THE ATP-DEPENDENT MECHANISM OF COHESIN FUNCTION IN CHROMOSOME SEGREGATION

Stefan Weitzer

Thesis presented for the degree of
Doctor of Philosophy from the University of London

September 2004

Chromosome Segregation Laboratory
Cancer Research UK London Research Institute
44 Lincoln´s Inn Fields
London WC2A 3PX

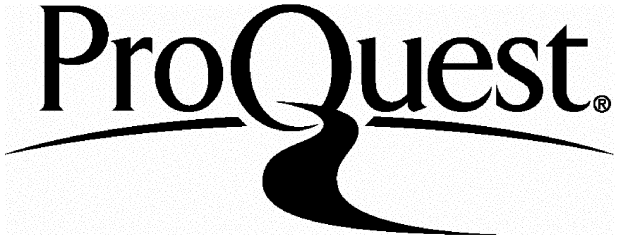

ABSTRACT

Equal chromosome distribution during mitotic cell divisions is necessary for maintaining genomic stability in eukaryotes. An essential prerequisite is the alignment of sister chromatid pairs in metaphase. Pairing or cohesion between sister chromatids is established during DNA replication and is promoted by the chromosomal cohesin complex. The budding yeast *Saccharomyces cerevisiae* cohesin complex consists of four core subunits, Smc1 and Smc3, both members of the Structural Maintenance of Chromosome (SMC) protein family, and the Scc1 and Scc3 subunits. At the anaphase onset cohesion is suddenly lost by proteolytic cleavage of cohesin's Scc1 subunit, leading to dissociation of cohesin from chromosomes and separation of sister chromatids getting pulled towards opposite cell poles by spindle microtubules. The mechanism by which cohesin binds to DNA initially, how cohesion is established during DNA replication and how cohesin dissociates from chromosomes in anaphase, is unknown.

In this study, cohesin bound to chromatin which likely represents the functional pool of the complex, was biochemically characterised. Cohesin was found to associate with chromatin in clusters but size, shape and subunit composition does not change during cohesion establishment. This suggests that the molecular function of cohesin is inherent of the complex and may have to be sought in its characteristic architecture and conserved domains.

Cohesin's Smc1 and Smc3 subunits are largely composed of long stretches of antiparallel intramolecular coiled coils which are flanked at one end by putative ATP-Binding Cassette (ABC) ATPase head domain. Heterodimerisation of Smc1 and Smc3 results in the formation of a proteinaceous ring, large enough to embrace two strands of DNA which has lead to the hypothesis that cohesion is mediated by entrapment of both sister chromatids within the ring.

This study shows that cohesin has indeed ATP binding activity. The two SMC subunits by themselves form a ring, closed at their interacting ATPase head domains in an ATP-dependent and independent fashion. Disruption of this interaction and opening of the ring is triggered by a cleavage fragment of the Scc1 subunit. To assess the role of ATP in cohesion, point mutations were introduced that were designed to prevent ATP binding or hydrolysis by the Smc1 subunit. ATP binding was found to be essential for cohesin complex assembly whereas a motif implicated in ATP hydrolysis is required for loading of cohesin onto DNA. In addition, an intact SMC ring is indispensable for DNA binding, indicating that ATP hydrolysis may be coupled to DNA transport into the ring.

These data suggest that ATP hydrolysis is necessary for loading of cohesin onto chromatin, whereas a prerequisite for DNA unloading of cohesin during anaphase is the disruption of the ring promoted by a Scc1 cleavage fragment. The analysis of ATP function in the context of cohesin's ring structure contributes to a biochemical understanding of the establishment and resolution of sister chromatid cohesion. In addition, since ring structure and functional domains appear to be conserved within related Smc protein complexes, similar mechanisms might apply to their multiple roles in chromosome biology like DNA condensation.

TABLE OF CONTENTS

ABSTRACT *2*

TABLE OF CONTENTS *3*

LIST OF FIGURES *7*

LIST OF TABLES *9*

ABBREVIATIONS *10*

ACKNOWLEDGEMENTS *12*

CHAPTER 1: Introduction *13*

1.1 The concept of sister chromatid cohesion **13**

1.2 The cohesin complex **16**

1.3 Sister chromatid cohesion and the cell cycle **20**

1.3.1 Cohesin binding to DNA 20

1.3.2 Establishment of cohesion 22

1.3.3 Bi-orientation of sister chromatids 24

1.3.4 Events leading to resolution of cohesion 25

1.4 Architecture of cohesin **29**

1.5 Cohesin association with DNA **35**

1.5.1 The cohesin ring model of DNA strand entrapment 35

1.5.2 DNA binding activities of cohesin 38

1.6 SMC complexes and their biochemical activities **39**

1.6.1 The SMC protein family 39

1.6.2 Bacterial SMC complexes 40

1.6.3 The Condensin Smc2/4 complex 41

1.6.4 The Smc5/6 complex 44

1.7 Role of ATP in architecture of SMC proteins and ABC ATPases **45**

1.7.1 SMC heads are ABC ATPases 45

1.7.2 Dimer organisation of ABC ATPases 46

1.7.3 ATP-induced dimerisation of an SMC related ABC ATPase, the Rad50 protein 49

1.8 Open questions addressed in this thesis and summary of results **54**

CHAPTER 2: Purification and characterisation of chromatin bound cohesin *58*

2.1 Purification of chromatin bound cohesin **58**

2.2 Subunit composition and hydrodynamic properties of cohesin during chromatin binding or cohesion establishment **60**

2.3 Cohesin associates with chromatin in clusters **61**

2.3.1 Electron microscopy of cohesin/DNA complexes 61

2.3.2 Cohesin associates with chromatin in clusters 63

2.4 Summary **64**

CHAPTER 3: ATP binding activity of cohesin and ATP-dependent complex assembly *71*

3.1 ATP binding activity of cohesin **71**

3.2 Construction and expression of Smc1 ATPase motif mutants **72**

3.3 The ATPase motifs in Smc1 are essential for sister chromatid cohesion **74**

3.4 ATP binding is required for cohesin complex formation **75**

3.4.1 Coimmunoprecipitation of ATPase motif mutant Smc1 with other cohesin subunits 75

3.4.2 An ATP-dependent in vitro reconstitution system for cohesin 76

3.5 Summary **77**

CHAPTER 4: Interaction analysis of cohesin SMC heads *83*

4.1 The SMC head interaction is independent of Scc1 ..... **83**

4.2 Smc1 and Smc3 form a closed ring independently of Scc1 ..... **84**

4.3 ATP-dependent and independent interactions between SMC heads **85**

4.4 Both Smc1 and Smc3 heads are required for Scc1 binding **86**

4.5 Summary **88**

CHAPTER 5: DNA loading and unloading of cohesin *93*

5.1 The C-motif of Smc1 is not required for chromosome segregation **93**

5.2 The C-motif of Smc1 is required for DNA loading of cohesin **94**

5.3 A closed cohesin ring is essential for DNA binding **95**

5.4 A closed Smc1/3 ring is not sufficient for cohesin binding to DNA **97**

5.5 Hydrolysable ATP stimulates dissociation of Scc1 from the SMCs *in vitro* **98**

5.6 A role for the C-terminal Scc1 cleavage product in unloading of cohesin from DNA **99**

5.7 Summary **100**

CHAPTER 6: Discussion *109*

6.1 The chromatin bound cohesin complex **109**
6.1.1 Is the ring structure sufficient for the chromosomal activities of cohesin? 109
6.1.2 Chromosomal cohesin is a monomeric complex: Implications for models of sister chromatid cohesion 112
6.1.3 The binding mode of cohesin on chromosomes 114

6.2 ATPase motif mutants as a tool to analyse the role of ATP in cohesion **115**

6.3 The assembly of the cohesin complex **117**
6.3.1 ATP binding of cohesin is required for complex formation 117
6.3.2 Interactions at the SMC head domains and Scc1 binding 119

6.4 A model for ATP hydrolysis-dependent binding of cohesin to DNA **120**

6.5 DNA unloading of cohesin **125**

6.6 DNA binding by ATP hydrolysis-dependent transport: Applicable for related SMC complexes? **128**

CHAPTER 7: Materials and Methods *133*

7.1 Molecular biology **133**
7.1.1 Polymerase chain reaction (PCR) 133
7.1.1.1 PCR for epitope tagging of endogenous cohesin subunits 133
7.1.1.2 PCR for cloning of cohesin subunit variants 135
7.1.1.3 PCR to introduce point mutations into Smc1 135
7.1.2 Restriction enzyme digestion and Klenow fill-in reaction of DNA overhangs 136
7.1.3 Phosphorylation and annealing of DNA linker oligonucleotides 137
7.1.4 Agarose gel electrophoresis 137
7.1.5 Isolation of DNA from agarose gels 137
7.1.6 Dephosphorylation of vector DNA and ligation reaction 138
7.1.7 Transformation of E. coli with plasmid DNA 138
7.1.8 Isolation of plasmid DNA from E. coli 139
7.1.9 DNA sequence analysis 139

7.2 Yeast biology **140**
7.2.1 Growth of cells and maintenance 140
7.2.2 Transformation 140
7.2.3 Synchronisation of cells and cell cycle experiments 141
7.2.4 Protein expression and depletion by the galactose inducible promoter 142
7.2.5 Flow cytometry 142

7.3 Biochemistry **142**
7.3.1 Preparation of yeast protein extracts 142
7.3.2 Purification and immunoprecipitation of cohesin and SMC complexes 143
7.3.3 SDS-PAGE and Western blot analysis 144
7.3.4 Coomassie and silver staining 145
7.3.5 Radioactive labelling of DNA in cohesin/DNA complexes 145
7.3.6 Gel filtration and glycerol gradient centrifugation 146
7.3.7 Quantification of chromatin bound cohesin 147
7.3.8 ATP crosslinking to cohesin 149
7.3.9 In vitro reconstitution system for cohesin 149
7.3.10 Assay for testing ATP-dependent disassembly of cohesin 149

7.4 Microscopy 150
7.4.1 Sister chromatid separation assay 150
7.4.2 Chromosome spreading 150
7.4.3 Electron microscopy of cohesin/DNA complexes 151
7.5 Table of DNA vectors 153
7.6 Table of yeast strains 158

CHAPTER 8: References 162

LIST OF FIGURES

CHAPTER 1

Figure 1.1. The chromosome mechanics during mitosis. 15
Figure 1.2. The cohesin cycle. 19
Figure 1.3. Chromosome segregation during mitosis. 26
Figure 1.4. Cohesin removal and chromosome condensation in mitosis. 30
Figure 1.5. Architecture of SMC proteins. 33
Figure 1.6. The ring structure of cohesin 34
Figure 1.7. Models for cohesin's association with DNA 37
Figure 1.8. Architecture of ABC ATPases. 47
Figure 1.9. The ATP-dependent dimerisation of Rad50 head domains. 50
Figure 1.10. Hypothetical ATP-binding and hydrolysis cycle of ABC ATPases. 53

CHAPTER 2

Figure 2.1. A purification strategy to isolate chromatin bound cohesin 65
Figure 2.2. Purification of chromatin bound cohesin. 66
Figure 2.3. Comparison of cohesin subunit composition in soluble or chromatin fractions. 67
Figure 2.4. Chromosomal cohesin is a monomeric complex and does not change its size or shape during cohesion establishment 68
Figure 2.5. Electron micrographs of cohesin/DNA complexes 69
Figure 2.6. Cohesin binds to chromatin in clusters. 70

CHAPTER 3

Figure 3.1. ATP crosslinking to purified cohesin 78
Figure 3.2. Construction and expression of Smc1 ATPase motif mutants 79
Figure 3.3. ATP binding and hydrolysis motifs in Smc1 are essential for sister chromatid cohesion. 80
Figure 3.4. C-motif but not Walker A and B motif mutant Smc1 supports complex formation with Scc1. 81
Figure 3.5. ATP binding is required for Scc1 binding to Smc1. 82

CHAPTER 4

Figure 4.1. Interactions between Smc1 and Smc3 heads do not require Scc1. 89
Figure 4.2. Sedimentation properties of Smc1/3 complexes without Scc1 are consistent with closed rings. 90

Figure 4.3. ATPase motif mutant Smc1 heads interact with Smc3 in an ATP-dependent and independent manner. 91
Figure 4.4. Smc1 and Smc3 heads are both required for Scc1 binding. 92

CHAPTER 5

Figure 5.1. The C-motif of Smc1 is not required for chromosome segregation. 102
Figure 5.2. C-motif mutant Smc1 prevents cohesin binding to DNA. 103
Figure 5.3. A closed cohesin ring is required for DNA binding. 105
Figure 5.4. An Smc1/3 ring does not bind to DNA by itself. 106
Figure 5.5. Hydrolysable ATP stimulates the release of Scc1 from the SMCs. 107
Figure 5.6. Expression of the C-terminal Scc1 cleavage product disrupts the Smc1/3 head interaction and causes chromosome segregation in metaphase. 108

CHAPTER 6

Figure 6.1. The assembly of the cohesin complex. 118
Figure 6.2. ATP hydrolysis-dependent DNA binding of cohesin 122
Figure 6.3. DNA unloading of cohesin. 127
Figure 6.4. A model for chromosome condensation by DNA entrapment. 129

CHAPTER 7

Figure 7.1. Schematic overview of PCR-based epitope tagging of genes by homologous recombination. 135
Figure 7.2. Scheme of overlap extension PCR for site-directed mutagenesis. 136

LIST OF TABLES

CHAPTER 1

Table 1.1. Subunit composition of the cohesin complex from different species. 18
Table 1.2. Subunit composition of eukaryotic SMC complexes from different species. 40

ABBREVIATIONS

aa, amino acid
ABC, ATP-binding cassette
ADP, adenosine diphosphate
AMP-PNP, adenylyl-imidodiphosphate
ATP, adenosine triphosphate
    ATPγS, adenosine-5'-O- (3-thiotriphosphate)
    dATP, deoxyadenosine triphosphate
AFM, atomic force microscopy
APC, anaphase promoting complex
bp, basepair
BSA, bovine serum albumin
°C, degrees Celsius
CHIP, chromatin immunoprecipitation
DAPI, 4´,6-diamidino-2-phenylindole
Δ, deletion
DMSO, dimethyl-sulfoxide
DNA, deoxyribonucleic acid
    dsDNA, double-stranded DNA
    ssDNA, single-stranded DNA
DNase, deoxyribonuclease
dNTP, deoxyribonucleotide triphosphate
DTT, dithiothreitol
EM, electron microscopy
FISH, fluorescent *in situ* hybridisation
Gal, galactose
GAL1, galactose-inducible promoter 1
g, gram
    µg, micrograms
    mg, milligrams
h, hour(s)
HA, hemagglutinin
Hepes, N-(2-Hydroxyethyl)-piperazine-N´-2-ethanesulfonic acid
HU, hydroxyurea
Ig, immunoglobulin
IP, immunoprecipitation
IPTG, isopropyl β-D-thiogalactoside
kb, kilobase
kDa, kilodalton
l, litre(s)
    µl, microlitre(s)
    ml, millilitre(s)
M, molar
    µM, micromolar
    mM, millimolar
m, metre(s)
    µm, micrometre(s)
    mm, millimetre(s)
    nm, nanometre(s)
mA, milli Ampère
MAT, mating type
Mb, megabase
min, minute(s)
MN, micrococcal nuclease
noc, nocodazole

OD, optical density
ORF, open reading frame
PAGE, polyacrylamide gel electrophoresis
PBS, phosphate buffered saline
PCR, polymerase chain reaction
PIPES, 1,4-piperazine-diethane-sulphonic acid
PMSF, phenylmethylsulphonyl fluoride
rpm, revolutions per minute
SDS, sodium dodecyl sulphate
sec, second(s)
TAP, tandem affinity purification
TEV, tobacco etch virus
TPI1, triosephosphate isomerase 1 promoter
Tris, tris-hydroxymethyl-amino-methane
UV, ultraviolet
V, volt

ACKNOWLEDGEMENTS

I would like to thank my supervisor Frank Uhlmann for giving me the opportunity to work in his laboratory and for his assistance, constant support and encouragement throughout my projects. I am especially grateful for letting me share his enthusiasm and excitement about all topics within the chromosome biology field, and for teaching me the principles of protein science and experimental biochemistry.

I would like to acknowledge all members of the CSL lab past and present for their input into my work, for all the scientific and non-scientific discussions and for the great working environment they created. In particular I want to thank Chris for cloning, protein purifications and her support and help in every respect during my project which would have never worked out without her. I am very grateful to Matt for his interest in my work and for all discussions and comments on my experiments. Especially I would like to thank him for encouraging me to be critical with my own and other people's results and their interpretations, and for making me realise that the controls are the most important part of an experiment. A special thank-you to both of them for friendship, fun, going out or away, dragging me out of the cold room on a Friday night, improving my knowledge about football, tennis and Elvis but most importantly for listening to me and cheering me up when things were bad.

I want to thank everybody else at the institute, who made it such a great place to work at, especially Anna and Clare whom I had innumerable enjoyable evenings in the pub with, and for sharing gossip with me. Thanks also to Julia, Sabine and Mark who I joined for many country walks, museum trips, concert and cinema evenings. I also would like to acknowledge my friend Stefan in Cambridge whom I could always visit when I needed to escape London for a couple of days. I am very grateful to all my other friends back home in Austria who kept in touch with me and updated me with all the important stories and news from there.

Finally I would like to thank my family for keeping faith in me, and Tumee for waiting for me.

CHAPTER 1: Introduction

1.1 The concept of sister chromatid cohesion

Genetic information lies encoded and is packaged in chromosomes. When cells proliferate, chromosomes are duplicated in the process of DNA replication and two identical copies, the sister chromatids, are produced. During mitosis sister chromatids are then segregated to opposite cell poles, and cells are divided to give rise to two daughter cells. Each daughter cell has to be provided with a complete and identical set of chromosomes, a prerequisite for cell survival, controlled proliferation and growth. To maintain genomic stability throughout generations, mechanisms exist that control faithful segregation of sister chromatids thereby ensuring accurate transmission of chromosomes. Failures in these mechanisms during mitosis lead to chromosome missegregation, resulting in cells with too few or too many chromosomes (aneuploidy) which is often associated with the formation of malignant tumour cells (reviewed in Jallepalli and Lengauer, 2001). The precise segregation of chromosomes is likewise essential during meiotic cell divisions. Here, cells with initially two sets of chromosomes (diploids) undergo one round of DNA replication followed by two rounds of subsequent chromosome segregation. This results in the production of four haploid cells harbouring a single chromosome set. Chromosome missegregation during meiosis contributes to congenital aneuploidies like trisomies which are caused by the inheritance of an extra chromosome copy. A common example is trisomy of chromosome 21 leading to Down´s Syndrome (reviewed in Hassold and Hunt, 2001).

To guarantee accurate chromosome segregation in mitosis, sister chromatids have to become pairwise aligned at a zone between the two cell poles, the metaphase plate, prior to their separation (Figure 1.1). Positioning of chromosomes at the metaphase plate is brought about by the action of spindle microtubules. These emanate from spindle poles at opposite sides of the cell and attach to chromatids at specialised structures located at the centromeric regions, the kinetochores. Accurate chromosome segregation is only possible if microtubules are attached to all kinetochores in a fashion that microtubules

attached to one of the sister kinetochores have opposite orientations to those attached to the other, a formation also known as bi-orientation. By exerting pulling forces on kinetochore pairs during metaphase, microtubules attempt to move sister chromatids away from each other towards opposite poles. The resulting force on sister kinetochores has to be counteracted by an opposing force that holds them together. Without this counterforce, sister chromatids would never become pairwise aligned at the metaphase plate, and as a consequence would segregate randomly. It is sister chromatid cohesion that represents this counteracting force by providing a physical connection between pairs of sisters (reviewed in Nasmyth, 2001). The presence of sister chromatid cohesion is the prerequisite for the tension between sister kinetochores, which in turn is required for bi-orientation. Once sister chromatids of all chromosomes are bi-oriented, cohesion is suddenly destroyed at the anaphase onset leading to loss of tension between them and to their irreversible segregation towards opposite poles caused by the pulling force of the spindle (Figure 1.1).

It is also sister chromatid cohesion that links synthesis of sister chromatids that takes place in S-phase of the cell cycle, to their segregation in mitosis. During S-phase cohesion is established and identifies newly replicated sister chromatids as pairs (Tomonaga et al., 2000; Uhlmann and Nasmyth, 1998). In this way, sisters are kept tightly linked together during the gap between S-phase and mitosis, the G2 phase. The tight and permanent coupling of sisters during G2 is crucial since it can last for long time periods, in the case of human oocytes up to five decades.

In addition, sister chromatid cohesion facilitates DNA repair in G2. If one DNA strand breaks or is damaged, its sister strand can serve as a template for repair by homologous recombination. Cohesion efficiently tethers sisters together and thereby keeps the template strand in close proximity to the damaged strand so that its original sequence can be restored (Sjögren and Nasmyth, 2001).

What is the molecular basis for sister chromatid cohesion and who are the players involved? Genetic screens initially performed in yeast have led to the identification of specific proteins that mediate cohesion. Four of them were found to be present in a conserved protein complex, the cohesin complex. Cohesin forms a proteinaceous linkage between sister strands thereby holding them together from the time of their synthesis until metaphase. This connection is destroyed at the anaphase onset by

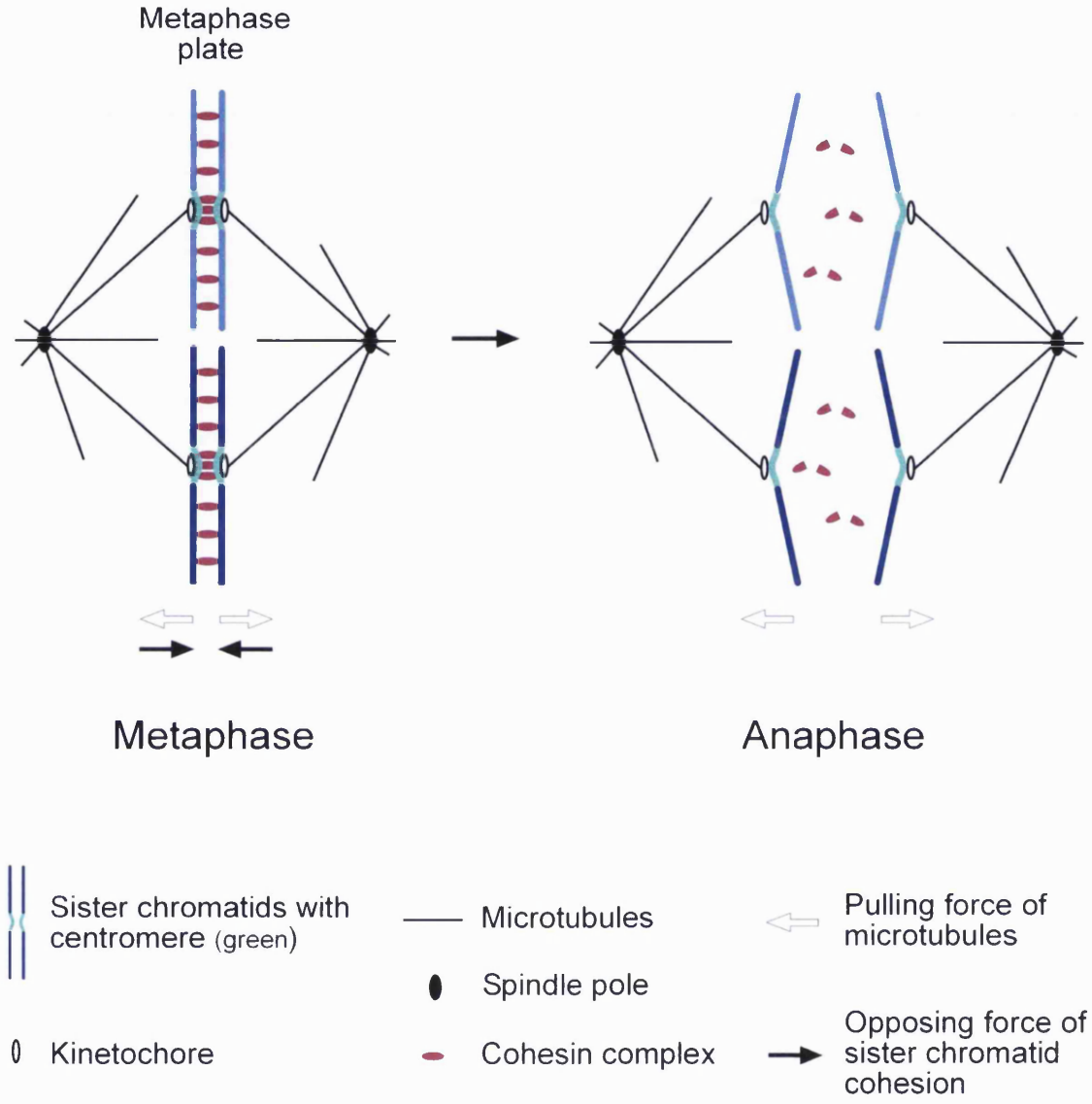

Figure 1.1. The chromosome mechanics during mitosis.

During mitotic divisions, a series of events is necessary in order to equally distribute replicated DNA into two daughter cells. Coincidently with DNA replication in S phase, sister chromatids become linked together along their entire length by cohesion, mediated by the cohesin complex. Kinetochores are assembled at the centromeric regions of each of the sisters and become attached to microtubules emanating from the spindle poles. In metaphase, chromosomes are aligned between the spindle poles when spindle microtubules attached to pairs of kinetochores face opposite directions (bi-orientation). Thus, forces are exerted on chromosomes that pull them to opposing spindle poles. This force is counteracted by cohesin that holds sisters together. At anaphase, cohesin is proteolytically destroyed and cohesion along chromosomes is lost. This allows the pulling force of the spindle microtubules to segregate the sister chromatids to opposite poles.

proteolytic cleavage of one of cohesin's subunits leading to its dissociation from chromosomes and initiation of sister chromatid segregation to opposite poles.

1.2 The cohesin complex

The cohesin complex contains the Scc1, Scc3, Smc1 and Smc3 proteins as core subunits, all of them essential proteins that are conserved in yeast, flies, worms and vertebrates (Table 1.1.) Their function in mediating cohesion between sister chromatids was first demonstrated in the budding yeast *Saccharomyces cerevisiae.* Here, sister chromatid sequences remain closely aligned from S-phase until metaphase, but their separation depends on the activation of an ubiquitin protein ligase at anaphase onset, the APC or Anaphase-promoting complex (Irniger et al., 1995). Since APC mutants fail to separate sisters, mutants capable of separation in the absence of APC function were likely playing a part in cohesion. Genetic screens designed to identify such components uncovered the subunits of the cohesin complex and additional proteins that are not part of the complex but have other roles in sister chromatid cohesion (Guacci et al., 1997; Michaelis et al., 1997; Tóth et al., 1999). Unlike these components, core proteins of the cohesin complex are necessary for both establishment of cohesion during DNA replication and its maintenance until metaphase.

Budding yeast's Scc1 (for sister chromatid cohesion) subunit is also known as Mcd1 (mitotic chromosome determinant) for its requirement in chromosome condensation, the longitudinal compaction of chromosomes during mitosis (Guacci et al., 1997). The orthologue in the fission yeast *Schizosaccharomyces pombe* is named Rad21 since it was initially characterised as a component required for double strand break repair (Birkenbihl and Subramani, 1995). This function is well conserved, since deletion of Scc1 in chicken cells or mutation of Scc1 in budding yeast shows defective recombinational repair between sister strands (Sjögren and Nasmyth, 2001; Sonoda et al., 2001). Budding yeast Scc1 is detectable from late G1 phase until metaphase, with a large fraction tightly associated with chromatin. Scc1 disappears entirely from chromosomes at anaphase onset, precisely when cohesion is dissolved (Michaelis et al., 1997; Tóth et al., 1999). Subsequent studies revealed that Scc1 is proteolytically cleaved during anaphase (Uhlmann et al., 1999) (Figure 1.2). It is cleavage of Scc1 that causes release of cohesin from chromatin and that was shown to be both required and

sufficient to trigger sister chromatid segregation (Uhlmann et al., 2000). Scc1 is replaced by its homologous Rec8 subunit in meiosis during which Rec8 is also proteolytically cleaved to allow two successive rounds of chromosome segregation (Buonomo et al., 2000).

Another core component of the cohesin complex is the Scc3 subunit, present in budding yeast as a single genomic copy (Tóth et al., 1999). In human and mouse cells, three Scc3 homologues exist, called SA1-SA3. SA1 and SA2 are mitotic forms of Scc3 which both are part of two distinct 14 S cohesin complexes (Sumara et al., 2000). *Xenopus* XSA1 and XSA2 are components of a 14 S and 12.5 S cohesin complex, respectively (Losada et al., 2000). The reason for the existence of cohesin complexes with different Scc3 isoforms in somatic vertebrate cells and whether these distinct cohesin complexes perform different functions, remains unclear. SA3 or STAG3 is the mammalian meiotic Scc3 homologue involved in chromosome pairing (Pezzi et al., 2000; Prieto et al., 2001). Likewise, fission yeast contains two different Scc3 homologues, Psc3 and Rec11. Psc3 is expressed during mitosis and meiosis. It colocalises with the other cohesin members on mitotic chromosomes but it fails to interact with them in solution under the experimental conditions that were used (Tomonaga et al., 2000). Rec11 is meiosis-specific and is targeted specifically to chromosome arms, whereas Psc3 is bound to the centromeric regions in meiosis (Kitajima et al., 2003). The different localisation pattern of both proteins is consistent with their different functions in meiotic cohesion. Whereas Rec11 along chromosome arms is essential for meiotic recombination, cohesin containing Psc3 is required for maintaining sister chromatid cohesion at centromeres throughout both meiotic divisions (Kitajima et al., 2003).

The SMC subunits of the cohesin complex, Smc1 and Smc3, belong to the Structural Maintenance of Chromosomes family. Members are highly conserved from bacteria to humans, and in addition to sister chromatid cohesion they have roles in chromosome condensation, recombination, gene dosage compensation and DNA repair (reviewed in Jessberger, 2002). They share a common structure that is based on five different domains. Two amino- and carboxy-terminal domains containing motifs highly conserved in ATPases are flanked by two long stretches of coiled coil domains that are separated by a central hinge domain (see chapter 1.4 for more details). Mammalian Smc1 and Smc3 subunits have also been isolated as components of the RC-1 complex

that promotes recombinational repair of double-stranded gaps and deletions (Jessberger et al., 1996). In addition to its role in DNA repair, Smc1 has been shown to function in a DNA damage response pathway mediated by the ATM checkpoint kinase (Kim et al., 2002; Kitagawa et al., 2004; Yazdi et al., 2002). Like the other members of cohesin, a meiosis specific variant of Smc1 exists in mammals, the SMC1β subunit (Revenkova et al., 2001).

Although not considered as a stoichiometric subunit of the cohesin complex in budding yeast, the Pds5 protein associates with core components of fission yeast, *Xenopus* and human cohesin (Sumara et al., 2000; Tanaka et al., 2001). Pds5 is an orthologue of *Aspergillus nidulans* BIMD and *Sordaria macrospora* Spo76 which have essential functions in chromosome segregation, DNA repair and meiotic sister chromatid cohesion (Denison et al., 1993; Holt and May, 1996; van Heemst et al., 1999). Pds5 is required for maintaining cohesion during G2 until mitosis in budding yeast, colocalises with cohesin on chromosomes from S-phase until metaphase, and dissociates from chromosomes in anaphase upon Scc1 cleavage (Panizza et al., 2000). In fission yeast, Pds5 becomes essential for cohesion only after prolonged cell cycle arrest in G2 (Tanaka et al., 2001), and in budding and fission yeast it is not required for cohesion establishment. It is currently unclear if Pds5 has any structural function within the cohesin complex or rather a regulatory role in maintenance of cohesion.

		S. cerevisiae	*S. pombe*	*C. elegans*	*D. melanogaster*	*X. laevis*	*H. sapiens*
SMCs		Smc1	Psm1	SMC-1	DmSMC1	XSMC1	hSMC1α
							hSMC1β
		Smc3	Psm3	SMC-3	DmSMC3	XSMC3	hSMC3
Non-SMCs	Kleisin	Scc1	Rad21	COH-2	DmRAD21	XRAD21	hSCC1
		Rec8*	Rec8*	REC-8*			hRec8*
		Scc3	Psc3	SCC-3	DmSA	XSA1, XSA2	hSA1, hSA2
			Rec11*				hSTAG3*
		Pds5	Pds5	PDS-5		XPDS5	hPDS5

Table 1.1. Subunit composition of the cohesin complex from different species. Proteins marked with asterisks (*) are specifically expressed during meiosis.

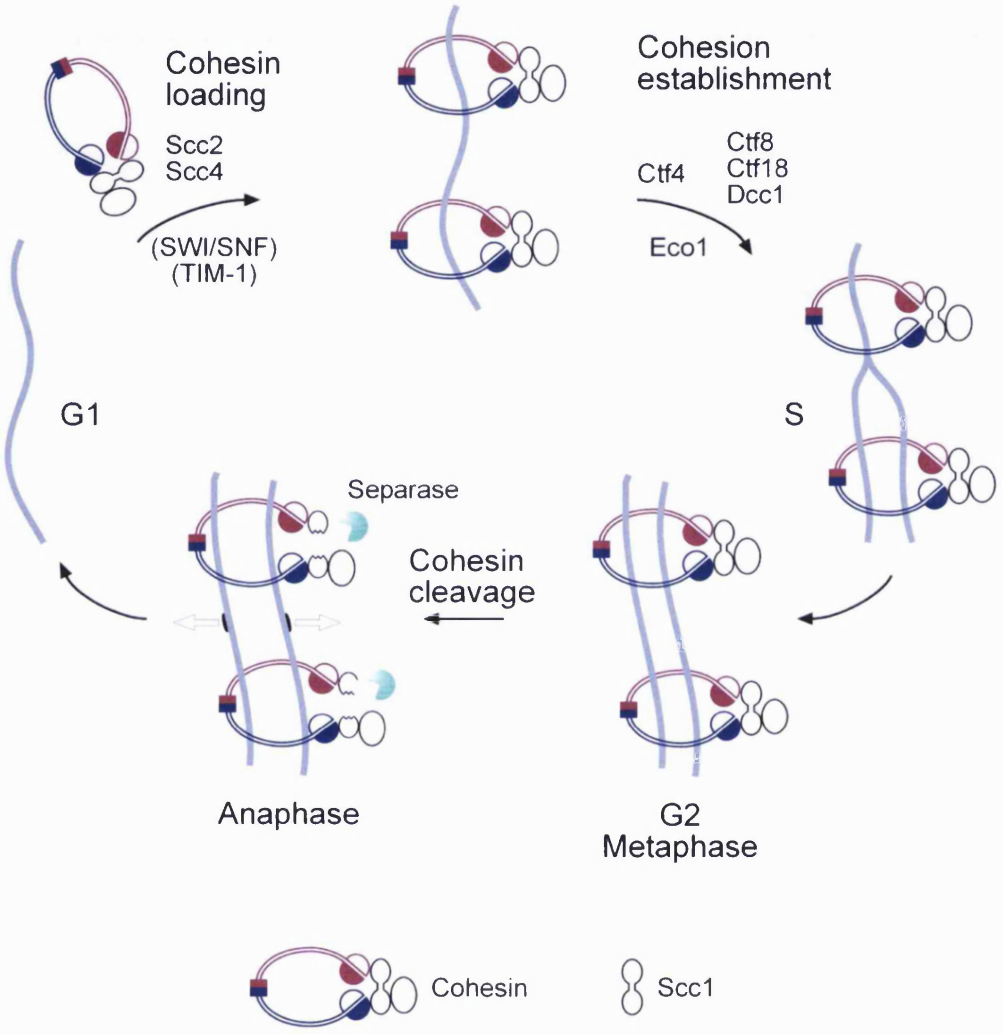

Figure 1.2. The cohesin cycle.

Cohesin is loaded onto chromosomes before the onset of DNA replication, either during G1 phase (budding yeast) or in telophase of the previous cell cycle (vertebrates). Loading is promoted by the Scc2/Scc4 proteins in budding yeast. Proteins such as the SWI/SNF chromatin remodelling complex and TIM-1 are involved in cohesin's association with chromosomes in humans and *C. elegans*, respectively. During DNA replication in S phase, cohesion is established between newly synthesised sister chromatids, which requires the activity of Eco1, Ctf4 and the alternative RFC complex containing Ctf8, Ctf18 and Dcc1. In metaphase, once all chromosomes are bi-oriented on the mitotic spindle, cohesin's Scc1 subunit is cleaved by separase. Consequently, cohesin is released from chromosomes and cohesion between sisters is lost, thereby triggering their movement to opposite poles of the cell during anaphase.

1.3 Sister chromatid cohesion and the cell cycle

1.3.1 Cohesin binding to DNA

In budding yeast, cohesin binds to chromosomes from late G1 phase until anaphase, from the time just before cohesion establishment until its resolution (Michaelis et al., 1997; Tanaka et al., 1999). In mammalian cells, cohesin is found associated with chromatin throughout interphase (Losada et al., 1998; Losada et al., 2000; Sumara et al., 2000; Waizenegger et al., 2000). It is removed from chromosomes during mitosis but reassociates already in telophase and remains on chromosomes until the next mitosis (Waizenegger et al., 2000). However, the complete removal of cohesin from chromosomes in mitosis as a prerequisite for sister separation is not as clear in fission yeast. Here, cohesin binding to centromeres is nearly constant throughout the cell cycle but is only slightly reduced in anaphase (Tomonaga et al., 2000). This might be due to a very transient dissociation of cohesin from chromosomes during anaphase and therefore beyond the limits of experimental resolution.

The localisation of cohesin on chromosomes is not random but occurs on specific cohesin association sites or Cohesin Associated Regions (CARs) which has been demonstrated by chromatin immunopreciptiation (CHIP) experiments (Blat and Kleckner, 1999; Laloraya et al., 2000; Lengronne et al., 2004; Megee et al., 1999; Tanaka et al., 1999). In budding yeast, the size of a CAR was shown to be about 0.8-1.0 kb. CARs are found on average every 15 kb, mostly in intergenic regions. Cohesin preferentially binds to AT-rich sequences which is presumably a consequence of its association with intergenic regions. Recent experiments revealed that the intergenic localisation of cohesin is at places of convergent transcription in budding and fission yeast, and that active transcription may be responsible for this localisation (Lengronne et al., 2004). In addition, cohesin is highly enriched around centromeres, the region where cohesin is most required to resist the pulling forces of spindle microtubules. In mammalian cells, location and distribution of CARs are not yet known, so far only some copies of the Alu class of short interspersed repeats was found to be cohesin-bound (Hakimi et al., 2002) .

In budding yeast, loading of cohesin to arms and centromeres of chromosomes requires the presence of an essential protein complex, composed of the Scc2 and Scc4 proteins (Ciosk et al., 2000; Michaelis et al., 1997) (Figure 1.2). These proteins are not stoichiometric components of the cohesin complex but were found to interact with soluble cohesin (Arumugam et al., 2003). However, on chromosomes Scc2/4 do not colocalise with cohesin and do not bind to CARs (Lengronne et al., 2004). Both proteins are required for establishment but not for maintenance of sister chromatid cohesion during metaphase, suggesting their function in cohesion is restricted to the initial loading process of cohesin onto chromosomes. The homologue of Scc2 in fission yeast, Mis4, was likewise found to be necessary for sister chromatid cohesion and deposition of cohesin on chromosomes (Tomonaga et al., 2000; Toyoda et al., 2002). Nipped B, the Scc2 homologue in *Drosophila melanogaster*, is required for sister chromatid cohesion and is implicated in mediation of long-range enhancer-promoter interaction, possibly by chromatin loop formation (Rollins et al., 2004; Rollins et al., 1999). The role of Scc2/4 could therefore be to generate chromatin domains which then would become permissive for cohesin loading, but the precise loading mechanism remains yet to be elucidated.

Recently, factors which load cohesin onto particular chromosome loci have been identified. In fission yeast, the Swi6 (HP1) protein is responsible for cohesin recruitment specifically to pericentromeric regions but not to the central core of centromeres or chromosome arms (Bernard et al., 2001; Nonaka et al., 2001). Swi6 binds to nucleosomes with histone H3 methylated at lysine 9 and promotes heterochromatin assembly. It also directly binds to the Psc3 subunit of cohesin, thereby depositing it onto pericentromeric loci. Loss of genomic integrity at the heterochromatic mating type locus in Swi6 or Psc3 mutants indicates that Swi6-dependent recruitment of cohesin may be a general positioning mechanism for cohesin onto heterochromatic regions.

TIM-1, the *Caenorhabditis elegans* homologue of the *Drosophila* circadian rhythm protein TIMELESS, has been shown to interact with cohesin and is required for homologue chromosome pairing in early meiosis (Chan et al., 2003). Inactivation of TIM-1 results in premature sister chromatid separation due to a failure of the Rec8 and Scc3 cohesin subunits to associate with chromatin, yet binding of the SMC subunits to chromosomes is unaffected. This suggests that cohesin assembly and its association

with chromatin occurs successive, the SMC subunits bind to chromatin independently of the non-SMCs. TIM-1 might promote binding of non-SMC subunits to chromatin-bound SMCs, but the molecular mechanism remains to be analysed.

Another factor involved in DNA loading of cohesin has been identified as the human SWI/SNF2 containing chromatin remodelling complex (Hakimi et al., 2002). It copurifies with cohesin, and its ATPase activity is required for cohesin loading onto Alu repeats. Mutations in two subunits of the budding yeast SWI/SNF related RSC nucleosome-remodelling complex also specifically prevented cohesin recruitment to chromosome arms but not centromeres, resulting in precocious loss of arm cohesion (Huang et al., 2004). This indicates that chromatin remodelling activity might be a prerequisite to allow accessibility for cohesin to nucleosomal DNA. However, the preferred type of DNA substrate for cohesin binding, whether it is naked chromosomal DNA, nucleosomal DNA or distinct chromatin structures, is unknown.

1.3.2 Establishment of cohesion

Cohesin loading onto chromosomes is essential but not sufficient for mediating sister chromatid cohesion. If Scc1 is expressed only after S-phase is completed, cohesin is still able to bind to chromosomes but sister chromatid cohesion is not generated (Uhlmann and Nasmyth, 1998). Therefore, cohesin is required to be present during DNA replication to confer cohesion establishment. This is reasonable since an inherent coupling of DNA replication with cohesion establishment would result in cohesion only between two newly synthesised sister strands emerging from the replication fork. Cohesion is thus prevented between mere related sequences, such as homologous chromatids in diploid cells, or completely unrelated sequences.

Specific proteins are required for cohesion establishment during S-phase (Figure 1.2). Budding yeast mutants in Eco1/Ctf7 (for establishment of cohesion, or chromosome transmission fidelity) load cohesin normally in G1 but fail to establish cohesion during S-phase (Skibbens et al., 1999; Tóth et al., 1999). Eco1 is not required for maintaining cohesion once it is established, and therefore its role in cohesion is limited to S-phase. Eco1 shows sequence similarity to acetyl-transferases, and it is capable of acetylating itself and cohesin subunits *in vitro* (Ivanov et al., 2002). However, acetylation activity *in vivo* has not been detected. Similarly, two proteins in

Drosophila, san (for separation anxiety) and deco (for Drosophila Eco1), both required for establishment of centromeric cohesion, are predicted to encode for acetyl-transferases (Williams et al., 2003).

The Eco1 homologue in fission yeast Eso1 is also essential for establishment but not for maintenance of cohesion (Tanaka et al., 2001; Tanaka et al., 2000a). Surprisingly, its requirement for cohesion establishment becomes completely negated in the absence of Pds5 suggesting a role for Pds5 in suppressing cohesion establishment until it is counteracted by Eso1. Paradoxically, once cohesion is established, Pds5 is necessary to maintain cohesion during prolonged G2 arrest, therefore playing a dual role in establisment and maintenance of cohesion. Pds5 hindrance of cohesion establishment might be to ensure that cohesion is only established between replication products by Eso1 in S-phase, and not before or afterwards between unrelated sequences, yet its precise role remains elusive.

Other proteins involved in the establishment of cohesion are functionally related to the DNA replication machinery. During DNA replication, Replication Factor C (RFC) is required for DNA loading of the trimeric sliding clamp PCNA (Proliferating Cell Nuclear Antigen). RFC consists of five subunits, Rfc1-Rfc5. Recently an alternative version of RFC, containing the Ctf8, Ctf18 and Dcc1 proteins instead of the Rfc1 subunit, has been identified in budding yeast (Hanna et al., 2001; Mayer et al., 2001). Although not essential, the deletions of either of these proteins result in defects in sister chromatid cohesion and high levels of chromosome loss. Whether this alternative RFC complex is also recruiting PCNA onto DNA *in vivo* is not known, although such an activity has been observed *in vitro* (Bermudez et al., 2003). In addition, PCNA genetically interacts with Eco1, and its overexpression suppresses a temperature-sensitive allele of Eco1 (Skibbens et al., 1999). During DNA replication PCNA associates with and promotes DNA polymerase processivity at the replication fork. DNA polymerases are indeed involved in sister chromatid cohesion. The replication initiator DNA polymerase α shows genetic and physical interaction with Ctf4, a protein required for robust cohesion (Formosa and Nittis, 1999). Mutants in the large subunit of DNA polymerase ε, responsible for processive leading strand synthesis, are defective in cohesion, and this protein shows genetic interactions with cohesin subunits (Edwards et al., 2003). In addition, the N-terminus of fission yeast Eso1 is homologous to DNA polymerase η involved in DNA repair (Tanaka et al., 2000a). Whether the role of the

alternative RFC complex is to recruit a clamp that associates with special polymerases for replication through cohesin associated chromosome regions, is not yet known. However, these findings indicate that cohesion is actively established at the replication fork with assistance of components of the DNA replication apparatus. However, the mechanism how these processes are coupled and its requirement for cohesion maintenance has remained unclear.

1.3.3 Bi-orientation of sister chromatids

Accurate chromosome segregation requires bi-orientation of chromosomes in metaphase. Bi-orientation is generated when a pair of sister kinetochores is attached to spindle microtubules emanating from two opposite spindle poles (bipolar attachment) rather than from the same pole (monopolar attachment, Figure 1.3A). Microtubule attachments to kinetochores are transient and unstable but become stabilised in the presence of tension between sister kinetochores. Tension is only generated if kinetochores become bipolar attached. A prerequisite for bipolar attachment is the Aurora B kinase (Adams et al., 2001; Biggins et al., 1999; Kaitna et al., 2002; Tanaka et al., 2002). Mutations in its homologue in budding yeast, the Ipl1 kinase, result in attachment of sister kinetochores preferentially with the spindle pole inherited from the previous division (Tanaka et al., 2002). Ipl1 therefore is responsible for resolving initial monopolar to allow stable bipolar attachments with spindles emanating from the old and the newly synthesised spindle pole. Monopolar attachment was also observed in cohesin mutants (Janke et al., 2002; Tanaka et al., 2000b; Toyoda et al., 2002). The role of cohesin in bi-orientation is not kinetochore assembly to bring the sister kinetochores in proximity such that they face opposite directions. Cohesin´s role is rather the generation of tension between sister kinetochores since tension is the only requirement for bi-orientation. This was demonstrated by a study showing that kinetochores assembled on engineered, unreplicated dicentric chromosomes were efficiently bi-orientated in budding yeast (Dewar et al., 2004). This is also consistent with a recent study using vertebrate cells depleted for Scc1. If in these cells decatenation of replicated chromosomes was inhibited, chromosomes still showed bi-orientation even though Scc1 was absent (Vagnarelli et al., 2004). Therefore, any essential role for cohesin in kinetochore function can be ruled out. Another protein complex involved in bi-

orientation is the Dam/Duo kinetochore complex. Phosphorylation of Dam/Duo by Ipl1 kinase is involved in making erroneous kinetochore-microtubule attachments unstable (Cheeseman et al., 2002). However, the mechanism of how kinetochore-microtubule attachments that are under tension resist to be turned over by Ipl1 activity and therefore become stabilised, is unknown.

Cells do not undergo anaphase unless all chromosomes have reached bi-orientation. Initiation of anaphase onset is prevented by the spindle checkpoint which senses the existence of unattached kinetochores and consequently inhibits the anaphase promoting complex (APC) (reviewed in Yu, 2002). Mediators of the spindle checkpoint comprise members of the Bub and Mad protein family. The Mad2 protein is recruited to unattached kinetochores where it supports assembly of the mitotic checkpoint complex containing BubR1/Mad3, Bub3, Mad2 and the APC activator Cdc20. This complex, or its subcomplexes, is then thought to diffuse away and stoichiometrically interacts with the APC, thereby blocking its activity by a yet unknown mechanism. Ipl1 kinase was also found to take part in the spindle checkpoint as an upstream activator. It triggers the checkpoint in situations where sister kinetochores are not under tension, for example due to loss of cohesion (Biggins and Murray, 2001). Whether the checkpoint is activated as a direct consequence of Ipl1´s role in monitoring lack of tension at kinetochores, is unclear.

1.3.4 Events leading to resolution of cohesion

In addition to bi-orientation, chromosomes have to become compacted and severely reduced in length during mitosis to ensure their correct segregation. A multisubunit protein complex structurally similar to cohesin, called condensin, is essential for initiation and maintenance of this process known as chromosome condensation (see chapter 1.6.3 for more details). Condensin mutants show defects in chromosome segregation, with chromosome masses being pulled apart but never becoming completely segregated (Saka et al., 1994). Condensation might also be required to facilitate decatenation of entangled sister chromatids. As each sister chromatid condenses, individual sister axes are formed which separate from one another and thereby might provide directionality to topoisomerases.

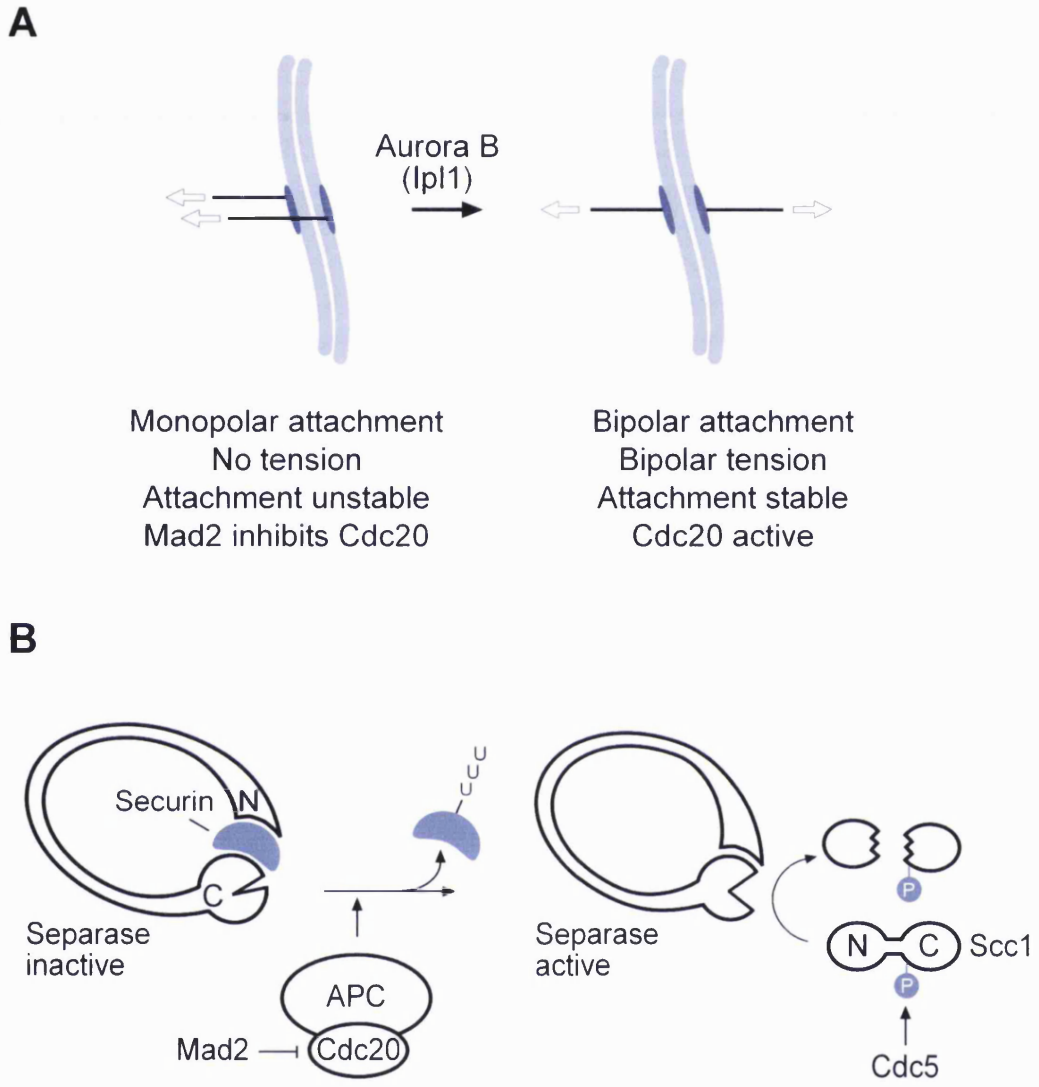

Figure 1.3. Chromosome segregation during mitosis.

(A) Bi-orientation of sister chromatids on the mitotic spindle. Microtubules of the mitotic spindle attach to kinetochores. This attachment is unstable due to the activity of Aurora B kinase unless bipolar tension between sister kinetochores is achieved. Mad2 recognizes free kinetochores and inhibits the Cdc20 activator of the anaphase promoting complex. Once bipolar tension is established, microtubule attachment becomes stabilised, and Mad2 relieves its inhibition on Cdc20.
(B) Regulation of anaphase onset. In metaphase, securin interacts with separase and inhibits its proteolytic activity. Securin is ubiquitylated by the Cdc20-activated anaphase promoting complex (APC) which targets securin for degradation. Upon liberation of securin, interaction of the N- and C-termini of separase becomes possible which fully activates its protease activity. Separase consequently cleaves Scc1, thus destroying cohesion. Budding yeast Polo-like kinase Cdc5 phosphorylates Scc1 in mitosis, a prerequisite for efficient cleavage by separase.

Once all sister chromatids are bi-oriented, Cdc20 is free to activate the APC thereby initiating anaphase onset and resolution of cohesion (Figure 1.3B). The APC is a multi-subunit ubiquitin protein ligase that polyubiquitinates mitotic cyclins and the anaphase inhibitor securin (in budding yeast Pds1, in fission yeast Cut2) which are then targeted for destruction by the 26S proteosome (Cohen-Fix et al., 1996); (Funabiki et al., 1996). In budding yeast, securin is the only protein that has to be degraded by the APC to allow sister chromatid segregation (Ciosk et al., 1998; Yamamoto et al., 1996). Cohesin subunits dissociate from chromosomes in dependency of APC activation, yet securin is not part of cohesin and securin mutants do not show premature sister separation. Securin was found to form a stable complex with separase (in budding yeast Esp1 for extra spindle poles, in fission yeast Cut1 for cells untimely torn) (Ciosk et al., 1998; Funabiki et al., 1996). Separase mutants are capable of destroying securin but cohesin fails to dissociate from chromosomes and sister chromatids do not separate. Based on these observations, securin was found to be an inhibitor of separase function in sister separation. Securin degradation by the APC releases this inhibition and separase becomes activated to trigger sister chromatid segregation. Loss of cohesion coincides with cleavage of cohesin's Scc1 subunit into two fragments and its dissociation from chromosomes (Uhlmann et al., 1999). Scc1's cleavage is dependent on separase which turned out to be the actual protease that cleaves Scc1 (Uhlmann et al., 2000). In budding yeast, Scc1 cleavage alone triggers and suffices for chromosome segregation during anaphase. This was shown by replacement of Scc1's cleavage site for separase by that of a foreign protease which also causes cohesin release from chromosomes and segregation of sisters (Uhlmann et al., 2000). Another cleavage target for separase is Rec8, the meiosis specific version of Scc1, consistent with the requirement of separase during both mitotic and meiotic divisions (Buonomo et al., 2000).

An important prerequisite for high-fidelity chromosome segregation is the degradation of Scc1's C-terminal separase cleavage fragment. This fragment contains at its N-terminus an arginine, a destabilising residue in the N-end rule degradation pathway which is specifically recognised by the Ubr1 protein (Rao et al., 2001). Ubr1 is an E3 ubiquitin ligase and acts together with the ubiquitin-conjugating E1 and E2 proteins to link a multi-ubiquitin chain to its substrate for subsequent degradation by the 26S proteasome. If a non-degradable version of the C-terminal Scc1 fragment (created by replacing the destabilising residue with a stabilising residue) is expressed at wild-

type levels in cells, an increased frequency of chromosome loss was observed. A similar degree of chromosome loss was also observed in cells deleted for the *Ubr1* gene. Overexpression of such a stable fragment is toxic and transient overexpression during a metaphase block, but not during arrest in G1 or S-phase, inhibits cell growth. Therefore, degradation of the C-terminal Scc1 separase cleavage fragment by the N-end rule pathway is essential before cells progress into the next cell cycle.

Separase homologues in other organisms have been identified based on sequence conservation in the C-terminal part of the protein which contains the protease domain. This domain is defined by a signature characteristic for endopeptidases of the CD clan, a superfamily including caspases, which contains a catalytic dyad formed by a histidine and cysteine residue (Uhlmann et al., 2000). The N-terminus of separase folds back to its C-terminus, and this intermolecular interaction might be essential to activate the protease (Hornig et al., 2002) (Figure 1.3B). Securin inhibits separase by preventing access of the substrate to the active site of its protease domain. In addition, securin disrupts the interaction of the N- and C-termini of separase, thereby possibly inhibiting its protease activity. Securin does not only have inhibitory function on separase, paradoxically it is also needed for its activation. It promotes nuclear accumulation of separase where it cleaves Scc1, and is required for separase to become fully active in anaphase (Agarwal and Cohen-Fix, 2002; Hornig et al., 2002; Jensen et al., 2001).

Despite securin's importance in regulating separase, several other securin–independent mechanisms of separase regulation have been discovered. For example, human separase is inhibited by high cyclin-Cdk activity in cell extracts lacking securin (Stemmann et al., 2001). This inhibition depends on phosphorylation of a single serine residue in separase that has to be removed in anaphase for its activation. Securin's function to inhibit separase activation is not the only mechanism that controls cleavage of cohesin. Budding yeast securin mutants are viable and show cohesin cleavage occuring with normal kinetics (Alexandru et al., 2001). This could be explained if regulation of cleavage occurs at the level of the substrate Scc1. Indeed, Scc1 is phosphorylated by Polo-like kinase Cdc5 just before anaphase, and it is phosphorylation that is required for efficient cleavage of Scc1 by separase (Alexandru et al., 2001; Hornig and Uhlmann, 2004; Uhlmann et al., 2000) (Figure 1.3B).

Whereas in budding yeast most cohesin dissociates from chromosomes in anaphase upon Scc1 cleavage, in other eukaryotes including vertebrates the bulk of cohesin is

already released from chromosome arms during prophase independently of cohesin cleavage (Losada et al., 2000; Waizenegger et al., 2000) (Figure 1.4). Only a small fraction of cohesin mostly around centromeres is retained and is required for maintenance of cohesion until metaphase. Loss of cohesion during anaphase is likely to be a consequence of destruction of the remaining cohesin by separase cleavage (Hauf et al., 2001; Waizenegger et al., 2000). Cohesin removal in prophase appears to be required for individualisation of chromosome arms and coincides with association of condensin onto chromosomes. Consequently, sister chromatids become compacted along their axes, resulting in the X-like structure of chromosomes in metaphase arrested cells. The mechanism for specific cohesin removal from chromosome arms, known as the prophase pathway, depends on the activity of Polo-like kinase (PLK) and Aurora B kinase (Losada et al., 2002; Sumara et al., 2002). The Scc1 and Scc3 (SA) subunits of cohesin can be phosphorylated by PLK *in vitro*. Phosphorylated cohesin binds less efficiently to sperm chromatin assembled in *Xenopus* extracts than the non-phosphorylated form, suggesting that phosphorylation of cohesin contributes to its dissociation from chromosomes during prophase. The role of Aurora B kinase in this process is not known since it does not appear to phosphorylate cohesin *in vitro*. However, Aurora B activity clearly triggers cohesin dissociation from chromosomes and sister chromatid resolution in mitosis, and works in synergy with PLK to promote these processes (Losada et al., 2002).

1.4 Architecture of cohesin

The structure of the cohesin complex is determined by the distinctive shape of the Smc1 and Smc3 proteins. SMCs are very large proteins of around 1000-1500 amino acids. They mostly consist of an alpha-helical coiled coil segment, about 900 residues or 100 nm in length, which is interrupted in the centre by a globular hinge domain. SMCs´ coiled coils are flanked at their amino- and carboxy termini by globular domains that contain sequences conserved in ATP-Binding Cassette (ABC) ATPases (Figure 1.5A). The N-terminal domain bears a Walker A or P-loop motif, whereas the C-terminal domain contains the Walker B motif and the C-motif, also known as the signature motif.

SMC proteins are dimeric, either forming homodimers as in the prokaryotic SMC proteins, or heterodimers between different SMC proteins in eukaryotes, like cohesin´s

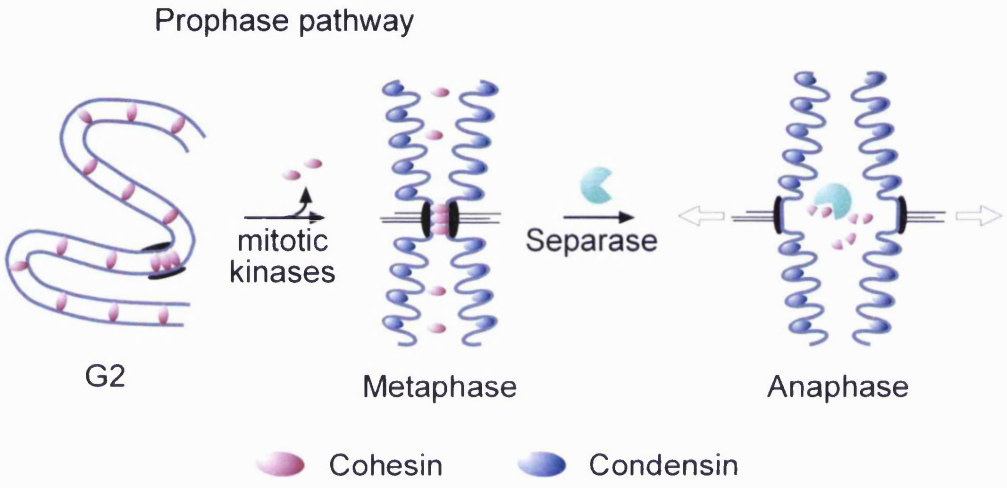

Figure 1.4. Cohesin removal and chromosome condensation in mitosis.

Cohesin locates all along the chromosome to maintain sister chromatid cohesion during G2. In mitosis, the condensin complex binds to and compacts chromosomes. At the same time part of cohesin dissociates from chromosome arms promoted by mitotic kinases (prophase pathway). This Scc1 cleavage-independent removal pathway for cohesin has only been shown for eukaryotes other than budding yeast, whose chromosomes condense to a lower degree. A crucial pool of cohesin must be maintained around centromeres to maintain cohesion in metaphase. At anaphase onset chromosome-bound cohesin is cleaved by separase to trigger sister chromatid segregation.

Smc1/3 heterodimer. Electron microscopy studies of *Escherichia coli* SMC-like MukB protein revealed that the coiled coil domain is antiparallel (Melby et al., 1998). If a fibronection domain is fused to the N-terminus of MukB, it is seen projecting from each end of the V-shaped dimer and not just from one end in the case of parallel coiled coils. SMC proteins could in principle be folded in two ways to represent antiparallel dimers. Either they dimerise along their entire length to form intermolecular coiled coils, or they fold back onto themselves, thereby creating intramolecular coiled coils, and dimerise at their hinge domains (Figure 1.5B). This would result in interaction of the amino- or carboxy terminal domains of either two different SMC proteins or the same protein, respectively. Recently, biochemical studies on budding yeast's cohesin subunits expressed in baculovirus-infected insect cells have addressed this issue of different modes of dimerisation (Haering et al., 2002). Smc3 with its hinge domain being replaced with an Smc1 hinge fails to interact with Smc1 but is able to form a homodimer with another Smc3 protein. If the hinge domain of Smc1 was exchanged for an Smc3 hinge, no heterodimerisation with Smc3 was observed unless Smc3 contained an Smc1 hinge. These data suggest that Smc1/3 dimerisation is solely conferred by their hinge domains, thereby supporting a model of two SMC proteins folding back onto themselves and connected at their hinges. The importance of the hinge domain for dimerisation was also shown by mutational studies of the BsSMC hinge (Hirano et al., 2001). SMC hinge domains contain four glycine residues highly conserved in all SMC proteins [consensus sequence $G(X)_6G(X)_3GG$], with an additional glycine being invariant in bacterial SMC proteins. Glycine residues potentially break α-helices and thereby contribute to structural flexibility of proteins. Exchanging four of the conserved glycines for alanines in the BsSMC hinge leads to monomeric proteins which appear as single-armed structures in electron micrographs (Hirano et al., 2001). Indeed, crystal structure analysis of the *Thermotoga maritima* SMC hinge showed that these glycines are located in the dimerisation interface, and their mutations therefore are expected to disrupt hinge interactions (Haering et al., 2002). These structural studies have also confirmed the intramolecular interaction mode of SMC coiled coils since they show amino- and carboxy terminal helices of the same protein chain forming a coiled coil domain. All N- and C-termini emerge from one side of a doughnut-shaped globular core structure formed by two interacting hinges. Both coiled coils are therefore expected to

originate at a fixed narrow angle from a stable hinge dimer, yet open and closed conformations of the coiled coils are possible due to their intrinsic flexibility.

The antiparallel and intramolecular nature of SMC coiled coils has important implications for the structure of the SMC amino- and carboxy terminal domains. The antiparallel alignment of coiled coils mediates proximity of N- and C-terminal domains to form an SMC head domain, and their intramolecular interactions would ensure that head domains are composed of termini of the same SMC molecule (Figure 1.5B). The crystal structure of the N-terminal domain of MukB showed that the Walker A motif is exposed on the surface and suggested that the N- and C-terminal domains of the SMC proteins have to associate to create a functional ATPase domain (van den Ent et al., 1999). This was further confirmed in a structural study analysing the *T. maritima* SMC N- and C-terminal domains (Löwe et al., 2001). These two domains form one single globular SMC head domain with structural features of an ATPase, supporting the antiparallel interaction mode of SMC coiled coils. Crystal structural analysis of cohesin´s SMC heads have not been performed yet, which for the first time would reveal structural features of an SMC head that is heterodimeric.

Electron microscopy studies of human and *Xenopus* cohesin have provided important insight into the overall shape of the complex (Anderson et al., 2002) (Figure 1.6A). The two SMC arms of the coiled coils have an open conformation with an angle of about 90°, although in a different report a more closed hinge of an angle of approximately 35° was found for budding yeast cohesin´s Smc1/3 (Haering et al., 2002). Strikingly, one arm of the SMCs often shows a sharp bend or kink located approximately one third away from the hinge to the head domain. A bioinformatics study describes disruptions of coiled coil sequences whose positions but not their sequences are conserved within the SMC family, and which could contribute to the formation of the kink (Beasley et al., 2002). However, whether the kink is located within Smc1 or Smc3 is unknown. Its function is also unclear, but it could support arm flexibility *in vivo*.

More importantly, these structural studies showed the location of the non-SMC proteins, Scc1 and Scc3 (SA), as a globular complex in close vicinity of the Smc1 and Smc3 head domains and suggest their association together (Anderson et al., 2002). This was further confirmed by biochemical analyses of variants of budding yeast´s cohesin subunits that were coexpressed in insect cells (Haering et al., 2002). The Scc1 subunit

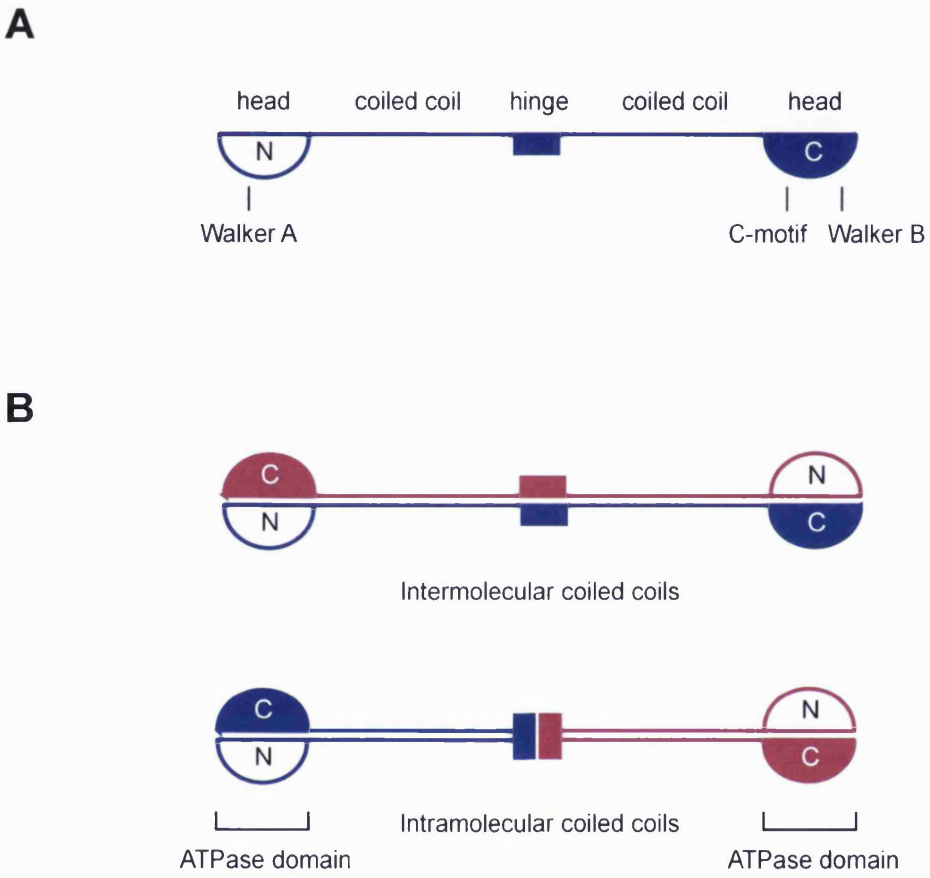

Figure 1.5. Architecture of SMC proteins.

(A) Protein domains within the SMCs. The SMC proteins are composed of five domains. These are the amino- and carboxy terminal heads which are separated by two stretches of alpha-helical coiled coil and the globular hinge domain in the centre of the molecule. The head domains harbour protein motifs characteristic for ATP-Binding Cassette (ABC) ATPases, which are the Walker A motif located within the N-terminal head and the Walker B and C-motifs in the C-terminal head.
(B) Two modes of antiparallel SMC protein folding and heterodimerisation. Upper panel: The two SMC proteins align along their entire length to form intermolecular coiled coils. This allows interactions between all of their domains. Lower panel: Each SMC polypeptide is folded back onto itself by intramolecular interaction between the coiled coils. Dimerisation occurs by association of the hinge domains. This model has proven to be correct. The antiparallel binding mode of the SMCs results in close proximity of the N- and C-terminal heads to form an ATPase domain.

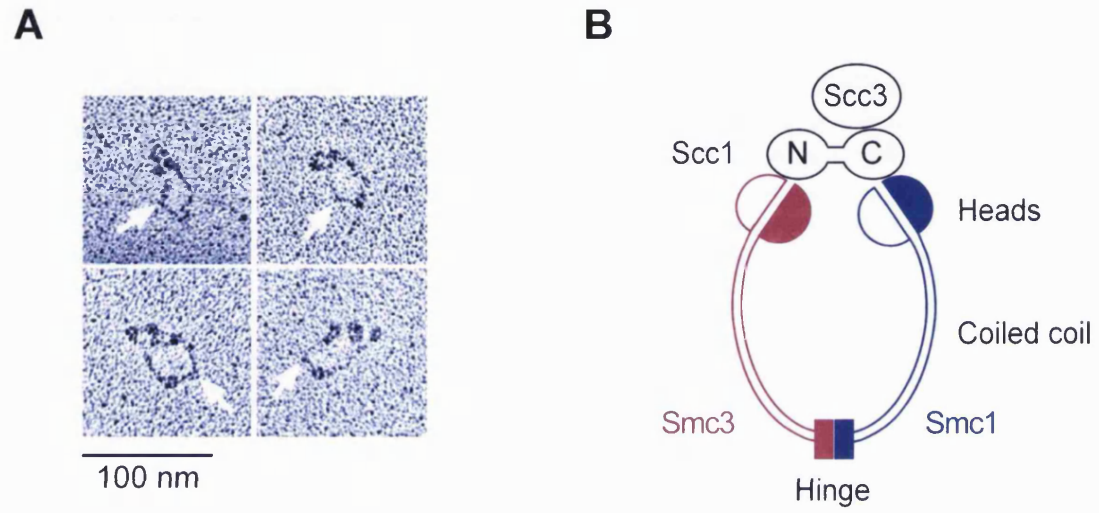

Figure 1.6. The ring structure of cohesin.

(A) Electron micrographs of the human cohesin complex. Cohesin appears as a ring-shaped structure with the two coiled-coil arms of the SMC subunits spread apart from each other in an open conformation. Arrows indicate the position of the kink frequently observed in the coiled-coil of one of the SMCs. The non-SMC proteins form a globular complex which binds to the head domains of the SMC heterodimer. In the first row this complex is found mostly superimposed with the heads. Alternatively, this might be the result of a close association of the heads. In the second row the heads are separated with the non-SMCs located between them (from Anderson et al., 2002).
(B) Architecture of cohesin. Biochemical studies revealed that the four subunits of cohesin, Scc1, Scc3, Smc1 and Smc3, are associated with each other to form a ring structure. This ring is closed on one side by interactions of the SMCs at a dimer interface located within the hinge. On the other side, the SMC heads are thought to be held together by the Scc1 subunit whose N-terminal end interacts with the Smc3 head and the C-terminus with the Smc1. The Scc3 subunit is associated with the Smc1/3 dimer by binding to the C-terminal half of Scc1.

was indeed found to interact with the heads of Smc1 and Smc3, since an SMC dimer lacking both heads did not interact with Scc1 (Figure 1.6B). Experiments on the binding mode between Scc1 and the SMC heads showed that the N-terminus of Scc1 interacts with the Smc3 head whereas its C-terminus binds the Smc1 head domain: The N-terminal Scc1 separase cleavage fragment was capable of binding to an Smc1/3 dimer missing the Smc1 but not the Smc3 head, and the C-terminal fragment interacts with Smc1/3 lacking only Smc3´s but not Smc1´s head. Scc1 is also capable to bring together Smc1 and Smc3 versions that have lost their potential to dimerise via their hinges. These results suggest that Scc1 functions as a bridge between the two SMC heads which are brought together by interacting with Scc1´s N- and C-terminal regions. Similarly, the N-terminal region of Rec8, the meiotic counterpart of Scc1, binds to Smc3´s head, and its C-terminus to Smc1 (Gruber et al., 2003). Scc1 and Rec8 are conserved in their N- and C-terminal globular domains and belong to the kleisin superfamily (Schleiffer et al., 2003). Kleisins are defined by their sequence similarity in these two domains and may also be part of SMC complexes, potentially by interacting with SMC head domains. The other non-SMC protein, Scc3, was found to interact with the Smc1/3 heterodimer via binding to Scc1´s C-terminal half (Figure 1.6B).

Taken together, these structural features based on *in vitro* studies together with electron micrographs of soluble cohesin suggest that cohesin forms a large proteinaceous ring. The ring is closed by association of Smc1 and Smc3 hinge domains at one end, at the other end by their head domains connected by the Scc1 subunit. A recent *in vivo* study presented data that are consistent with the existence of cohesin´s ring structure on chromatin and provided evidence for its importance in sister chromatid cohesion (Gruber et al., 2003).

1.5 Cohesin association with DNA

1.5.1 The cohesin ring model of DNA strand entrapment

In budding yeast, all four subunits of cohesin bind to chromosomes only as part of the holocomplex. Loss of function or absence of a single subunit abolishes chromatin loading of the others, suggesting that the complex has to be fully assembled before it can be loaded onto DNA. In addition, cohesin subunits colocalise on chromosome

spreads, indicating that cohesin might be associated with DNA as a complex (Panizza et al., 2000; Tóth et al., 1999). But how does DNA-bound cohesin mediate linkage between sister chromatids? Several models have been suggested that were aimed to combine cohesin´s ring structure with its function to connect sister strands. One model postulates that each of cohesin´s SMC head domains binds to one sister chromatid in conjunction with the non-SMC subunits (Anderson et al., 2002) (Figure 1.7A). However, this model does not explain how cohesion is suddenly lost in anaphase upon Scc1 cleavage, since cleavage would only result in a weakening but not in an entire loss of cohesion. Another model proposes that cohesion is mediated by a topological entrapment of both sister chromatids within cohesin´s ring (B) (Haering et al., 2002). This ´ring model´ would explain the tight association of cohesin with chromosomes which resists high salt treatment (Ciosk et al., 2000; Sumara et al., 2000). It would also explain the rapid dissociation of cohesin from chromosomes upon cleavage of Scc1 by separase. Cleavage would result in opening of the ring and the entrapped DNA would be released. The diameter of vertebrate cohesin, visualised by electron microscopy after rotary shadowing, is approximately 30 nm (Anderson et al., 2002). A ring with such dimension would be sufficient to accommodate two 10 nm chromatin fibres which represent nucleosomal DNA, but could enclose only one 30 nm chromatin fibre. The linkage of two such fibres would become possible by dimeric versions of the ring model. One variation is the entrapment of each chromatid within different cohesin rings which are connected either topologically or by protein-protein associations, for example via coiled coil interactions (C) (Milutinovich and Koshland, 2003). Alternatively, such cohesin dimers are formed if Scc1 connects the SMC heads of not a single but two different cohesin rings to form a large loop around both chromatids (D).

The ring model of DNA strand entrapment would clearly find support if the existence of cohesin´s ring structure on chromosomes could be demonstrated. Moreover, further evidence would be provided by showing that the integrity of a closed ring is essential for DNA binding. In a biochemical approach aimed to address these issues, the coiled coil domain of Smc3 was modified to contain a recognition sequence for a foreign protease (Gruber et al., 2003). Cleavage of this site resulted in dissociation of cohesin from chromosomes and loss of cohesion, consistent with a model of chromosome entrapment. This study has also shown that *in vitro* cleavage of the Scc1 subunit of chromatin bound cohesin leaves the N- and C-terminal Scc1 cleavage

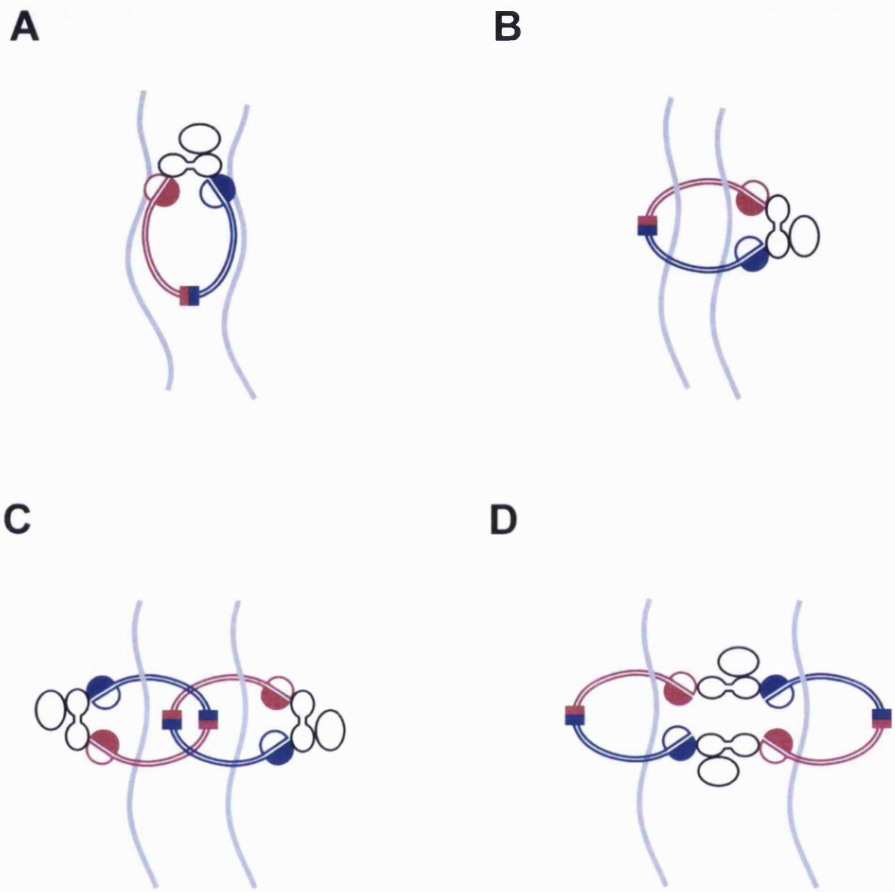

Figure 1.7. Models for cohesin's association with DNA

(A) One model predicts that the SMC proteins interact directly with DNA whereby each of the head domains binds to one sister chromatid.
(B) The cohesin ring model proposes that a single cohesin complex embraces two sister chromatids which thereby become linked together. Cleavage of Scc1 in anaphase opens the ring which allows sisters to be pulled away from each other.
(C - D) A variation of the ring model is the formation of dimeric cohesin rings. Two cohesin rings may be connected with each other either by intercatenation or protein-protein interactions, for example through their coiled coil (C). Alternatively, two rings might dimerise by binding of Scc1 to the Smc1 and Smc3 heads of two different complexes (D).

fragments associated with the complex via their interactions with the Smc3 and Smc1 heads, respectively. The integrity of the Smc3 subunit is required for this association, since it gets destroyed by cleavage of both, the Scc1 and the Smc3 subunits, at the same time. These findings suggest that chromosomal bound cohesin indeed forms a closed ring structure, and any breakage of the ring destroys its closure and therefore its potential for trapping DNA. However, whether chromatids are embraced by the ring and whether their association with DNA is merely topological or includes protein-DNA interactions, remains to be determined.

1.5.2 DNA binding activities of cohesin

Although the ring model provides an attractive way to explain how cohesion between sisters is generated, the actual mode of cohesin interaction with DNA is completely unclear. DNA binding activity of cohesin has been observed *in vitro* but experimental evidence for specific cohesin/DNA interactions are rather limited. Early reports investigated DNA binding of terminal regions of cohesin´s Smc1 and Smc3 proteins. Only C-terminal but not N-terminal domains were found to bind to dsDNA, preferentially with secondary structures such as stem-loops or palindromic sequences (Akhemedov et al., 1998). In addition, DNA interactions with Smc3´s coiled coils were observed (Akhmedov et al., 1999). A recent report describes association of the Smc1/3 hinge with dsDNA which requires dimerisation of the two SMC hinge domains (Chiu et al., 2004). Such hinge-mediated DNA interactions were also observed in *B. subtilis* SMC (Hirano and Hirano, 2002). However, the importance of these results, obtained from individual SMC protein domains, in the context of a model of topological DNA entrapment within cohesin´s ring, remains to be determined.

The purified cohesin holocomplex shows DNA binding activity, in contrast to purified Smc1/3 heterodimers (Kagansky et al., 2003). This is consistent with the interdependence of cohesin subunits for chromosome association. Biochemical activities of cohesin reflecting its *in vivo* function have also been reported. Purified cohesin promotes catenation of nicked circular DNA in the presence of topoisomerase II, an enzyme mediating DNA strand passages (Losada and Hirano, 2001). Furthermore, end-to-end joining of linear DNA molecules in the presence of DNA ligase was

observed. These results are consistent with cohesin's role in mediating intermolecular DNA interactions.

1.6 SMC complexes and their biochemical activities

1.6.1 The SMC protein family

Experimental data of cohesin activities obtained so far cover only a few aspects of the role of the complex in cohesion. In addition, the molecular actions observed *in vitro* do not require the presence of ATP which is predicted to have some function as ATPase motifs are contained in cohesin's SMC subunits (Kagansky et al., 2003; Losada and Hirano, 2001). In contrast, studies of related SMC complexes have provided more insight into biochemical activities of SMCs, in particular into how ATP affects their DNA modulation activities. The SMC (Structural Maintenance of Chromosomes) protein family has first been identified by genetic analysis of budding yeast's Smc1 which was found to be required for minichromosome stability during mitosis (Strunnikov et al., 1993). At about the same time, its homologue in chicken, ScII, the condensin SMCs Cut3 and Cut14, and *Xenopus* SMCs were described (Hirano and Mitchison, 1994; Saitoh et al., 1994; Saka et al., 1994). Since then, members of the SMC protein family have been discovered in organisms ranging from bacteria to human, and are implicated in various aspects of chromosome dynamics. In most eubacterial and archeal genomes, a single gene encodes for SMC suggesting prokaryotic SMCs form homodimers. This was confirmed in structural and hydrodynamic studies of the *Bacillis subtilis* SMC and of the SMC-like MukB protein in *Escherichia coli* (Hirano and Hirano, 1998; Melby et al., 1998). In contrast, all eukaryotic SMCs are heterodimers and are classified in three groups, cohesin's Smc1/3, condensin's Smc2/4 and the Smc5/6 DNA repair complex. Similar to cohesin, all of these SMC dimers interact with non-SMC subunits to form a functional holocomplex. An overview of all known members of SMC complexes is presented in Table 1.2.

			S. cerevisiae	*S. pombe*	*C. elegans*	*D. melanogaster*	*X. laevis*	*H. sapiens*
Condensin	SMCs		Smc4	Cut3	SMC-4	DmSMC4 (Gluon)	XCAP-C	hCAP-C
			Smc2	Cut14	MIX-1	DmSMC2	XCAP-E	hCAP-E
	Non-SMCs	**Kleisin**	Brn1	Cnd2		Barren	XCAP-H[a] XCAP-H2[b]	hCAP-H[a] hCAP-H2[b]
			Ycg1 (Ycs5)	Cnd3			XCAP-G[a] XCAP-G2[b]	hCAP-G[a] hCAP-G2[b]
			Ycs4	Cnd1			XCAP-D2[a] XCAP-D3[b]	hCAP-D2[a] hCAP-D3[b]
Smc5/6 complex	SMCs		Smc5	Spr18		DmSMC5		hSMC5
			Rhc18	Rad18				hSMC6
	Non-SMCs		Nse1	Nse1				
				Nse2				

Table 1.2. Subunit composition of eukaryotic SMC complexes from different species. Proteins marked with ([a]) are members of the condensin I complex, and ([b]) members of condensin II.

1.6.2 Bacterial SMC complexes

Bacterial SMC proteins have been implicated in regulating chromosome organisation and compaction and are required for chromosome partitioning. For example, SMC null mutants in *B. subtilis* show a variety of phenotypes including abnormal nucleoid morphology and accumulation of anucleate cells (Britton et al., 1998; Moriya et al., 1998). These phenotypes are indistinguishable from those observed in mutants of *E. coli's* MukB indicating that both proteins have analogous functions (Niki et al., 1991). Although MukB has only very limited sequence homology to SMC proteins, it shows a similar two-armed structure in electron micrographs (Melby et al., 1998). The MukB dimer forms a complex with two other proteins, MukE and MukF,

encoded in the same operon (Yamazoe et al., 1999). Likewise, *B. subtilis* SMC interacts at its catalytic head domains with ScpA, a kleisin family member, and ScpB (Mascarenhas et al., 2002; Soppa et al., 2002; Volkov et al., 2003). Mutants in these non-SMC proteins display similar phenotypes to that of the corresponding SMCs suggesting that they work in concert *in vivo*.

Bacteria lack a mitotic apparatus equivalent to that of eukaryotes, and duplication of the circular chromosome, condensation and separation occurs simultaneously in the cell. The mechanism how bacteria compact their DNA is not clear but given their mutant phenotypes, bacterial SMCs are a major contributor in this process. One way of compacting chromosomes might be via supercoiling of chromosomal DNA. Bacterial proteins involved in supercoiling include DNA gyrase which introduces negative supercoils, and topoisomerase I that relaxes them. Interestingly, the MukB and BsSMC phenotypes can be suppressed by mutations in topoisomerase I, and mukB mutants are hypersensitive to inhibitors of DNA gyrase (Onogi et al., 2000; Sawitzke and Austin, 2000; Weitao et al., 1999). In addition, BsSMC was found to affect supercoiling of plasmid DNA *in vivo* (Lindow et al., 2002). These data support a crucial role for bacterial SMCs in regulating DNA topology and thereby organising higher-order chromosome structures.

In vitro studies in BsSMC have for the first time revealed biochemical activities of an individual SMC protein (Hirano and Hirano, 1998). Purified BsSMC preferentially binds to single-stranded DNA (ssDNA) but shows also low-affinity binding to double-stranded DNA (dsDNA). In addition, BsSMC exhibits two forms of ATPase activities, a basal activity in the absence of DNA and an ATPase activity greatly stimulated by DNA. Although DNA binding activity is ATP-independent, BsSMC can form higher order DNA aggregates in the presence of ATP (Hirano and Hirano, 1998). It is unclear whether the energy-dependent aggregation of DNA is relevant to BsSMC function *in vivo* but it could represent a primitive type of chromosome condensation.

1.6.3 The Condensin Smc2/4 complex

Condensin is required for chromosome reorganisation, compaction and segregation during mitosis. In addition, condensin plays an important function in global gene regulation and dosage compensation. Members of the condensin complex were initially

identified biochemically by their purification from mitotic chromosomes assembled in *Xenopus* cell-free extracts (Hirano et al., 1997; Hirano and Mitchison, 1994). The condensin complex consists of five subunits, the two SMC subunits (Smc2/CAP-E and Smc4/CAP-C) and the three non-SMC subunits (CAP-D2, CAP-G and the kleisin CAP-H). Similar to cohesin, the SMCs of condensin form a large ring structure with the non-SMCs bound to their catalytic head domains (Anderson et al., 2002). Condensin is required for both establishment and maintenance of chromosome condensation. If compact sperm chromatin is incubated with mitotic egg extracts immunodepleted of the condensin holocomplex, it is progressively converted into a diffuse mass. Adding back purified condensin rescued the condensation defect (Hirano et al., 1997; Hirano and Mitchison, 1994). Recently, a second class of condensin has been reported in vertebrates, termed condensin II, which shares the SMC subunits of the canonical complex (condensin I), but contain a different set of non-SMCs (CAP-D3, CAP-G2 and CAP-H2) (Ono et al., 2003). Both condensin complexes localise differently on mitotic chromosomes and make distinct contributions to chromosome architecture. Immunodepletion of condensin I in *Xenopus* extracts results in a more severe defect in chromosome compaction compared to depletion of condensin II, indicating condensin I having a predominant role in the overall chromosome assembly.

The *S. pombe* cut3 (Smc4) and cut14 (Smc2) subunits of the condensin complex were discovered in screens designed to isolate mutants in chromosome segregation (Saka et al., 1994). Mutants in these subunits cause a 'cut' (cells untimely torn) phenotype when unsegregated DNA masses are cut through by the division septum at the cell centre. FISH (fluorescent *in situ* hybridisation) analysis of these mutants showed decreased chromosome compaction along chromosome arms but normal centromere separation, indicating that the 'cut' phenotype is the consequence of a condensation rather than a cohesion defect. The non-SMC subunits of *S. pombe's* condensin complex Cnd1-3 were later purified as interaction partners of cut3/cut14 (Sutani et al., 1999). Similarly, mutants of condensin subunits in *S. cerevisiae* show chromosome condensation and transmission defects, in particular impaired segregation of the heterochromatic rDNA region where condensin is found concentrated during mitosis (Freeman et al., 2000; Strunnikov et al., 1995).

Besides its crucial role during mitosis, condensin has several non-mitotic functions. One example is its requirement for mediating dosage compensation during sex

determination in *C. elegans*. The Smc2 orthologue MIX-1 and the Smc4 orthologue DPY-27 are part of a dosage compensation complex that promotes hermaphrodite development of XX animals by repressing a gene implicated in male development (Chuang et al., 1994; Lieb et al., 1998). In addition, it is specifically recruited to both X chromosomes in hermaphrodites and represses gene transcription by twofold, thereby equalising X-linked gene expression between XX hermaphrodites and XO males. The MIX-1 subunit is also part of a different complex containing another Smc4 homologue, termed SMC-4 (Hagstrom et al., 2002). This complex appears to be the functional *C. elegans* homologue of the condensin complex since it is required for mitotic chromosome structure and segregation.

Similarly, a role in regulation of gene expression has also been found for *Drosophila* condensin. The 'barren' subunit, a CAP-H orthologue, colocalises with Polycomb group proteins (PcG) to Polycomb response elements (PRE) (Lupo et al., 2001). PcG proteins act on PREs to transcriptionally repress chromosomal domains by inducing heterochromatin formation. A barren mutation relieved gene silencing mediated by one of the PREs, Fab-7, and resulted in misregulation of body-segment identity (Lupo et al., 2001). Therefore, condensin and PcG act together to maintain transcriptional repression possibly through heterochromatin assembly.

Although it is unclear how condensin interacts with chromatin and triggers its condensation, the condensin complex shows *in vitro* activities that might contribute to mitotic chromosome compaction. Condensin purified from *Xenopus* extracts binds to DNA independently of ATP (Kimura and Hirano, 1997). The presence of DNA stimulates condensin's ATPase activity, and superhelical tension is introduced into DNA in an ATP hydrolysis-dependent manner, as shown in two assays. In the first one, mitotic condensin mediated positive supercoiling of relaxed circular DNA in the presence of topoisomerase I which removes compensatory negative supercoils (Kimura and Hirano, 1997). In a second assay, condensin promoted knotting of nicked circular DNA in the presence of topoisomerase II, an enzyme which allows DNA strand passages by making and resealing dsDNA breaks (Kimura et al., 1999). In this assay, the predominant products were positive three-noded knots created by a single strand passage between two positive supercoils. The formation of such knots is only possible if condensin were to generate large positive writhes in the DNA that are constrained in the same relative orientation. This suggests that condensin is not only capable of producing

positive supercoils but also potentially of organising them into global loop structures, which could represent a mitosis-specific form of chromatin assembly. However, electron spectroscopic imaging failed to display such loop formation (Bazett-Jones et al., 2002). Instead, a local ATP hydrolysis-dependent conversion of a short stretch of DNA into two supercoils wrapped around a single condensin complex was observed. Compensatory supercoils in the DNA regions not bound by condensin can be visualised. However, they are unlikely to contribute to condensation *in vivo* as they can be easily removed by topoisomerases. It is also unlikely that simple wrapping of DNA would account for efficient chromosome condensation since its effect on compaction is very small. Therefore, it remains still to be shown whether the biochemical activities of condensin observed *in vitro* have physiological significance and whether they contribute to the mechanism underlying chromosome condensation.

1.6.4 The Smc5/6 complex

The Smc5/6 complex has essential functions in DNA repair, and was initially discovered by analysis of the Rad18 protein, the Smc6 homologue in *S. pombe* (Lehmann et al., 1995). The rad18-X mutant is sensitive to both UV and ionising irradiation with an inability to repair dsDNA breaks. Epistasis analysis showed that Rad18 takes part in a repair pathway which is different from the classical nucleotide excision repair pathway, and which likely uses recombination for the elimination of UV-induced lesions (Lehmann et al., 1995). Analysis of the rad18-74 allele revealed that Rad18 is required to maintain checkpoint arrest in G2 following DNA damage but not for its initiation, resulting in aberrant and lethal mitoses of mutant cells after re-entering the cell cycle (Verkade et al., 1999). Rad18 also genetically interacts with Brc1, a protein whose BRCT domains show homology to the breast and ovarian cancer susceptibility gene BRCA1, a G2 checkpoint protein (Verkade et al., 1999). In addition, Rad18 was found to interact physically and genetically with the DNA repair protein Rad60 but their functional relationship is unknown (Boddy et al., 2003; Morishita et al., 2002). Apart from their roles in response to extrinsic DNA damage, Rad18 and its homologue in *S. cerevisiae*, Rhc18, have also essential functions during normal mitotic growth.

The dimerisation partner of Rad18/Smc6 was identified as the Spr18/Smc5 protein, and both proteins are found in a high molecular weight complex (Fousteri and Lehmann, 2000). Recently, two other subunits of the Smc5/6 complex have been reported, the conserved non-SMCs Nse1 and Nse2 (Fujioka et al., 2002; McDonald et al., 2003). Both proteins are essential and mutants show similar phenotypes as those observed upon inactivation of Smc5 and Smc6. The precise role of the Smc5/6 complex in DNA repair is not yet known. A Rad18 mutation is synthetic lethal with topoisomerase II mutants, and could therefore be involved in chromatin organisation for establishing or maintaining chromosomal structures necessary for DNA repair (Verkade et al., 1999). The biochemical activities of the complex are also unknown. Although the Rad18/Spr18 complex has ATPase activity greatly stimulated by dsDNA (Fousteri and Lehmann, 2000), a potential role in modulating DNA remains yet to be analysed. Mutants in ATPase motifs of Rad18 do not rescue DNA repair deficiency of the rad18-X allele (Fousteri and Lehmann, 2000). In addition, overexpression of a Rad18 mutant in the Walker A motif (K129E) exerts a dominant negative effect on viability of wild-type cells, probably due to sequestering of endogenous Spr18. Mutants in Rad18 ATPase motifs also fail to rescue the viability of a Rad18 deletion strain with the exception of a particular mutation in the conserved C-motif, S1045A. Since this mutant is nonetheless deficient in DNA repair, it separates the role of Rad18 in DNA repair from its essential functions. These mutant analyses strongly support a crucial role for the Smc5/6 ATPase activity *in vivo*, but the mechanism of how it mediates DNA repair remains to be investigated.

1.7 Role of ATP in architecture of SMC proteins and ABC ATPases

1.7.1 SMC heads are ABC ATPases

Biochemical activities of SMCs found *in vitro* and phenotypes observed by expression of ATPase motif mutant SMC versions *in vivo,* clearly suggest that SMCs are functional ATPases. To get insight into potential mechanisms of SMC action driven by ATP, it is required to identify the type of ATPase that is represented by the SMCs. As mentioned above, all SMC proteins contain sequences highly conserved in ATPases which are the Walker A and B motifs (Walker et al., 1982), and the C-motif (Figure

1.5A). The glycine rich Walker A motif (GXXXXGKS/T) or P-loop lies within the N-terminal domain. Residues of this motif interact with the phosphate groups and the magnesium of bound Mg-ATP (Saraste et al., 1990; Smith and Rayment, 1996). The Walker B motif or DA box (hhhhD, h corresponds to hydrophobic residues) is located within the C-terminal SMC domain. Its conserved aspartate residue coordinates the hydrated Mg^{2+} ion which is in turn coordinated by the phosphates of ATP. The key role of the Walker A and B motif is therefore the formation of a binding pocket for ATP within the catalytic core of the protein. Immediately upstream of the Walker B motif resides the C-motif, also known as the signature motif (LSGG) (Bianchet et al., 1997). The C-motif is diagnostic of ATP-Binding Cassette (ABC) ATPases which if mutated, abolishs ATP hydrolysis and impairs their function. Since the C-motif is present in all SMC proteins (with the only exception of Spr18 that contains QSGG), their head domains potentially constitute an ABC ATPase. This was indeed shown by crystal structure analysis of a fusion protein composed of the N- and C-terminal domains of *T. maritima* SMC which were linked together by a short peptide segment (Löwe et al., 2001) (Figure 1.8A). The structure contains three β-sheets, each of the N- and C-terminal domains contributes one of them but the central β-sheet contains elements of both, two strands from the N-terminal and four strands from the C-terminal domain. Therefore both domains come together to form a single globular domain, the SMC head. If the structure is superimposed with catalytic domains of known members of the ABC ATPase family, like the histidine permease protein HisP from *Salmonella typhimurium* or the dsDNA repair protein Rad50 from *Pyrococcus furiosus*, a strong similarity of their folds is observed (Löwe et al., 2001). All motifs and loops involved in ATP binding and hydrolysis are found aligned within the three-dimensional protein structure, which emphasises the close relationship between SMCs and ABC ATPases.

1.7.2 Dimer organisation of ABC ATPases

The ABC ATPase family is a large group of transmembrane proteins involved in ATP-dependent transport of a variety of substrates across cellular membranes. This family includes bacterial transporters that export complex molecules like lipids, polysaccharides or proteins, or import small nutrients such as amino acids, peptides, or sugar molecules (reviewed in Holland and Blight, 1999). Prominent family members in

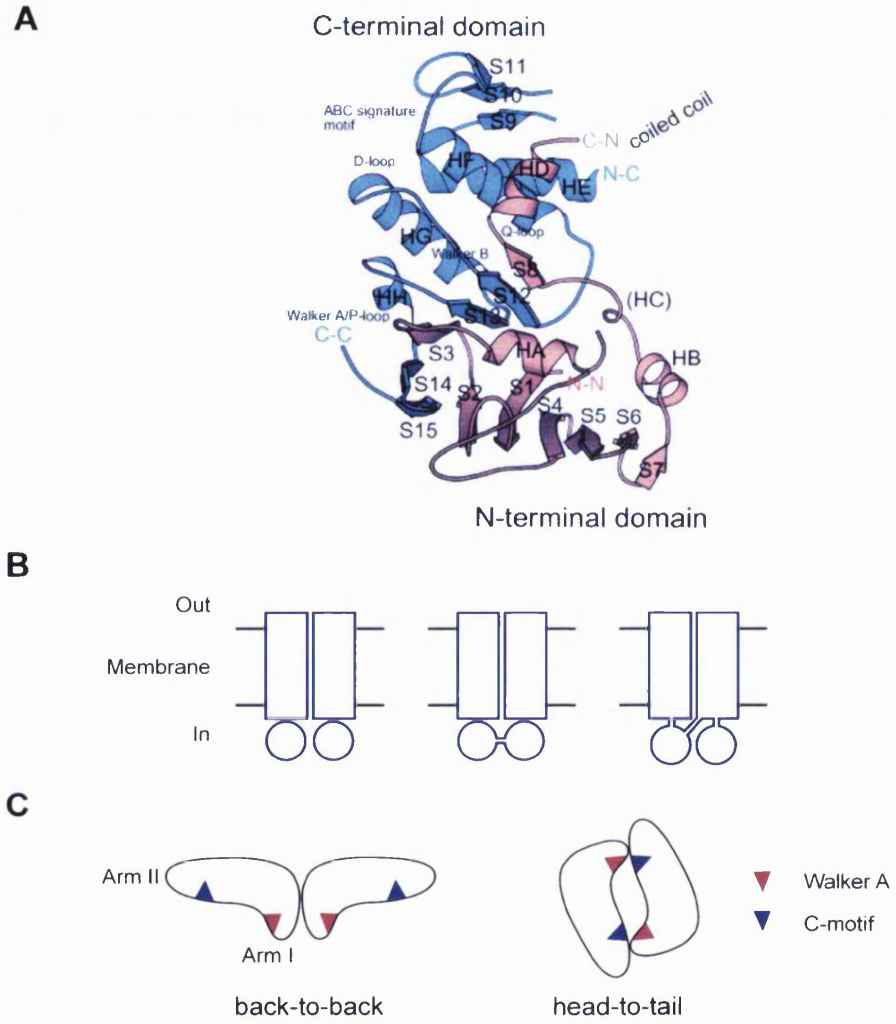

Figure 1.8. Architecture of ABC ATPases.

(A) Crystal structure of the N- and C-terminal domains of *Thermotoga maritima* SMC. These domains were expressed and crystallised as a fusion protein linked together with a short peptide segment which replaced the coiled coil and hinge. The fold is closely related to the ABC ATPase family of proteins. The ATPase domain is formed by association of the N-terminal (red) and C-terminal domains (blue). Both domains contribute to the central β-sheet, the N-terminal domain contributes strands S3 and S8 and the C-terminal domain contributes strands S12-S15 (from Löwe et al., 2001).
(B) Schematic structure of ABC transporters. Left panel: In prokaryotes, most transporters consist of two transmembrane subunits (rectangles) and two cytoplasmic ATPase domains (circles). The two ATPase domains can often be found fused into a single protein (middle panel). Right panel: In most fungal and animal transporters, all of the domains are fused into a single polypeptide.
(C) Proposed arrangement of ATPase dimers. Left panel: The first structure of an ATPase dimer (HisP) was proposed as a two-armed ´back-to-back´ conformation with the Walker A and C-motif of different catalytic domains in distance from each other. Right panel: In the ´head-to-tail´ conformation, first revealed in Rad50, the Walker A and C-motif of different domains are in close proximity to each other.

eukaryotes are the cystic fibrosis transmembrane conductance regulator (CFTR) or multidrug resistance proteins such as the P-glycoprotein that pumps out many anticancer agents. ABC transporters are composed of four different domains or subunits, the two transmembrane domains determining substrate specificity and the two catalytic ATPase subunits peripherally associated at their cytoplasmic side (Figure 1.8B). These two domains are mostly expressed as single subunits in prokaryotes but can also be found fused together, however, in fungal and animal transporters all four domains are largely fused into a single polypeptide. The ATPase motifs at the N-and C-termini of the catalytic domains are arranged in the same way as in SMC proteins but in contrast are not separated by long coiled coils. The active transport across membranes requires ATP hydrolysis, but how both events are coupled is unclear (reviewed in Davidson, 2002). Up to the time when the first crystal structures of ABC ATPases were solved, it was also not clear why two ATPase subunits are present in one ABC transporter. However, both domains are required because ATPase activity and transport is abolished if the function of one domain is inactivated (Al-Shawi and Senior, 1993; Azzaria et al., 1989; Davidson and Sharma, 1997; Loo and Clarke, 1996). In addition, ATP hydrolysis shows positive cooperativity suggesting that the two ATP binding sites are in close proximity (Davidson et al., 1996; Loo and Clarke, 1997). A series of crystal structures of dimerised ATPase subunits have been solved, the first one of the bacterial histidine permease HisP (Hung et al., 1998). In the ATP-free structure of the HisP dimer, each monomer forms an L-shaped molecule with two arms. Arm I contains the Walker A and B ATP binding motifs, whereas arm II contains the C-motif. The monomers are oriented to each other in a ´back-to-back´ conformation with the dimer interface formed by components of arm I of both monomers and the C-motifs facing outwards (Figure 1.8C, left). An interaction of the C-motifs with ATP would be necessary to explain why most mutations in the C-motif abolish ATP hydrolysis, but in this structure the C-motifs are too far apart to interact with ATP bound to arm I. However, this could be explained by an alternative configuration in which the C-motif of one monomer faces the Walker motifs of the other (´head-to-tail´), thereby becoming involved in catalysis of the ATP buried in the interface between them (Jones and George, 1999) (Figure 1.8C, right). Such a structure would also be consistent with the arrangement of ATPase domains in some bacterial and fungal ABC transporters that have both catalytic domains fused together as part of a single polypeptide. Here, the N-

terminal ATPase domain contains non-functional Walker A and B motifs but a canonical C-motif, whereas in the C-terminal domain the Walker A and B motifs are canonical but the sequence of the C-motif is altered, thereby creating at least one functional ATPase domain.

The question of how ATPase motifs are oriented to each other was also addressed biochemically in the MalK catalytic subunit of the bacterial maltose transporter (Fetsch and Davidson, 2002). The experiments are based on the ability of vanadate to stabilise the ATPase transition state immediately after ATP hydrolysis, by binding to one of the two nucleotide binding sites at positions adjacent to ADP. Subsequent UV irradiation induces a specific cleavage of the polypeptide backbone nearby the vanadate ion. The photocleavage pattern of MalK showed that either the Walker A motif or the C-motif is cleaved in a given monomer, indicating that both motifs are in close proximity during ATP hydrolysis. This result further supports a model in which Walker motifs of one monomer are positioned opposite the C-motif of the other and cooperate in ATP hydrolysis.

1.7.3 ATP-induced dimerisation of an SMC related ABC ATPase, the Rad50 protein

The final proof for the opposite arrangement of Walker and C-motifs was provided by crystal structure analysis of ATP-bound *P. furiosus* Rad50 head domains, an ABC ATPase. Rad50 homologues are found from bacteria to man and play an important role in genomic stability and repair of double-strand breaks during homologous recombination or non-homologous end-joining (reviewed in D'Amours and Jackson, 2002). The Rad50 complex contains a heterotetramer composed of the Rad50 protein and the Mre11 nuclease, both forming homodimers in the complex (Figure 1.9A). In contrast to ABC transporters, the catalytic domains of Rad50 are not associated with membrane-spanning domains. The Rad50 dimer rather has an overall structure similar to SMC proteins with which it also shares some sequence similarity. The Rad50 heads reconstitute ABC ATPase domains with the Walker A motif at the N-terminus and Walker B and C-motifs at the C-terminus of each monomer. These terminal regions are separated by intramolecular and antiparallel long coiled coils, however, unlike in SMCs

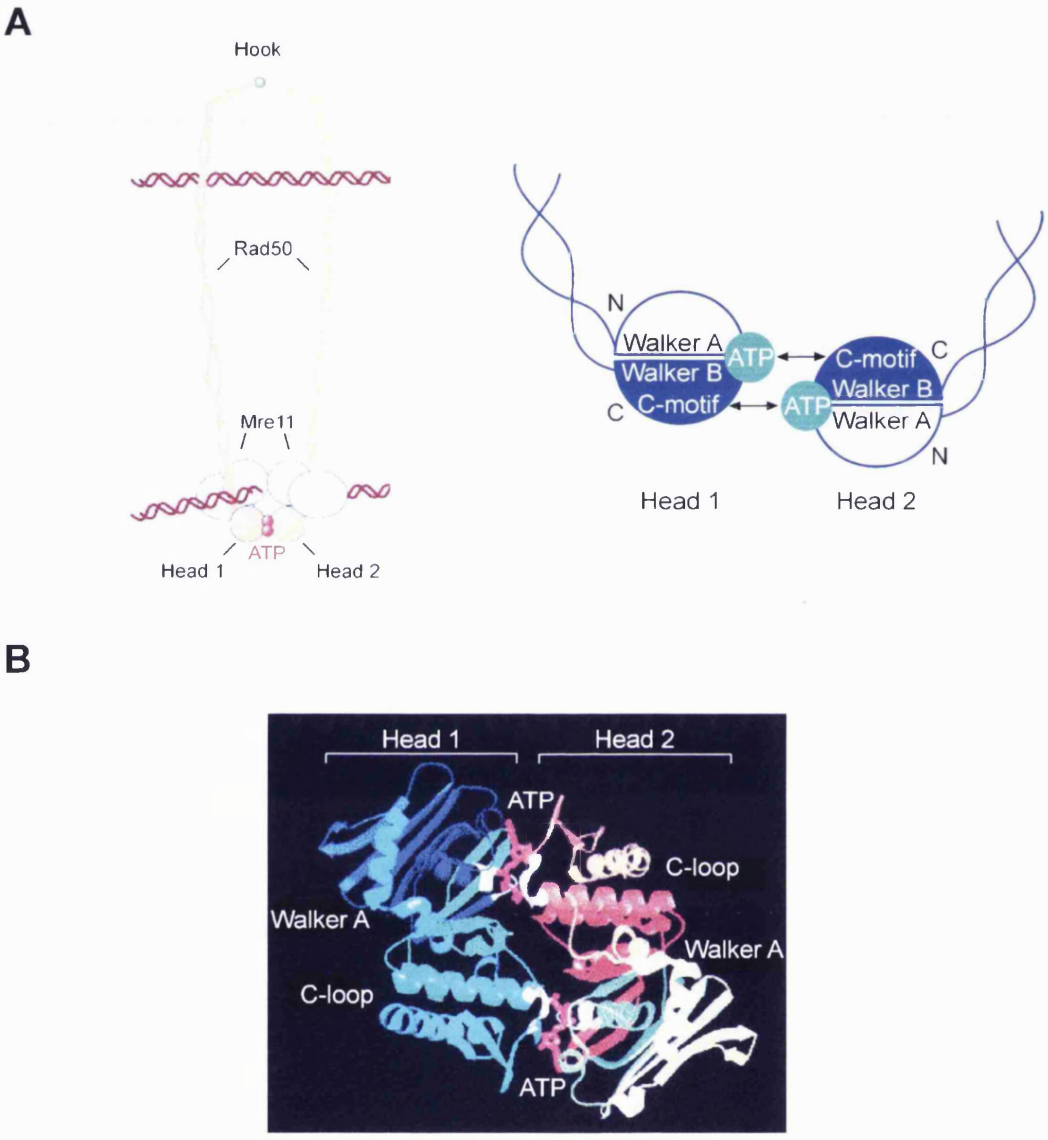

Figure 1.9. The ATP-dependent dimerisation of Rad50 head domains.

(A) Left panel: Architecture of the Rad50 complex. The Rad50 complex is a heterotetramer composed of the Rad50 and the Mre11 homodimers. The overall structure of Rad50 is similar to SMC proteins but dimerisation occurs at zinc-bound hook regions instead of interaction at the hinges. Two Rad50 head domains and the Mre11 homodimer assemble to form a head complex which may associate with DNA. Mre11 binds to a stretch of coiled coil adjacent to the heads. Two heads interact with each other and dimerise in an ATP-dependent manner (from Hopfner and Tainer, 2003). Right panel: In Rad50 and other ABC ATPases, ATP binds to the Walker A and B motifs of each head and interacts with the C-motif of the respective opposite head via its γ-phosphate. Head-to-head interaction occurs by sandwiching two molecules of ATP within the dimer interface.
(B) Crystal structure of the Rad50 head dimer bound to ATP (from Schmitt and Tampé, 2002).

they are not disrupted by a central hinge domain. Instead, in the centre of the Rad50 molecule a non-helical hook-shaped region is located that contains a conserved Cys-X-X-Cys motif (Hopfner et al., 2002). The motifs of two Rad50 molecules dimerise and form interlocking hooks with a zinc atom bound within their interface. At the opposite side of the hook region, each of the two Mre11 subunits probably binds to a stretch of Rad50 coiled coil adjacent to the head domain, thereby becoming part of a tetrameric head complex (Hopfner et al., 2001). In electron micrographs this complex was observed to associate with DNA which consequently becomes accessible for the exo- and endonucleolytic activities by Mre11 (de Jager et al., 2001; Hopfner et al., 2001). Since the coiled coils appear to be highly flexible, association of two Rad50 complexes, each providing one DNA-bound head complex, potentially could bring together two broken DNA ends for repair by non-homologous end-joining, or bridge two sister chromatids to stabilise DNA intermediates during repair by homologous recombination.

Self-dimerisation of Mre11 may promote the pre-assembly of the tetrameric head complex. However, biochemical analysis revealed that the remaining two catalytic Rad50 head domains can only dimerise in the presence of ATP or the non-hydrolysable ATP analogue AMP-PNP. The ATP-dependent dimer formation was confirmed in the crystal structure of the Rad50 head domain that was solved in the ATP-free and ATP-bound form (Hopfner et al., 2000). A comparison of both structures revealed an ATP induced conformational change in each head domain whereby ATPase motifs become correctly positioned for ATP to promote dimerisation. The two head domains associate in a 'head-to-tail' orientation in the presence of ATP or AMP-PNP, the Walker motifs of each head mutually bind to the C-motif of the opposing head (Figure 1.9A right panel, and B). In this conformation, two ATP molecules become buried in the dimer interface. Within a given head, each ATP is bound with the β-phosphate to the Walker A motif and by association with hydrated Mg^{2+} to the Walker B motif, whereas the γ-phosphate interacts with the serine and one glycine residue of the 'LSGG' C-motif of the opposite head. Therefore, the role of the C-motif appears to be a sensor for a γ-phosphate of an ATP that is associated with an opposing molecule, and by binding consequently triggers head dimerisation. Interestingly, upon dimerisation a positively charged groove is formed at the dimer interface that has dimensions suitable for DNA binding. A dependency of ATP-induced head dimerisation for protein-DNA binding would be consistent with the observed ATP-stimulated dsDNA binding activity of the

Rad50 catalytic domain. However, such a mechanism remains to be tested. The ATP-induced head-head interaction also implies that breakage of the P_β-O-P_γ bond during ATP hydrolysis is likely to induce their disengagement, and subsequently upon ADP/ATP exchange the ATP-binding and hydrolysis cycle is restarted (Figure 1.10).

Recently, ATP-stimulated dimer formation has also been shown in crystal structures of two ABC-transporters, the *E. coli* MalK ATPase subunit and the putative ABC domain MJ0796 from *Methanococcus janaschii* (Chen et al., 2003; Smith et al., 2002). In the latter protein, dimerisation was only possible upon substitution of a particular residue (E171Q, 'transition state mutation') next to the Walker B motif which abolished ATP hydrolysis and increased affinity between isolated subunits in the presence of ATP. These structural studies provide growing evidence that the ATPase cycle of domain engagement/disengagement is a common mechanism in most ABC ATPases and by similarity to Rad50, could be the basis for chromosomal functions of SMCs. Preliminary insight into the ATPase regulation of SMC proteins and its role in DNA modulation was provided by mutational studies in *B. subtilis* SMC (BsSMC) (Hirano et al., 2001). Point mutations were introduced in BsSMC's Walker A (K37I) and Walker B (D1117A) motifs, both of which abolished ATPase acitivity due to a failure in ATP binding. A mutant in the C-motif (S1090) was capable of ATP binding but nevertheless was defective in ATP hydrolysis. This is consistent with the role of the C-motif in mediating head-to-head interaction, a requirement for subsequent ATP-hydrolysis. All three ATPase motif mutants have a dominant-negative effect on the DNA-stimulated ATPase activity of wild-type protein. Therefore, the DNA-bound BsSMC ATPase resembles other ABC ATPases which are known to abolish ATP hydrolysis if one of their two catalytic domains is not functional. In contrast to Rad50, ATP is not required for the basal DNA binding activity of BsSMC. However, ATP-induced dimerisation of BsSMC heads seems to be important for DNA association since the introduction of a 'transition state mutation', which upon ATP binding captures the dimerised form, is necessary to support stable binding to dsDNA, but not a C-motif mutation or even wild-type protein (Hirano T., unpublished results). The ATP-dependent interaction of two SMC heads has remained unproven, therefore biochemical and crystal structure studies will be necessary to confirm the implicated functions of the amino acid substitutions in the above analyses. Nevertheless, due to the high conservation of ATPase motifs shared

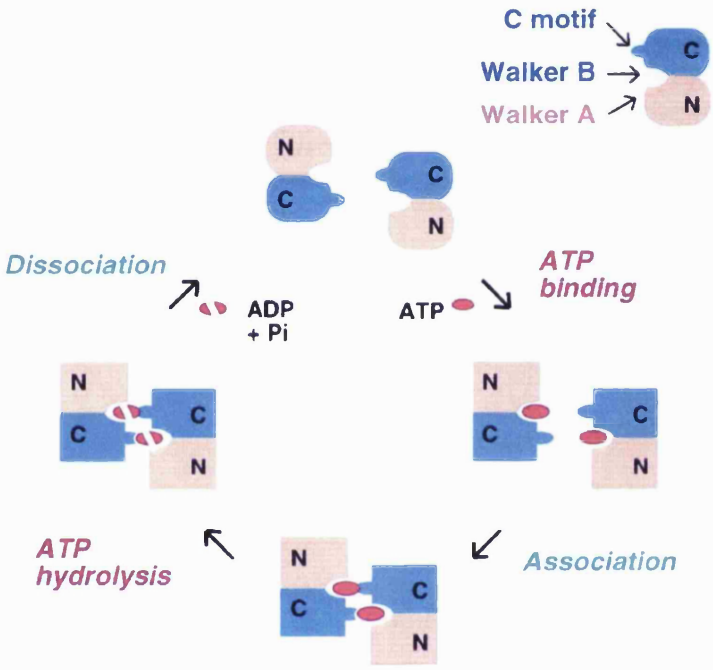

Figure 1.10. Hypothetical ATP-binding and hydrolysis cycle of ABC ATPases.

ATP binding to the Walker A and B motifs within the catalytic domain of an ABC ATPase may cause its engagement by contacting the C-motif of another domain. Engagement triggers ATP hydrolysis resulting in disengagement of both domains. This subsequently promotes a new cycle of ATP binding and hydrolysis (from Hirano, 2002).

between Rad50, ABC transporters and SMC proteins it is reasonable to assume that similar alterations in these motifs affect similar ATP-dependent mechanisms.

1.8 Open questions addressed in this thesis and summary of results

Since the discovery of the cohesin complex, genetic and biochemical approaches have identified proteins that are required for loading of cohesin onto chromosomes, for establishment and for resolution of sister chromatid cohesion. However, despite the progress being made in isolation of factors involved in cohesion, the biochemical mechanism how the four stoichiometric subunits of cohesin are initially assembled and the complex loaded onto specific loci on chromosomes, the cohesin association sites, has remained obscure. Cohesin has mostly been characterised in studies performed with protein isolated from soluble fractions (Losada et al., 1998; Sumara et al., 2000; Tóth et al., 1999). These analyses did not lead to identification of any additional cohesin-associated proteins that might confer loading of the complex onto specific chromosomal regions. It is possible that cohesin bound to chromosomes differs from soluble cohesin and may be associated with such additional factors. Other factors may include proteins that assist the complex to establish cohesion between sister chromatids. Therefore, an important approach to get insight into cohesin function is the isolation and biochemical characterisation of the chromosomal cohesin complex. For this, a purification strategy was established to isolate cohesin released from budding yeast chromatin. The analysis of subunit composition of purified complexes, included in chapter 2, revealed that cohesin bound to chromosomes is biochemically similar to previously characterised cohesin from soluble fractions.

In addition to subunit composition, the binding mode of cohesin to chromatin has also remained elusive. Preliminary structural studies of cohesin assembled onto DNA or chromatin *in vitro* have not been conclusive (Sakai et al., 2003). A more physiological approach to address how cohesin is bound to DNA is the isolation of cohesin/DNA complexes directly from chromatin for subsequent structural analysis. Chapter 2 includes an electron microscopy study of such cohesin/DNA complexes purified *ex vivo* which revealed that cohesin associates with chromatin in clusters. This was further supported by data obtained by quantitative Western analysis.

A major breakthrough for a potential mechanism of cohesin binding to DNA and cohesion establishment came from combined structural and biochemical studies that revealed that cohesin has the shape of a large proteinaceous ring. This ring structure has prompted the hypothesis that cohesin binds to DNA by topological embrace. Although yet unproven, an attractive model of cohesion establishment is the entrapment of two sister chromatids within a cohesin ring during DNA replication which thereby become linked together. In a simplistic view, such a scenario would imply cohesin to be a monomeric complex before and after replication. However, other models include dimerisation of cohesin during cohesion establishment. The molecular weight of native chromosomal cohesin is unknown. In addition, changes in size and shape of chromatin bound cohesin during cohesion establishment have hitherto not been investigated, and thus alternative models of sister chromatid cohesion remain possible. Measurement of hydrodynamic properties, described in chapter 2, demonstrated that chromosomal cohesin is a monomeric complex and does not change its size or shape during cohesion establishment, thereby limiting the number of possible models of sister chromatid cohesion.

Cohesin SMC heads share protein motifs with the large family of ABC ATPase. The presence of these ATPase motifs suggests a role for ATP in cohesion, similar to the requirement of ATP in the various chromosomal activities of related bacterial and eukaryotic SMC complexes. Therefore, despite the homology between members of the SMC protein family, it has remained elusive if ATP is indeed a prerequisite for cohesin function *in vivo*. So far biochemical analysis of cohesin *in vitro* did not reveal a contribution of ATP to its DNA binding activities (Losada and Hirano, 2001; Kagansky et al., 2003). Approaches to address ATP´s potential role in cohesion are described in chapter 3. These include crosslinking experiments which showed that cohesin has indeed ATP binding activity. To assess the *in vivo* function of ATP in cohesion, point mutations were introduced in the Walker motifs or C-motif of Smc1 that were implicated in ATP binding or hydrolysis, respectively. Genetic analysis of the mutant Smc1 proteins revealed that the ATPase motifs are essential for sister chromatid cohesion. Smc1, mutant in the ATP binding motifs but not in the ATP hydrolysis motif failed to interact with the Scc1 subunit in coimmunoprecipitation experiments. Therefore binding of ATP to Smc1 appears to be required for complex assembly which was further confirmed in an *in vitro* reconstitution assay (chapter 3).

If the model of cohesin binding to DNA by topological entrapment is correct, the question how DNA is initially threaded into cohesin's ring that is thought to be closed by interaction of the Scc1 subunit with the SMC head domains, is currently a matter of debate. SMC heads are similar in architecture to the interacting heads of Rad50 and other ABC ATPase domains, crystal structure studies of which have revealed an ATP-dependent cycle of their engagement and disengagement. In analogy, a similar mechanism could play a role in cohesin loading onto DNA whereby ring opening at the heads would allow the initial transport of DNA into the ring and reclosure its entrapment. However, a prerequisite to apply such a mechanism is a direct interaction of the SMC heads independently of Scc1, which has hitherto not been detectable (Haering et al., 2002). Experiments in chapter 4 revealed that cohesin's Smc1 and Smc3 subunits by themselves form a closed ring structure through direct interaction of their head domains, independently of Scc1. The SMC head dimerisation was found to be mediated by ATP-dependent and independent interactions and might be required for the assembly of the Scc1 subunit onto the Smc1/3 ring (chapter 4).

In contrast to Smc1 mutated in the ATP binding motifs, the ATP hydrolysis mutant supports intact complex formation and also forms closed cohesin rings. However, chromosome spread experiments, shown in chapter 5, revealed that DNA binding of cohesin was abolished in this mutant. This result indicates that ATP hydrolysis may be required for loading cohesin onto DNA. Deletion and depletion studies of cohesin subunits demonstrated that in addition to functional ATPase heads, an intact cohesin ring composed of all four subunits is essential for DNA binding. This suggests that ATP hydrolysis may be coupled to DNA transport into the cohesin ring. Whereas this is an attractive way to explain DNA loading of cohesin, mere cleavage of Scc1 during anaphase would not be predicted to open up the cohesin ring to release DNA since SMC head domains interact with each other independently of Scc1. Instead, the C-terminal cleavage fragment of Scc1 was found to play an active role in disrupting the SMC head interaction and to trigger sister chromatid segregation (chapter 5).

Taken together, the results presented in this thesis describe a potential role of ATP in the function of cohesin. Evidence is provided that the SMC proteins, independently of Scc1, form a ring and that ATP binding is required for association of the SMC ring with Scc1. Complex assembly and ring formation, however, are not sufficient to bind to chromatin. Mutant analysis indicates that ATP hydrolysis by Smc1 is required for this

step. These results lead to a model consistent with ATP hydrolysis-dependent transport of DNA into the cohesin ring.

CHAPTER 2: Purification and characterisation of chromatin bound cohesin

Biochemical characterisation of cohesin has largely been restricted to material recovered from soluble supernatant fractions after cell extraction (Losada et al., 1998; Tóth et al., 1999; Sumara et al., 2000; Haering et al., 2002). These studies have defined cohesin as a monomeric ring-shaped complex which is composed of four core subunits, the Scc1, Scc3, Smc1 and Smc3 proteins. However, cohesin that is bound to chromatin likely represents the functional pool of the complex. Thus, as a first step in order to study cohesin function it is necessary to assess if chromosomal cohesin differs in any way from cohesin in cell supernatants. Such differences between chromatin bound and unbound forms of cohesin may be detected by analysing the subunit composition, size and shape of the complex. Changes in these parameters could in particular become apparent during cohesion establishment because this process transforms cohesin that is bound to one DNA strand before DNA replication into a proteinaceous structure that holds two sister strands together after replication.

In order to analyse subunit composition of chromosomal cohesin, the complex was purified from chromatin of budding yeast. Biochemical analysis included measurements of its hydrodynamic properties during cohesion establishment. In addition, structural studies of cohesin/DNA complexes isolated *ex vivo* were performed to get insight into the binding mode of cohesin to DNA.

2.1 Purification of chromatin bound cohesin

To characterise the chromosomal cohesin complex of budding yeast, a purification strategy was developed to isolate cohesin from chromatin fractions. After cell extraction, most of the cellular cohesin is tightly associated with a nuclear chromatin pellet. This is demonstrated in Figure 2.1A by the presence of about two-third of the total pool of Scc1 in the chromatin fraction. Previous studies have shown that chromatin

bound cohesin cannot be solubilised even with high salt concentrations (Ciosk et al., 2000; Sumara et al., 2000). However, cohesin can be efficiently released from chromatin under mild conditions by nuclease treatment and recovered in a soluble fraction (Ciosk et al., 2000). The type of nucleases used for cohesin release was either DNase I, which digests most of the DNA in the chromatin pellet, or micrococcal nuclease (MN). Chromosomal DNA can be cut by MN into nucleosomal arrays of different lengths depending on the enzyme concentration, which therefore potentially allows copurification of DNA fragments with cohesin for structural studies. In order to isolate cohesin from supernatant fractions after release, Scc1 was chosen as bait to purify the holocomplex as it directly interacts with all the other cohesin subunits (Haering et al., 2002). The genomic copy of the SCC1 gene was modified to encode a C-terminal HA_6 epitope tag, separated by a peptide recognition motif for tobacco etch virus (TEV) protease (Dougherty et al., 1989). This allowed one-step affinity purification of cohesin either from the soluble fraction after cell lysis or from chromatin after solubilisation. For this, released extracts containing tagged Scc1 were incubated with anti-HA antibody that was then coupled to protein A beads, and subsequently the holocomplex was eluted from the beads by cleavage with TEV protease (Figure 2.1B). This purification method turned out to be the most successful and efficient way to isolate chromatin bound cohesin. Two-step purification strategies, for which affinity tags such as the Tandem-Affinity-Purification (TAP) tag (Rigaut et al., 1999) or an HA_3-TEV-His_6 tag were C-terminally fused to the Scc1 subunit, failed as they abolished cohesin release from chromatin after nuclease treatment or produced too many unspecific protein bindings, respectively (data not shown).

Silver stain analysis of proteins in the eluate identified all known core subunits, the Scc1 subunit at approximately 80 kDa which was poorly stained as has previously been observed (Tóth et al., 1999), and the Smc1, Smc3 and Scc3 proteins which migrate around 160 kDa (Figure 2.2A). Protein bands of Smc1 and Scc3 comigrate, but increasing the size by tagging either proteins with a myc epitope, that was introduced at their genomic loci, confirmed the presence of both subunits in the eluate after silver staining (data not shown). The identity of cohesin subunits was further verified by Western analysis (data not shown). To estimate the yield of cohesin after purification, known amounts of bovine serum albumin were loaded next to cohesin and band intensities compared after silver staining (data not shown). The total amount of purified

protein usually obtained from one litre of a logarithmically growing yeast culture was about 1.25 µg after a complete DNA digest by DNase I and MN, and 125 ng after partial MN digest that releases less cohesin from chromatin.

To determine whether DNA fragments could be copurified after cohesin release from chromatin by MN treatment, the eluate was subjected to radioactive DNA end-labelling. Since MN digests create DNA fragments with 5´ overhangs, a fill-in reaction using Klenow polymerase and α-^{32}P-dATP was performed. Purified cohesin was indeed found to associate with DNA fragments that are in length up to 1 kb after complete MN digest, and larger than 5 kb after partial digest (Figure 2.2B and C). In addition, this method also allowed determination of the minimal size of chromatin fragments bound to cohesin, which was estimated to be 300 bp, the length of dinucleosomes. This parameter has never been precisely determined before as the highest resolution of currently available CHIP data on cohesin association sites is about 0.8-1 kb (Laloraya et al., 2000).

2.2 Subunit composition and hydrodynamic properties of cohesin during chromatin binding or cohesion establishment

It appears at first sight that apart from known cohesin subunits, additional proteins do not interact with chromosomal cohesin in a stoichiometric manner (see Figure 2.2A). To directly assess whether proteins specifically associate with the chromatin bound form of cohesin, the complex was isolated from solubilised chromatin as well as from cell supernatants. In addition, to study possible changes to cohesin during the establishment of sister chromatid cohesion, cells arrested before or after DNA replication were used for the purification. Half of the culture was treated with the replication inhibitor hydroxyurea (HU), the other half was treated with the spindle poison nocodazole that arrests cells in metaphase. Cohesin was isolated as described above but to block unspecific protein bindings, bovine serum albumin was added to the extraction buffer. In addition, to increase the protein yield in the preparations, the TEV protease elution step was omitted and instead proteins were eluted with SDS from the beads, and subsequently analysed by SDS-PAGE. As shown in Figure 2.3, after extensive silver staining several sub-stoichiometric or background protein bands

became visible, but there was no evidence for specific association of polypeptides to chromatin bound cohesin either before or after DNA replication.

The failure to detect changes to the subunit composition did not exclude the possibility that cohesin may form dimers or higher-order oligomers during chromatin binding or cohesion establishment. Therefore, the hydrodynamic properties of cohesin solubilised from chromatin of HU or nocodazole arrested cells were determined using size exclusion chromatography and glycerol gradient centrifugation. Fractions were collected and analysed by Western blotting using antibodies raised against the endogenous Scc1 and Smc1 proteins. In addition, the Scc3 subunit was detected by anti-HA antibody (data not shown) as endogenous Scc3 was tagged with an HA_3 epitope. All these subunits coeluted in the same fractions. The Stokes radius of cohesin, measured by gel exclusion chromatography, was 8.5 nm (Figure 2.4A) while the sedimentation coefficient, determined by glycerol gradient centrifugation, was 14.1 S (Figure 2.4B). Both values did not change before or after DNA replication. The molecular weight of cohesin derived from these values by the method of Siegel and Monty (see chapter 7.3.6) is about 500 kDa. This is consistent with a complex of one subunit each of Smc1, Smc3, Scc1, and Scc3, for which the calculated molecular weight is 480 kDa. Thus, cohesin bound to chromosomes is biochemically similar to previously characterised cohesin in cell supernatants and no major alteration to the size or shape of cohesin is detectable during cohesion establishment.

2.3 Cohesin associates with chromatin in clusters

2.3.1 Electron microscopy of cohesin/DNA complexes

To determine how cohesin is bound to chromosomal DNA, structural studies using electron microscopy (EM) were performed on cohesin/DNA complexes. This work was carried out in collaboration with Dr Nasser Hajibagheri at the Electron Microscopy Unit at CR-UK, London. It was possible to obtain such cohesin/DNA complexes since DNA copurified with cohesin after release from chromatin by complete or partial MN digest (see Figure 2.2B and C). Samples were subjected to several procedures recommended for visualisation of protein/DNA complexes. One method, the monolayer technique according to Kleinschmidt (Kleinschmidt, 1968), has in particular proven successful to

effectively spread DNA bound to cohesin onto carbon coated EM grids that were used in the experiments. Before samples were spread, the EM grids were glow discharged to facilitate absorption of DNA molecules to the carbon films. To analyse cohesin/DNA structures, the dark-field technique was applied, a method in transmission EM that allows high-contrast visualisation of specimens that are not metal-shadowed.

Eluates after one-step purification show only little impurities as judged by silver staining (see Figure 2.2A). However, to ensure that structures observed by electron microscopy are indeed cohesin/DNA complexes, preparations from tagged and untagged strains were analysed. In the control samples obtained from untagged strains but also surprisingly in samples from tagged strain after complete MN digest, no structures were observed by EM. The latter case was probably due to a failure of the relatively short DNA fragments to adhere to the grids. In contrast, protein/DNA complexes were present in samples derived from tagged strains after partial digest (Figure 2.5) that produces longer DNA fragments. As these studies are very preliminary, the identity of cohesin was not confirmed by techniques such as immunogold labelling. In addition, statistics on the distribution of protein on DNA and length measurements of DNA fragments were not performed. It can be assumed that DNA fragments are over 5 kb in length (see Figure 2.2C), and therefore should cover at least one entire cohesin association site that has an estimated length of about 1 kb. The size of the smallest single protein complex associated with DNA appeared not to exceed 10 nm (Figure 2.5, arrows) which is much less than previous length measurements of soluble human cohesin (65 nm) in electron micrographs or soluble fission yeast Psm1/3 (25-45 nm) in AFM (atomic force microscopy) experiments (Anderson et al., 2002; Sakai et al., 2003). However, the discrepancy in size of the complex might be due to association of protein with DNA which could result in an overall compaction of the complex. Another possibility is that the relatively thin coiled coil domains that contribute to most of the size of cohesin were not visualised, and other techniques like metal-shadowing would be required. Strikingly, in the cohesin/DNA electron micrographs the majority of proteins were present as part of accumulations (Figure 2.5, arrowheads). This suggests that cohesin associates with chromatin in form of clusters which might represent the preferred binding mode of cohesin to DNA.

2.3.2 *Cohesin associates with chromatin in clusters*

So far it remained elusive whether each genomic cohesin association site represents binding of one or more cohesin complexes. Therefore the question was addressed whether in theory it is possible that cohesin associates with chromatin in clusters as suggested by EM (see above). It has previously been shown that cohesin association sites can be found on average every 15 kb along budding yeast chromosomes (Blat and Kleckner, 1999; Laloraya et al., 2000). Hence, there are about 800 cohesin association sites in the 12 Mb genome. Cytological observations suggest only about 200 of these may be used in individual cells (Michaelis et al., 1997; Klein et al., 1999). To estimate how many cohesin complexes are present per genome, quantitative Western analysis was performed. As a first step, the amount of cohesin in chromatin fractions of a known number of cells was determined. To obtain a standard protein to quantify amounts of cohesin, recombinant Scc1 was produced by overexpression and purification in bacteria.

For this, the SCC1 gene was cloned into the bacterial pET30 expression vector for inducible expression by isopropyl β-D-thiogalactoside (IPTG) of a C-terminally His_6 tagged protein in *E. coli*. Test inductions had shown that the protein is insoluble under every condition that was used (data not shown). Finally, parameters for induction were chosen that yielded maximum protein amounts. Protein expression was induced over a period of two hours at 37°C by addition of 1 mM IPTG to *E. coli* transformed with the pET30-SCC1 construct. Successful expression of Scc1 was analysed by Coomassie staining and protein identity confirmed by Western blotting (Figure 2.6A, left panels). The inclusion bodies containing insoluble Scc1 were isolated and the protein recovered by denaturing extraction in urea. Recombinant Scc1 was subsequently purified by gel filtration followed by a dialysis step to renature the protein after which the protein remained soluble (see chapter 7.3.7). Protein concentration of Scc1 was measured by quantitative Coomassie staining and Bradford assay with bovine serum albumin as standard (Figure 2.6A right panel and data not shown).

For quantitative Western analysis, a fraction representing chromatin from 2 x 10^7 cells determined by a haemacytometer as well as by using a Coulter Counter, was loaded next to known amounts of recombinant Scc1 (Figure 2.6B). Western membranes were probed with an anti-Scc1 antiserum and subsequently with a fluorescent dye-coupled secondary antibody for quantification by an infrared imager (see chapter 7.3.7).

Relative protein amounts (pixels) were measured, and the pixel value obtained for chromatin Scc1 was fitted into a standard curve derived from values of recombinant Scc1 (Figure 2.6C). The amount of Scc1 in the chromatin fraction was calculated to be about 8.3 ng. Using a molecular weight for Scc1 of 63 kDa, this amount corresponded to 4000 molecules of cohesin per haploid genome. Therefore, 5-20 cohesin complexes, depending on the actual number of cohesin association sites (200-800, see above), are present at each site. This result confirmed the observation in electron micrographs of cohesin/DNA complexes, and suggests that cohesin may indeed associate with chromatin in clusters.

2.4 Summary

- Purification and analysis of subunit composition revealed that chromatin bound cohesin is biochemically similar to cohesin isolated from cell supernatants and does not seem to associate with any additional polypeptides.

- Measurement of hydrodynamic properties showed that chromosomal cohesin is a monomeric complex with a molecular weight of about 500 kDa and does not change size and shape during cohesion establishment.

- Analysis of cohesin/DNA complexes isolated from chromatin indicated that cohesin preferentially binds to DNA in the form of clusters.

- Quantitative Western analysis provided evidence that a chromosomal cohesin association site is likely to represent binding of not a single cohesin molecule but rather a cluster composed of 5-20 cohesin complexes.

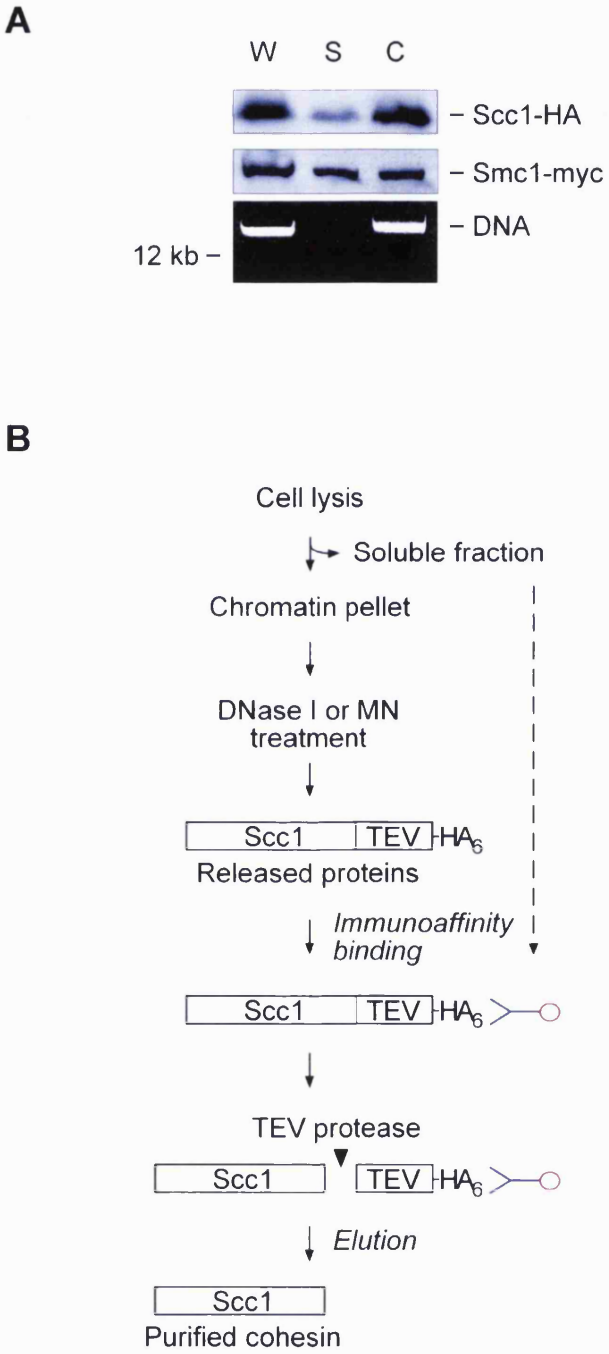

Figure 2.1. A purification strategy to isolate chromatin bound cohesin.

(A) Whole cell extracts (W) of strain Y613 (*MAT*a, *pep4Δ, SCC1-HA6, SMC1-myc18*) were separated into soluble (S) and chromatin fractions (C). Equivalent protein and DNA aliquots were analysed by Western blotting and agarose gel electrophoresis, respectively.
(B) Purification scheme for the isolation of cohesin from soluble and chromatin fractions.

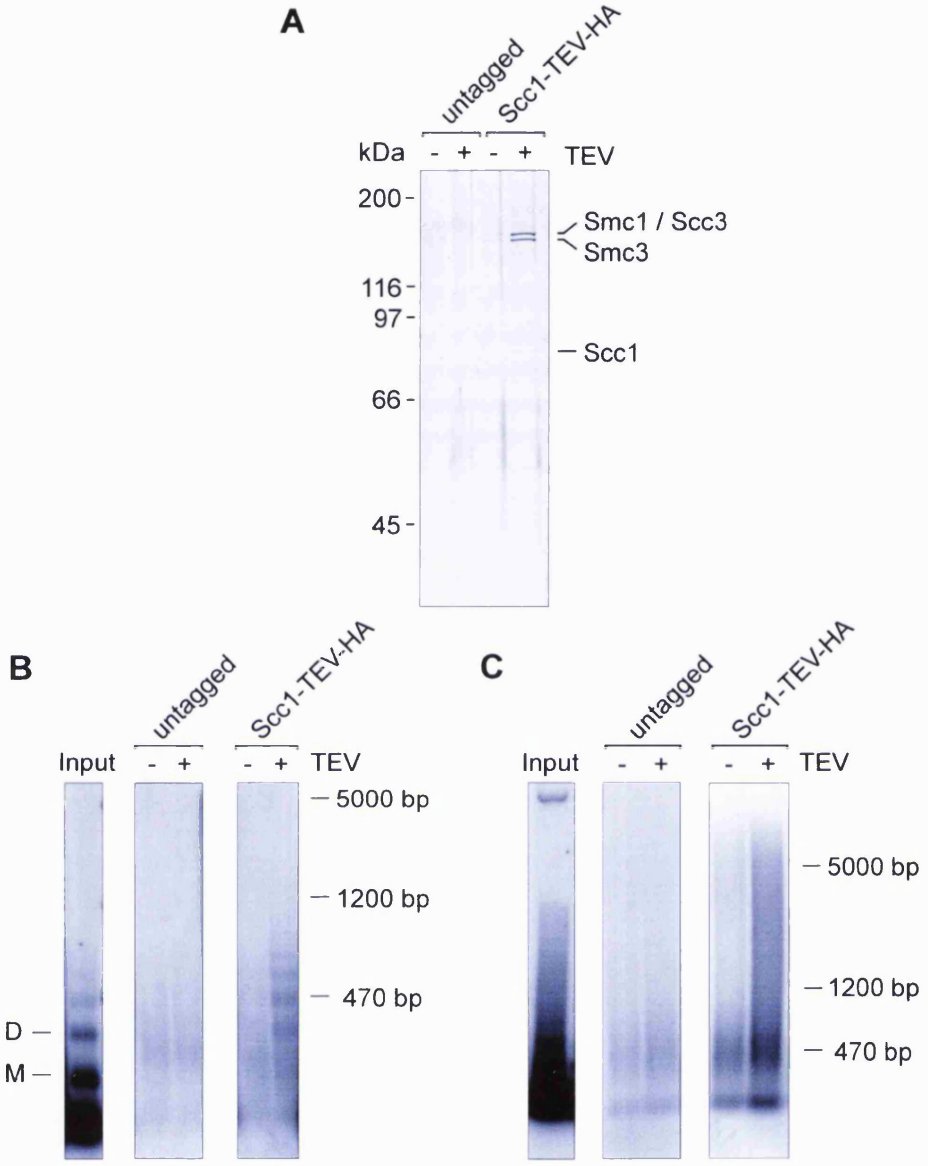

Figure 2.2. Purification of chromatin bound cohesin.

(A) Cohesin from chromatin of strain Y618 (*MAT*a, *pep4Δ, SCC1-TEV-HA6*) was released by micrococcal nuclease treatment and immunopurified by HA pulldown followed by TEV cleavage. The eluate was analysed by SDS-PAGE followed by silver staining. Smc1 and Scc3 comigrate; the Scc1 subunit stains poorly with silver (Tóth et al., 1999). Extracts from a control strain lacking the HA epitope were subjected to the same purification procedure. TEV, elution with TEV protease.
(B) and **(C)** Copurification of DNA fragments with cohesin. DNA present in input and eluate fractions after a complete (B) or partial (C) micrococcal nuclease release of cohesin was radioactively end-labelled using Klenow Polymerase. Labelled DNA fragments were separated by agarose gel electrophoresis and analysed by autoradiography. As a marker, DNA fragments of a known size, derived from digested plasmid DNA, were labelled and loaded. M, expected size of a mononucleosome DNA fragment; D, dinucleosome-size fragment.

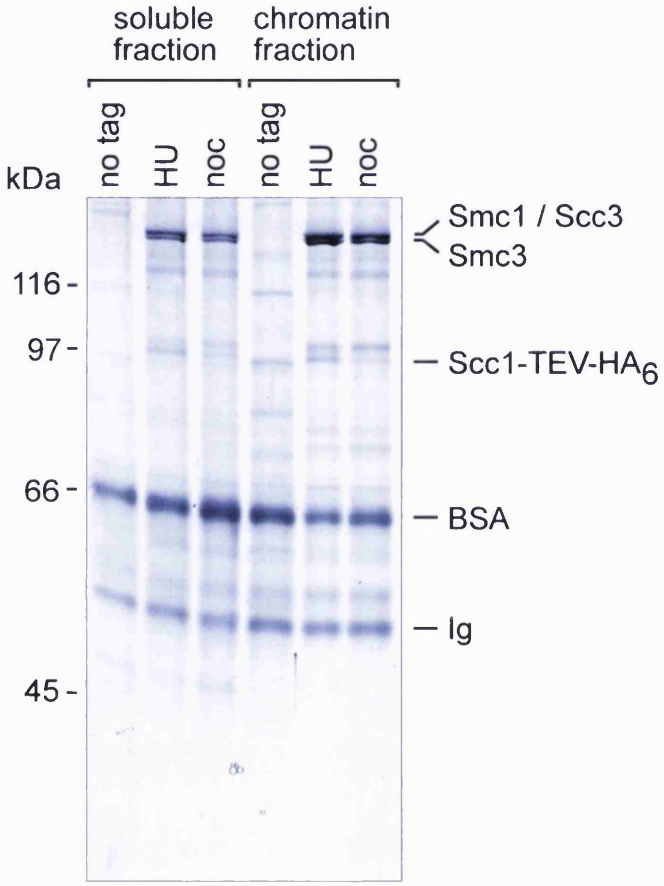

Figure 2.3. Comparison of cohesin subunit composition in soluble or chromatin fractions.

Cells from strain Y618 were arrested by hydroxyurea (HU) or nocodazole (noc) treatment, and cohesin was immunopurified from soluble fractions or DNase I-treated chromatin by HA pulldown followed by SDS elution. As a control, a logarithmically growing strain lacking the HA epitope tag was used. Proteins were separated by SDS-PAGE and analysed by silver staining.

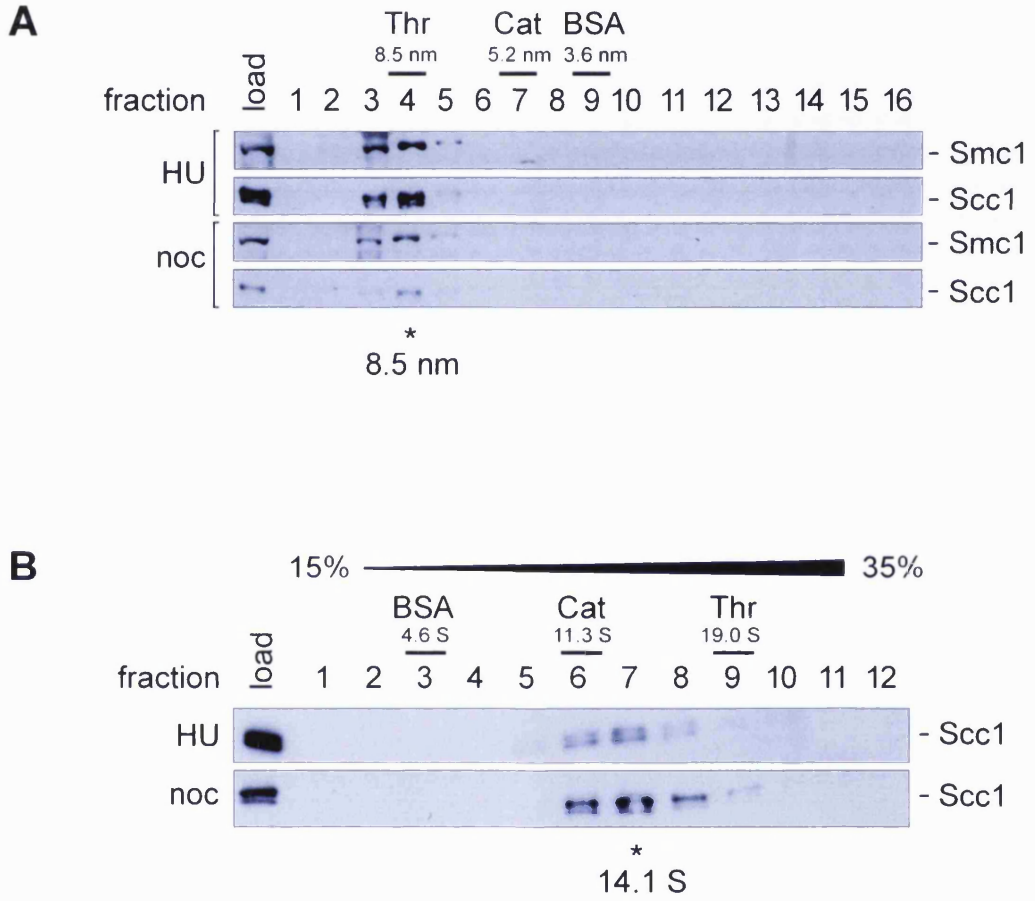

Figure 2.4. Chromosomal cohesin is a monomeric complex and does not change its size or shape during cohesion establishment.

(A) Gel exclusion chromatography of cohesin solubilised by DNase I from chromatin after hydroxyurea or nocodazole treatment of strain Y458 (*MAT*a, *pep4Δ, SCC3-HA3*). The Scc1 and Smc1 subunits were detected by Western blotting using polyclonal antisera. Scc3-HA3 co-elutes with Scc1 and Smc1 (data not shown). Marker proteins used for calibration were: Thr, thyroglobulin; Cat, catalase; BSA, bovine serum albumin. Asterisks (*) mark peak fractions of cohesin.
(B) Glycerol gradient centrifugation of cohesin from similar preparations as in (A). Marker proteins were analysed in a parallel gradient.

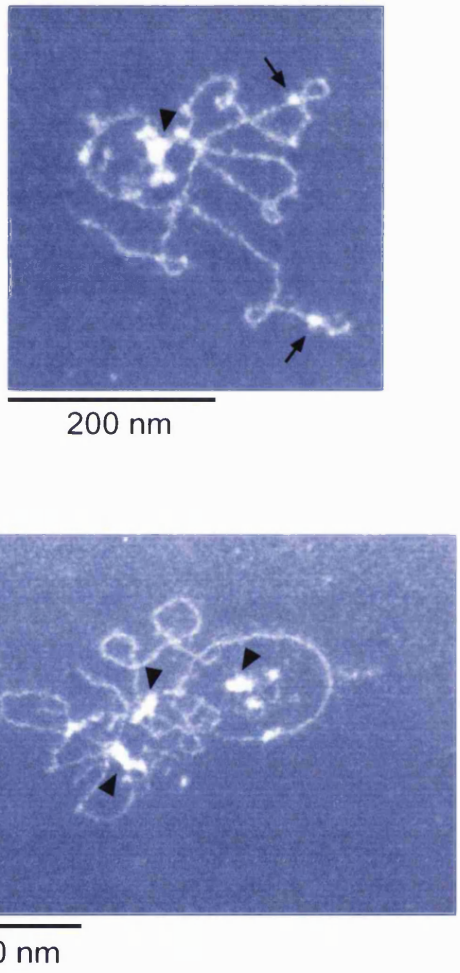

Figure 2.5. Electron micrographs of cohesin/DNA complexes.

Chromatin of strain Y618 and an untagged control strain was digested by micrococcal nuclease, and cohesin was affinity-purified from the released fraction. The purity of cohesin was confirmed by silver staining and copurification of DNA fragments by end-labelling followed by autoradiography (compare Figure 2.2). An aliquot of the eluate was spread onto glow discharged EM grids and visualised by dark-field EM. The images represent structures present in eluates that contain cohesin/DNA complexes released from partially digested chromatin. Arrows indicate single protein complexes on DNA, whereas arrowheads mark clusters of protein.

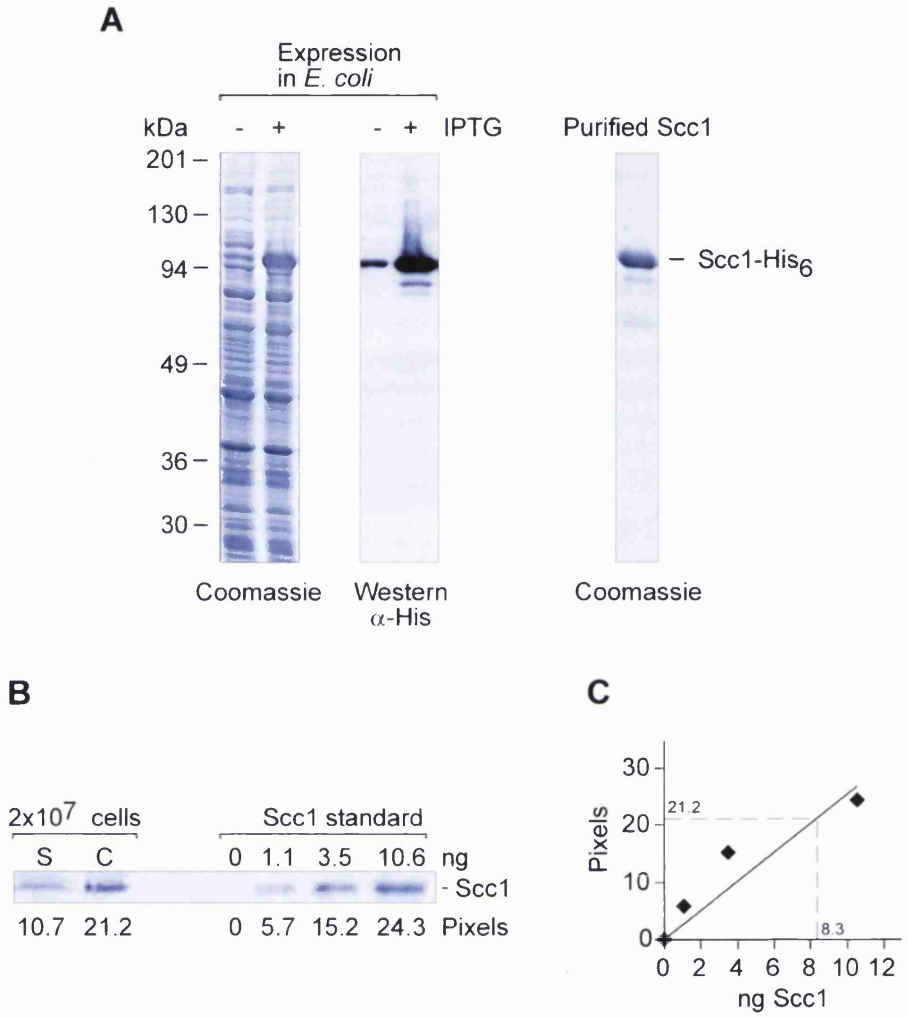

Figure 2.6. Cohesin binds to chromatin in clusters.

(A) Bacterial expression and purification of recombinant Scc1. Expression of His_6-tagged Scc1 was induced in *E. coli* with 1 mM IPTG at 37°C. Aliquots of cell extract samples before (uninduced) and two hours after the induction were analysed by Coomassie staining and Western blotting (left panels). Bacterial inclusion bodies containing insoluble Scc1 were isolated, the protein solubilised in urea and purified by gel filtration. The protein concentration of purified Scc1 in the preparation was measured by quantitative Coomassie staining and Bradford assay using bovine serum albumin as standard, and was 0.25 mg/ml (data not shown). 1.2 µg of protein was loaded on a gel and stained by Coomassie (right panel).
(B) and **(C)** Quantification of cohesin bound to chromatin. Soluble and chromatin fractions from 2 x 10^7 cells, and known amounts of recombinant Scc1 were subjected to SDS-PAGE. Relative protein amounts (pixels) of Scc1 were measured by quantitative Western blotting using polyclonal anti-Scc1 antiserum (B). Known amounts of recombinant Scc1 were plotted against their pixel values. Subsequently, the protein amount of Scc1 in the chromatin fraction was derived from this standard curve (C).

CHAPTER 3: ATP binding activity of cohesin and ATP-dependent complex assembly

Cohesin isolated from soluble and chromatin fractions do not differ biochemically (see chapter 2). This suggests that chromosomal cohesin is sufficiently described by its known distinctive ring structure and that chromosomal activities may be intrinsic to the complex. A feature of cohesin that has not been explored in previous analysis are the predicted ATPase domains that are formed by the heads of the two SMC subunits. Each head is composed of the amino- and carboxy-terminal domains of a single SMC protein. These domains contain the conserved ATPase protein motifs required for ATP binding and hydrolysis which are the Walker A motif, located at the amino-terminus, and the Walker B and C-motifs at the carboxy-terminus. Binding of ATP to an isolated cohesin SMC domain, the N-terminal Smc1 head, has been reported (Akhemedov et al., 1998) but so far a contribution of ATP to cohesin activities *in vitro* could not be detected (Losada and Hirano, 2001; Kagansky et al., 2003).

To assess whether ATP is involved in cohesin function, the ATP binding activity of purified cohesin was tested. In addition, mutant analysis of the ATPase motifs in Smc1 were performed *in vivo* to investigate whether ATP binding and hydrolysis play a role in sister chromatid cohesion.

3.1 ATP binding activity of cohesin

To test if cohesin shows any ATP binding activity, crosslinking of ATP to the complex was attempted. For this, cohesin was purified from soluble yeast extracts using the one-step purification strategy (see chapter 2.1). Affinity-bound cohesin was eluted by TEV protease, and the eluate was split into two aliquots to which the ATP-analogue 8-azido-[α-^{32}P]ATP was added. Azido-ATP specifically interacts with nucleotide-binding sites of proteins, and becomes covalently attached with their target after photochemical cross-linking. To test the specificity of ATP binding, one of the aliquots was supplemented with an excess of non-radioactive ATP. After an incubation step to

allow ATP binding, both reactions were subjected to UV-crosslinking and proteins analysed by SDS-PAGE followed by autoradiography. As shown in Figure 3.1, a protein of the size of the SMC subunits was crosslinked to ATP in the purified material. The ATP binding was specific as the signal was abolished in the competition reaction containing unlabelled ATP and no band was detected in the control purification. The protein bands of Smc1 and Smc3 show similar gel migrations, and even if one of the subunits was tagged with an HA_6 epitope to increase its size, differentiation between ATP binding to both or only one of the proteins was not possible (data not shown). Since ATP binding motifs are contained in both proteins, it is conceivable that both Smc1 and Smc3 may bind ATP. The level of ATP binding to cohesin appeared to be very low when compared to another ATP binding protein, recA (Weinstock et al., 1979), of which a similar amount of recombinant protein was subjected to a parallel ATP crosslinking reaction (Figure 3.1, right panel). In addition, if the non-hydrolysable ATP analogue ATPγS, that is expected to stably bind to the SMCs, was used instead of azido-ATP, no increase in ATP binding activity was observed (data not shown). Purified cohesin/DNA complexes were also tested for ATP binding since it has been shown that ATP hydrolysis activity of *B. subtilis* SMC (BsSMC) was greatly stimulated by DNA (Hirano and Hirano, 1998). However, the level of crosslinking was similar compared to soluble cohesin and therefore the association of DNA with cohesin did not appear to stimulate binding to ATP (data not shown).

3.2 Construction and expression of Smc1 ATPase motif mutants

To analyse a possible contribution of ATP binding or hydrolysis to cohesin function, point mutations were introduced into the conserved ATPase motifs within Smc1. Three mutations were constructed that have previously been characterised in BsSMC *in vitro* (Hirano et al., 2001). Both a lysine to isoleucine mutation in the Walker A motif and an aspartate to alanine mutation in the Walker B motif prevented binding of ATP to BsSMC. Mutation of a conserved serine in the C-motif to arginine allowed ATP binding but prevented ATP hydrolysis. The amino acid sequences of the N-terminal head domains of BsSMC and budding yeast Smc1 show 28 % identity (BsSMC amino acids 1-161 vs. Smc1 1-163 aa), whereas the C-terminal heads are 38 % identical (BsSMC 1036-1186 aa vs. Smc1 1068-1225 aa). Sequence comparisons were performed using

the ALIGN program (Pearson et al., 1997) (http://xylian.igh.cnrs.fr/bin/align-guess.cgi). Structural analyses of both ATPase domains and therefore three-dimensional alignments have not been reported, but the high sequence conservation suggests that the identical mutations may have the same effect in cohesin SMCs. The corresponding amino acid changes were introduced into the Walker A, Walker B and C-motifs of Smc1 which are K39I, D1157A and S1130R, respectively (Figure 3.2A). To construct the mutant variants, the *SMC1* gene was cloned into a vector of the YIplac series which were designed to allow their genomic integration at marker loci by homologous recombination (Gietz and Sugino, 1988). The *SMC1* gene was inserted into the vector downstream of the galactose-inducible *GAL1* promoter and was C-terminally tagged with an HA_6 epitope. Introduction of point mutations into the ATPase motifs was then performed by site-directed mutagenesis using overlap extension PCR (see chapter 7.1.1.3). For testing the *in vivo* function of the ATPase motifs, the vectors containing the Smc1 constructs were subsequently integrated into a yeast strain containing a temperature sensitive allele of the *SMC1* gene (*smc1-259*), which had been isolated in a screen for proteins required for sister chromatid cohesion (Michaelis et al., 1997) .

To assess if the amino acid changes introduced into the ATPase motifs of Smc1 affect its protein stability *in vivo*, the expression levels in yeast of the mutant Smc1 proteins were analysed. Strains which contain the wild-type or *SMC1* mutant constructs were grown up and the *GAL1* promoter was induced for two hours by adding galactose to the medium. In order to compare levels of protein expression from the *GAL1* and endogenous Smc1 promoter, a strain in which the endogenous *SMC1* gene was tagged with an HA_6 epitope, was included in the experiment. Protein expression was carried out at the permissive temperature of 25°C and additionally at 35.5°C, the restrictive temperature of the $smc1^{ts}$ strain. As shown by Western analysis, Smc1 mutant and wild-type proteins were expressed at similar levels at both temperatures (Figure 3.2B). The *GAL1* inducible proteins were expressed at about 2 to 3 times the level of endogenous Smc1. The result shows that the ATPase motif mutations do not appear to have an impact on protein stability of Smc1.

3.3 The ATPase motifs in Smc1 are essential for sister chromatid cohesion

In order to investigate if the ATPase motifs have any function *in vivo,* it was tested whether the mutant Smc1 proteins support cell viability. Strains expressing wild-type Smc1 or the Smc1 ATPase motif mutants were streaked on medium containing galactose and incubated at the permissive or restrictive temperature. Only wild-type Smc1 but none of the ATPase motif mutants rescued growth of the *smc1*^{ts} strain at the restrictive temperature (Figure 3.3A). This suggests that the ATPase motifs and therefore ATP binding and hydrolysis by Smc1 may be essential. Expression of the mutant Smc1 proteins did not have a dominant effect on the function of endogenous Smc1 since viability of the mutant strains was not reduced at the permissive temperature.

To find out why the Smc1 ATPase motif mutations were lethal, their effect on sister chromatid cohesion was analysed. In cohesion-deficient cells, sister chromatids are expected to become separated even before they undergo anaphase. The premature loss of cohesion can be observed in cells arrested in metaphase. For this, the promoter of the Cdc20 activator of the APC was replaced with the methionine-repressible *MET3* promoter in strains expressing wild-type and ATPase motif mutants (Uhlmann et al., 2000). In addition, these strains harbour multiple repeats of Tetracycline (Tet) operators at the *URA3* locus adjacent to the centromere of chromosome V, and express a Tet repressor fused to GFP (Michaelis et al., 1997). In this system the Tet operators become visible as green fluorescent dots within nuclei thereby marking this chromosomal locus. Strains were grown up at the permissive temperature and proteins constitutively expressed by the presence of galactose in the medium. Metaphase arrest of logarithmically growing cells was then induced by addition of methionine that resulted in depletion of the Cdc20 protein. At the same time, cells were shifted to the restrictive temperature and separation of GFP dots, indicating loss of sister chromatid cohesion, was scored over a time period of five hours. Complete metaphase arrest of the cells was confirmed by FACS analysis of DNA content (data not shown). During the time course, *smc1*^{ts} cells showed increasing loss of cohesion that was only suppressed by expression of wild-type Smc1 but not the ATPase motif mutants. The degree of sister separation of cells expressing the ATPase motif mutants did not differ from that observed in *smc1*^{ts}

cells alone, indicating that there was not even a partial suppression by the mutants (Figure 3.3B). This result indicates that the lethality of the Smc1 ATPase motif mutants was caused by a cohesion defect, and suggests that ATP binding and hydrolysis by Smc1 may be required for sister chromatid cohesion.

3.4 ATP binding is required for cohesin complex formation

3.4.1 Coimmunoprecipitation of ATPase motif mutant Smc1 with other cohesin subunits

To assess why the Smc1 ATPase motif mutants failed in sister chromatid cohesion, it was tested whether any of the mutations affected the formation of an intact cohesin complex. Wild-type or mutant Smc1 proteins were expressed and immunoprecipitated with anti-HA antibody from soluble extracts of cells containing endogenous Scc1 fused to a myc_9 epitope tag. Western analysis showed that Scc1 coprecipitated with wild-type and also with C-motif mutant Smc1, although with somewhat reduced efficiency with the latter. Scc1 did not coprecipitate with Walker A and B motif mutant Smc1 (Figure 3.4A). To confirm this result, the reciprocal immunoprecipitation experiment was performed. Scc1 was immunopurified with anti-myc antibody, wild-type or C-motif mutant Smc1 copurified but only little Walker A and no Walker B motif mutant Smc1 could be detected (Figure 3.4A). This result indicates that intact Walker A and B motifs but not the C-motif are required for Smc1 to form a cohesin complex that includes the essential Scc1 subunit.

The composition of the immunopurified cohesin complexes were further analysed by SDS-PAGE followed by silver staining (Figure 3.4B). This analysis revealed that the Smc3 subunit coprecipitated with wild-type and all mutant Smc1 proteins. Interaction of Smc3 with Smc1 in the absence of Scc1 was expected because the two SMC proteins bind each other independently of the heads via the hinge.

The Scc3 subunit is thought to associate with cohesin via its interaction with Scc1. C-motif mutant Smc1 was shown to bind Scc1. To test if therefore C-motif mutant Smc1 is also capable of interacting with Scc3, HA_6 tagged wild-type and C-motif mutant Smc1 were expressed and immunoprecipitated from cells containing the

endogenous Scc3 protein tagged with a Pk_3 epitope. As expected, Scc3 copurified with both wild-type as well as C-motif mutant Smc1, although less efficiently with the latter (Figure 3.4C). The reduced efficiency of Scc3 binding was expected due to the weaker binding of Scc1 (compare Figure 3.4A). Taken together, the results suggest that intact Walker A and B motifs in Smc1 are indispensable for the binding of Scc1. Cohesin containing C-motif mutant Smc1 was found to be mostly indistinguishable from wild-type cohesin in its subunit composition, yet a somewhat reduced binding of Scc1 was observed.

3.4.2 An ATP-dependent in vitro reconstitution system for cohesin

The failure of Walker A and B motif mutant Smc1 to recruit Scc1 indicated that ATP binding by Smc1 was required for cohesin complex assembly. To analyse ATP dependency of complex formation directly, cohesin was reconstituted from its components *in vitro* (Figure 3.5A). For this, two yeast strains were used, in both the Scc1 gene was deleted and instead myc_{18} epitope tagged Scc1 was expressed from the galactose-inducible *GAL1* promoter. In one strain, this promoter was repressed by growing cells for three hours in medium containing glucose whereby the cellular pool of Scc1 became depleted. In addition, the endogenous Smc1 subunit in this strain was tagged with an HA_6 epitope. In the other strain, Smc1 was not tagged, but Scc1-myc_{18} was expressed from the induced *GAL1* promoter. Extracts were prepared from both strains and split into three aliquots. The extract from one aliquot was depleted of ATP by apyrase treatment, the others left untreated, or supplemented with an ATP regenerating system. Similarly treated extracts of both strains were mixed and incubated to allow complex assembly. Subsequently, the Smc1 subunit was immunoprecipitated with anti-HA antibody to assay complex formation between Smc1-HA_6 and Scc1-myc_{18}. Scc1 associated with Smc1 only in extracts that were supplemented with ATP, as shown in Figure 3.5B. This association was also found if non-hydrolysable ATPγS was used instead of the ATP regenerating system (data not shown). However, the interaction between both subunits appeared to be less reproducible, as ATPγS was presumably slowly hydrolysed in the crude extracts used in the experiments. In summary, these results suggest that ATP binding, but not hydrolysis, by the Smc1 subunit is required for cohesin complex assembly. This is consistent with the

observation that functional ATP binding motifs within Smc1 are prerequisites for complex formation but not an intact ATP hydrolysis motif (see previous chapter).

3.5 Summary

- The SMC subunits of purified cohesin show ATP binding activity *in vitro* as revealed by crosslinking experiments.

- Mutant analysis showed that the ATPase motifs in Smc1 are essential for sister chromatid cohesion.

- Coimmunoprecipitation experiments revealed that Smc1 mutated in the Walker A and B motifs failed to associate with Scc1, whereas a mutation in the C-motif did not affect complex formation. This suggests that ATP binding but not ATP hydrolysis by Smc1 is required for cohesin complex assembly.

- In an *in vitro* reconstitution assay ATP was found to be required for Scc1 binding to Smc1. This is consistent with ATP binding to the Smc1 subunit being a prerequisite for cohesin complex formation.

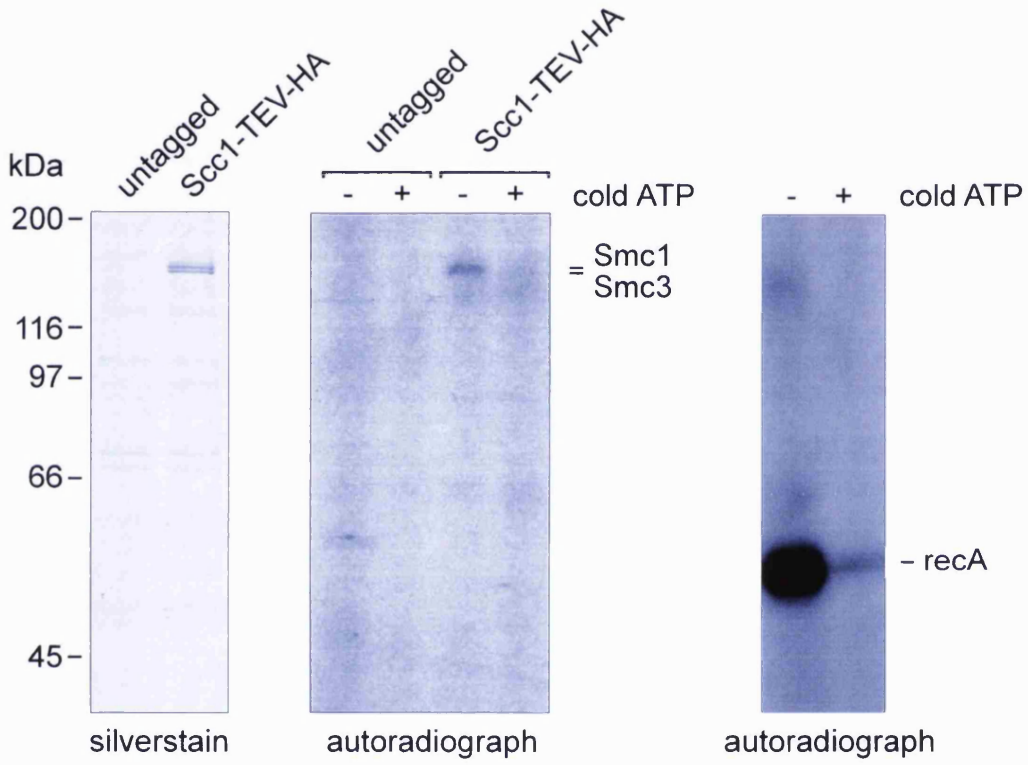

Figure 3.1. ATP crosslinking to purified cohesin.

Cohesin was immunopurified from soluble fractions of strains Y618 (left panel) and crosslinked with 8-azido-[α-^{32}P]ATP (middle panel). The specificity of crosslinking was confirmed by competition with cold ATP. As a positive control, a similar amount of recombinant RecA protein was crosslinked in a parallel reaction (right panel). Images of the middle and right panel are from the same gel and exposure time.

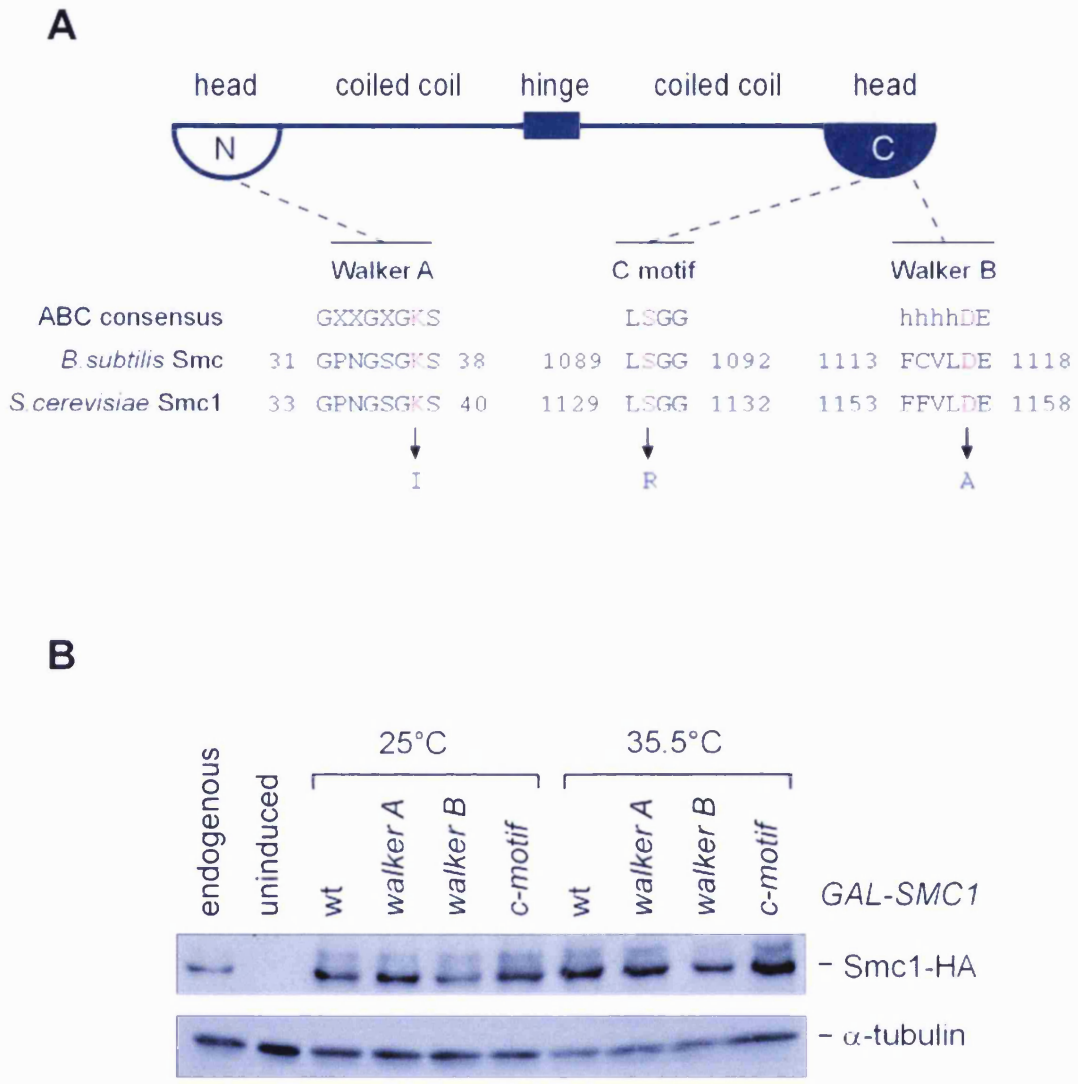

Figure 3.2. Construction and expression of Smc1 ATPase motif mutants.

(A) Alignment of the conserved ABC ATPase motifs within *B. subtilis* SMC (BsSMC) and budding yeast Smc1. The indicated amino acid changes were introduced into the ATPase motifs of the Smc1 protein. These point mutations have previously been characterised in BsSMC and were shown to prevent ATP binding (Walker A and B motif) or ATP hydrolysis (C-motif).
(B) Wild-type (Y754: *MAT*a, *smc1-259, GAL-SMC1-HA6*), Walker A (Y782), Walker B (Y784), or C-motif mutant (Y783) Smc1 was expressed under control of the *GAL1* promoter at 25°C or 35.5°C. Protein extracts were prepared and expression levels of wild-type and mutant proteins were assessed by Western blotting against the HA_6 epitope tag fused to Smc1. In order to compare protein levels by *GAL1* induced expression with endogenous Smc1 levels, extracts of strain Y752 (*MAT*a, *SMC1-TEV-HA6*) was prepared and included in the Western analysis. Equal loading of protein extracts was confirmed by probing against α-tubulin.

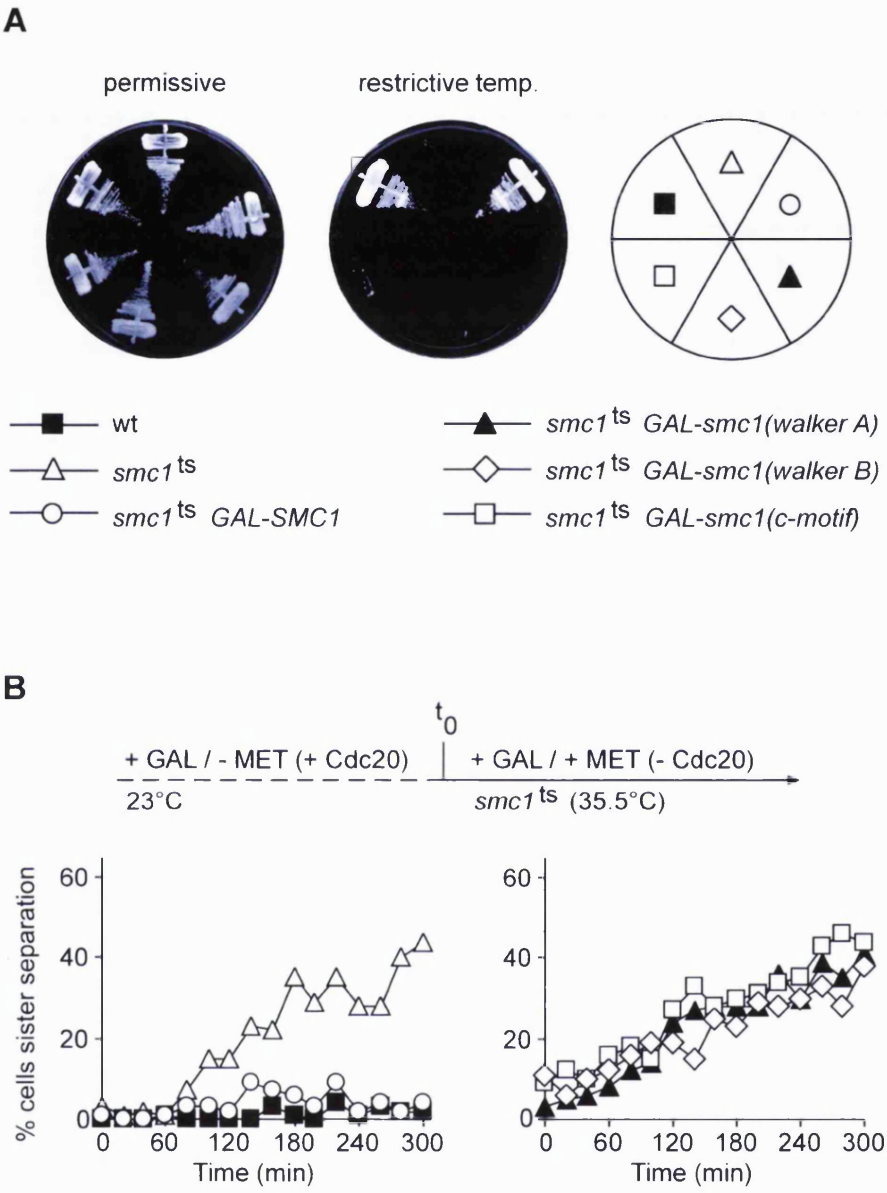

Figure 3.3. ATP binding and hydrolysis motifs in Smc1 are essential for sister chromatid cohesion.

(A) Walker A, Walker B, or C-motif mutant Smc1 does not rescue growth of an *smc1*^{ts} strain. *smc1*^{ts} strains expressing wild-type (Y754: *MAT*a, *smc1-259, GAL-SMC1-HA6*), Walker A (Y782), Walker B (Y784), or C-motif mutant (Y783) Smc1 under control of the *GAL1* promoter were streaked on medium containing 2 % galactose for induction and incubated at the permissive or restrictive temperature.
(B) Cohesion defect in Smc1 ATPase motif mutants. *smc1*^{ts} strains expressing wild-type (Y821: *MAT*a, *smc1-259, MET3-CDC20, TetR-GFP, TetOs::URA, GAL-SMC1-HA6*), Walker A (Y793), Walker B (Y795), or C-motif mutant Smc1 (Y794) were arrested in metaphase by Cdc20 depletion at 35.5°C. Separation of sister chromatids was analysed at indicated time points. Metaphase arrest of cells was confirmed by FACS analysis (data not shown). Symbols as in (A).

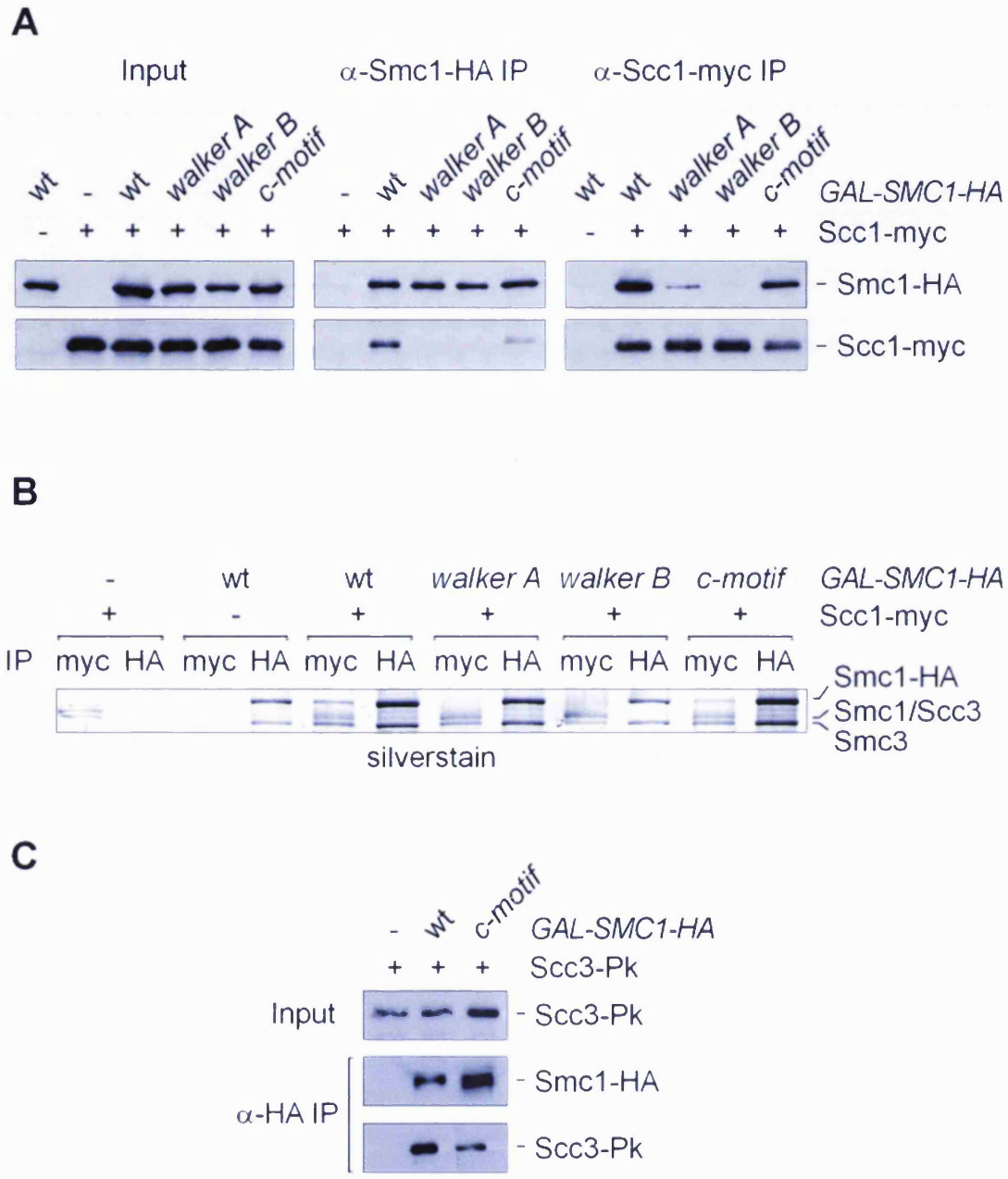

Figure 3.4. C-motif but not Walker A and B motif mutant Smc1 supports complex formation with Scc1.

(A) Smc1-HA or Scc1-myc was immunoprecipitated from strains expressing wild-type (Y797: *MAT*a, *smc1-259, SCC1-myc9, GAL-SMC1-HA6*), Walker A (Y839), Walker B (Y827), or C-motif mutant Smc1 (Y826). Coprecipitation was analysed by Western blotting.
(B) Silver staining of the immunoprecipitates described in (A).
(C) Scc3 is present in cohesin containing C-motif mutant Smc1. Wild-type (Y1573: *MAT*a, *smc1-259, SCC3-Pk3, GAL-SMC1-HA6*) or C-motif mutant Smc1 (Y1574) was expressed and coprecipitation of Scc3 with Smc1-HA was analysed.

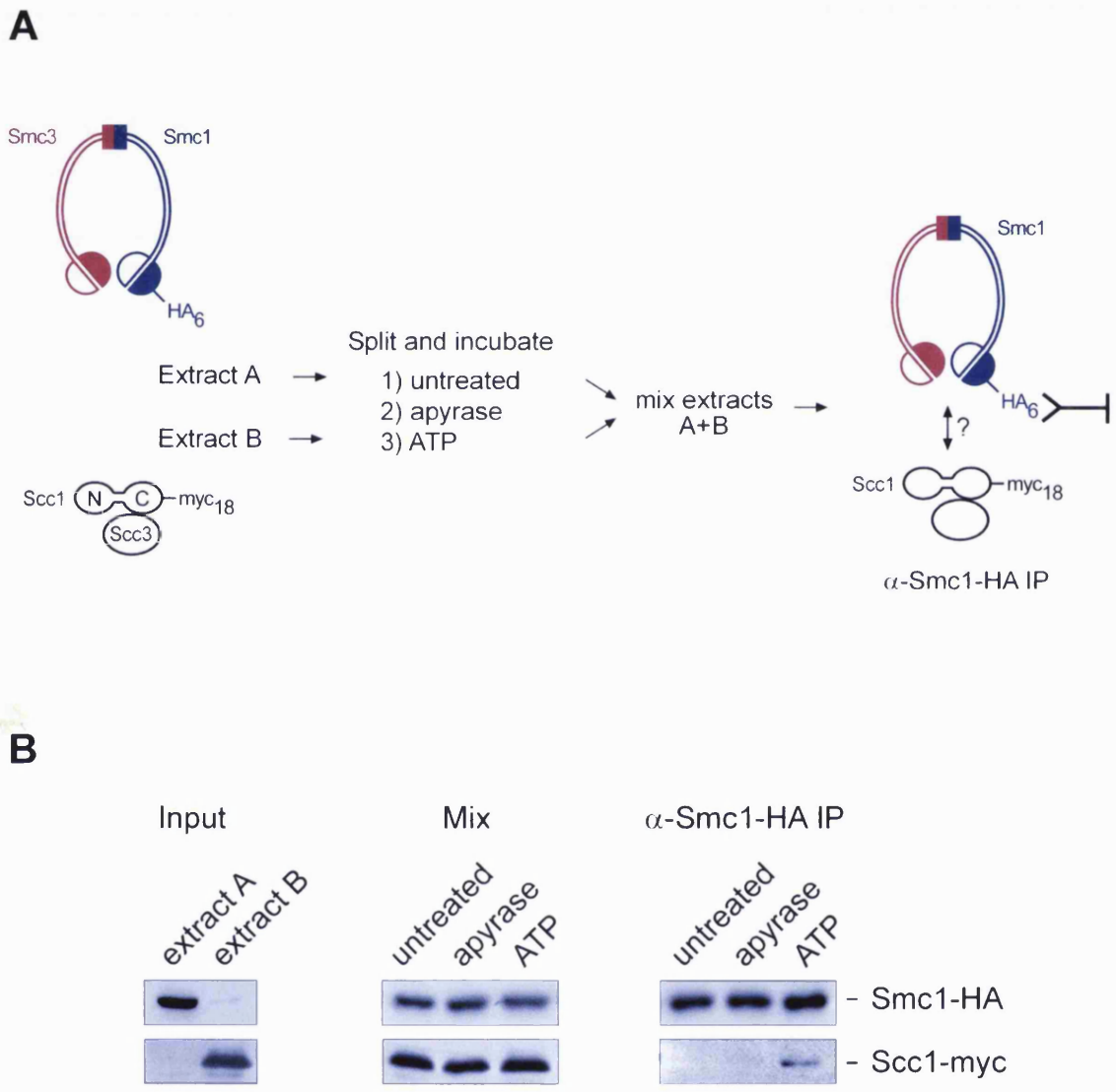

Figure 3.5. ATP binding is required for Scc1 binding to Smc1.

(A) Scheme of the *in vitro* reconstitution system for cohesin described in (B).
(B) Extracts of strain Y749 (*MAT*a, *scc1Δ, GAL-SCC1-myc18, SMC1-HA6*) depleted of Scc1 (extract A), and K7062 (*MAT*a, *scc1Δ, GAL-SCC1-myc18*) expressing Scc1 (extract B) were prepared (left panel, Input) and left untreated or supplemented with apyrase or an ATP regenerating system. Similarly treated extracts from both strains were mixed (middle panel, Mix). Smc1-HA was immunoprecipitated and coprecipitation of Scc1 was analysed (right panel).

CHAPTER 4: Interaction analysis of cohesin SMC heads

Since the suggested role for ATP in sister chromatid cohesion was confirmed (see chapter 3), its function within the catalytic ATPase head domains of cohesin SMCs was analysed. SMC head domains belong to the family of ABC ATPases (Löwe et al., 2001). A common feature of ABC ATPases is the ATP-mediated interaction of their catalytic domains. This has first been discovered by crystal structural analysis of the DNA repair protein Rad50, a close SMC relative that has ATPase heads of similar architecture (Hopfner et al., 2000). In Rad50, ATP binds to Walker A and B motifs in each head and makes contact with the C-motif within the respective opposite head (see Figure 1.9). Two heads are therefore thought to bind to each other, sandwiching a pair of ATP molecules.

So far biochemical analysis of the cohesin complex could not provide evidence for a direct interaction between the Smc1 and Smc3 heads. Instead, it has been shown that both heads are bridged by the Scc1 subunit, whereby each of the terminal Scc1 regions binds to one of the SMC heads to form a closed cohesin ring (Haering et al., 2002). As these studies were performed using recombinant proteins in an insect cell expression system, in this chapter an *in vivo* approach in yeast cells is described to reveal potential head interactions. It was further investigated if such interactions are dependent on ATP binding, as shown for Rad50 and other ABC ATPases, and also whether both SMC heads are required for the association of Scc1 to the Smc1/3 complex.

4.1 The SMC head interaction is independent of Scc1

To test if an interaction between Smc1 and Smc3 is possible even in the absence of Scc1, a 'head-only' version of Smc1 was constructed. This was necessary to assess interactions specifically at the head domains since both SMC proteins also associate with each other at the hinge. The head construct contained the N-terminal domain of Smc1 plus 52 amino acids of coiled coil (1-215 aa) and the C-terminal domain plus 45 amino acids of coiled coil (1023-1225 aa) (Figure 4.1A). Both domains were fused together by a peptide linker of ten glycines. Coiled coil probability for the Smc1

sequence was predicted using the COILS programme (Lupas et al., 1991) (http://www.ch.embnet.org/software/COILS_form.html). At the C-terminus of the Smc1 head, a double protein A tag was inserted. The protein was expressed from the constitutive triose-phosphate isomerase 1 (*TPI1*) promoter in a strain in which Scc1 could be depleted under control of the *GAL1* promoter (see chapter 3.4.2). In addition, this strain contained the endogenous Smc3 protein tagged with an HA_3 epitope. Extracts were prepared from logarithmically growing strains expressing or depleted for Scc1, and the Smc1 head was affinity-purified by binding to IgG sepharose. As shown in Figure 4.1B, Smc3 associated with the Smc1 head both in the presence or absence of Scc1. In a similar experiment, direct head interactions were also detected in cells arrested in G1 phase by alpha-factor or in metaphase by nocodazole, and therefore do not seem to be restricted to a particular cell cycle stage (data not shown). These results suggest that Scc1 is not required for interactions of the SMC heads in yeast cells. This is in contrast to previous data obtained using an insect cell expression system showing a requirement of Scc1 for the interaction between the heads (Haering et al., 2002). Scc1 may stabilise the interaction between Smc1 and Smc3 heads, however, the efficiency of copurification of Smc3 with Smc1 heads was not increased in the presence of Scc1 (Figure 4.1B). Nevertheless, these results do not exclude an Scc1-mediated association of the heads. Two alternative modes of interactions between the SMC heads may therefore exist, a direct interaction as well as an indirect interaction via Scc1.

4.2 Smc1 and Smc3 form a closed ring independently of Scc1

The direct interaction between the SMC heads implies that Smc1 and Smc3 may form a closed ring structure independently of Scc1. If this is correct then hydrodynamic properties of an Smc1/3 dimer is expected to be similar to the wild-type cohesin ring but should differ from an open ring. To test this possibility, three different strains were constructed, all in which Scc1 could be depleted by repressing the *GAL1* promoter. The strains constitutively expressed under control of the *TPI1* promoter either HA epitope tagged wild-type Smc1, Walker A motif mutant Smc1 or Smc1 lacking both N- and C-terminal domains ('headless Smc1'). This headless Smc1 construct spanned amino acids 164-1067 fused at the C-terminus to an HA_3 epitope tag (compare Figure 4.1A). Headless Smc1 was used as a control that was expected to be unable to form a closed

ring with Smc3 (see Figure 4.2B). To allow one-step purification of Smc1/3 complexes, strains also contained the endogenous Smc3 subunit C-terminally fused to a TEV protease cleavage site and Pk_3 epitope tag (see chapter 2.1).

Strains were depleted of Scc1 and extracts were prepared. Smc1/3 complexes were purified by incubation with anti-Pk antibody and coupling to protein A beads, from which they were then eluted by TEV protease. Subsequently the complexes were subjected to glycerol gradient centrifugation. Fractions were collected and analysed by Western blotting using anti-HA antibody to detect the Smc1 protein in the Smc1/3 complexes (Figure 4.2A). As an indicator for the shape of the protein complexes the S_{max}/S ratio was determined. S_{max} is the maximal sedimentation coefficient proteins could display if they were globular in shape, reflecting the molecular weight, and S is the observed sedimentation coefficient (see chapter 7.3.6). The complex of Smc3 with either wild-type or Walker A motif mutant Smc1 sedimented at 9.9 S corresponding to an S_{max}/S ratio of 1.6, indicative of a moderately elongated shape (Figure 4.2B). The S_{max}/S ratio of 14 S wild-type cohesin was also 1.6 (compare Figure 2.4B), consistent with a similar overall shape irrespective of whether Scc1 and Scc3 are bound. The S_{max}/S ratio of Smc3 in complex with headless Smc1 was 1.8, indicating a more elongated shape, in agreement with an open ring formation lacking head-to-head interaction. This result suggests that the Smc1/3 complex forms a closed ring *in vivo*, even in the absence of Scc1.

4.3 ATP-dependent and independent interactions between SMC heads

In ABC ATPases, the interaction between both catalytic domains is mediated by two molecules of ATP, each of which binds to the Walker A and B motifs of one domain and contacts the C-motif of the opposite domain. To test whether head-to-head interaction of cohesin SMCs is mediated in the same manner, point mutations as described in chapter 3.2 were introduced into the Walker A, Walker B and C-motifs within the Smc1 head construct. The Walker A and B mutation is expected to abolish ATP binding to Smc1, and the mutation in the C-motif is expected to allow ATP binding in Smc1 but to prevent interaction with ATP bound to the Smc3 head (Figure 4.3A, scheme). The Smc1 head versions were C-terminally tagged with an HA_3 epitope. Wild-type and the mutant Smc1 heads were expressed under control of the *GAL1*

inducible promoter in a strain that contained the endogenous Smc3 protein tagged with a myc_9 epitope. Extracts were prepared and Smc3 was immunoprecipitated using anti-myc antibody. As shown in Figure 4.3A, the Walker A, Walker B and C-motif mutant Smc1 heads copurifed with Smc3 as efficiently as the wild-type Smc1 head. This suggests that deficiency of ATP binding to the Smc1 head does not affect its association with the Smc3 head, nor does the expected inability of an Smc1 head to interact with an ATP-bound Smc3 head.

An alternative interpretation of this result is that direct interactions between the heads were entirely lost but their association was via the Scc1-dependent binding mode of SMC heads (Figure 4.3B, scheme). This possibility requires Scc1 to be part of a complex with the Smc1 head versions. To test this, wild-type and mutant Smc1 heads were expressed in a strain in which endogenous Scc1 was myc_9 epitope tagged. The Scc1 protein was immunoprecipitated and copurification of Smc1 heads analysed. The wild-type Smc1 head associated with Scc1 but not the Walker A and to a reduced extent Walker B motif mutant heads (Figure 4.3B). This was consistent with previous experiments showing that Scc1 binding is not supported by Walker A and B motif mutant Smc1 (see chapter 3.4.1). Thus, Scc1 did not appear to contribute to their interactions with Smc3 heads.

One possibility to explain the remaining head-to-head interactions of Walker A or B motif mutant Smc1 is that they are mediated by ATP bound to the Smc3 head. Therefore, an Smc1 head construct was made that contained mutations in both Walker A and C-motif, which is expected to abolish all ATP-dependent interactions between the heads. Surprisingly, such double-mutant Smc1 heads still associated with Smc3, although with reduced efficiency (Figure 4.3A), indicating loss of interactions that were ATP-dependent. This suggests that two different sets of interactions exist between the SMC heads, ATP-dependent as well as ATP-independent interactions.

4.4 Both Smc1 and Smc3 heads are required for Scc1 binding

In budding yeast, cohesin is assembled *de-novo* during G1 and S phase when the Scc1 protein is synthesised (Michaelis et al., 1997; Ciosk et al., 2000). Scc1 binds to the Smc1/3 heterodimer which is present in cells throughout the cell cycle. Since the SMC heads can either interact directly with each other or indirectly via Scc1, there are

two possibilities of how the heads initially reside before Scc1 binding. In the first scenario the heads are separated, and the terminal regions of Scc1 bind to the Smc1 and Smc3 heads (Figure 4.4A, model A). In this model, a single SMC head domain may be sufficient for Scc1 binding to the Smc1/3 dimer. This is supported by studies in yeast cells showing that the N- or C-terminal fragments of Scc1 after being cleaved by separase are bound to Smc3 or Smc1, respectively, whose head domains were separated (Gruber et al., 2003). In addition, after coexpression of the recombinant proteins using an insect cell expression system, each of the monomeric SMC proteins copurified with full length Scc1 (Haering et al., 2002). Consistently, the N-terminal half of Scc1 bound to an Smc1/3 dimeric complex lacking Smc1´s head and the C-terminal Scc1 half associated with an Smc1/3 complex lacking Smc3´s head. The other possibility is that the Smc1 and Smc3 heads are both required to associate with Scc1 (model B). In this scenario, interactions between both heads may contribute to a binding platform for Scc1. In contrast to the previous model, a single head domain is therefore not sufficient to recruit the protein.

In order to assess if a single SMC head is sufficient or both SMC heads are required for Scc1 binding, strains were constructed that expressed under *GAL1* promoter control either wild-type proteins or versions of Smc1 or Smc3 missing their entire head domain (Figure 4.4B). The Smc1 construct contained amino acids 164-1067 C-terminally tagged with an HA_3 epitope (compare Figure 4.1A), and the Smc3 construct spanned amino acids 171-1044 fused to an HA_9 tag. To define the flanking regions of the headless Smc3 construct, the COILS program was used again (Lupas et al., 1991). In the strains, the endogenous Scc1 protein was tagged with a myc_9 epitope. The HA-tagged Smc1 or Smc3 proteins were immunoprecipitated and coprecipitation of Scc1 was analysed. Scc1 copurifed only with complexes containing wild-type SMC proteins but not with those containing a headless SMC protein (Figure 4.4B). To confirm in these complexes the expected formation of SMC heterodimers via the hinge, the endogenous Smc1 or Smc3 proteins in strains expressing wild-type or headless Smc3 and Smc1, respectively, were additionally tagged with a Pk_3 epitope. As shown in Figure 4.4B (middle panel), endogenous wild-type SMC proteins that provided intact head domains were present in complexes with the headless SMC versions. Therefore, a single head domain does not support complex formation with Scc1 in yeast cells suggesting that both Smc1 and Smc3 heads are essential for Scc1 binding. This result is

consistent with the idea that head-to-head interactions between both SMC proteins may be a prerequisite for the recruitment of Scc1 (model B). This interpretation finds support in the observation that Smc1 heads containing mutations in the Walker A or B motifs did not support complex formation with Scc1 (see chapters 3.4.1 and 4.3). These complexes contained both SMC heads, but their ATP-dependent interaction may have been compromised. However, at this stage it is not possible to rule out 'model A' that requires presence of both intact SMC heads but not necessarily contact between them for the interaction with Scc1.

4.5 Summary

- As shown by Scc1 depletion experiments, Smc1 and Smc3 heads interact independently of the Scc1 subunit in yeast cells. This represents a novel binding mode of cohesin's SMC heads in addition to Scc1-dependent head interactions that have previously been reported in a different system.

- The Smc1 and Smc3 subunits form a complex whose hydrodynamic properties are indistinguishable from those of the closed cohesin ring. Therefore, the SMC subunits by themselves form a closed ring, consistent with their observed head-to-head interactions in the absence of Scc1.

- Coimmunoprecipitation studies of ATPase motif mutant Smc1 proteins suggest that interactions between cohesin SMC heads are ATP-dependent as well as ATP-independent.

- In yeast cells, Scc1 is not part of Smc1/3 complexes lacking one of the two SMC heads, as shown by coimmunoprecipitation. Therefore, both SMC heads are required for binding of Scc1 to the Smc1/3 complex.

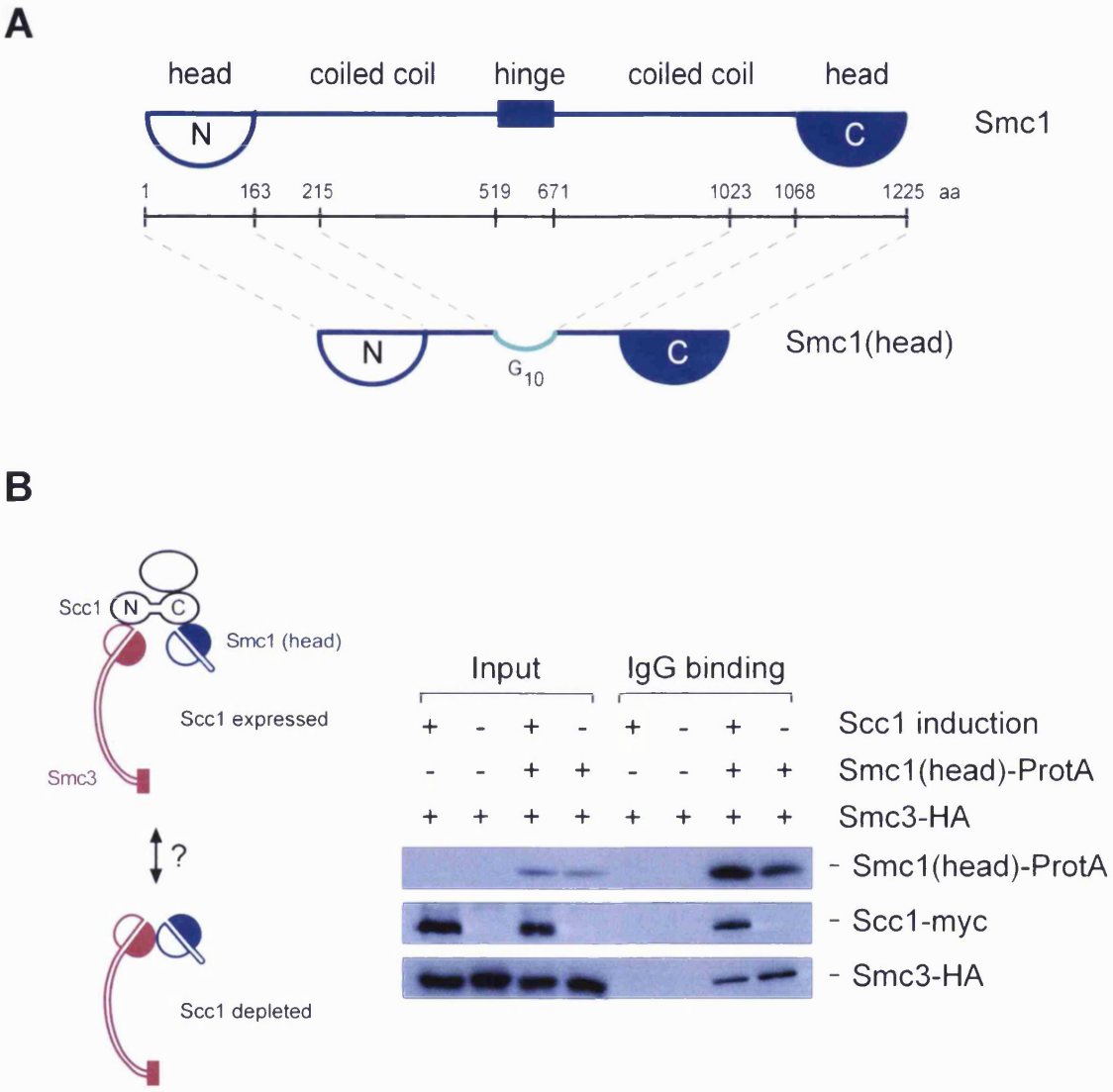

Figure 4.1. Interactions between Smc1 and Smc3 heads do not require Scc1.

(A) Scheme of the Smc1 head construct. Protein domains within Smc1 were defined by their coiled coil probability according to the COILS algorithm (Lupas et al., 1991). G_{10}, peptide linker of ten glycines.
(B) Scc1 was either expressed or depleted from strain Y1172 (*MAT*a, *scc1Δ, GAL-SCC1-myc18, SMC3-HA3, TPI-SMC1(head)-ProtA*) in which Smc1 heads were constitutively expressed. Copurification of Smc3 with Smc1 heads was tested.

A

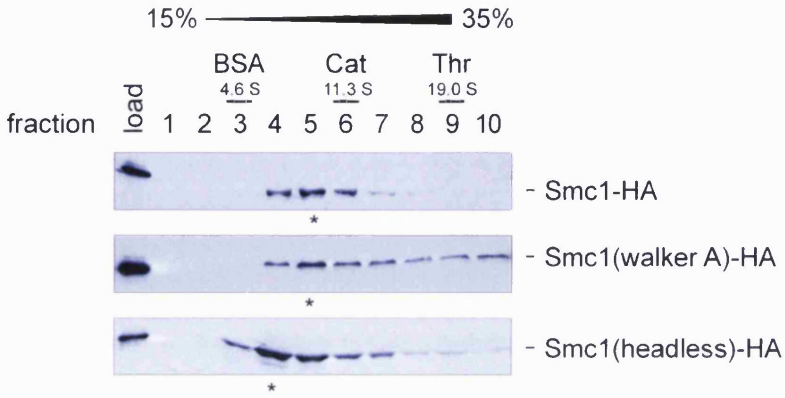

B

	MW (kDa)	S_{max}	S	S_{max}/S
Smc1 Smc3 + Scc1/3	488	22.4	14.1	1.6
Smc1 Smc3	291	15.9	9.9	1.6
Smc1(walkerA) Smc3	291	15.9	9.9	1.6
Smc1(headless) Smc3	251	14.4	7.8	1.8

Figure 4.2. Sedimentation properties of Smc1/3 complexes without Scc1 are consistent with closed rings.

(A) Three different strains were used that constitutively expressed either wild-type Smc1 (Y1418: *MAT*a, *scc1Δ, GAL-SCC1-myc18, SMC3-TEV-Pk3, TPI-SMC1-HA6*), Walker A motif mutant Smc1 (Y1419), or headless Smc1 (Y1420). Scc1 was depleted from these strains by repression of the *GAL1* promoter, and Smc1/3 complexes purified by pulldown of Smc3 via the Pk tag. Complexes were eluted by TEV cleavage and subjected to glycerol gradient centrifugation. Western analysis of the fractions was performed to detect the Smc1 protein in the complexes. Asterisks (*) indicate the peak fractions of the complexes.
(B) The shape of the Smc1/3 complexes (depicted on the left side) was analysed by determination of the S_{max}/S ratio. S_{max} is the maximal sedimentation coefficient that represents the molecular weight, and S is the observed sedimentation coefficient of the complexes. The S value for wild-type cohesin was derived from Figure 2.4B.

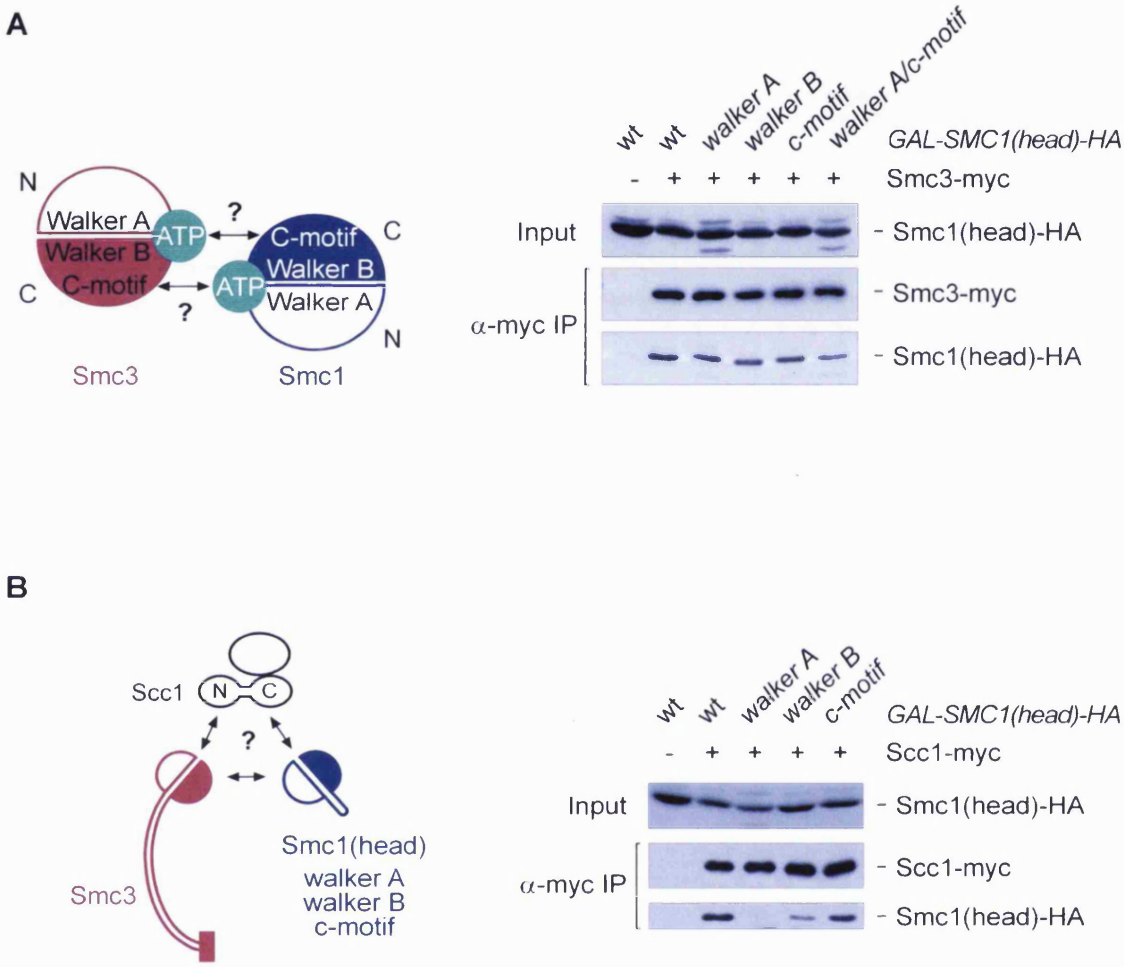

Figure 4.3. ATPase motif mutant Smc1 heads interact with Smc3 in an ATP-dependent and independent manner.

(A) Binding of ATPase motif mutant Smc1 heads with Smc3. Left panel: Model of potential ATP-mediated interactions between the Smc1 and Smc3 heads based on analogy to head interactions in Rad50. Right panel: Extracts of strains expressing wild-type (Y1000: *MAT*a, *pep4Δ, SMC3-myc9, GAL-SMC1(head)-HA3*), Walker A (Y1321), Walker B(Y1322), C-motif (Y1001), or double Walker A and C-motif mutant Smc1 heads (Y1478) were prepared and binding to Smc3-myc was analysed.
(B) Walker A and B mutant Smc1 heads bind to Smc3 independently of Scc1. Left panel: Scheme of possible interactions between Smc1 and Smc3 heads and Scc1. Right panel: Wild-type (Y956: *MAT*a, *pep4Δ, SCC1-myc9, GAL-SMC1(head)-HA3*), Walker A (Y1319), Walker B (Y1320), or C-motif mutant Smc1 heads (Y999) were expressed and their coprecipitation with Scc1-myc was tested.

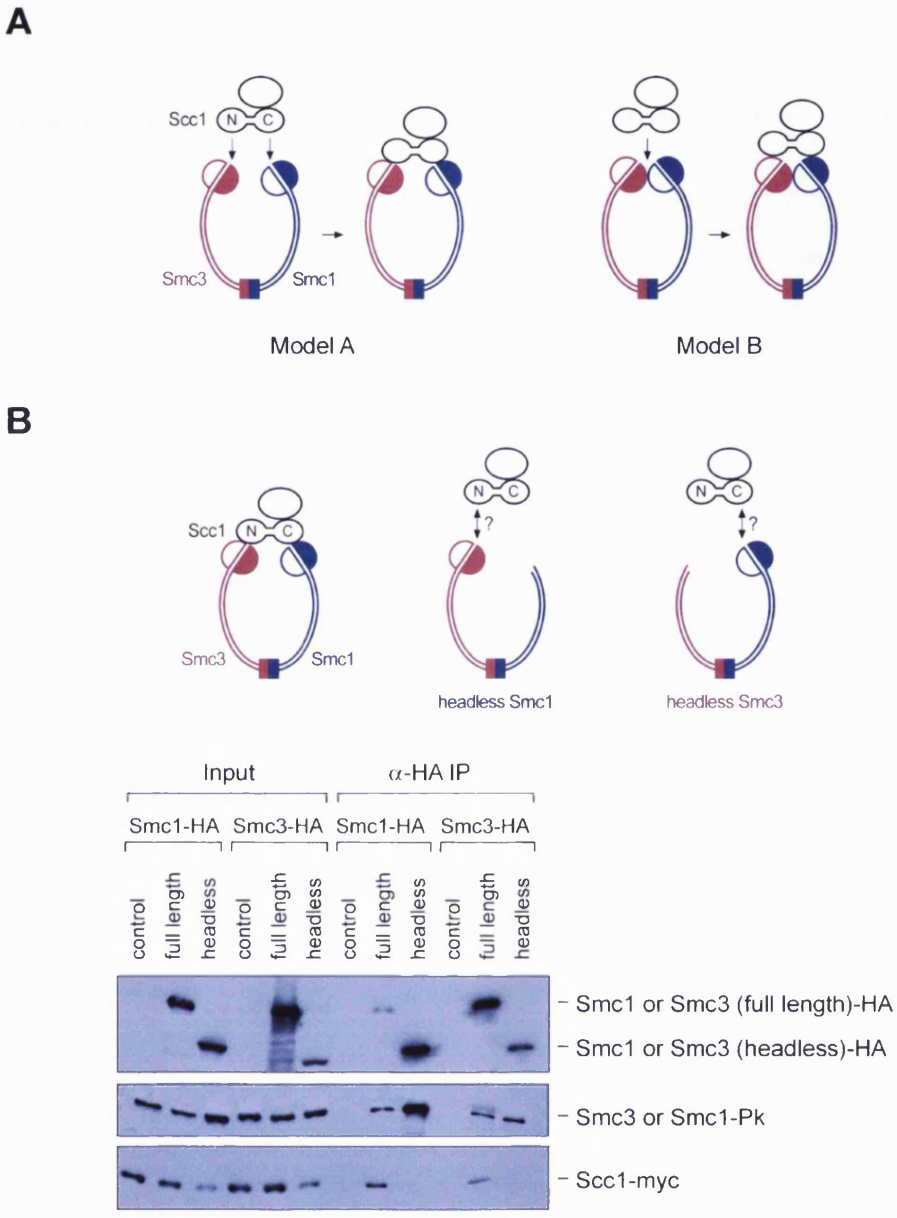

Figure 4.4. Smc1 and Smc3 heads are both required for Scc1 binding.

(A) Two models of Scc1 assembly onto the Smc1/Smc3 dimer. In model A, SMC heads are separated. Binding to Scc1 is mediated by interaction of the heads with the Scc1 termini. Model B suggests that interactions between the SMC heads may be required to allow Scc1 binding.
(B) Scc1 does not bind to an SMC dimer lacking one of the heads. Wild-type Smc1 (Y1719: *MAT*a, *pep4Δ, SMC3-Pk3, SCC1-myc18, GAL-SMC1-HA6*) or a headless version of Smc1 Y1720) as well as wild-type Smc3 (Y1721: *MAT*a, *pep4Δ, SMC1-Pk3, SCC1-myc18, GAL-SMC3-HA9*) or headless Smc3 (Y1722) were expressed and immunopurified. Coprecipitation of Scc1 and the respective other SMC subunit was analysed (compare with scheme in the upper panel).

CHAPTER 5: DNA loading and unloading of cohesin

The cohesin complex is assembled when the Scc1 protein is synthesised during G1 and S phase in budding yeast. Scc1, together with the Scc3 subunit, binds to the Smc1/3 heterodimer, and only once cohesin is fully assembled, does it associate with chromatin (Michaelis et al., 1997; Tóth et al., 1999; Ciosk et al., 2000). The mechanism how cohesin is loaded onto chromatin is completely unclear. A possible model for cohesin binding to chromatin is provided by its ring structure that could topologically embrace DNA. If this is correct, how then is DNA initially transported into the cohesin ring that is closed at its interacting SMC ATPase heads (compare chapter 4)? In ABC ATPases, ATP hydrolysis causes disengagement of catalytic domains which in analogy could allow such transport of DNA.

A mutant in the C-motif of the Smc1 ATPase head which is expected to abolish ATP hydrolysis did not support cell viability and sister chromatid cohesion, even though an intact cohesin complex was formed (compare chapter 3). Experiments in the present chapter address whether the C-motif is essential for cohesin binding to chromatin which would then indicate a potential role for ATP hydrolysis in this process.

If DNA is entrapped in cohesin's ring, how does cohesin become unloaded from DNA in anaphase? Interactions between the SMC head domains would have to become disrupted to allow DNA release from the ring. This chapter analyses the requirements that enable head separation to allow cohesin unloading from DNA.

5.1 The C-motif of Smc1 is not required for chromosome segregation

In order to reveal the function of the Smc1 C-motif, it was characterised in more detail. As shown in Figure 3.3A, C-motif mutant Smc1 does not support cell viability. This was surprising since subunit composition of cohesin formed by C-motif mutant Smc1 appears to be mostly indistinguishable from wild-type complexes (Figure 3.4). One possibility is that ATP hydrolysis might not be required for cohesion establishment but for loss of cohesion. If this is true then chromosome segregation during anaphase is

expected to be impaired when sisters are held together by cohesin containing C-motif mutant Smc1. To test this, a strain was used that contained a temperature sensitive allele of the *CDC15* gene (*cdc15-2*) which is required for cells to exit from mitosis (Fitch et al., 1992). At the restrictive temperature of 37°C, this strain arrests in telophase, and if sister chromatid segregation was unaffected, sisters will be present in both mother and daughter cells at that stage. To visualise sister segregation, the Tet-Operator/Tet-Repressor-GFP system was used as described before (see chapter 3.3). Wild-type or C-motif mutant Smc1 were expressed and cells were treated at the permissive temperature of 23°C with pheromone (alpha-factor) that synchronised cells in G1 phase. Cells were then released into the cell cycle at the restrictive temperature and sister chromatid segregation was scored until complete telophase arrest. To confirm arrest in G1 and telophase, the budding index, as an indication of cells passing through S-phase, was measured. As shown in Figure 5.1, the degree of sister chromatid segregation was identical in wild-type and C-motif mutant Smc1 expressing cells which in both was about 80%. The remaining population of cells showed only sister separation and not segregation which was probably due to a minor segregation defect inherent to the *cdc15-2* strain at the restrictive temperature. This result demonstrates that C-motif mutant Smc1 does not interfere with loss of cohesion and sister chromatid segregation. Therefore ATP hydrolysis rather appears to be required for processes leading to the establishment or maintenance of a linkage between replicated sisters, consistent with the inability of C-motif mutant Smc1 to support sister chromatid cohesion (compare Figure 3.3B). This result is also consistent with the previous data showing that expression of C-motif mutant Smc1 did not exert a dominant negative effect on cell viability (compare Figure 3.3A).

5.2 The C-motif of Smc1 is required for DNA loading of cohesin

The Smc1 C-motif mutant does not affect segregation of sister chromatids but does not support cohesion between them. To further assess potential functions of the C-motif, it was next tested whether cohesin complexes formed by the mutant protein were able to bind to chromatin. The HA_6-epitope tagged wild-type or C-motif mutant Smc1 proteins were expressed at the permissive temperature of 22°C in an *smc1*^{ts} strain containing Scc1 as a myc_9 epitope tagged protein. The cells were synchronised by alpha-factor

treatment in G1 phase. Then cells were released into the cell cycle at the restrictive temperature of 35.5°C and arrested in metaphase by nocodazole treatment. Budding index of cells were measured that confirmed G1 and metaphase arrest. During a time course after release from G1, samples were taken for chromosome spreading. Using this technique, cohesin binding to chromatin was visualised by immunostaining of the myc_9 epitope tagged Scc1 protein. Cells expressing wild-type Smc1 efficiently loaded cohesin onto chromatin (Figure 5.2A). In contrast, Scc1 did not associate with chromosomes in cells expressing C-motif mutant Smc1 or in cells that do not express Smc1. Western analysis confirmed the same expression levels of wild-type and mutant proteins in metaphase (Figure 5.2B). This result shows that C-motif mutant Smc1 does not support cohesin binding to chromosomes and suggests that the Smc1 C-motif is required for DNA loading of cohesin.

5.3 A closed cohesin ring is essential for DNA binding

One reason why the C-motif mutation prevented chromatin binding of cohesin could be that even though all subunits assembled into a complex, a closed ring structure was not formed. DNA would thereby never become fully embraced by cohesin's ring, and any association of cohesin with chromosomes would not be maintained. However, analysis of head interactions described in chapter 4 has shown that a C-motif mutant Smc1 head copurified in immunoprecipitations of the Smc3 protein (see Figure 4.3A). This indicates that rather a reaction involving an intact C-motif and therefore possibly hydrolysis of ATP is required for loading cohesin onto DNA.

The role of ATP hydrolysis might be to transiently open up the head-to-head interaction, as observed in ABC ATPases. This would then allow transport of DNA into the cohesin ring. Alternatively, ATP hydrolysis might be required for a DNA binding reaction different from DNA transport and the SMC heads themselves might mediate DNA binding. Such binding of DNA to ATPase heads has been proposed in structural studies of the Rad50 protein complex (Hopfner et al., 2000). If this also holds true for cohesin, then DNA binding should be observed in a complex that contains intact SMC heads but is disrupted at the hinge. To test this, the Smc1 head construct, that included part of the coiled coil but lacked the hinge, was used again (see Figure 4.1A). Firstly it had to be ensured that the Smc1 head was part of an intact SMC head complex

including Smc3, Scc1 and Scc3. The Smc1 head bound to Smc3 and Scc1 which has previously been shown (see Figure 4.3). To test association with Scc3, the HA_3 epitope tagged Smc1 head was expressed in a strain in which endogenous Scc3 was present as a Pk_3 epitope tagged protein. The Scc3 protein was then immunoprecipitated using anti-Pk antibody. As shown in Figure 5.3A, copurification of the Smc1 head was observed which confirmed that both proteins are part of the same complex. Next, in order to assess chromatin binding of such complexes, the Smc1 head construct was expressed in *smc1*^{ts} cells containing endogenous Scc1 protein tagged with a myc_9 epitope. Cells were released from G1 arrest into metaphase at the restrictive temperature as described before and chromosome spreading used to analyse Scc1-myc_9 binding to chromatin. As shown in Figure 5.3B, the Smc1 head complex did not associate with chromatin, suggesting that an intact SMC head complex is not sufficient for DNA binding.

The above cohesin head complex lacked part of the Smc1 coiled coil and hinge. It was next tested whether these parts of Smc1 might directly contribute to chromatin binding. This is conceivable since DNA binding activity of the hinge region has been reported for *B. subtilis* BsSMC and bovine Smc1/3, and additionally cohesin coiled coils were found to associate with DNA (Akhmedov et al., 1999; Hirano and Hirano, 2002; Chiu et al., 2004). For this study, the headless Smc1 construct (described in chapter 4.2) was used since it contained the hinge and coiled coil. When expressed in cells, the headless Smc1 protein assembled into an SMC dimer that does not form closed rings and does not bind Scc1 (compare Figures 4.2 and 4.4B). This allowed to directly assess any contribution of the SMC´s coiled coil and hinge domains to cohesin loading onto chromatin. The headless Smc1 was expressed as an HA_3 epitope tagged protein and immunostained on chromosome spreads of cells taken during a release from G1 into metaphase. The SMC dimer formed by the headless Smc1 protein did not show any association with chromatin, indicating that cohesin´s coiled coil and hinge domains by themselves are not sufficient for DNA binding (Figure 5.3C).

Taken together, these results suggest that all parts of Smc1 are necessary for cohesin´s binding to DNA. The failure of DNA association with the SMC head complex alone could be explained by the absence of a topological trap provided by Smc1´s coiled coil and hinge. However, it cannot be excluded that both domains are required for a DNA binding reaction by the SMC heads other than providing a trap. Nevertheless, the results altogether suggest that the integrity of Smc1 is a prerequisite for chromatin

association of cohesin. This strongly indicates that a closed cohesin ring is essential for DNA binding, consistent with a model of topological DNA entrapment and a role for ATP hydrolysis in transporting DNA into the ring.

5.4 A closed Smc1/3 ring is not sufficient for cohesin binding to DNA

Results presented in the previous chapter suggested that a closed cohesin ring is required for binding to DNA. As shown in chapter 4, the Smc1/3 complex by itself forms a closed ring by interaction of the SMC head domains. If the mere ring structure of cohesin is sufficient for stable DNA binding, then an Smc1/3 complex without the Scc1 and Scc3 subunits should associate with chromatin. This possibility was tested using cells in which the Scc1 subunit could be depleted. In these cells, the Scc3 protein is also not expected to be part of the Smc1/3 complex because studies using the insect cell expression system have shown that it binds to the complex via Scc1. However, to confirm this in yeast, cells were used in which the endogenous Smc1 protein was tagged with an HA_6 epitope and Scc3 with a Pk_3 epitope. Scc1 was depleted from these cells by repressing its expression controlled by the *GAL1* promoter. In immunoprecipitates of Scc3-Pk_3, Smc1 was only detected in the presence but not in the absence of Scc1 (Figure 5.4A). This result excludes that the Scc1 and Scc3 subunits are part of the Smc1/3 complex which could influence its potential association with chromatin.

To test binding of the Smc1/3 ring to chromatin, Scc1 was depleted from cells containing the endogenous Smc1 protein tagged with an HA_6 epitope. The cells were then released from G1 into metaphase, and chromatin association of Smc1 analysed on chromosome spreads using anti-HA antibody. As shown in Figure 5.4B, Smc1 was not detectable on spreads in the absence of Scc1. This suggests that the Smc1 and Smc3 subunits by themselves do not bind to DNA *in vivo* even though they assemble into a closed ring structure. This is also consistent with previous observations showing that only fully assembled cohesin can bind to chromatin in yeast (Tóth et al., 1999). Therefore, the Smc1/3 ring requires the Scc1/3 sub-complex for the initial loading onto DNA and/or the maintenance of a stable association with DNA.

5.5 Hydrolysable ATP stimulates dissociation of Scc1 from the SMCs *in vitro*

If disengagement of the SMC heads caused by ATP hydrolysis allows entry of DNA into the ring, how then does DNA initially pass by the Scc1 protein whose terminal regions are bound to them? ATP hydrolysis or the separation of the heads themselves may stimulate transient dissociation of Scc1 from the SMCs which is sufficient for DNA getting transported into the ring. If this is correct then ATP but maybe not ADP or the non-hydrolysable ATP analogue, ATPγS, might promote transient disassembly of cohesin. To test whether evidence for such cycles of engagement and disengagement of the SMC heads could be obtained (Figure 5.5A), an *in vitro* reaction was set up. In this reaction Scc1 was immobilised on beads, and it was measured whether SMC proteins could be released from the beads and recovered in a supernatant fraction in a manner that depends on hydrolysable ATP. To test this possibility, a strain was used in which endogenous Smc1 was tagged with a myc_{18} epitope and Scc1 with an HA_6 epitope. Cells were blocked in metaphase by nocodazole treatment, when cohesin is fully assembled, and extracts were prepared. Cohesin was immunoprecipitated via Scc1 using anti-HA antibody and protein A beads, and immunoprecipitates were subsequently split into five aliquots. The aliquots were either supplemented with ADP, ATP, ATPγS, an ATP regenerating system or left untreated, and were then incubated. Protein released from the beads was separated from protein bound to the beads, and aliquots representing equal protein distribution analysed by Western blotting. Smc1 was partially released from Scc1 bound to the beads only in the presence of ATP and the ATP regenerating system but not with ADP or ATPγS (Figure 5.5B). ADP did not promote release possibly due to the inability of the complex to become re-assembled for the next cycle of SMC head engagement/disengagement, and ATPγS might have inhibited disengagement of the heads. This result suggests that ATP hydrolysis by the SMC heads or their subsequent separation may transiently disrupt Scc1-SMC interactions. This is consistent with the idea that ATP hydrolysis is required for DNA to enter the cohesin ring.

5.6 A role for the C-terminal Scc1 cleavage product in unloading of cohesin from DNA

Cohesin dissociates from chromatin in anaphase upon cleavage of the Scc1 subunit by separase (Uhlmann et al., 1999; Uhlmann et al., 2000). According to the cohesin ring model, DNA release is only possible if the ring becomes disrupted. SMC heads can interact with each other independently of Scc1, and simply destroying Scc1 would not be predicted to disrupt the cohesin ring. Alternatively, even if heads associate via Scc1 and the ring gets disrupted by its cleavage, what prevents the heads interacting with each other before all DNA is released from the ring?

One possibility is that the Scc1 cleavage products play an active role during anaphase in opening up the cohesin ring or maintaining an open conformation. While the N-terminal Scc1 fragment after cleavage remains in cells throughout the cell cycle, the C-terminal cleavage product is degraded by the N-end rule pathway shortly after it is created (Rao et al., 2001). The N-terminal arginine of the cleavage product is recognised by the Ubr1 protein that targets it for degradation by the proteosome. A non-degradable version can be made by replacing arginine with a stabilising residue that is not recognised by Ubr1. Overexpression of such a non-degradable version in cells is lethal, and stabilisation of the C-terminal Scc1 cleavage product by deleting the *Ubr1* gene causes high frequency of chromosome loss. Therefore, its destruction in anaphase seems to be crucial for some aspects of cohesin function.

To test if the C-terminal cleavage product of Scc1 (269-566 aa) can potentially disrupt the SMC head interaction, a non-degradable FLAG epitope tagged version was used in which the N-terminal arginine was replaced with a stabilising methionine (Rao et al., 2001). The fragment was expressed by induction of the *GAL1* promoter in cells arrested by alpha-factor in G1 phase when endogenous Scc1 is absent (Michaelis et al., 1997). In these cells, the Smc1 head construct, tagged with a protein A epitope, was constitutively expressed from the *TPI1* promoter. The Smc1 head was affinity purified by binding to IgG sepharose and copurification of endogenous HA_3 epitope tagged Smc3 analysed. Smc3 copurified with the Smc1 head but only in the absence of the Scc1 fragment. After induction of the *GAL1* promoter, the Scc1 fragment bound to the Smc1 head and displaced Smc3 (Figure 5.6A). This indicates that the C-terminal cleavage product of Scc1 has the potential to disrupt the interaction between the Smc1

and Smc3 heads. Expression of the Scc1 fragment caused separation of the heads even if this experiment was performed in metaphase arrested cells when endogenous Scc1 is stably bound to cohesin. Therefore, the exogenously expressed fragment appears to counteract in a dominant manner Scc1's proposed function of holding SMC heads together (data not shown).

The above experiments have shown that the C-terminal Scc1 fragment disrupts SMC head interactions when ectopically expressed in cells. To assess whether the endogenous cleavage fragment was sufficient to separate SMC heads, the following experiment was conducted. Cells were arrested in G1 but the fragment was not ectopically expressed. Instead, cells were deleted for the *Ubr1* gene which stabilised the endogenous C-terminal Scc1 cleavage product throughout the cell cycle (Rao et al., 2001). However, endogenous amounts of the fragment in G1 did not cause measurable disruption of the head interaction (data not shown). This suggests that the Scc1 fragment produced by separase during anaphase has the potential for separation of SMC heads, but that additional regulation might control this process *in vivo*.

Unloading of cohesin from DNA is thought to require opening of the ring by disrupting the SMC head interactions. If this is correct then expression of the Scc1 fragment in metaphase arrested cells should be sufficient for DNA release, thereby causing sister chromatid separation. To test this, cells were arrested in metaphase by depletion of Cdc20 under control of the methionine repressible promoter, and the Scc1 cleavage fragment was expressed by induction of the *GAL1* promoter. Sister separation was analysed using the Tet-Operator/Tet-Repressor-GFP system. Upon expression of the Scc1 cleavage fragment, sister chromatids separated in a significant fraction of cells, in contrast cohesion between sisters was maintained in control cells (Figure 5.6B). The metaphase arrest during the experiment was confirmed by measuring the budding index (data not shown). Thus, the C-terminal Scc1 cleavage fragment has the potential to trigger sister chromatid segregation by opening up the cohesin ring.

5.7 Summary

- The C-motif of Smc1 is essential for cohesion between sister chromatids but is not required for their segregation in anaphase.

- Further characterisation of the mutant using chromosome spreading indicated that an intact C-motif of Smc1, and therefore possibly hydrolysis of ATP, is required for loading cohesin onto DNA.

- An intact SMC head complex or the hinge is not sufficient for binding of cohesin to DNA. A closed ring of Smc1 and Smc3 also does not bind to DNA by itself. Only a closed ring that is fully assembled with all cohesin subunits is loaded onto DNA. This is consistent with a model in which the SMC heads, together with Scc1 and Scc3, transport DNA into the cohesin ring whose role it is to enclose DNA.

- In an *in vitro* assay, ATP but not non-hydrolysable ATP stimulates Scc1 dissociation from Smc1. This suggests that ATP hydrolysis might not only cause disengagement of the SMC heads but subsequently might also promote transient release of Scc1 from the SMCs. This may allow DNA to initially pass by Scc1 to enter the cohesin ring.

- Expression of the C-terminal Scc1 cleavage product causes disruption of SMC head interactions and triggers sister chromatid segregation. It might therefore play an active role in opening up the cohesin ring or maintain it open during anaphase to allow release of DNA from the ring.

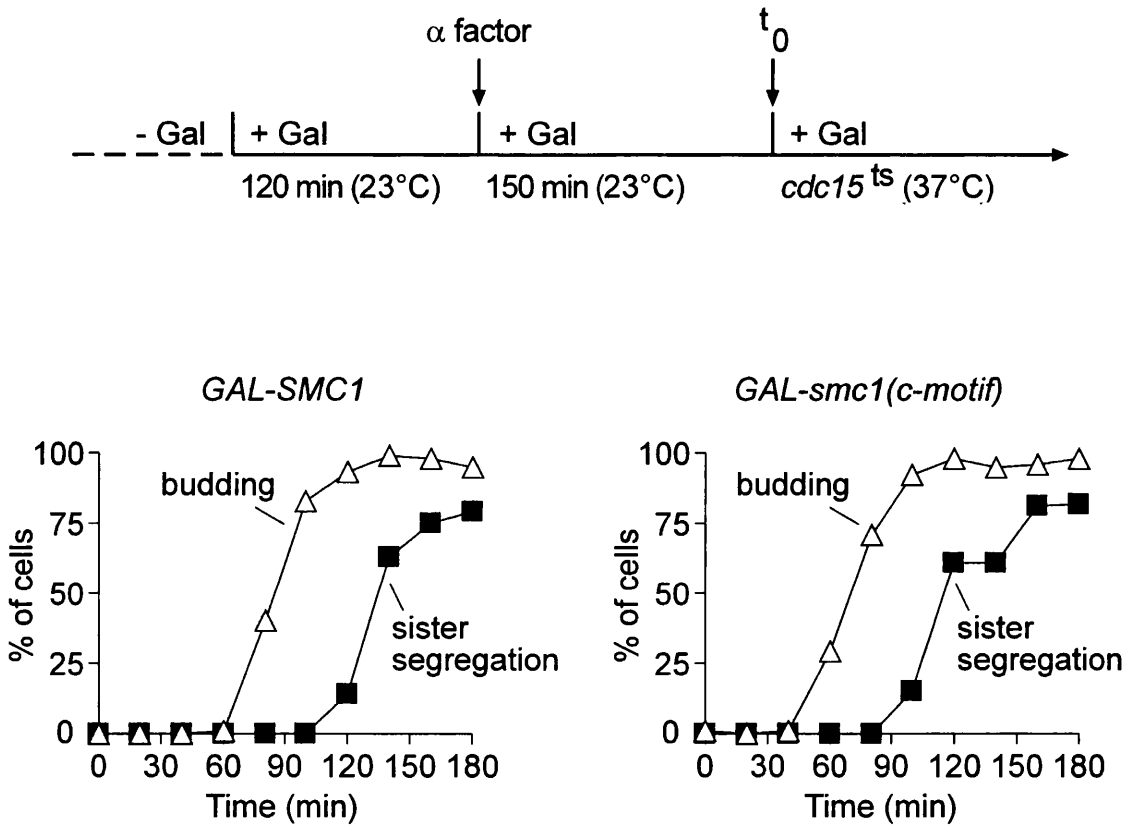

Figure 5.1. The C-motif of Smc1 is not required for chromosome segregation.

cdc15^{ts} strains expressing wild-type (Y917: *MAT*a, *cdc15-2*, *TetR-GFP*, *TetOs::URA*, *GAL-SMC1-HA6*) or C-motif mutant Smc1 (Y918) were blocked in G1 by alpha-factor treatment at 23°C and released at 37°C to arrest cells in telophase. Segregation of sister chromatids and budding index was analysed at indicated time points.

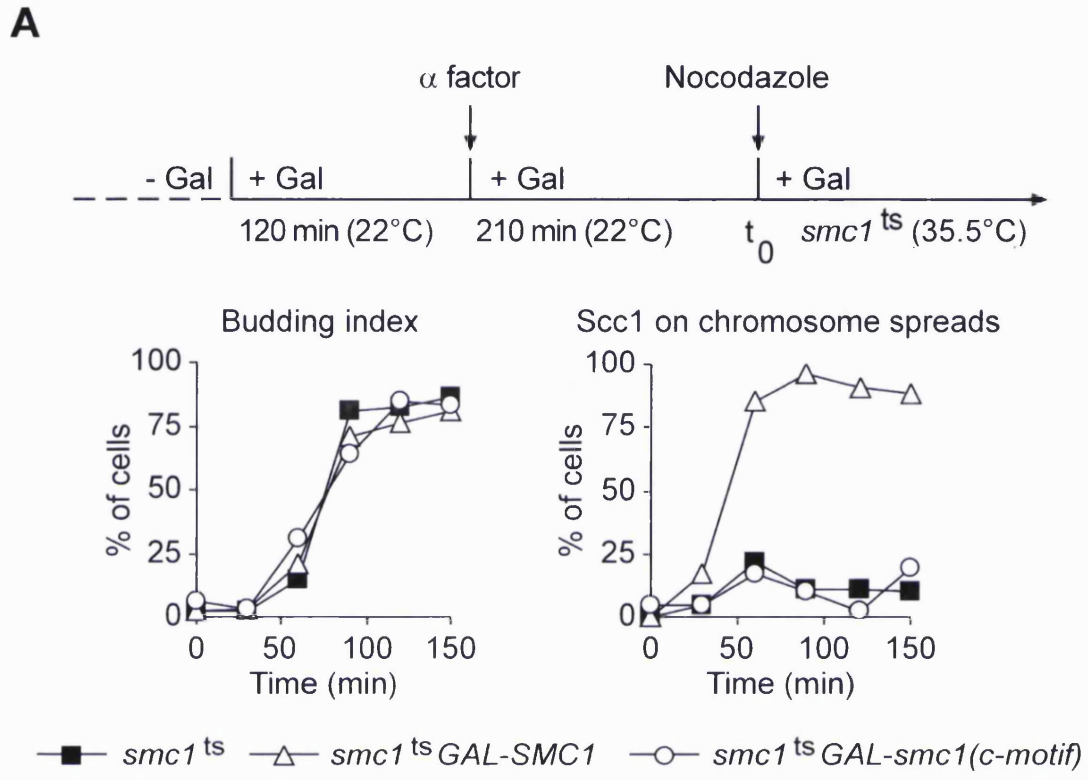

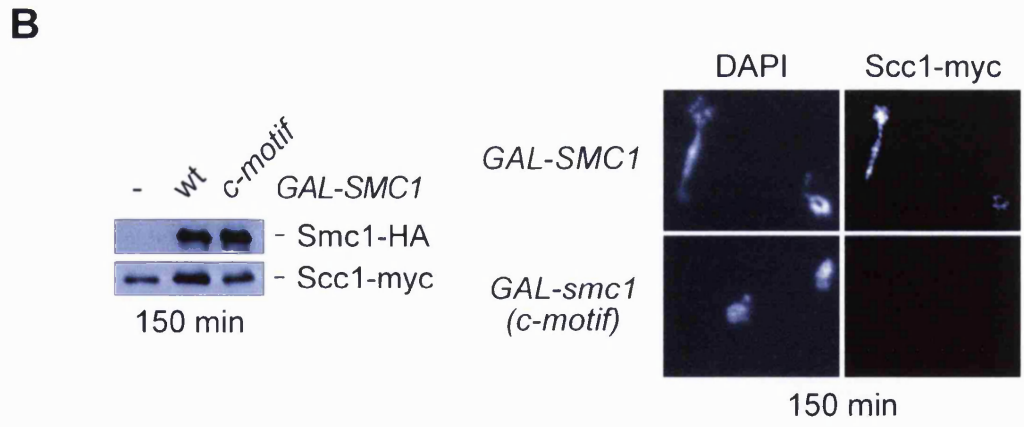

Figure 5.2. C-motif mutant Smc1 prevents cohesin binding to DNA.

(A) *smc1*^{ts} strains expressing wild-type (Y797) or C-motif mutant Smc1 (Y826) were arrested in G1 by alpha-factor treatment at 22°C, released at 35.5°C and blocked in metaphase by addition of nocodazole. Chromatin association of cohesin at indicated times was analysed by immunostaining of Scc1-myc on chromosome spreads.
(B) Expression levels of Smc1 and Scc1 (left panel) and an example of chromosome spreads (right panel) at 150 min after release are shown. Scc1-myc was detected on chromosome spreads using monoclonal antibody 9E10, DNA was visualised by 4′,6-diamidino-2-phenylindole (DAPI) staining.

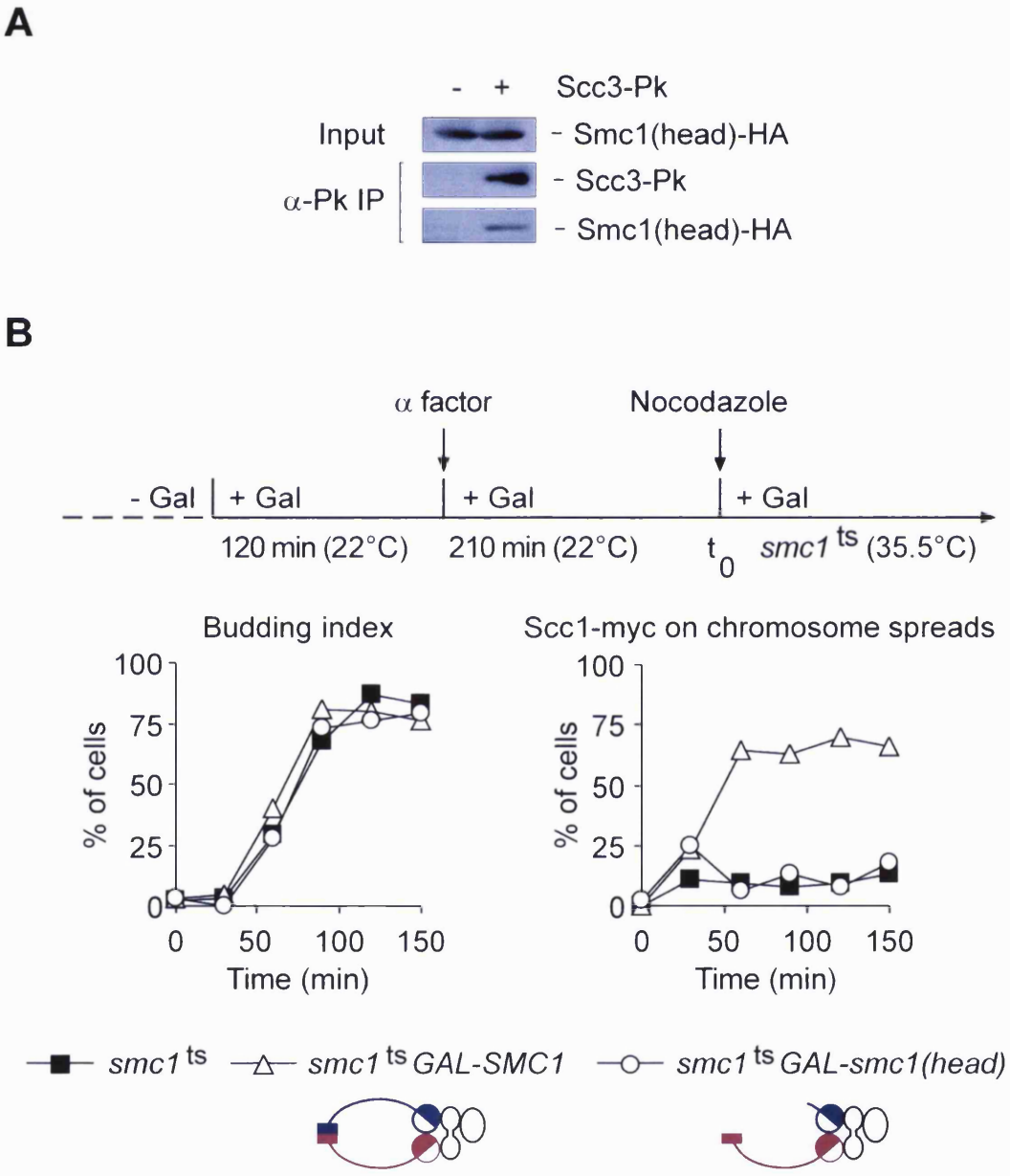

Figure continues…

...Figure continued

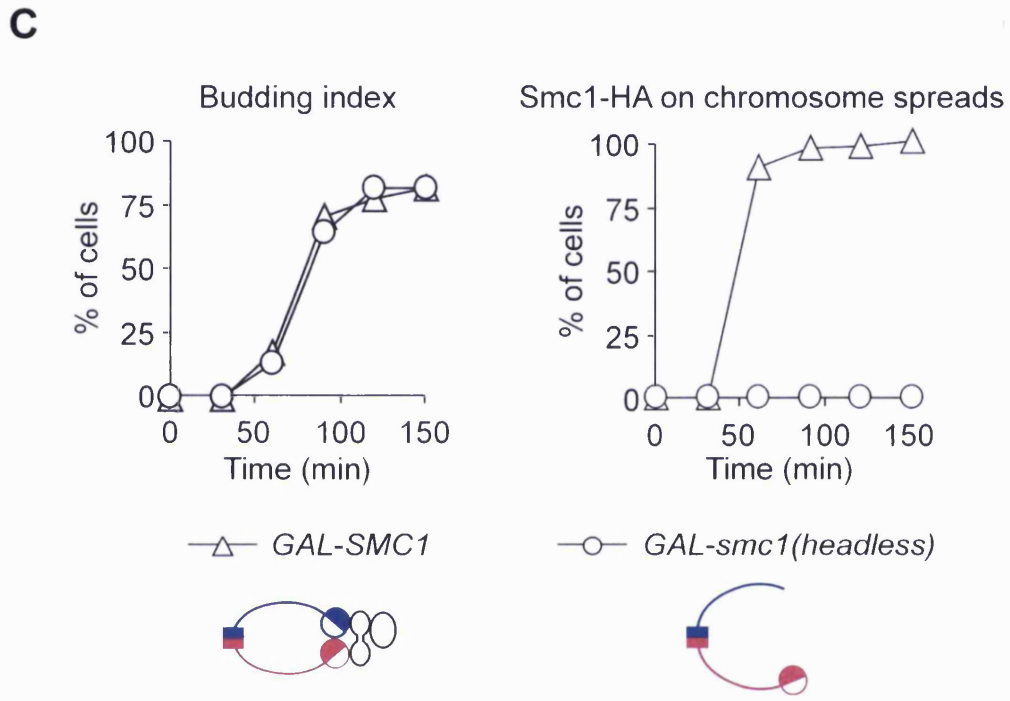

Figure 5.3. A closed cohesin ring is required for DNA binding.

(A) Scc3 is present in the complex formed with Smc1 heads. Smc1 head was expressed in strain Y1542 (*MAT*a, *pep4Δ, SCC3-Pk3, GAL-SMC1(head)-HA3*), and coprecipitation with Scc3 was analysed.
(B) An SMC head complex is not sufficient for binding to DNA. *smc1*^{ts} strains expressing wild-type Smc1 (Y797) or the Smc1 head construct (Y1065) were arrested in G1 by alpha-factor treatment at 22°C, released at 35.5°C and blocked in metaphase by addition of nocodazole. Chromatin association of cohesin was analysed as in Figure 5.2.
(C) A complex containing headless Smc1 does not bind to DNA. *smc1*^{ts} strains expressing wild-type Smc1 (Y797) or a headless version of Smc1 (Y1225) were released from G1 arrest into metaphase. Smc1-HA staining on chromosome spreads was detected using monoclonal antibody 16B12.

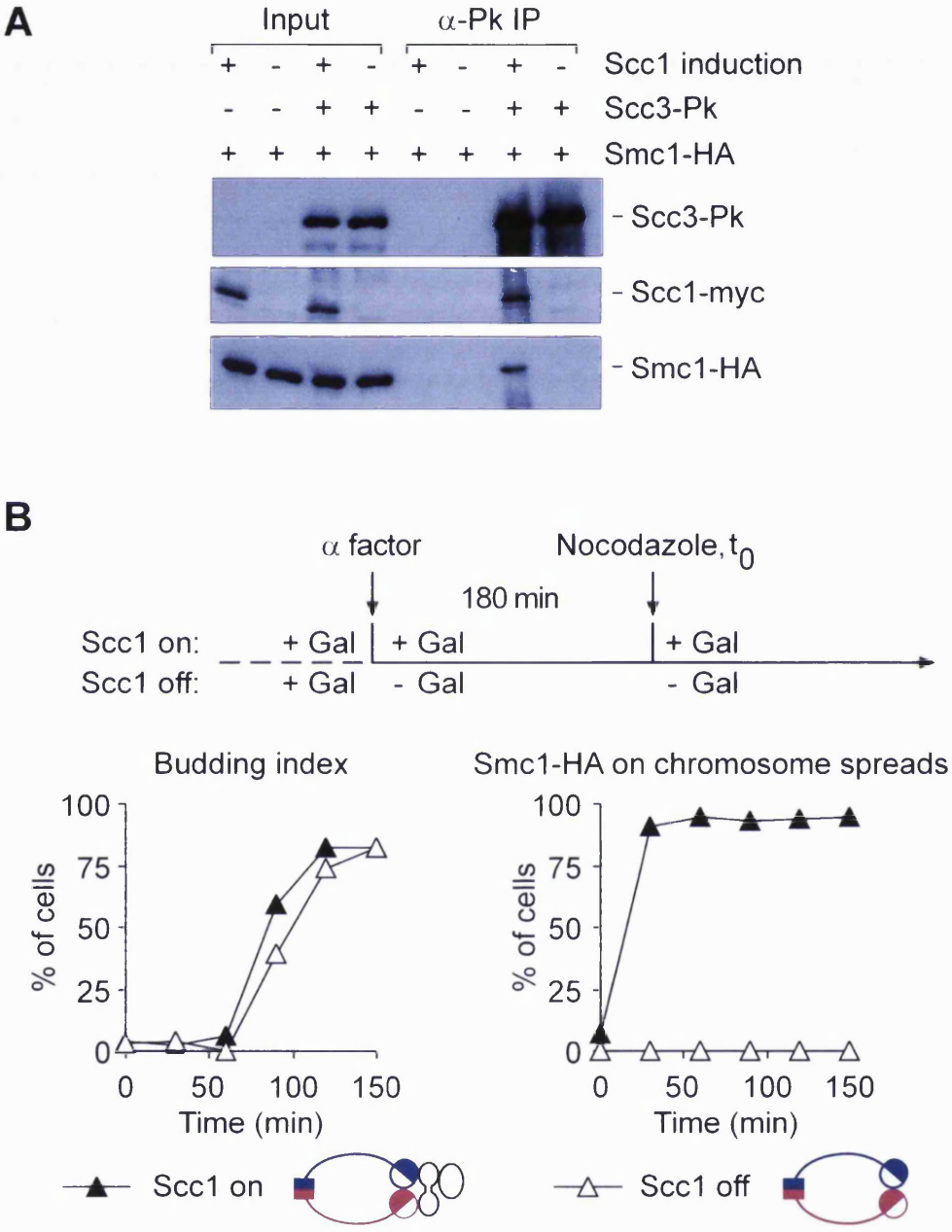

Figure 5.4. An Smc1/3 ring does not bind to DNA by itself.

(A) Scc3 does not bind to Smc1/3 in the absence of Scc1. Scc1 was either expressed or depleted from strain Y1674 (*MAT*a, *scc1Δ, GAL-SCC1-myc18, SMC1-TEV-HA6, SCC3-Pk3*) and copreciptiation of Smc1 with Scc3-Pk was analysed.
(B) Scc1 was either expressed (Scc1 on) or depleted (Scc1 off) in strain Y749 (*MAT*a, *scc1Δ, GAL-SCC1-myc18, SMC1-TEV-HA6*). Cells were blocked in G1 and released into metaphase. Smc1-HA was detected on chromosome spreads using monoclonal antibody 16B12.

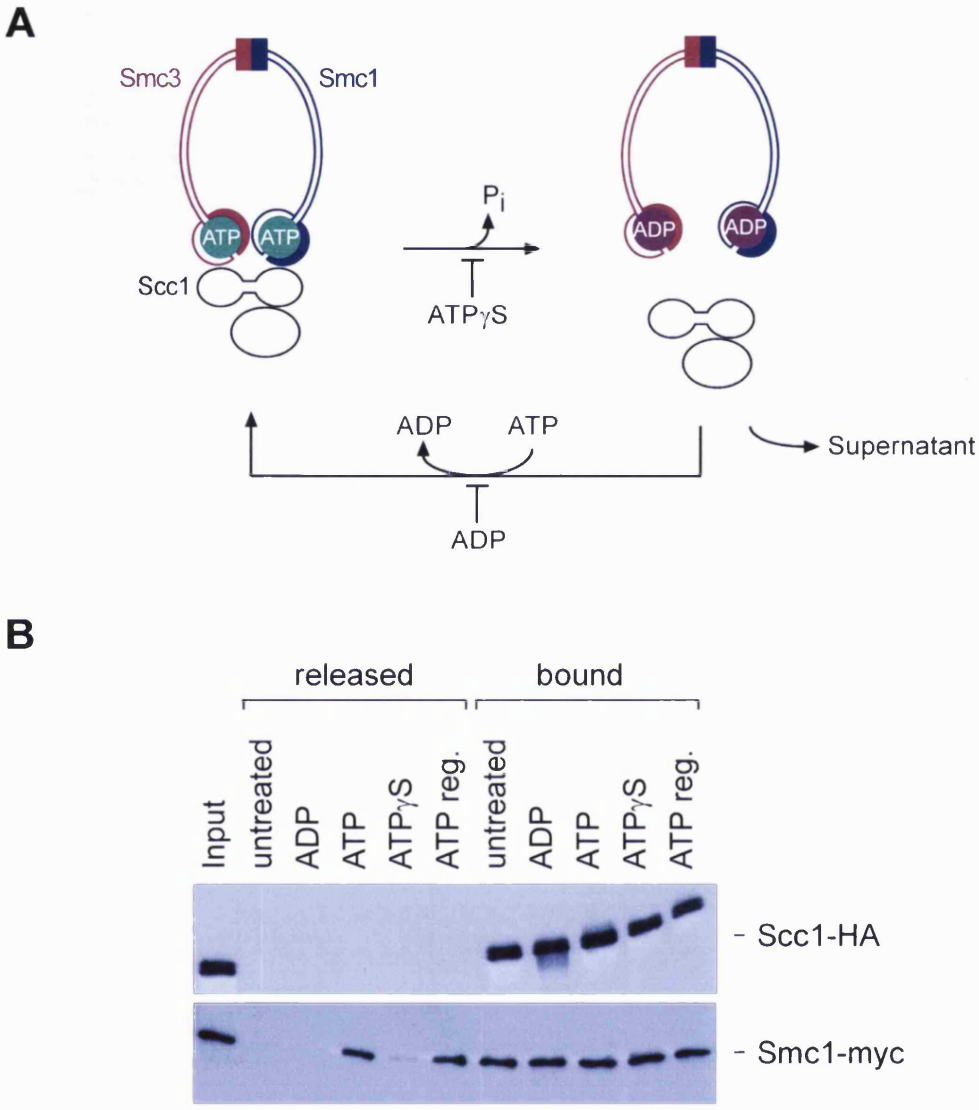

Figure 5.5. Hydrolysable ATP stimulates the release of Scc1 from the SMCs.

(A) Model of how ATP might stimulate Scc1 dissociation from the SMCs. ATP hydrolysis causes the disengagement of the SMC heads and transient release of Scc1. In multiple cycles of head engagement and disengagement, depending on the presence of ATP but prevented by ADP or ATPγS, this release may become apparent in an *in vitro* reaction described in (B).
(B) Strain Y613 (*MAT*a, *pep4Δ, SCC1-HA6, SMC1-myc18*) was blocked in metaphase by nocodazole and Scc1-HA immunoprecipitated. The immunoprecipitation beads were aliquoted into six parts. One part was loaded directly for Western analysis (Input), the others were supplemented with ADP, ATP, ATPγS, or an ATP regenerating system (ATP reg.), or left untreated. Proteins released from the immunoprecipitates (released) were separated from the beads (bound) before loading.

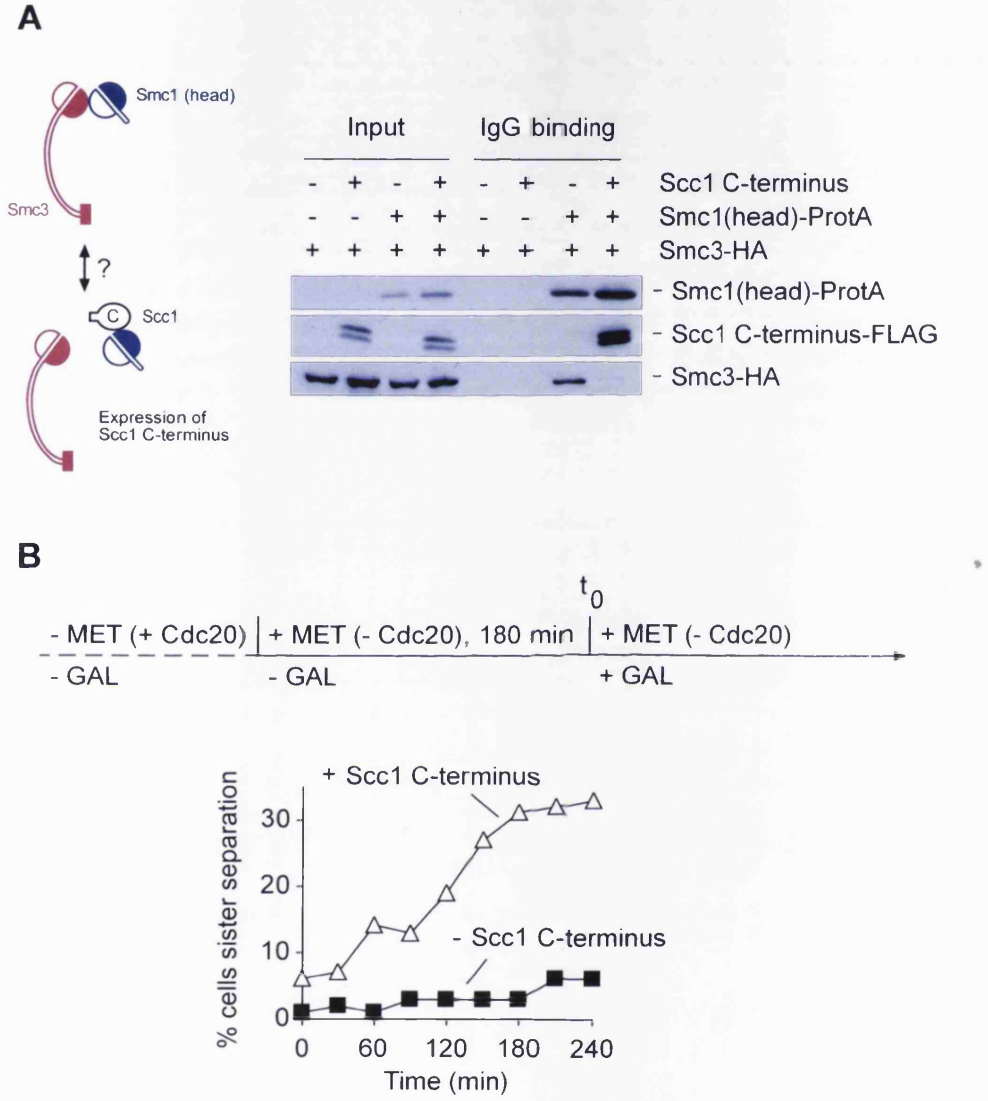

Figure 5.6. Expression of the C-terminal Scc1 cleavage product disrupts the Smc1/3 head interaction and causes chromosome segregation in metaphase.

(A) The C-terminal Scc1 cleavage product disrupts the interaction between Smc1 heads and Smc3. Strain Y1281 (*MAT*a, *pep4Δ, SMC3-HA3, GAL-SCC1(Met269-566)-FLAG, TPI-SMC1(head)-ProtA*) was arrested in G1, with or without induction of the Scc1 fragment. Extracts were prepared and binding of Smc3 and the Scc1 fragment to Smc1 heads analysed (compare left panel).
(B) Loss of sister chromatid cohesion caused by the Scc1 fragment. Strain Y1565 (*MAT*a, *MET3-CDC20, TetR-GFP, TetOs::URA, GAL-SCC1(Met269-566)-FLAG*) was arrested in metaphase by Cdc20 depletion, then the C-terminal Scc1 fragment was induced. Separation of sister chromatids was analysed at indicated time points. Strain Y115, lacking the Scc1 fragment expression construct, was used as a control. Mitotic arrest over the duration of the experiment was confirmed by scoring the budding index (data not shown).

CHAPTER 6: Discussion

6.1 The chromatin bound cohesin complex

6.1.1 Is the ring structure sufficient for the chromosomal activities of cohesin?

The crucial role of the cohesin complex in sister chromatid cohesion is well established, however, its molecular function is largely unknown. A major goal of this study was the biochemical characterisation of cohesin bound to budding yeast chromatin as it represents the cellular pool of the complex that mediates sister chromatid cohesion. One aim was to identify polypeptides specifically interacting with chromosomal cohesin in addition to the core components of previously characterised cohesin of soluble fractions after cell extraction (Losada et al., 1998; Tóth et al., 1999; Sumara et al., 2000). Such candidate proteins may include factors involved in the loading of cohesin onto chromosomes, maintaining the complex on chromosomes or in targeting cohesin onto distinct chromosomal regions. Other potential proteins associated with cohesin may be implicated in establishment of sister chromatid cohesion which takes place during DNA replication. Recent studies in yeast and other organisms have indeed identified factors interacting with cohesin and required for its chromosomal loading or targeting. The Scc2/Scc4 complex binds to cohesin in soluble fractions of budding yeast and is essential for cohesin's association with chromosomes (Ciosk et al., 2000; Arumugam et al., 2003). The TIM-1 protein and a chromatin remodelling complex containing SWI/SNF2 are interacting with cohesin and are involved in loading of the complex onto chromosomes in *C. elegans* and humans, respectively (Hakimi et al., 2002; Chan et al., 2003). Furthermore, the Psc3 subunit of fission yeast cohesin binds to the heterochromatic Swi6 (HP1) protein *in vitro* which was shown to position cohesin to pericentromeric regions (Bernard et al., 2001; Nonaka et al., 2001).

In the present study, cohesin was isolated from chromatin fractions after nuclease release and its subunit composition was analysed. Only the four core components of cohesin, Smc1, Smc3, Scc1 and Scc3 were detectable and there was no indication for

binding of additional polypeptides in a stoichiometric manner (Figure 2.2A and 2.3). The subunit composition of cohesin isolated from soluble and chromatin fractions did not appear to be different before or after DNA replication (Figure 2.3). In addition, the molecular weight of chromosomal cohesin is consistent with the complex being exclusively composed of each of the core components, as previously suggested (Haering et al., 2002) (Figure 2.4). However, these analyses do not exclude the presence of small or substoichiometric polypeptides associated with cohesin, transient interactions and also other proteins whose association with cohesin may have been lost during cell extraction or release from chromatin. Nevertheless, they indicate that cohesin bound to chromosomes may be biochemically similar to the soluble complex that displays the characteristic ring-shaped structure.

This result raises the question whether chromosomal activities of cohesin can be explained merely by the distinctive ring structure of the complex formed by its core components. Is there any requirement for chromosomal cohesin to be associated with other proteins that facilitate its loading onto chromosomes, its positioning to specific chromosomal regions, the maintenance of its binding to chromosomes, or the establishment of cohesion? According to the ring model, cohesin may bind DNA strands by embracing them (Haering et al., 2002; Gruber et al., 2003). In a simplistic view, the topological trap of DNA within cohesin´s closed ring could in principle be sufficient for the interaction of the complex with chromosomes, occurring between cohesin loading onto DNA in G1 and destruction of cohesion in anaphase in budding yeast. In addition, despite topological entrapment of DNA, parts of the SMC proteins were shown to have DNA binding activity *in vitro*, which could contribute to cohesin´s association with chromosomes (Akhemedov et al., 1998; Akhmedov et al., 1999; Chiu et al., 2004).

As mentioned above, cohesin-associated proteins have been isolated from soluble cell extracts and were shown to be essential for loading of cohesin onto chromosomes. Cytological analysis in budding yeast revealed that cohesin does not colocalise with the Scc2/Scc4 loading complex on chromatin, and indicated that sites of initial cohesin loading onto chromosomes may be different from known cohesin binding sites (Tóth et al., 1999). Thus, specific factors may associate with chromosomal cohesin and reposition it from sites of loading to permanent cohesin binding sites. However, recent data suggest that it is converging transcription rather than a ´targeting factor´ that

relocates cohesin to these sites (Lengronne et al., 2004). The cohesin ring might simply slide along chromosomes, responding to steric requirement of transcription, until becoming clustered between two transcriptionally active genes. These data nevertheless do not exclude that such targeting factors associate with cohesin on chromosomes, especially for positioning cohesin to sites associated with low transcriptional activity like centromeres. Such a factor was identified as the fission yeast Swi6 protein since it recruits cohesin to centromeric heterochromatin as well as to heterochromatic mating type loci (Bernard et al., 2001; Nonaka et al., 2001).

Does the cohesin ring alone suffice for the establishment and maintenance of cohesion between two sister chromatids? The cohesin ring model proposes that sister chromatid cohesion is mediated by two sister DNA molecules becoming entrapped within the same ring (see chapter 1.5.1). Therefore the ring alone might be enough for tethering sister strands together until its cleavage by separase at anaphase onset. However, if cohesin rings are preassembled around chromosomes before S-phase, how do sisters become entrapped within the same rings during DNA replication, the time period during which cohesion is established? Experiments presented in this thesis do not reveal any evidence for the association of proteins differentially bound to the complex before or after DNA replication which might regulate this process (Figure 2.3). The replication fork might simply pass through the cohesin ring thereby leaving two sisters trapped inside (Haering et al., 2002). This model is an attractive way to explain the inherent coupling of DNA replication to establishment of cohesion. However, it is hard to imagine how a replication fork could slide through a cohesin ring if DNA polymerases and accessory proteins were assembled into a single, stationary replicon, as has been suggested in bacteria (Lemon and Grossman, 2000). In addition, this model does not explain the requirement of proteins for the establishment of sister chromatid cohesion, such as Eco1/Ctf7 and components of the replication machinery (see chapter 1.3.2).

Taken together, if cohesin´s ring model proves correct, then the mere topological nature of the ring could in principle explain some of cohesin´s chromosomal activities, but not all of them such as cohesion establishment during DNA replication. Biochemical analyses presented in this thesis did not reveal any polypeptides directly interacting with chromosomal cohesin. However, association with other proteins or posttranslational modifications of cohesin subunits which may regulate chromatin

binding or cohesion establishment cannot be excluded. Nevertheless, the results emphasise that some cohesin activities may be intrinsic to the complex, which during the course of the thesis was demonstrated by studies on the ATPase domains of cohesin SMC proteins (see below).

6.1.2 Chromosomal cohesin is a monomeric complex: Implications for models of sister chromatid cohesion

Measurements of the hydrodynamic properties of cohesin released from chromatin revealed that the complex is monomeric before and after DNA replication (Figure 2.4). The finding of chromosomal cohesin to be a monomeric complex is in agreement with coimmunoprecipitation experiments on chromatin-released cohesin of budding yeast, showing that cohesin complexes contain only one copy of each core subunit (Haering et al., 2002). If in diploid strains the two alleles of either Scc1, Scc3, Smc1 or Smc3 were differentially epitope tagged, the two tagged versions of the same subunit cannot be coimmunoprecipitated. However, although release from chromatin was carried out under mild conditions (see chapter 7.3.2), it cannot be excluded that protein interactions, in particular those which might be DNA-dependent, may have been lost.

The only indication that SMC complexes might interact when associated with DNA comes from *in vitro* studies on *B. subtilis* SMCs (BsSMCs) (Hirano et al., 2001). In crosslinking experiments, the BsSMC homodimer displayed protein-protein interactions in the presence of DNA and ATP. However, BsSMC was also shown to stimulate ATP-dependent DNA aggregation (Hirano and Hirano, 1998), which could in principle be responsible for bringing DNA bound proteins in close proximity which are then likely to be crosslinked. In addition, these experiments were using only the purified SMC subunits of the BsSMC holocomplex in an *in vitro* system, and therefore might be unlikely to reflect the situation *in vivo*. Most of the size analyses of SMC complexes in cells have been restricted to proteins from soluble fractions. So far, no evidence has been found that cohesin and other SMC complexes are present other than as monomers, with the exception of the Smc5/Smc6 proteins that are part of a high molecular weight complex (Fousteri and Lehmann, 2000).

If chromatin-bound cohesin stays as a monomeric complex during cohesion establishment (Figure 2.4), how does that impinge on current models of sister chromatid cohesion? As mentioned in chapter 1.5.1, these include ones that propose sister chromatids becoming entrapped during DNA replication either within a single cohesin ring or alternatively becoming linked together by dimeric versions of the ring. Since cohesin appears to be monomeric on chromosomes in metaphase arrested cells (Figure 2.4), a stage when cohesion between sisters is expected to be fully established, such 'dimeric ring models' may not be applicable. However, how then could possibly two 30 nm chromatin fibres fit into a single ring with a diameter of approximately 30 nm? If the ring model of cohesin embracing DNA holds true, then an important step to address this question will be to assess if shortening the diameter of cohesin rings influences sister chromatid cohesion by any means. Alternatively, sister chromatids might not be located within the ring's centre but wrapped around the cohesin SMC heads, as suggested by electron spectroscopic imaging of DNA bound to condensin's Smc2/Smc4 head domains (Bazett-Jones et al., 2002).

Previous models for linkage of two DNA strands by SMC proteins also suggest that each head domain of an SMC dimer interacts with one DNA strand, thereby tethering strands together. This is achieved by the ring opening up, which results in the SMC dimer adopting an open conformation made possible by a wide hinge angle (Hirano et al., 2001; Anderson et al., 2002;). As shown in Figure 2.4B, glycerol gradient analysis does not reveal any change in the shape of chromatin released cohesin before or after DNA replication. The shape of the complex was consistent with cohesin rings being closed at both stages (Figure 4.2). A conformation of cohesin consistent with an open ring, as judged by sedimentation analysis, was not observed, which makes such models questionable.

Altogether, the finding that chromosomal cohesin during cohesion establishment does not form dimers or higher-order oligomers and does not appear to undergo conformational changes, limits the number of possible models for sister chromatid cohesion.

6.1.3 The binding mode of cohesin on chromosomes

In an attempt to study the structure and binding mode of cohesin on chromosomes, cohesin/DNA complexes were purified from chromatin after release by micrococcal nuclease treatment (Figure 2.2). The advantage of this approach was the isolation of such complexes *ex vivo*, as opposed to reconstituting cohesin/DNA complexes *in vitro*, and which are thus more likely to represent interactions of cohesin with DNA on chromatin. In electron micrographs, proteins associated with DNA strands, most likely representing cohesin, appear as single complexes but mostly as part of clusters (Figure 2.5). However, these studies are preliminary, and the identity of cohesin needs to be confirmed in future analyses by methods such as immunogold labelling. No particular structural features of the DNA bound protein complexes could be observed, in contrast to electron micrographs obtained of cohesin purified from soluble extracts (compare Figure 1.6A) (Anderson et al., 2002). Techniques such as rotary shadowing may help to enhance resolution of protein structures, especially to possibly visualise coiled coil domains of the SMCs. Alternatively, other approaches such as atomic force microscopy (AFM) might have to be applied. AFM has proven to be suitable to visualise condensin assembled on naked DNA *in vitro*, and revealed a particular protein domain, the SMC hinge domain, to interact with DNA (Yoshimura et al., 2002). The same technique was applied to visualise cohesin bound to naked DNA or reconstituted chromatin *in vitro* (Sakai et al., 2003). However, binding of cohesin to naked DNA was rare, and although cohesin did interact with chromatin, the images did not give any insight into the binding mode of cohesin with DNA.

In electron micrographs, cohesin was found to associate with DNA as clusters (Figure 2.5). Quantitative Western analysis could further confirm that cohesin may preferentially bind to chromatin in clusters of 5-20 complexes per cohesin association site (Figure 2.6). This is an interesting observation as it raises the possibility that a single cohesin complex may not be sufficient to mediate sister chromatid cohesion at a given site. If sister DNA strands are entrapped merely within a single ring, they are expected to be tightly linked. However, it is currently unclear whether the cohesin complex is turned over on chromosomes and therefore the presence of additional 'backup' rings are required to assure continuous maintenance of cohesion at the same

site. Alternatively, a single ring might simply not fulfill the physical strength that is needed to locally hold sisters together.

Although highly speculative, a different interpretation is that cohesin's accumulation on chromatin might support the formation of higher order chromosomal structures. Beside others, the function of such structures may be to facilitate the assembly of chromosomal insulator/boundary elements. These elements are known to separate transcriptional units, thereby restricting the spread of silenced chromatin or the influence of silencer or enhancer elements between them (reviewed in West et al., 2002). Indeed, mutations in Smc1 and Smc3 reduce the ability of a boundary flanking the yeast HMR silent mating-type locus to block the spread of gene-silencing protein complexes, and Scc1 locates to this boundary (Donze et al., 1999; Laloraya et al., 2000). A similar function by the Scc3/Stromalin cohesin subunit in contributing to insulator function has recently been proposed in *Drosophila* (Rollins et al., 2004). RNA interference of Scc3 reduced the effect of the *Drosophila* gypsy insulator on blocking enhancer-promoter communication at the *cut* gene, necessary for cell type specification at wing margins. Another function of boundaries assembled at cohesin association sites may be to restrict condensin activity to defined chromosomal domains. This was suggested by the observation that cohesin is required to regain condensed chromosome structure upon returning temperature-sensitive condensin mutants to the permissive temperature (Lavoie et al., 2002).

Clearly, future biochemical and structural studies on the binding mode of cohesin with DNA and chromatin will become necessary as a first step towards an understanding of cohesin's role in higher order chromosome dynamics.

6.2 ATPase motif mutants as a tool to analyse the role of ATP in cohesion

Previous studies on the cohesin complex did not investigate the function of the predicted ABC-like ATPase domains formed by the heads of the Smc1 and Smc3 subunits. In cohesin, the heads are thought to be linked together by the Scc1 subunit whose cleavage in anaphase destroys sister chromatid cohesion. These head domains are conserved in all members of the SMC protein family, and in some of them the essential

role of ATP as a prerequisite for their diverse activities is well established. Therefore, it was conceivable to assume that ATP might play a key role in cohesin function. Crosslinking experiments presented in this thesis indeed revealed that the SMC subunits of cohesin, purified from yeast cell extracts, have ATP binding activity (Figure 3.1). In similar crosslinking experiments, ATP binding to the purified N-terminal but not C-terminal Smc1 head domain could be demonstrated (Akhemedov et al., 1998). The binding of ATP to the SMCs was low compared to another ATP binding protein (RecA). One reason for the low binding activity might be that cohesin´s ATP hydrolysis rate is minimal and therefore exchange of ATP that is already bound to the SMC heads is a rare event. This is consistent with the proposed role for cohesin´s SMCs to transport DNA by a conformational switch of their head domains (see below) rather than function as motor proteins which are predicted to display high ATP hydrolysis activity.

To assess the *in vivo* function of ATP binding and hydrolysis of cohesin SMCs, point mutations were introduced in residues of the Smc1 ATPase motifs, located in the head domains that are predicted to be essential for these activities (Figure 3.2A). Based on *in vitro* studies of *B. subtilis* SMCs, amino acid substitutions in the Walker A and B motif are expected to abolish ATP binding whereas a mutation in the C-motif should prevent ATP hydrolysis (Hirano et al., 2001). The primary sequences of *B. subtilis* and yeast cohesin SMC heads show a high percentage of identity (N-terminal heads, 28 %; C-terminal heads 38 %), therefore it is likely that the same amino acid changes may have similar effects. This is also supported by crystal structure analyses of related proteins like Rad50 and ABC transporters, showing that the corresponding residues in the ATPase motifs are involved in ATP binding or hydrolysis (Hopfner et al., 2000; Smith et al., 2002; Chen et al., 2003). However, future studies will be needed to confirm that the ATP ´binding´ and ´hydrolysis´ Smc1 mutants are really defective in these processes. This will presumably become a challenging task, given that ATP binding activity of cohesin is low, compared to another ATP binding protein (RecA) (Figure 3.1), and it has so far not been possible to detect hydrolysis of ATP by cohesin. In addition, recombinant Smc1 or Smc3 head domains did not show any ATP binding activity (data not shown).

6.3 The assembly of the cohesin complex

6.3.1 ATP binding of cohesin is required for complex formation

The expression of any of the Smc1 ATPase mutants in a strain carrying a temperature-sensitive allele of the *SMC1* gene did not support cell viability and sister chromatid cohesion at the restrictive temperature (Figure 3.3). The mutants appeared to be defective in establisment or maintenance rather than resolution of cohesion. This opened the possibility that ATPase motifs of Smc1 may be required for processes such as complex assembly of cohesin, which takes place in budding yeast during G1/S phase when newly synthesised Scc1 (and associated Scc3) binds to the Smc1/3 dimer, or subsequent loading of assembled cohesin onto chromosomes. Indeed, the Walker A and B motif mutants that are expected to compromise ATP binding to Smc1 heads, but to a much lesser extent the C-motif (ATP hydrolysis) mutant, abolished complex formation with Scc1 (Figure 3.4A). Consistently, the presence of ATP was a prerequisite for the assembly of Scc1 onto the Smc1 subunit in an *in vitro* complex reconstitution assay (Figure 3.5). Scc1 binding to Smc1 was also observed, although less reproducibly, when the non-hydrolysable ATP analogue, ATPγS, was included in this assay (data not shown). Therefore, ATP binding and not hydrolysis by Smc1 seems to be necessary for the interaction with Scc1. But is it sufficient for recruiting Scc1 to the SMC head domains, or is in addition ATP binding by the Smc3 head required? During the course of this thesis, similar mutational studies were performed on the ATPase motifs of the Smc3 protein (Arumugam et al., 2003). Here, the equivalent amino acid substitutions, as described for the Smc1 subunit, were introduced into Smc3´s Walker A, B and C-motif. Similarly, the Smc3 ATPase motif mutants showed a cohesion defect, yet complex formation was not affected by any of the mutations. Therefore it seems that only ATP binding by the Smc1 head and not by Smc3 is needed for the Smc1/3 dimer to associate with Scc1. The C-terminal part of Scc1 has previously been shown to interact with an Smc1 head whereas the N-terminus of Scc1 binds to Smc3 (Haering et al., 2002). Thus, the initial and essential step in the formation of cohesin might be the association of the C-terminal Scc1 domain to an Smc1 head bound to ATP, and this association may be required for the N-terminal part of Scc1 to subsequently interact with an Smc3 head (Figure 6.1). This is consistent with the notion that Scc1´s C-terminal domain alone can

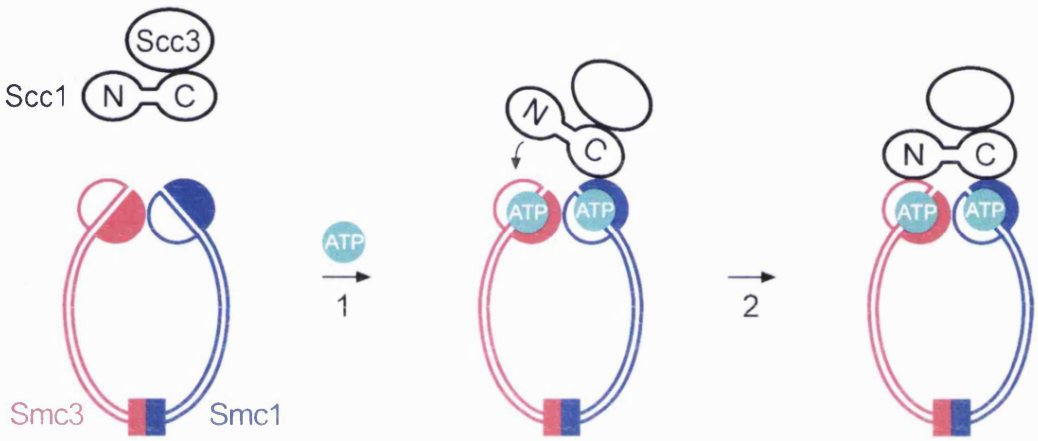

Figure 6.1. The assembly of the cohesin complex.

The cohesin SMC dimer forms a ring closed by the interacting Smc1 and Smc3 head domains. (1) ATP binding by the head of Smc1 is required for the association of the C-terminal domain of Scc1 when the protein is synthesised during G1/S phase. In addition to ATP, the Smc3 head is essential for this association, most likely via its interaction with the Smc1 head, thereby contributing to a binding platform for Scc1. (2) Upon initial Scc1 binding to the Smc1 head, Scc1´s N-terminus subsequently interacts with the Smc3 head.

bind *de novo* to the Smc1/3 complex *in vivo* (compare Figure 5.6A), but not its N-terminal domain (Arumugam et al., 2003 and data not shown).

6.3.2 Interactions at the SMC head domains and Scc1 binding

Crystal structure studies of Rad50 and other ABC ATPases have demonstrated that two catalytic ATPase domains interact with each other by ATP bound to the Walker A/B motif of one domain contacting the C-motif of another (see chapter 1.7). Since SMC heads constitute ABC ATPases, similar interactions were expected to exist between cohesin´s Smc1 and Smc3 heads. However, direct interactions between both heads have hitherto not been detected and it has been thought that it is the Scc1 subunit that connects both heads to form ´tripartite rings´ (Haering et al., 2002). Results presented in this thesis have shown that an Smc1 ´head-only´ version was capable to directly bind to Smc3 in the absence of Scc1, therefore providing evidence for the existence of ´bipartite rings´, closed at the two interacting SMC head domains (Figure 4.1). This is consistent with sedimentation analyses suggesting rings only composed of the Smc1/3 dimer may be closed by interaction of both head domains (Figure 4.2). SMC heads may therefore associate with each other in two different modes, either directly and independently of Scc1 or indirectly via Scc1. Such alternative binding modes are in agreement with electron micrographs of the vertebrate cohesin complex, showing the two SMC heads either in close proximity or separated but bridged by the non-SMC subunits (Anderson et al., 2002) (compare Figure 1.6A).

Immunoprecipitaton experiments revealed that the direct interactions between Smc1 and Smc3 may be ATP-dependent as well as ATP-independent. This became evident since an Smc1 head mutated in the Walker A and C-motif, and therefore predicted to abolish all ATP-mediated interactions, still bound to Smc3, although to a reduced level (Figure 4.3A). This was rather unexpected, as the crystal structure of the Rad50 dimer interface suggests contacts between the heads mostly depended on ATP, and in addition no dimerisation was observed in biochemical analyses in the absence of ATP (Hopfner et al., 2000). Although direct ATP-independent protein-protein interactions across the dimer interface of other catalytic ABC ATPase subunits such as MalK or MJ0796 were detected, it is unclear to what extent they contribute to stable dimer formation (Smith et al., 2002; Chen et al., 2003). It is also possible that ATP-independent interactions

between cohesin SMC heads were mediated by coiled coils that are part of the 'Smc1 head construct', rather than by residues of the nucleotide-binding interface. Future biochemical analyses on cohesin SMC heads will certainly be needed to determine the prerequisites for dimer formation, for example by assessing if isolated Smc1 and Smc3 heads require ATP for their interaction *in vitro*.

The existence of two binding modes of cohesin SMC heads to Scc1 raises the question whether interactions between the heads are needed for the initial association of the Scc1 subunit with the Smc1/3 complex. Experiments in yeast have shown that once Scc1 is bound to the complex, its domains are capable of remaining associated even if the heads are separated: After Scc1 cleavage by separase, each of the terminal domains of Scc1 is bound to one of the SMC heads (Gruber et al., 2003). Therefore, binding of Scc1 to just one of two separated head domains could in principle be sufficient for its association with the Smc1/3 dimer. This could be via the ATP-bound Smc1 head that recruits the C-terminal part of Scc1. However, results included in this thesis demonstrated that not a single but rather both heads are required for Scc1 binding (Figure 4.4), and therefore the Smc3 head, although not necessarily ATP binding to it (see previous chapter), becomes additionally essential. It is very likely that both heads or parts of them contribute to a binding platform for Scc1, and only when ATP binds to Smc1, conformational changes within this platform are induced that allow Scc1 to associate. Conformational changes within catalytic domains in other ABC ATPases upon ATP binding have indeed been observed (Hung et al., 1998; Hopfner et al., 2000). Head-to-head contacts might contribute to this platform. However, it is questionable whether these contacts are ATP-dependent as Scc1 was still capable to interact with an Smc1/3 complex mutated in Smc3's Walker A and C-motif (Arumugam et al., 2003). Clearly, crystal structure analyses of SMC head domains bound to Scc1 will be needed to gain insight into the interaction map of these proteins.

6.4 A model for ATP hydrolysis-dependent binding of cohesin to DNA

Smc1 mutated in the C-motif, that was predicted to abolish ATP hydrolysis, was capable of forming intact cohesin complexes, albeit somewhat less efficiently (Figure 3.4A). In addition, closed rings were formed in such complexes, thereby ruling out that their architecture differed from wild-type cohesin which may have contributed to the

inability to support sister chromatid cohesion (Figure 4.3A). However, the Smc1 C-motif mutation abolished binding of cohesin to chromatin, suggesting a role for ATP hydrolysis by cohesin in this process (Figure 5.2). Similarly, mutation of Smc3´s C-motif, even though capable of assembling closed cohesin rings that were also indistinguishable from wild-type complexes, did not support chromosome association of the complex (Arumugam et al., 2003). It therefore appears that a mutation in the C-motif of only one head prevented ATP hydrolysis by the other, resulting in a full inactivation of its function, which is consistent with hydrolysis of the two ATP molecules bound by ABC transporters being a simultaneous and cooperative event (Azzaria et al., 1989; Al-Shawi and Senior, 1993; Loo and Clarke, 1996; Davidson and Sharma, 1997; Stray and Lindsley, 2003).

If ATP hydrolysis is indeed required for binding cohesin to chromosomes, what then is its role in this process? In ABC ATPases, ATP hydrolysis is thought to result in disengagement of two interacting catalytic domains (see chapter 1.7). If it is correct that cohesin binds to DNA by topological entrapment, then disengagement of the SMC heads would allow DNA to enter cohesin´s ring (Figure 6.2). In such a model, the two heads may initially represent a closed transport gate, interacting with bound ATP, and thereby preventing access of DNA to the interior of the ring. Hydrolysis of ATP would then lead to separation of the heads and transport of DNA into the ring. Such a model of ATP hydrolysis-dependent DNA transport into the cohesin ring by the SMC heads might be evolutionary analogous to the transport of cargo across membranes by the structurally related catalytic domains of ABC ATPases. DNA itself could induce ATP hydrolysis as has been observed in *B. subtilis* SMC and condensin (Kimura and Hirano, 1997; Hirano et al., 2001). Alternatively, the cohesin associated Scc2/4 complex could promote hydrolysis of ATP, since mutations in these proteins prevent cohesin binding to chromatin in yeast, resembling the phenotype of the SMC C-motif mutants (Arumugam et al., 2003; Ciosk et al., 2000).

If it is true that DNA becomes entrapped by cohesin after its transport into the ring, then any loss of its integrity is expected to result in loss of cohesin´s association with chromosomes. Consistent with this assumption, cohesin containing an intact SMC head complex but disrupted at the Smc1 hinge and coiled coil did not bind to chromatin (Figure 5.3B). In addition, cohesin missing Smc1´s head but containing its coiled coil and hinge domains was incapable of associating with chromatin (Figure 5.3C).

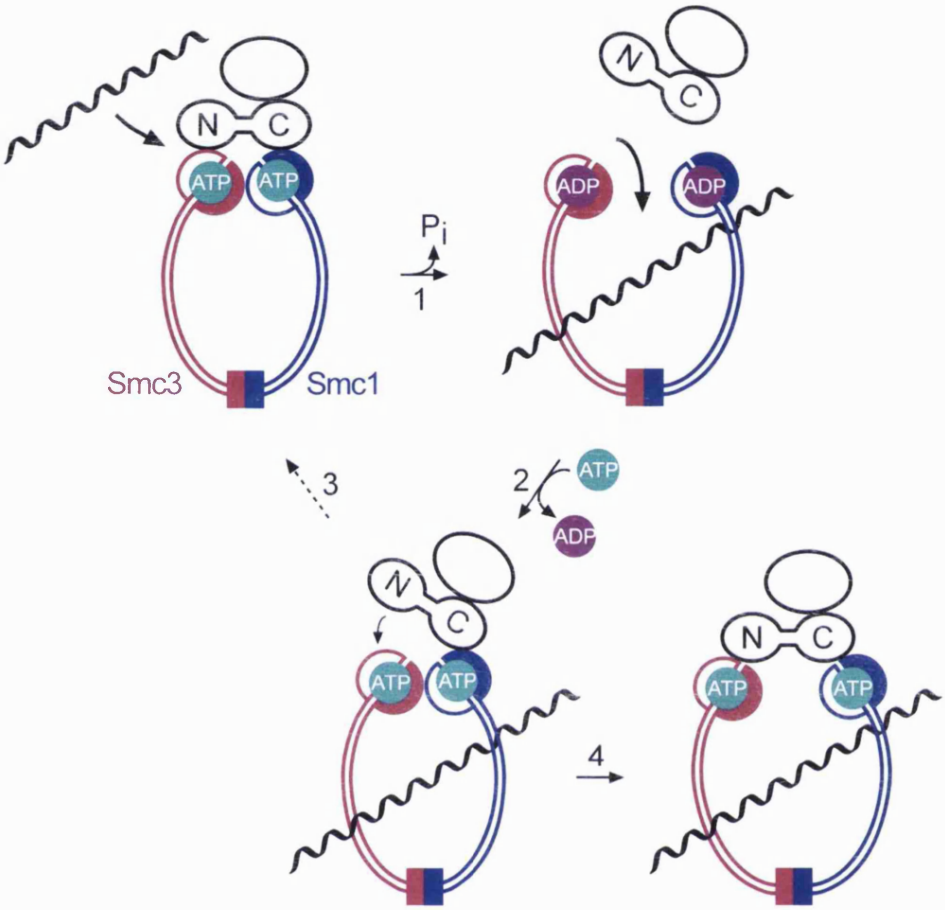

Figure 6.2. ATP hydrolysis-dependent DNA binding of cohesin.

(1) ATP bound to the SMC heads is hydrolysed in a cooperative manner, and this could possibly be stimulated by DNA or the Scc2/4 complex. Upon ATP hydrolysis, the heads become separated and Scc1 transiently dissociates from one or both heads. This results in ring opening, allowing DNA transport into the ring. (2) Subsequent *de novo* ATP binding to the heads might promote their reassociation and Scc1 binding, thereby the ring becomes closed and DNA topologically entrapped. (3) If the ATP binding/hydrolysis cycle is reversible, cohesin could potentially undergo another cycle of DNA transport and become loaded around two sister strands during DNA replication for cohesion establishment. (4) To maintain sister chromatid cohesion, it is crucial to secure a closed conformation of the ring, leaving both sisters trapped inside. One possibility to achieve this is to keep both heads apart, resulting in inhibition of ATP hydrolysis. The C-terminal Scc1 domain could play a role in this process since it prevents the SMC head-to-head interaction.

Therefore, after DNA transport, the role of Smc1´s coiled coil and hinge may be to provide a topological trap for DNA. Alternatively, cohesin might bind DNA in an ATP hydrolysis-dependent manner different from transport. Such binding might take place at the SMC head complex itself, as proposed for Rad50 whose head domains join a positively charged groove suitable to engulf DNA (Hopfner et al., 2000). This is unlikely to be the case, as an intact ATPase head complex was incapable of binding to chromatin (Figure 5.3B). However, these results altogether do not exclude that the Smc1 hinge and coiled coils may have another yet unknown role during an ATP hydrolysis-dependent DNA binding reaction by the heads other than forming a trap for DNA. Certainly, the ultimate goal for future studies will become the establishment of an *in vitro* system for ATP-dependent DNA loading of cohesin which will help to assess (a) if ATP hydrolysis is indeed required for cohesin binding to DNA, as suggested by *in vivo* analysis of the C-motif mutants, and (b) if DNA becomes topologically entrapped by cohesin after its loading.

Once DNA is transported inside, what then prevents it from exiting the ring? Obviously, it is very important that sister DNA strands remain stably enclosed by cohesin to maintain sister chromatid cohesion from the time of its establishment in S-phase until metaphase. Above results suggest a role for the Smc1 C-motif in opening cohesin´s DNA entry gate by ATP hydrolysis driving heads apart. But is opening the gate the sole function of ATP hydrolysis or does it also play a role in closing the gate after DNA transport? The failure of C-motif mutants to associate with chromatin could arise due to failure of either opening or closing the ring. However, it seems rather likely that the defect lies in gate opening, as C-motif mutants are capable of forming closed rings, at least in soluble fractions (Figure 4.3A). What then closes the gate after DNA entry? One possibility is that the Scc1-dependent interaction mode of SMC heads might take over, and separated heads become bridged by Scc1 to ensure maintenance of their topological connection. This is also consistent with the observation that a ring solely composed of an Smc1/3 dimer but lacking Scc1 does not bind chromatin (Figure 5.4B). An alternative and not inconceivable interpretation is that Scc1´s association with the SMC heads plays a crucial role in DNA transport itself by stimulating ATP hydrolysis. Interestingly, current evidence also suggests that cohesin SMCs are capable of stably binding to chromatin in a different manner that does not require their interaction with kleisin subunits. During meiosis in *C. elegans*, inactivation of the TIM-1 protein

abolished binding of the cohesin Rec8 kleisin to chromatin, but Smc1 and Smc3 still associated with chromosomes (Chan et al., 2003).

Separation of the heads would certainly be necessary for DNA transport into the ring. But how does DNA pass by the Scc1 subunit that forms an obstacle for entry as its terminal regions bind to the heads? ATP hydrolysis followed by head separation might induce conformational changes leading to a transient dissociation of either one or both terminal parts of Scc1 from the heads (Figure 6.2). This is plausible as ATP binding to the heads is a prerequisite for their association with Scc1 (see previous chapter). Indeed, indications for such a mechanism have been observed, since release of Scc1 from the SMCs was promoted by ATP but not by the non-hydrolysable ATP analogue ATPγS, or by ADP (Figure 5.5B). Although not tested yet, ATP hydrolysis mutants would also be predicted to be incapable of Scc1 dissociation, leaving the ring locked, and thereby blocking transport of chromosomal DNA. Subsequent reconnection of Scc1 with the heads after DNA transport would require *de novo* ATP binding by the Smc1 subunit. If this ATP binding/hydrolysis cycle, regulating Scc1´s association with the Smc1/3 dimer, proves correct, it will be interesting to see whether cohesin could undergo only one or multiple cycles of DNA transport. This will determine whether cohesin embracing one DNA strand before the replication fork dissociates from chromosomes but could shortly thereafter become reloaded around two sisters after they emerge from the replication fork. Alternatively, cohesin could be loaded once onto DNA before replication, resulting in cohesion establishment as the replication fork slides through the ring (Haering et al., 2002).

One of the key issues for the future will also be to assess what closes the DNA entry gate permanently after both sister strands are loaded within cohesin´s ring in order to maintain sister chromatid cohesion. For this, the inhibition of the ATP binding/hydrolysis cycle would become essential. One possibility is to prohibit ATP hydrolysis by preventing head engagement, thereby blocking the C-motif of one head from interacting with the other ATP-bound head. This could be the function of the C-terminal domain of Scc1 by sterically blocking engagement of the Smc1 and Smc3 heads (see Figure 5.6 and next chapter). If that is the case, then heads are expected to be separated at the latest from the time of cohesion establishment until metaphase, before cohesion is resolved. *In vivo* analyses that assess the ´binding state´ between the two

SMC heads at various stages of the cell cycle will certainly become necessary to address this issue.

6.5 DNA unloading of cohesin

In budding yeast, cohesin is unloaded from DNA and dissociates from chromosomes during anaphase, dependent on cleavage of the Scc1 subunit by the protease separase at the metaphase-anaphase transition (Uhlmann et al., 1999; Uhlmann et al., 2000). To fully understand the consequences of Scc1 cleavage for DNA unloading of cohesin it will be important to know in which mode of interaction the SMC heads rest in metaphase. In the case of a head-to-head interaction in metaphase, mere Scc1 cleavage would not result in opening of the ring to allow DNA to exit cohesin. Alternatively, if already during DNA binding of cohesin or establishment of cohesion the heads are separated but bridged by Scc1 (see previous chapter), cleavage of Scc1 may then simply destroy this bridge and allow DNA to leave the ring. Inactivation of Scc1 in metaphase via a temperature-sensitive version of the protein also leads to sister separation, consistent with the latter possibility (Ciosk et al., 2000). However, if heads are separated, what then prevents after Scc1 cleavage the SMC head interaction from being reestablished before sister strands have entirely left cohesin´s ring?

A possible solution to this puzzle is the finding that ectopic expression of a stable version of the C-terminal Scc1 cleavage fragment disrupts the interaction between the SMC heads by binding to Smc1 and displacing Smc3 (Figure 5.6A). The cohesin ring thereby becomes opened up which would then allow sister chromatids to exit the ring (Figure 6.3). This is consistent with the observation that expression of the cleavage fragment in metaphase triggered sister chromatid segregation (Figure 5.6B). The potential of the C-terminal fragment to actively break open cohesin might also explain why its expression is toxic in both yeast (Rao et al., 2001) and mammalian cells (Hoque and Ishikawa, 2002).

The stability of the C-terminal cleavage fragment in cells is limited by its degradation via the N-end rule pathway (Rao et al., 2001). Interestingly, half life of the fragment derived from pulse-chase experiments *in vivo* appeared to be short ($t_{1/2} \approx 2$ min), in contrast to the half life of the fragment after Scc1 cleavage by

separase ($t_{1/2} \approx 20$ min) (Rao et al., 2001). It will be interesting to see whether the maintenance of the fragment is regulated before degradation, possibly by monitoring DNA release from cohesin, to secure complete chromosome segregation. However, additional regulations are likely to exist that control head separation *in vivo*: The endogenous C-terminal fragment can be stabilised by deleting the *UBR1* gene, which encodes the ubiquitin ligase that targets N-end rule substrates for degradation. However, the endogenous amounts of the fragment did not appear to disrupt head interactions (data not shown).

How does expression of the C-terminal Scc1 fragment trigger separation of the SMC heads? In metaphase arrested cells, expression of the cleavage fragment caused separation of the heads (data not shown) and triggered chromosome segregation, even though full length Scc1 is stably associated with cohesin (Figure 5.6B). It is therefore likely that the binding site of the Scc1 cleavage fragment at the Smc1 head is different from the one of full length Scc1. During a normal cell cycle, the C-terminal Scc1 fragment might thus become repositioned at the Smc1 head during or shortly after it is produced by separase, thereby causing conformational changes that are incompatible with two SMC heads being engaged. Further analyses are certainly required to assess if binding of full length Scc1 and its cleavage fragment to the Smc1 head are both possible at the same time or are mutually exclusive.

The potential of a separase cleavage fragment of Scc1 to open up the cohesin ring for unloading of DNA is consistent with a model of topological DNA trapping by cohesin. However, such a model does not explain why cohesin can dissociate from chromosome arms without the apparent requirement of Scc1 cleavage in most eukaryotes during prophase (see chapter 1.3.4). The release of cohesin from chromosomes requires the activity of mitotic kinases such as Polo-like kinase (PLK) and Aurora B kinase (Losada et al., 2002; Sumara et al., 2002). Purified PLK can phosphorylate the Scc1 and Scc3 (SA) subunits of cohesin *in vitro* which reduces cohesin´s binding efficiency to chromatin (Sumara et al., 2002). These subunits are also phosphorylated in metaphase *in vivo,* depending on the presence of PLK. It therefore appears that cohesin´s dissociation from chromosome arms during prophase might be triggered by phosphorylation of its subunits by PLK. Phosphorylation might directly cause the release of the Scc1 subunit from one or both SMC heads followed by DNA

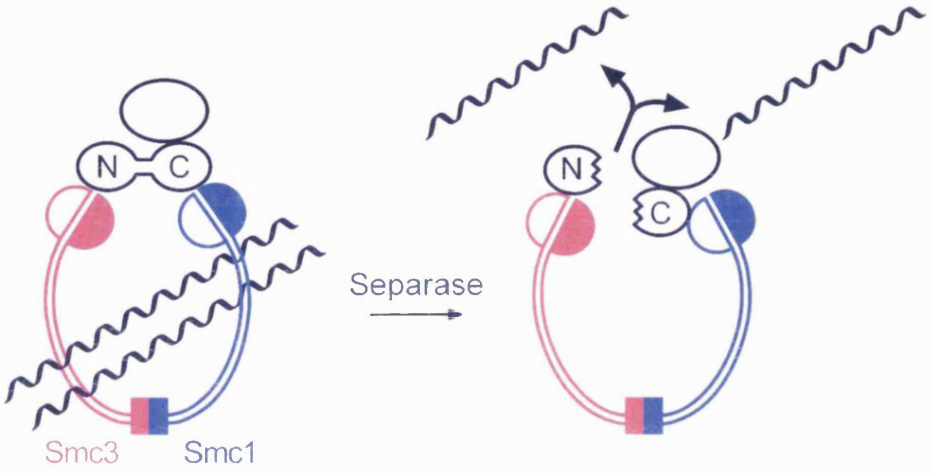

Figure 6.3. DNA unloading of cohesin.

At anaphase onset Scc1 is cleaved by separase. The C-terminal cleavage product of Scc1, bound to Smc1, prevents the SMC heads from interacting and actively breaks open the cohesin ring. Upon cleavage, this fragment might become repositioned at the Smc1 head, causing conformational changes that are incompatible with head-to-head interactions. Ring opening subsequently allows release of sister strands from cohesin.

exiting the ring. Alternatively, phosphorylation may activate the ATP binding/hydrolysis cycle by the SMC heads resulting in dissociation of Scc1 and subsequent DNA release (see previous chapter). As a first step to test such hypotheses, it will be essential to assess whether PLK has any effect on the integrity of the cohesin complex *in vitro*.

6.6 DNA binding by ATP hydrolysis-dependent transport: Applicable for related SMC complexes?

If cohesin is loaded onto DNA by ATP hydrolysis-driven transport into its ring, is it then conceivable that similar mechanisms for DNA binding also exist in related SMC complexes? The condensin complex, composed of the Smc2, Smc4 and three non-SMC subunits located at the SMC's head domains, is responsible for chromosome compaction in order to prevent sister chromatid entanglement during mitosis. *In vitro* activities of condensin include positive supercoiling of circular DNA (Kimura and Hirano, 1997). Although so far no direct evidence has been found *in vivo,* condensin might promote the coiling of chromosomal DNA in order to compact chromosomes. Like cohesin, condensin displays a ring-shaped structure of similar dimensions suitable for a topological entrapment of DNA (Anderson et al., 2002). For chromosome compaction, the condensin ring might transport and embrace DNA strands from the same chromatin fibre within its ring (Figure 6.4). Thus, condensin could mediate intra-chromatid cohesion, as opposed to inter-chromatid cohesion promoted by the cohesin complex. DNA strands could become transported into the ring at the base of a chromosomal coil, resulting in entrapment of DNA loops with a defined chirality (Kimura et al., 1999) (Figure 6.4). The occurrence of such loops might be a consequence of DNA becoming wrapped around head or coiled coil domains after its transport into condensin's ring (Bazett-Jones et al., 2002). Similar to Scc1's proposed function for cohesin binding to chromosomes, the condensin's non-SMC subunits could close the entry gate to maintain DNA's stable entrapment within the ring (compare Figure 6.2). The role of the non-SMCs could also be to stimulate DNA transport into the ring. In agreement with such hypotheses, the purified *Xenopus* condensin SMCs, XCAP-C (Smc4) and XCAP-E (Smc2), do not associate with chromatin in the absence

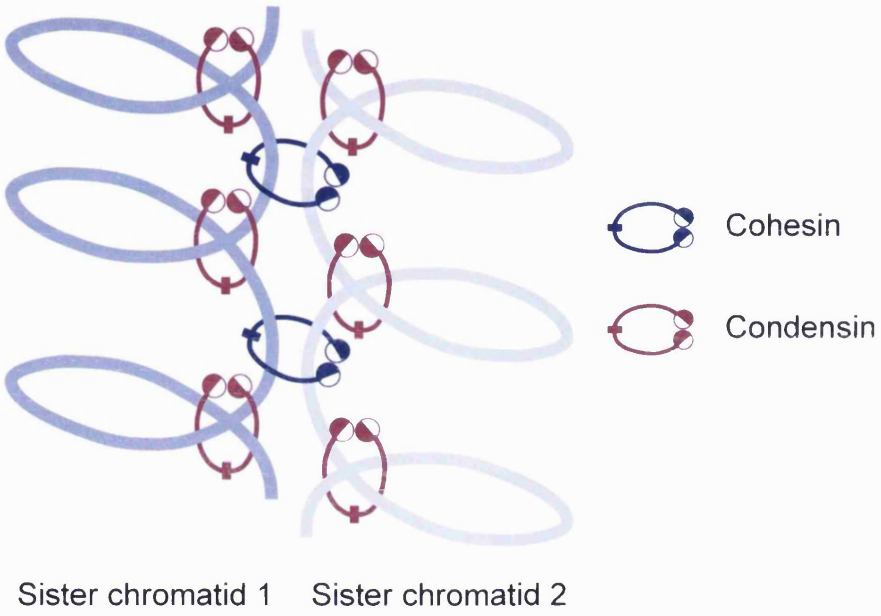

Figure 6.4. A model for chromosome condensation by DNA entrapment.

The cohesin complex might tether two sister chromatids together by embracing them in the same ring to promote inter-chromatid cohesion. In contrast, the condensin complex might embrace two different segments of the same chromatid within the same ring to promote intra-chromatid cohesion. In that way, an array of chromosomal loops might be generated that are entrapped at their base and which might promote chromosome compaction.

of the non-SMC subunits *in vitro* (Kimura and Hirano, 2000). Depletion of the non-SMCs, hCAP-G and hCAP-G2, using RNA interference also abolished chromosomal binding of the hCAP-E SMC subunit in human cells (Ono et al., 2003). In addition, mutants in yeast condensin's non-SMCs, Brn1, Ycg1 and Ycs4 do not support chromatin association of Smc4 at the restrictive temperature (Lavoie et al., 2002).

The essential roles of condensin's non-SMC subunits for DNA binding would thus fit a model of DNA entrapment by the complex, similar to the one proposed for cohesin. But are the known requirements for ATP in condensin activities also consistent with such a model? The DNA supercoiling activity of vertebrate condensin is dependent on ATP hydrolysis by the complex but it is currently unclear how ATP hydrolysis contributes to this activity (Kimura and Hirano, 1997; Kimura et al., 2001). One prediction from a model of DNA transport into condensin's ring is that ATP is a prerequisite for the binding of the complex to DNA. However, so far no evidence has been reported that ATP is essential for this association *in vitro* (Kimura and Hirano, 1997; Kimura et al., 1999; Strick et al., 2004). In addition, mutant versions of the purified yeast Smc2/4 complex, which are incapable of ATP hydrolysis, still bound DNA. Furthermore, the absence of ATP or the presence of non-hydrolysable ATP in a binding reaction did not prevent association of the Smc2/4 complex with DNA (Stray and Lindsley, 2003). Thus, if DNA is transported into the condensin ring, then transport may rather occur in an ATP-independent manner, and merely entrapping DNA would also certainly not account for the activities of the complex observed *in vitro.* Alternatively, the ATP-independent DNA binding mode of condensin does not involve entrapment, and condensin might bind to DNA by other means, for example by interaction via its hinge domains (Yoshimura et al., 2002). Only upon ATP binding, DNA would become transported and subsequently entrapped by condensin's ring. To get more insight into the binding mechanism of condensin to DNA, it will become essential in future studies to assess whether mutations in condensin's SMC ATPase motifs have any effect on the association of the complex with chromatin *in vivo.* Although cohesin binding to DNA was found to be ATP-independent *in vitro* (Losada and Hirano, 2001; Kagansky et al., 2003), the mutation analysis presented in this thesis strongly indicates a crucial role for ATP in chromatin binding of the complex.

The Smc5/6 (Spr18/Rad18) complex is involved in repair of DNA damage caused by ionising and UV irradiation. Structural studies of the Smc5/6 complex have hitherto

not been carried out. However, it is reasonable to assume that it also forms a ring-like structure similar to cohesin or condensin, given the conservation between SMC proteins. The Spr18/Rad18 complex was shown to have DNA stimulated ATPase activity, and phenotypes of ATPase motif mutants in the essential Rad18 protein have been studied *in vivo* (Fousteri and Lehmann, 2000). Rad18 mutants in the ATP binding (Walker A and B) motifs as well as in the ATP hydrolysis motif (C-motif) are deficient in DNA repair upon ionising and UV irradiation of cells. Similar to the proposed function of cohesin in DNA repair, the Smc5/6 complex might hold sisters or homologues together at the site of DNA damage. This would ensure that a damaged strand is in close proximity to its template strand so that its original sequence can be restored by homologous recombination. Topological entrapment of two DNA strands might be one possibility to achieve this. Epistasis analysis indeed suggests that Rad18 is a player in a DNA repair pathway involving recombination (Lehmann et al., 1995). In future studies it will therefore be interesting to see whether the reasons for the DNA repair defects by the Rad18 ATPase motif mutants were similar to the ones observed for the ATPase motif mutants of cohesin's Smc1 protein. This will certainly contribute to an understanding whether activities between both complexes underlie unique ATP-dependent mechanisms.

The *B. subtilis* 'condensin' implicated in bacterial chromosome compaction is a ternary complex composed of an SMC homodimer (BsSMC), the kleisin ScpA and the ScpB protein with both Scp subunits bound to the BsSMC head domains. The BsSMC dimer by itself shows DNA binding and DNA-stimulated ATPase activity *in vitro* (Hirano and Hirano, 1998). However, DNA binding alone was independent of ATP. The presence of ATP or non-hydrolysable ATP caused DNA aggregation by BsSMC (Hirano and Hirano, 1998). Given the unspecific binding of BsSMC to DNA, it is difficult to apply a model that involves ATP hydrolysis-dependent transport of DNA across interacting head domains. Is it then plausible to assume that BsSMC does not bind to DNA by topological entrapment? In surface plasmon resonance experiments, purified BsSMC was shown to bind stronger to closed DNA as compared to linear DNA, suggesting that binding was via a ring-like structure with the heads closed and DNA trapped between the arms (Volkov et al., 2003). It thus seems that BsSMC binds to DNA via embracement, and the head domains might operate the entry gate for DNA. Due to their binding to the head domains, ScpA and ScpB could stabilise the ring

closure. Although *in vitro* studies have not provided any evidence so far for DNA binding by BsSMC depending on ATP hydrolysis, such binding cannot entirely be excluded.

Many of the chromosomal activities by SMC complexes may be explainable by the ´ring model´ of topological DNA entrapment. However, it is likewise possible that different SMC rings may also have different modes of DNA binding, which might be necessary to facilitate their variety of tasks in chromosome dynamics.

CHAPTER 7: Materials and Methods

This chapter summarises the molecular biological and biochemical methods as well as yeast techniques used throughout this thesis. It also includes details of DNA constructs and genotypes of yeast strains referred to in chapters 2-5.

7.1 Molecular biology

7.1.1 Polymerase chain reaction (PCR)

7.1.1.1 PCR for epitope tagging of endogenous cohesin subunits

In order to fuse HA, myc or Pk epitope tags to the C-termini of genomic copies of cohesin subunits, a PCR-based technique was used as described (Knop et al., 1999). Briefly, forward and reverse primers were designed that were complementary at their 3´ ends to epitope tag-marker cassettes consisting of the respective epitope tag next to a selectable auxotrophic marker gene. The 5´ ends of the primers were complementary to the appropriate region of homology with the yeast genome, about 50 nucleotides, to allow in-frame fusion of the epitope downstream of the gene of interest (Figure 7.1). Vectors containing the epitope tag-marker cassettes used as template for PCR are listed in chapter 7.5. For purification of cohesin or SMC complexes, a peptide recognition site for TEV protease (5´ GAG AAT TTG TAT TTT CAG GGT 3´) was inserted into the forward primer downstream of the open reading frame of Scc1 or Smc3, respectively. Yeast cells were transformed with the PCR product to allow integration into the genome by homologous recombination (see chapter 7.2.2). Transformants were subsequently selected using the auxotrophic markers. These were heterologous markers derived from *K. lactis* or *S. pombe* to reduce the likelihood of recombination at the endogenous marker locus rather than at the gene of interest.

The PCR reaction mix was set up as follows:

10 ng template DNA
0.5 µM forward primer
0.5 µM reverse primer
200 µM of each dNTP
10 µl Expand High Fidelity Buffer (10x concentrated with 15 mM $MgCl_2$; Roche)
3.5 U Expand High Fidelity Taq Polymerase (Roche)
dH_2O to 100 µl

PCR reactions were usually performed with the following cycling parameters using Peltier Thermal Cycler-200 (MJ Research):

1 cycle:	3 min at 94°C
10 cycles:	20 sec at 94°C
	30 sec at the primer annealing temperature (normally 50-60°C)
	2 min at 72°C
10 cycles:	20 sec at 94°C
	30 sec at the primer annealing temperature
	2 min (+ 5 sec extension time after each cycle) at 72°C
1 cycle:	5 min at 72°C

The resulting PCR product was analysed by agarose gel electrophoresis (see chapter 7.1.4), and precipitated by the addition of 1/10 volume of 3 M sodium-acetate pH 5.2 and 3 volumes of absolute ethanol. Precipitations were placed at -20°C for 30 min prior to centrifugation at 13000 rpm for 30 min. DNA pellets were washed with 70 % ethanol to remove salt and air-dried. DNA was resuspended and stored in 50 µl of deionised water at -20°C to be used for subsequent yeast transformations (see chapter 7.2.2).

Figure 7.1. Schematic overview of PCR-based epitope tagging of genes by homologous recombination.

7.1.1.2 PCR for cloning of cohesin subunit variants

For cloning of full-length, head and headless SMC constructs, DNA was amplified by PCR using plasmids as templates containing the genomic clones (see chapter 7.5). The parameters for PCR are mostly the same as described for epitope tagging. PCR products were run on an agarose gel from which DNA fragments were subsequently extracted (see chapter 7.1.5), digested and ligated into the desired vector (see chapters 7.1.2 and 7.1.6).

7.1.1.3 PCR to introduce point mutations into Smc1

To create ATPase motif mutant Smc1 versions, site-directed mutagenesis using overlap extension PCR was performed. In a first round of PCR, two parallel reactions were carried out with two different sets of primers. One set contained a forward primer upstream of the point mutation harbouring a restriction site for cloning, and a reverse primer containing the mutation and extending 15 nt on either side of the mutation. The other set contained a forward primer with the mutation and a reverse primer located downstream that contained a restriction site. Both PCR fragments were extracted from agarose gels, and equal amounts of PCR products were used as a template for a second round of a single PCR reaction including the primers located upstream and downstream of the point mutation (Figure 7.2). The PCR product was extracted from gels and subjected to cloning steps to exchange the wild-type DNA fragment using the restriction sites within the primers. The successful introduction of the mutation was confirmed by DNA sequencing (see chapter 7.1.9). The composition of all PCR reaction mixtures and

PCR parameters was as described for epitope tagging except for increasing the amount of DNA template to 100 ng and decreasing the total number of cycles during the extension reaction from 20 (2 x 10 cycles) to 15 (1 x 10 cycles + 1 x 5 cycles) during both rounds of PCR.

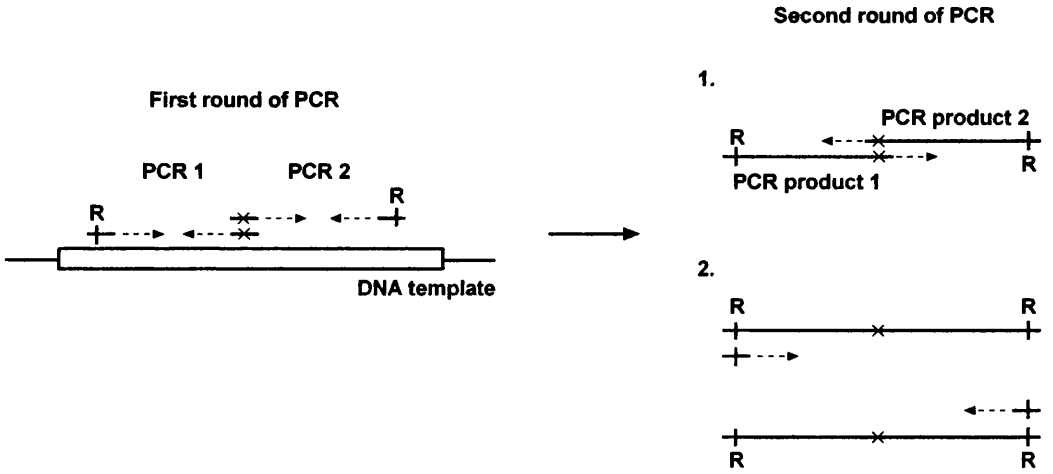

Figure 7.2. Scheme of overlap extension PCR for site-directed mutagenesis. (R, Restriction site; the red cross indicates the point mutation to be introduced).

7.1.2 Restriction enzyme digestion and Klenow fill-in reaction of DNA overhangs

DNA was in general digested in 50 µl of total volume for 2 hours at the recommended temperature of the restriction enzyme. The amount of DNA that was digested per reaction was usually about 0.1 - 1 µg. The DNA concentration was determined according to the following formula: Absorbance of one A_{260} unit (at a path distance of 1 cm) corresponds to a DNA concentration of approximately 50 µg/ml. The volume of restriction enzyme stock in digest reactions did not exceed 10 % (v/v) so that glycerol was kept below 5 % (v/v) to prevent 'star' activity. Enzymes were obtained from New England Biolabs, and digests were performed in appropriate buffers, supplied by the manufacturer with the enzyme.

For converting 5′ overhangs into blunt ends, a Klenow fill-in reaction was performed. For this, 0.1 mM dNTPs and 5 U Klenow Polymerase (New England Biolabs) was added to 50 µl of restriction digest and incubated for 15 min at 25°C. All

digests and fill-in reactions were analysed by agarose gel electrophoresis followed by extraction from the gel.

7.1.3 Phosphorylation and annealing of DNA linker oligonucleotides

To generate DNA linker sequences, two oligonucleotides that were in reverse antiparallel orientation to each other, were designed. Each of the oligonucleotides was added at 2.25 μg in a separate mix containing 1 mM ATP, 10 U T4 Polynucleotide kinase (PNK, New England Biolabs) and 10x PNK buffer, which was incubated for 20 min at 37°C to allow phosphorylation of 5´ DNA ends. Both reactions were mixed and NaCl was added at 100 mM followed by incubation for 10 min at 65°C. Subsequently oligonucleotides were allowed to anneal by cooling down the mix at room temperature, and the resulting dsDNA linker was used directly for ligation reactions.

7.1.4 Agarose gel electrophoresis

Agarose gels (1–2 % w/v in TAE; 40 mM Tris-acetate, pH 7.5, 2 mM EDTA) were prepared with ethidium bromide (about 1 μg/ml). The percentage of agarose in gels was determined according to the size of DNA fragments to be resolved (1 % for fragments larger than 0.5 kb, 2 % for fragments smaller than 0.5 kb). Samples containing DNA to be analysed were supplemented with 6x DNA loading buffer (15 % w/v Ficoll, 0.1 % w/v Bromophenol blue). A 1 kb DNA ladder (Gibco) was run in parallel with samples to indicate length of DNA fragments. Gels were generally run at 100 V in 1x TAE buffer using Anachem electrophoresis cells, and DNA was visualised using a UV transilluminator.

7.1.5 Isolation of DNA from agarose gels

Following agarose gel electrophoresis, DNA fragments visualised by UV light were excised from gels as slices. DNA was extracted from these gel slices using Qiaquick columns (Qiagen) according to the manufacturer´s protocol, and eluted from the silica-based solid support with 30-50 μl deionised water.

7.1.6 Dephosphorylation of vector DNA and ligation reaction

To prevent religation of vector DNA, dephosphorylation of the linearised vector DNA was performed using 20 U alkaline Phosphatase from calf intestine (New England Biolabs) in a reaction volume of 50 µl after restriction digest followed by incubation for 1 h at 37°C. Vector DNA was subsequently extracted from agarose gels, and purifed DNA was resuspended in deionised water and stored at -20°C until further use.

For ligation of vector and insert DNA, following reaction mix was set up:

10 ng vector DNA
3x molar excess of insert DNA compared to vector DNA
2 µl 10x ligation buffer (New England Biolabs)
400 U T4 DNA Ligase (New England Biolabs)
dH_2O to 20 µl

Ligation was carried out at 16°C overnight or for 1 h at 25°C. 10 µl of the reaction mix was subsequently used for transformation of chemical competent *E. coli* (DH5α) cells.

7.1.7 Transformation of E. coli with plasmid DNA

Chemical competent *E. coli* (DH5α) cells for transformation with plasmid DNA were prepared as follows: A single bacterial colony was inoculated into 2 ml of Luria Broth medium (LB; 1 % w/v bactotryptone, 0.5 % w/v Bacto-yeast extract and 170 mM NaCl) and grown overnight at 37°C. 1 ml of this culture was added to 500 ml LB/10 mM $MgCl_2$ medium and grown with vigorous shaking at 18°C until $OD_{596\ nm}$ = 0.25-0.7 (about 2-3 days). The culture was placed on ice for 10 min and cells were harvested by centrifugation at 3000 rpm for 10 min. The cell pellet was resuspended in 80 ml ice-cold TB buffer (10 mM Pipes/KOH [pH 6.7], 55 mM $MnCl_2$, 15 mM $CaCl_2$ and 250 mM KCl) and incubated in an ice bath for 10 min. Cells were harvested again and resuspended by gentle swirling in 20 ml TB/7 % DMSO and incubated in an ice bath for

a further 10 min. Subsequently cells were aliquoted and immediately snap frozen in an ethanol/dry-ice bath, and stored at -80°C.

For transformation, aliquots of cells were thawed on ice and 100 µl of cell suspension was incubated with 10 µl of ligation mix for 10 min on ice. Subsequently cells were heat-shocked for 2 min at 42°C and added back on ice for 3 min. 1 ml of LB medium was added and cells were allowed to recover for 45 min at 37°C. Cells were plated on LB-agar (2 % w/v agar) containing the appropriate antibiotics and incubated at 37°C overnight. Resulting colonies were used for inoculating 5 ml of LB medium plus antibiotics (ampicillin with a final concentration of 100 µg/ml, and kanamycin at 50 µg/ml), and small-scale plasmid isolation ('mini-preps') was carried out the following day. Plasmid DNA was subjected to restriction enzyme digest and sequencing to check the insert.

7.1.8 Isolation of plasmid DNA from E. coli

Routine large-scale ('maxi-preps') plasmid DNA isolations were carried out using the Qiagen MAXI prep kit according to the manufacturer's instructions (Qiagen), while plasmid mini-preps were either carried out using the Qiagen MINI prep kit or the mini-prep service facility at CR-UK. The plasmid isolation procedure using Qiagen kits is based on the alkaline cell lysis but using a silica-based chromatography column to purifiy isolated DNA.

7.1.9 DNA sequence analysis

PCR cycle sequencing using fluorescent dye-labelled terminator nucleotides during the enzymatic extension reactions was employed for all DNA sequencing. All sequencing PCR reactions were set up as follows:

8 µl Terminator Ready Reaction mix (see below)
200-500 ng DNA template
5 pmol primer
dH_2O to 20 µl

The terminator ready reaction mix contained the ABI Prism Dye Terminator Cycle Sequencing Ready Reaction Mix (Perkin Elmer) and AmpliTaq DNA polymerase (Roche). Following thermal cycling, unincorporated nucleotides were removed by ethanol precipitation, and sequencing reactions were loaded on automated sequencing machines (Applied Biosystems) at the sequencing service of CR-UK.

7.2 Yeast biology

7.2.1 Growth of cells and maintenance

Yeast strains were grown either in liquid culture using YEP medium (1.1 % w/v yeast extract, 2.2 % w/v bacto-peptone and 0.0055 % w/v adenine) containing 2 % w/v D-glucose (YEP-D) or 2 % w/v galactose and 2 % w/v raffinose (YEP-Raf/Gal), or on corresponding agar plates containing 2 % w/v agar. Strains in which promoters of essential genes were exchanged with the methionine-repressible *MET3* promoter, were grown up in synthetic medium (YNB; 0.8 % w/v yeast nitrogen base, sugar (2 % w/v D-glucose or raffinose/galactose), adenine (60 μg/ml), uracil (60 μg/ml) and the following amino acids (60 μg/ml each): arginine, tryptophan, histidine, leucine, isoleucine, lysine, phenylalanine, threonine, tyrosine) lacking methionine. For long-term storage, yeast strains were maintained as stocks in 15 % glycerol at -80°C.

7.2.2 Transformation

Yeast cells were transformed with purified PCR products for epitope tagging, or with linearised plasmid DNA for integration of promoter-gene cassettes or exchange of endogenous promoters of essential genes against the *MET3* promoter as follows: About 10^8 cells in mid-log phase were spun down and washed in 1 ml deionised water and 1 ml TEL buffer (10 mM Tris/HCl [pH 7.5], 0.1 mM EDTA and 100 mM Lithium acetate) before being resuspended in 100 μl TEL buffer. 50 μl of the cell suspension was added to 1 μg of PCR product or linearised plasmid DNA (in a maximum volume of 8 μl) and 2 μl 10 mg/ml denatured salmon sperm DNA. Then 300 μl TELP buffer (TEL buffer plus 40 % polyethyleneglycol 3350 or 4000) was added followed by short vortexing, and the suspension was incubated for 2-4 h at 25°C. Subsequently cells were

heat-shocked for 15 min at 42°C and spun for 2 min at 6000 rpm. Cells were washed in 1 ml 1 M sorbitol and then plated on selective YNB agar plates (containing sugar, adenine, uracil and amino acids except the one selected for [in case of integration of promoter-gene cassettes] or lacking methionine [in case of promoter exchange]). Amino acid markers used were *LEU2, URA3, HIS3* and *TRP1*. Plates were incubated at 25°C, colonies were repatched and checked for positive transformants. This was done either by protein extraction followed by Western analysis to confirm protein expression (integration of promoter-gene cassettes) or by testing the inability to form colonies when transformants were patched on plates containing methionine (promoter exchange).

7.2.3 Synchronisation of cells and cell cycle experiments

An arrest of cells in G1 phase was carried out using alpha-factor pheromone treatment. 0.4 μg/ml alpha-factor peptide (provided by the CR-UK peptide service) was added to a culture of about 10^6 cells/ml in mid-log phase. After 1 and 2 h another 0.3 μg/ml alpha-factor was added. G1 arrest was checked under the microscope, indicated by unbudded cells with a ´shmooing´ cell shape. To release cells from the arrest, cells were filtered onto a cellulose membrane (1.2 μm; Schleicher and Schuell) using a Sartorius filter device. Cells were washed with YEP medium and transferred into fresh medium. Synchrony of cells during cell cycle experiments was determined by measuring the budding index (n = 100) and by assessing the DNA content by flow cytometric analysis (FACS).

Arrest of cells in S phase was achieved by treating cells in mid-log phase with 100 mM hydroxyurea (HU; Sigma) for 2-3 hours. Arrest was checked under the microscope indicated by large budded cells.

To block cells in metaphase, cells in mid-log phase were treated with 5 μg/ml nocodazole (Sigma) for 2-3 hours. The presence of large budded cells indicated a metaphase arrest. For metaphase arrest by Cdc20 depletion under control of the methionine repressible *MET3* promoter, cells were grown up until mid-log phase in synthetic medium lacking methionine. Subsequently cells were filtered, washed and transferred into YEP medium (plus sugar) containing 2 mM methionine, and complete arrest was checked after 2-3 h.

7.2.4 Protein expression and depletion by the galactose inducible promoter

For inducing protein expression controlled by the *GAL1* promoter, cells were grown up in medium containing 2 % raffinose until mid-log phase, and 2 % galactose was added for a minimum of 2 h.

To deplete cells of proteins (i.e. Scc1) under control of the *GAL1* promoter, cells were grown up in YEP-Raf/Gal until mid-log phase and subsequently filtered and washed. The filter membrane was then transferred into fresh YEP-D or YEP-Raf medium (lacking galactose) and cells incubated for 3 h. Depletion of proteins from cells was checked by Western analysis.

7.2.5 Flow cytometry

To determine DNA content of cells by flow cytometry, 10^6-10^7 cells were fixed in 1 ml 70 % ethanol for 2 h on ice. Cells were spun down and the pellet resuspended in 1 ml buffer containing 50 mM Tris/HCl (pH 7.5) and 0.1 mg/ml RNase A followed by incubation for at least 2 h at 37°C. Cells were spun down and resuspended in 0.4 ml buffer containing 200 mM Tris/HCl (pH 7.5), 211 mM NaCl, 78 mM $MgCl_2$ and 50 µg/ml propidium iodide. Samples were sonicated for 10 sec (5 microns; Soniprep 150 sonicator, MSE) and analysed using a Becton-Dickinson FAC Scan apparatus (excitation wavelength of 488 nm; detection wavelength 510-550 nm) and CELL QUEST software.

7.3 Biochemistry

7.3.1 Preparation of yeast protein extracts

Protein extracts from yeast were mainly prepared using the NaOH lysis method (Kushnirov, 2000). About 10^8 cells were harvested by centrifugation (5 min, 3000 rpm) and washed with ice-cold deionised water. The cell pellet was resuspended in 100 µl water, 100 µl 0.2 M NaOH was added and the suspension incubated for 6 min at room temperature. Cells were pelleted and subsequently resuspended in 50 µl 2x SDS-PAGE loading buffer (100 mM Tris/HCl [pH6.8], 20% (v/v) glycerol, 4 % (w/v) SDS, 0.2 %

(w/v) Bromophenol blue, 100 mM DTT) and boiled for 5 min. 5 µl of protein extract was loaded on an SDS-polyacrylamide gel for Western analysis (see chapter 7.3.3).

7.3.2 Purification and immunoprecipitation of cohesin and SMC complexes

Cohesin or SMC complexes were isolated by affinity binding from soluble or chromatin fractions which were prepared as previously described (Liang and Stillman, 1997). 4x 10^9 cells were pelleted by centrifugation (3000 rpm, 10 min), resuspended in 5 ml PIPES/KOH buffer (100 mM PIPES/KOH [pH 9.3], 10 mM DTT and 0.1 % sodium azide) and incubated for 10 min at room temperature. Cells were pelleted (2000 rpm, 3 min) and resuspended in 5 ml KP_i/Sorbitol solution (50 mM KH_2PO_4/K_2HPO_4 [pH 7.4], 0.6 M sorbitol, 10 mM DTT). Zymolyase T-100 (MP Biochemicals) was added to a final concentration of 40 µg/ml and the suspension was incubated for 10 min at 37°C until complete spheroplastation of cells. Cells were collected by centrifugation (800 rpm, 5 min), washed once in 5 ml ice-cold wash buffer (50 mM HEPES/KOH [pH 7.5], 100 mM KCl, 2.5 mM $MgCl_2$ and 0.4 M sorbitol) and resuspended in 450 µl EB buffer (50 mM HEPES/KOH [pH 7.5], 100 mM KCl, 2.5 mM $MgCl_2$, 1 mM DTT, 1 mM PMSF, 2 mM benzamidine, 0.2 mg/ml bacitracin, 2 µg/ml leupeptin, 2 µg/ml aprotinin, 2 µg/ml pepstatin A, plus protease inhibitor tablets [Roche]). In some experiments, 5 mg/ml bovine serum albumin (Sigma) was included. Cells were lysed on ice by addition of 0.25 % Triton X-100 for 3 min, and the cell extract was layered onto 900 µl EBX-S (EB buffer/0.25 % Triton X-100/30 % sucrose). After centrifugation at 12000 rpm for 10 min, the supernatant fraction (about 900 µl) above the sucrose layer was recovered for subsequent immunoprecipitation of soluble proteins (see below). For isolating chromatin bound cohesin, the sucrose layer was removed by aspiration and the chromatin pellet was resuspended in 1 ml EB-X buffer (EB buffer/0.25 % Triton X-100). To digest all DNA in chromatin pellets, 1 mM $MnCl_2$ and 0.4 U/ml DNase I (Sigma) was added. To isolate cohesin/DNA complexes, 1 mM $CaCl_2$ and 3 mM units or 0.2 mM units micrococcal nuclease (Sigma) were added for a complete or partial DNA digest, respectively. Reactions were incubated for 10 min at 25°C, and centrifuged at 12000 rpm for 10 min. The supernatant fraction containing released cohesin was retrieved, from which cohesin was subsequently immunopurified.

For immunopurifcation of cohesin from soluble or chromatin-released extracts, the extracts were precleared by adding protein A sepharose beads (Amersham Biosciences) to 1/10 of total volume and incubated for 30 min at 4°C on a rotating wheel. Subsequently precleared extracts were incubated with anti-myc (9E10, CR-UK), anti-HA (12CA5, CR-UK) or anti-Pk (SV5-Pk1, Serotec) antibody at a concentration of 1:400 for 1 h on ice, followed by binding to Protein A beads (1/40 of total volume) for 30 min at 4°C on a rotating wheel. Alternatively, precleared extracts were incubated with IgG-Sepharose (Amersham Biosciences; 1/40 of total volume) to bind protein A tagged Smc1 heads. Beads were washed 6 times with 1 ml EB-X buffer and proteins were eluted in 2x SDS-PAGE loading buffer. Alternatively, proteins harbouring a TEV cleavage site upstream of the epitope tag were eluted from the beads by addition of 50 µl EB-X including 0.2 U/µl TEV protease (Invitrogen) followed by incubation under vigorous shaking for 2 h at 16°C. Proteins were further analysed by Western blotting or silver staining.

7.3.3 SDS-PAGE and Western blot analysis

Protein samples were resolved on separating gels containing 8 % - 15 % acrylamide/bis-acrylamide solution (37.5:1; Amresco) depending on the size of the proteins to be resolved (8 % for proteins bigger than about 80 kDa, higher percentage for proteins smaller than 80 kDa), 375 mM Tris/HCl (pH 8.8) and 0.1 % SDS. A stacking gel was used on top of all separating gels, containing 5 % acrylamide, 125 mM Tris/HCl (pH 6.8) and 0.1 % SDS. All gels were run at 20 mA through the stacking gel, and at 40 mA through the separating gel using SDS-PAGE running buffer (25 mM Tris, 250 mM glycine and 0.1 % SDS) and electrophoresis cells from C.B.S Scientific. To determine molecular weights of separated proteins, a prestained marker was used (New England Biolabs) for Western analysis, and a broad-range marker (Biorad) for silver stains.

For Western analysis, proteins were blotted onto Protran transfer membranes (Schleicher and Schuell) pre-equilibrated in transfer buffer (14.4 g/l glycine, 3 g/l Tris, 0.02 % SDS, 10% v/v methanol). Protein transfer was performed for 3 h at 1.2 mA/cm^2 gel area using semi-dry transfer units (Hoefer). Membranes were blocked for 1 h in blocking solution (PBS-A [170 mM NaCl, 3 mM KCl, 10 mM Na_2HPO_4, 2 mM

KH_2PO_4], 0.01 % Tween 20, 5 % low fat dried milk). Subsequently membranes were incubated with primary antisera, diluted in blocking solution, for 1 h. Antisera used were anti-myc (9E10, CR-UK, 1:2000), anti-HA (12CA5, CR-UK, 1:5000), anti-Pk (SV5-Pk1, Serotec, 1:2000), anti-FLAG (M2, Sigma, 1:1000), anti-His (Novagen, 1:2000), peroxidase coupled anti-peroxidase antibody (Sigma, 1:2000), anti-Scc1 (a gift from Dr Strunnikov, NIH Bethesda, 1:3000) and anti-tubulin (YOL1/34, Serotec, 1:1000). Membranes were washed 3 times for 10 min in a large excess of PBS-T (PBS-A/0.01 % Tween 20) and incubated for 30 min with horseradish peroxidase (HRP)-conjugated secondary antibody (Amersham, 1:8000, diluted in blocking solution). Membranes were washed again 3 times for 10 min in PBS-T, before developing using the ECL (enhanced chemiluminescence) reagent system (Amersham) according to the manufacturer's protocol.

7.3.4 Coomassie and silver staining

Coomassie staining of proteins resolved on SDS-PAGE gels was performed using the PhastGel Blue system (Amersham Biosciences) according to the manufacturer's instructions. For silver staining of proteins, gels were washed for 10 min in deionised water and fixed in ethanol/acetic acid/water (4:1:5) for 1 h. Gels were washed twice for 5 min with deionised water and soaked for 30 min in a solution containing 1 % (v/v) glutaraldehyde and 0.5 M sodium acetate. Gels were washed again 3 times for 15 min with water and stained for 30 min with a solution prepared by slowly adding 0.8 % $AgNO_3$ (Sigma) to a solution containing 0.33 % NH_3 and 20 mM NaOH to allow complete conversion into soluble silver-diammonium complexes. After four washes for 4 min, stains were developed by adding a solution containing 0.005 % (w/v) citric acid and 0.1 % (v/v) formaldehyde. The development of stains was stopped by immersing gels in 5 % Tris/2 % acetic acid, and gels were subsequently air-dried.

7.3.5 Radioactive labelling of DNA in cohesin/DNA complexes

In order to test copurification of DNA fragments with chromatin-released cohesin after micrococcal nuclease digest (see chapter 2.1), eluates after TEV cleavage were subjected to radioactive labelling. For this, 5 μl of eluate was mixed with 3.7 x 10^5 Bq

[α-^{32}P]dATP (220 TBq/mmol, Amersham Biosciences), 50 μM of dCTP, dGTP and dTTP (Roche) and 2.5 U Klenow Polymerase (New England Biolabs) and EB-X buffer in a total volume of 60 μl. The reaction mix was incubated for 15 min at 25°C. 3 μl 10 % SDS and 0.1 U Proteinase K (Sigma) were added and the mix was incubated for a further 15 min at 37°C. Subsequently the mix was spun through a G-50 column (Amersham Biosciences) to remove unincorporated nucleotides, and 6x DNA loading buffer was added to the flow-through. DNA fragments were resolved on an 1 – 1.5 % agarose gel which was subsequently vacuum-dried onto anion exchange chromatography paper (DE81, Whatman), and analysed by autoradiography.

7.3.6 Gel filtration and glycerol gradient centrifugation

To perform size analysis of chromatin bound cohesin (see chapter 2.2), fractions released from chromatin after DNase I treatment were directly applied onto a gel filtration column or layered on top of a 15 %-35 % glycerol gradient. In addition, to differentiate between open and closed forms of the cohesin ring (see chapter 4.2), immunopurifed complexes after TEV elution were subjected to glycerol gradient centrifugation.

Gradients were made by stepwise layering 420 μl of solutions containing different concentrations of glycerol (from bottom to top: 35 %, 30 %, 25 %, 20 % and 15 % in EB-X buffer with 0.05 % Triton X-100) on top of each other in tubes with 34 mm of height and 11 mm of diameter. The final volume of the gradient was therefore 2.1 ml onto which 100 μl of sample was applied. The centrifugation was carried out using a swinging tube rotor (TLS-55, Beckman Coulter) at 42000 rpm for 13 h. Fractions of 200 μl were collected manually from top to the bottom, and protein was precipitated by adding 8 % trichloroacetic acid. Samples were left for 10 min on ice before centrifuged for 10 min at 13000 rpm. Precipitated protein was washed twice with 1 ml ice-cold acetone, and dried by vacuum centrifugation. Subsequently the protein pellet was dissolved in 25 μl 6 M Urea/1 % SDS, and analysed by Western blotting to determine the S value (sedimentation coefficient) of peak fractions.

Gel filtration was performed using a Superdex 200 column (HR 10/30, Amersham Biosciences) preequilibrated in running buffer (EB-X [0.1 % Triton X-100]). 100 μl of DNase I-released chromatin fractions was loaded onto the column and run at 0.3

ml/min. Fractions of 500 µl were collected using an FPLC (Äkta system, Amersham Biosciences) and protein was precipitated as described above, followed by Western analysis to determine r_s (Stokes radius) of peak fractions.

For calibration, standard proteins were used (thyroglobulin r_s = 8.5 nm, 19.0 S; catalase r_s = 5.2 nm, 11.3 S; bovine serum albumin r_s = 3.6 nm, 4.6 S). The native molecular weight of cohesin was calculated by the method of Siegel and Monty (Siegel and Monty, 1966) using the following equation:

$M = S\ N_0\ (6\ \pi\ \eta\ r_s)\ /\ (1 - v_2\ \rho)$; M = molecular weight (Da), S = sedimentation coefficient (x 10^{-13} sec), N_0 = Avogadro's number (6.022 x 10^{23}), η = viscosity of the solvent (0.01 g/[cm x sec] for H_2O), r_s = Stokes Radius (nm x 10^{-7}), v_2 = partial specific volume (0.73 cm^3/g, assumed average for proteins), ρ = density of solvent (1.0 g/ cm^3 for H_2O).

To determine the shape of SMC complexes, the frictional ratio (S_{max} / S) was calculated. The value for S, which is the observed sedimentation coefficient, was obtained by linear regression of values from the standard proteins. S_{max} was calculated from the known molecular weights according to Bloomfield (Bloomfield et al., 1967) using the following equation: $S_{max} = 0.00361 \times M^{2/3}$.

7.3.7 Quantification of chromatin bound cohesin

To quantify the amount of chromatin bound cohesin, cells were lysed by spheroplastation according to chapter 7.3.2. Before harvesting, cells were counted using a haemacytometer (Assistent) as well as a Coulter Counter. A cell number of 3.75 x 10^9 was determined using both methods. After lysis, soluble proteins were recovered in 900 µl total volume of which 5 µl was loaded on an SDS-PAGE gel (corresponding to 2 x 10^7 cells). The chromatin pellet was resuspended in the equivalent volume of 900 µl of which also 5 µl were loaded. Next to them, known amounts of recombinant Scc1 that served as standard protein were loaded. After the gel-run, quantitative Western blotting was performed: Following the Western transfer, membranes were blocked with Odyssey buffer (LI-COR)/PBS-A (1:1), incubated with polyclonal anti-Scc1 antiserum and subsequently with an anti-rabbit IRDye800 coupled secondary antibody (Rockland).

Proteins were subsequently quantified by measuring the fluorescent signal at 785 nm using the Odyssey infrared imager (LI-COR) and Infrared Imaging System software.

To obtain recombinant Scc1, its ORF was cloned into the pET30a vector (Novagen) which was transformed into *E. coli* (BL21 CodonPlus, Stratagene). An overnight culture of 100 ml in LB (37°C, shaking at 220 rpm) was diluted into 2 l of LB medium to $OD_{600\ nm} = 0.05$, and after further incubation the Scc1 protein was expressed for 2 h at 37°C by addition of 1 mM isopropyl β-D-thiogalactoside (IPTG; Sigma) at an $OD_{600\ nm} = 0.4$. Cells were harvested by centrifugation (4000 rpm for 20 min) and the cell pellet was resuspended in 20 ml extraction buffer (50 mM Tris/HCl [pH 8], 300 mM NaCl, 5 mM β-mercaptoethanol, 10 mM benzamidine and 1 mM PMSF). The cells were lysed by sonication (6x 30 sec, 15 microns; Soniprep 150 sonicator, MSE) and centrifuged at 17000 rpm for 30 min. As Scc1 was present as insoluble protein, the supernatant fraction was discarded and the pellet containing the bacterial inclusion bodies was washed in three successive steps with 25 ml extraction buffer containing either 1 % Triton X-100, 2 % Triton X-100 or 1 % CHAPS (3-[(3-Cholamido-propyl)-dimethyl-ammonio]-1-propane-sulfonate) on a rotating wheel for 45 min and centrifugation steps of 10 min at 8000 rpm in between. The pellet was finally washed twice with 25 ml extraction buffer and recombinant Scc1 solubilised in 5 ml 8 M urea using a Dounce homogeniser (Wheaton). After urea treatment, the solution was diluted with deionised water to 6 M urea and centrifuged for 15 min at 20000 rpm. The supernatant containing denatured, soluble Scc1 was centrifuged again for 10 min at 45000 rpm before 1 ml was applied onto a Superdex 200 column (16/60, Amersham Biosciences) preequilibrated in 6 M urea as running solution. The sample was run at 0.8 ml/min and fractions of 2 ml were collected. Six peak fractions containing purified protein were pooled and dialysed in six successive steps using SnakeSkin dialysis bags (Pierce) against following solutions: 4 M, 3 M, 2 M, 1 M urea, and twice in low-salt extraction buffer (50 mM Tris/HCl [pH 8], 100 mM NaCl); each step was for 1 h. Finally the protein concentration was measured by Bradford using the ´Biorad dye reagent concentrate for protein assay´. In addition, quantitative Coomassie staining was performed whereby known amounts of BSA was loaded next to an aliquot of the Scc1 preparation, and relative protein amounts were determined by measuring the fluorescent signal at 685 nm using the Odyssey infrared imager (LI-COR) and Infrared Imaging System software.

Subsequently the protein amount of Scc1 that was loaded was derived from a standard curve, and the concentration of Scc1 in the preparation was calculated (0.25 mg/ml).

7.3.8 ATP crosslinking to cohesin

Crosslinking of ATP to cohesin was carried out with about 200 ng immunopurified cohesin, obtained after TEV elution (see chapter 7.3.2), and 7.4 x 10^4 Bq 8-N_3-[α-^{32}P]ATP (74-370 GBq/mmol, ICN) in 20 μl EB-X buffer. In competition experiments, 1 mM non-radioactive ATP (Roche) was included in the reaction. As a positive control, 200 ng recombinant RecA protein (a gift from Steve West, CR-UK) was subjected to crosslinking in a parallel reaction. Mixtures were incubated for 1 h on ice and irradiated in a UV crosslinker (Stratagene) with 1.5 J/cm^2 over 5 min. Proteins were subsequently analysed by SDS-PAGE followed by autoradiography.

7.3.9 In vitro reconstitution system for cohesin

In the complex reconstitution system, the supernatant fraction of cells expressing or depleted for Scc1, which contained soluble proteins after cell lysis (see chapter 7.3.2), was split into three aliquots of 200 μl each. One aliquot was left untreated, the others were supplemented with 3.5 U/ml apyrase (Sigma) or 20 μl 10x ATP regenerating system (50 mM HEPES/KOH [pH 7.5], 100 mM KCl, 10 mM $MgCl_2$, 10 mM ATP [Roche], 600 mM creatine phosphate [Roche], 1.5 mg/ml creatine kinase [Roche], 1 mM DTT, 10 % glycerol) and incubated for 10 min at 25°C. Similarly treated extracts were then mixed and incubated for 30 min at 25°C. Subsequently mixtures were subjected to immunoprecipitation against the HA_6 tagged Smc1 subunit (see chapter 7.3.2) to assess complex assembly.

7.3.10 Assay for testing ATP-dependent disassembly of cohesin

To test the effect of ATP on the interaction between Scc1 and the SMCs, HA_6 tagged Scc1 was immunoprecipitated (see chapter 7.3.2) in extracts incubated with 12CA5 antibody followed by coupling to 90 μl protein A beads. Beads were washed

and split into six tubes containing 15 µl beads. Beads of one tube were resuspended in 2x SDS-PAGE loading buffer to indicate 'protein input', the beads of the other tubes were resuspended in 40 µl EB-X buffer alone or containing 2 mM ADP (Roche), 2 mM ATP (Roche), 2 mM ATPγS (Roche) or supplemented with an ATP regenerating system (see chapter 7.3.9). The beads were incubated for 30 min at 25°C and spun down. Aliquots from the supernatant fraction were taken that contained released proteins. Beads were subsequently washed twice in EB-X buffer, and resuspended in 2x SDS-PAGE loading buffer. Equivalent fractions of released and bound proteins were loaded on SDS-PAGE and release of SMCs from immobilised Scc1 analysed by Western blotting.

7.4 Microscopy

7.4.1 Sister chromatid separation assay

Sister chromatid separation was scored by using the Tetracycline Operator/Repressor-GFP system described in Michaelis et al., 1997, whereby sister chromatids become visible as green fluorescent dots within the nuclei. For preparation of fixed cells, an aliquot of culture was centrifuged (1 min, 13000 rpm), the supernatant was poured off and the cell pellet was resuspended in 1 ml ice cold absolute ethanol and fixed for 2 h. 5 µl of the suspension was pipetted onto a thin 2 % agarose layer on top of a glass slide. The sample was covered with a cover slip, and chromosomes were visualised using an Axioplan 2 imaging microscope (Zeiss).

7.4.2 Chromosome spreading

To visualise chromatin bound cohesin and SMC complexes, chromosome spreading was carried out adapted from Michaelis et al., 1997. An aliquot of culture containing 1 x 10^7 cells was spun down (1 min, 13000 rpm) and the cell pellet resuspended in 1 ml of 'solution 1' (0.1 M KH_2PO_4/K_2HPO_4 [pH 7.4], 0.5 mM $MgCl_2$ and 1.2 M sorbitol. Samples were spun (1 min, 13000 rpm) and cells were resuspended in 200 µl 'solution 1' containing 100 mM DTT and 0.7 mg/ml zymolyase T-100. Cells were incubated for 5-10 min until complete spheroplastation, and then the reaction was stopped by adding

1 ml ice-cold 'solution 2' (0.1 M MES [2-(N-morpholino)-ethane-sulfonic acid]/KOH [pH 6.4], 0.5 mM $MgCl_2$, 1 M sorbitol, 1 mM EDTA) . Cells were spun (2 min, 4000 rpm) and resuspended in 200 µl 'solution 2'. 20 µl of the cell suspension was pipetted onto a glass slide (Menzel SuperFrost), followed by 40 µl of fixative (4 % paraformaldehyde, 3.4 % sucrose), 80 µl Lipsol (1 %, LIP Ltd.) and another 80 µl fixative. The resulting drop was distributed over the slide by moving a glass rod gently parallel to the slide and air-dried overnight. Slides were washed for 10 min in a jar with PBS-A, blocked for 20 min in blocking buffer (0.5 % BSA and 0.5 % gelatine in PBS-A) in a moist chamber and incubated for 2 h with the first antibody (anti-myc [9E10, CR-UK, 1:100] and anti-HA [16B12, Babco, 1:1000], diluted in blocking buffer), added at 50 µl. The slides were washed in PBS-A for 10 min, and 50 µl of second antibody (goat anti-mouse Cy3-coupled IgG, Amersham Biosciences, 1:1000, diluted in blocking buffer) was added followed by incubation for 2 h in the dark. Slides were again washed for 10 min in a jar with PBS-A and 30 µl DAPI/antifade solution (20 µl blocking buffer plus 10 µl antifade reagent [Biorad], containing 0.1 µg/ml DAPI [4',6-diamidino-2-phenylindole]) was added. Slides were covered with a cover slip and sealed with nail polish. Immunofluorescence stainings were analysed using an Axioplan 2 imaging microscope (Zeiss) attached to a Princeton Cool CCD digital camera, and images were processed using IPlab and Adobe Photoshop software.

7.4.3 Electron microscopy of cohesin/DNA complexes

Cohesin/DNA complexes were purified after release from chromatin by partial or complete micrococcal nuclease digest according to the protocol in chapter 7.3.2. The wash steps of cohesin bound beads before TEV elution was not carried out for six times with EB-X (0.25 % Triton X-100) buffer. Instead, beads were washed in six steps with EB-X buffer containing decreasing amounts of Triton X-100 (twice with EB-X [0.25 %], once with EB-X [0.1 %], once with EB-X [0.05 %] and twice with EB-X [0.02 %]; 1 ml of buffer per wash). TEV elution was carried out in EB-X buffer containing 0.02 % Triton X-100 since low detergent concentration increases attachment of protein or DNA to EM grids. Spreading of cohesin/DNA complexes was done in collaboration with Dr Nasser Hajibagheri at the Electron Microscopy Unit at CR-UK (London) using the Kleinschmidt technique (Kleinschmidt, 1968). Complexes were spread onto glow-

discharged, carbon-coated EM grids and visualised by darkfield transmission EM using a Jeol 1200WEXII electron microscope.

7.5 Table of DNA vectors

Vectors for bacterial expression of Scc1 (see chapter 7.3.7)

Number	Name	Description/cloning	Origin
61	YCplac111-SCC1	Genomic library clone of Scc1.	Christine Michaelis
203	pET30a-SCC1	The ORF of Scc1 was amplified by PCR using the 61 as template and inserted as NdeI/XhoI fragment into 206.	This thesis
206	pET30a	Bacterial expression vector for His6 tagged proteins	Novagen

Integrative vector for promoter exchange in yeast

Number	Name	Description/cloning	Origin
109	YIp22 MET3-CDC20	Construct to exchange the CDC20 promoter against the methionine-repressible promoter (marker: TRP1)	Frank Uhlmann

Vectors for epitope tagging in yeast

Number	Name	Description/cloning	Origin
33	pUC19-myc9-KlTRP1	One step tagging vector to fuse myc9 C-terminally to genes (marker: TRP1).	Wolfgang Zachariae
34	pUC19-myc18-KlTRP1	One step tagging vector to fuse myc18 C-terminally to genes (marker: TRP1).	Wolfgang Zachariae
35	pUC19-HA3-KlTRP1	One step tagging vector to fuse HA3 C-terminally to genes (marker: TRP1).	Wolfgang Zachariae
36	pUC19-HA6-SpHIS5	One step tagging vector to fuse HA6 C-terminally to genes (marker: *S. pombe* HIS5 which complements *S. cerevisiae* HIS3).	Gustav Ammerer
37	pUC19-HA3-SpHIS5	One step tagging vector to fuse HA3 C-terminally to genes (marker: *S. pombe* HIS5 which complements *S. cerevisiae* HIS3).	Wolfgang Zachariae, Marta Galova
38	pUC19-myc18-SpHIS5	One step tagging vector to fuse myc18 C-terminally to genes (marker: *S. pombe* HIS5 which complements *S. cerevisiae* HIS3).	Wolfgang Zachariae, Marta Galova
554	pUC19-3Pk-KITRP1	One step tagging vector to fuse Pk3 C-terminally to genes (marker: TRP1).	Wolfgang Zachariae

Vectors for cloning of cohesin subunit variants

Number	Name	Description/cloning	Origin
17	pGEX-KG	Bacterial expression vector for GST tagged proteins	Neil McDonald
18	pCITE-2a	Vector for *in vitro* translation	Novagen
19	pCITE-2b	Vector for *in vitro* translation	Novagen
125	pFastBac HA3-Smc3	Full length Smc3 cloned into pFastBac vector (Gibco) as HA3 fusion.	Andreas Hochwagen
161	YCp111-SMC1	Genomic library clone of Smc1	Christine Michaelis
162	YCp111-SMC3	Genomic library clone of Smc3	Christine Michaelis
254	pCITE-2a-SMC1 (N-terminal head + coiled coil)	The N-terminal head plus coiled coil (215 aa) of Smc1 was amplified by PCR adding an NdeI site at the 5´ end and an XhoI site at the 3´ end, and was subsequently cloned into 18.	Chris Lehane
310	pCITE-2b-SMC3	The BamHI fragment of full length Smc3 from 125 was cloned into 19 digested with BamHI/XbaI.	Chris Lehane
354	pCITE-2b-SMC3 (SpeI)	The NcoI/BstXI fragment of Smc3 from 310 was replaced with an NcoI/BstXI PCR fragment containing NcoI-Gly-SpeI at the 5´ end.	Chris Lehane
366	pCITE-2a-SMC1 (headless)	A Smc1 fragment excluding the head domains (164-1067 aa) was amplified by PCR and cloned into 18 as BclI/NheI fragment, destroying the BamHI/XbaI sites of the vector.	Chris Lehane
370	pCITE-2a-SMC1 (head)	A PCR fragment containing the C-terminal head plus coiled coil of Smc1 was amplified by PCR adding XhoI-(G_{10} linker)-NotI at the 5´ end and a SalI site at the 3´ end, and was cloned into 254 as a XhoI/SalI fragment, destroying the XhoI site in 254.	Chris Lehane
371	pCITE-2a-SMC3 (headless, SpeI)	A PCR fragment containing the headless region of Smc3 (171-1044 aa) including NcoI-ATG-SpeI at the 5´ end and XhoI at the 3´ end was cloned into 18 cut with NcoI and XhoI.	Chris Lehane
389	pGEX-KG-SMC1 (head)	The Smc1 (head) fragment was cut out with NdeI+blunt/XbaI from 370 and cloned into 17 (cut with BamHI+blunt/XbaI).	Chris Lehane
610	pGEX-KG-SMC1 (head, walker B)	The walker B mutation was introduced into a PCR fragment containing the C-terminal Smc1 region flanked by a NotI site at the 5´ end and an XbaI site at the 3´ end, and exchanged with the corresponding restriction fragment within 389.	This thesis

Basic vectors for gene integration into yeast

Number	Name	Description/cloning	Origin
1	YIplac128	LEU2 based intergrative vector	Gietz and Sugino
2	YIplac204	TRP1 based intergrative vector	Gietz and Sugino
13	YIplac128-GAL	GAL1-10 promoter inserted between EcoRI and BamHI of 1.	Frank Uhlmann
14	YIplac204-GAL	The GAL1-10 promoter was inserted between EcoRI and BamHI of 1.	Frank Uhlmann
466	YIplac128-TPI	The Triosephosphate isomerase 1 promoter was amplified by PCR from genomic DNA as template and cloned into 1 as BamHI/EcoRI fragment.	This thesis

The vectors of the YIplac series are described in Gietz and Sugino, 1988.

Vectors for integration of cohesin subunit variants into yeast

Number	Name	Description/cloning	Origin
41	pBS-HA3 (XbaI)	pBS vector containing the HA3 epitope that can be cut out as XbaI fragment.	D. Kornitzer
42	pBS-HA3 (NotI)	pBS vector containing the HA3 epitope that can be cut out as NotI fragment.	D. Kornitzer
157	pRS305-GAL-SCC1 (Met269-566)-FLAG	Intergrative plasmid to express a stable version of the C-terminal separase cleavage fragment (marker: LEU2).	Hai Rao (Alex Varshavsky)
457	YIplac128-GAL-SMC1-HA6	The N-terminal region of Smc1 was amplified by PCR until the unique BamHI site within Smc1, adding a BglII-ATG-XmaI site at the 5´ end, and inserted into 13 (cut with BamHI). The resulting vector was cut with BamHI/SphI, and an internal Smc1 fragment (BamHI/EcoRI) from 161 and a PCR fragment containing the C-terminal region of Smc1 (starting with EcoRI at the 5´ end and NotI-Stop-SphI at the 3´ end) was inserted by triple ligation. Subsequently a double HA3 tag from 42 (cut out with NotI) was inserted in the resulting vector (cut with NotI).	This thesis
458	YIplac128-GAL-SMC1 (walker A)-HA6	The walker A mutation was introduced into a PCR fragment containing the N-terminal Smc1 region flanked by an XmaI site at the 5´ end and an NcoI site at the 3´ end, and exchanged with the corresponding restriction fragment within 457.	This thesis
459	YIplac128-GAL-SMC1 (walker B)-HA6	The walker B mutation was introduced into a PCR fragment containing the C-terminal Smc1 region flanked by an XbaI site at the 5´ end and an SphI site at the 3´ end, and exchanged with the corresponding restriction fragment within 457.	This thesis

460	YIplac128-GAL-SMC1 (c-motif)-HA6	The C-motif mutation was introduced into a PCR fragment containing the C-terminal Smc1 region flanked by an XbaI site at the 5´ end and an SphI site at the 3´ end, and exchanged with the corresponding restriction fragment within 457.	This thesis
461	YIplac128-GAL-SMC1 (head)-HA3	The Smc1 (head)-fragment was amplified by PCR using 370 as template adding a KpnI site at the 5´ end and a PstI site at the 3´ end, and was subsequently cloned into 481 (cut with KpnI/PstI).	This thesis
462	YIplac128-GAL-SMC1 (head, c-motif)-HA3	The C-motif mutation was introduced into a PCR fragment containing the C-terminal Smc1 (head) region flanked by an XhoI site at the 5´ end and a PstI site at the 3´ end, and exchanged with the corresponding restriction fragment within 461.	This thesis
481	YIplac128-GAL-HA3	13 was cut with BamHI/SphI and a linker (BamHI-KpnI-PstI-NotI-Stop-SphI) was inserted. Subsequently an HA3 epitope tag cassette was inserted into the NotI site.	This thesis
600	YIplac128-GAL-SMC1(headless)-HA3	The C-terminal XbaI/PstI fragment of headless Smc1 in 366 replaced with a PCR fragment that does not contain a stop codon, then the resulting Smc1 (headless) cassette (cut with EcoRV/PstI) was inserted into 481 (cut with KpnI+blunt/PstI).	This thesis
601	YIplac128-TPI-SMC1 (head)-protein A	The Smc1 (head)-protein A cassette of 602 was cut out with KpnI+blunt/HindIII and inserted into 466 (cut with BamHI+blunt/HindIII).	This thesis
602	YIplac128-GAL-SMC1 (head)-protein A	The NotI-HA3-NotI cassette of 481 was exchanged with a NotI-protein A-NotI linker cassette, then the resulting vector was cut with Kpn//PstI and the Smc1 (head) cassette (KpnI/PstI) of 461 was inserted.	This thesis
614	YIplac128-TPI-SMC1(headless)-HA3	The C-terminal XbaI/PstI fragment of headless Smc1 in 366 replaced with a PCR fragment that does not contain a stop codon, then the resulting Smc1 (headless) cassette (cut with EcoRV/PstI) was inserted into YIplac128-TPI-HA3 (analogous to 481 but containing the TPI instead of GAL promoter).	This thesis

616	YIplac128-GAL-SMC1 (head, walker A/c-motif)-HA3	The walker A mutation was introduced into a PCR fragment containing the N-terminal Smc1 region flanked by an NdeI site at the 5´ end and a BamHI site at the 3´ end, and exchanged with the corresponding restriction fragment within 370. An N-terminal fragment containing the mutation was cut out of the resulting vector with MscI/XhoI and cloned into 462 by exchange with a fragment cut out with KpnI+blunt/XhoI.	This thesis
617	YIplac128-TPI-SMC1-HA6	The Smc1-HA6 cassette was cut out from 457 (XmaI+blunt/AflII) and inserted into 466 (cut with BamHI+blunt/AflII).	This thesis
618	YIplac128-TPI-SMC1(walker A)-HA6	The Smc1 (walker A)-HA6 cassette was cut out from 458 (XmaI+blunt/AflII) and inserted into 466 (cut with BamHI+blunt/AflII).	This thesis
621	YIplac128-GAL-SMC1 (head, walker B)-HA3	A fragment containing the walker B mutation within the Smc1 (head) was cut out with SpeI/BglII, and cloned into 461 by exchange with a fragment cut out with SpeI/BglII.	This thesis
622	YIplac204-TPI-SMC1 (head)-protein A	The TPI-Smc1 (head)-protein A cassette from 601 was cut out with NdeI/HindIII and inserted into 2 (cut with NdeI/HindIII).	This thesis
632	YIplac128-GAL-HA3-SMC3 (headless)	An HA3 tag from 41 (cut out with XbaI) was inserted into 371 (cut with SpeI), the resulting plasmid was then cut with NcoI+blunt/PstI and the HA3-Smc3 (headless) cassette was inserted into 13 (cut with BamHI+blunt/PstI).	This thesis
634	YIplac128-GAL-HA9-SMC3	A triple HA3 tag from 41 (cut out with XbaI) was inserted into 354 (cut SpeI), the resulting plasmid was then cut with NcoI+blunt/SalI and the HA9-Smc3 cassette was inserted into 13 (cut with BamHI+blunt/SalI).	This thesis
673	YIplac128-GAL-SMC1 (head, walker A)-HA3	The walker A mutation was introduced into a PCR fragment containing the N-terminal Smc1 region flanked by an NdeI site at the 5´ end and a BamHI site at the 3´ end, and exchanged with the corresponding restriction fragment within 370. The Smc1 (head, Walker A) cassette of the resulting vector was cut out with MscI/XhoI and cloned into 461 by exchange with a fragment cut out with KpnI+blunt/XhoI.	This thesis

PCR amplifications of regions within Smc1 and Smc3 were carried out using the genomic library clones 161 and 162 as templates. The vector number in this table corresponds to the number in the DNA database of the Uhlmann lab.

7.6 Table of yeast strains

Gene names are abbreviated by three italicised upper case letters followed by a number e.g. *SCC1*. Mutant alleles are indicated as italicised lower case letters e.g. *pep4*. Gene deletions are shown by the '::' or 'Δ' symbols, e.g. *pep4::URA3*, whereby *URA3* represents the marker gene which was used for replacement of *PEP4*. In addition, the marker behind the '::' symbol is integrated into the genome when used for epitope tagging (e.g. *SCC1-HA6::HIS3*), promoter-gene cassette integration (e.g. *GAL-SMC1-HA6::*LEU2) and promoter exchange (*MET3-CDC20::TRP1*). A temperature sensitive mutant allele, for example of *SMC1*, is indicated as $smc1^{ts}$ or *smc1-259*.

All strains are derivatives of W303 or backcrossed against this background, and are therefore *ade2-1, trp1-1, leu2-3, his3-11,15, ura3-1, can1-100*. The origin of all strains is this thesis, apart from strains K7062 (Christine Michaelis) and Y115 (Frank Uhlmann).

Strain	Genotype
K7062	*MATa barΔ scc1::URA3 GAL-SCC1-myc18*
Y115	*MATa MET3-CDC20::TRP1 TetR-GFP::HIS3 TetOs::URA3*
Y458	*MATa pep4::URA3 bar1::hisG SCC3-HA3::HIS3*
Y613	*MATa pep4::URA3 bar1::hisG SCC1-HA6::HIS3 SMC1-myc18::TRP1*
Y618	*MATa pep4::URA3 bar1::hisG SCC1-TEV-HA6::HIS3*
Y749	*MATa barΔ scc1::URA3 GAL-SCC1-myc18 SMC1-TEV-HA6::HIS3*
Y752	*MATa pep4::URA3 bar1::hisG SMC1-TEV-HA6::HIS3*
Y754	*MATa smc1-259 pep4::URA3 TetR-GFP::HIS3 TetOs::URA3 GAL-SMC1-HA6::LEU2*
Y782	*MATa smc1-259 pep4::URA3 TetR-GFP::HIS3 TetOs::URA3 GAL-SMC1(walker A)-HA6::LEU2*
Y783	*MATa smc1-259 pep4::URA3 TetR-GFP::HIS3 TetOs::URA3 GAL-SMC1(c-motif)-HA6::LEU2*
Y784	*MATa smc1-259 pep4::URA3 TetR-GFP::HIS3 TetOs::URA3 GAL-SMC1(walker B)-HA6::LEU2*

Y793	*MATa smc1-259 MET3-CDC20::TRP1 pep4::URA3 TetR-GFP::HIS3 TetOs::URA3 GAL-SMC1(walker A)-HA6::LEU2*
Y794	*MATa smc1-259 MET3-CDC20::TRP1 pep4::URA3 TetR-GFP::HIS3 TetOs::URA3 GAL-SMC1(c-motif)-HA6::LEU2*
Y795	*MATa smc1-259 MET3-CDC20::TRP1 pep4::URA3 TetR-GFP::HIS3 TetOs::URA3 GAL-SMC1(walker B)-HA6::LEU2*
Y797	*MATa smc1-259 TetR-GFP::HIS3 TetOs::URA3 SCC1-myc9::TRP1 GAL-SMC1-HA6::LEU2*
Y821	*MATa smc1-259 MET3-CDC20::TRP1 pep4::URA3 TetR-GFP::HIS3 TetOs::URA3 GAL-SMC1-HA6::LEU2*
Y826	*MATa smc1-259 TetR-GFP::HIS3 TetOs::URA3 SCC1-myc9::TRP1 GAL-SMC1(c-motif)-HA6::LEU2*
Y827	*MATa smc1-259 TetR-GFP::HIS3 TetOs::URA3 SCC1-myc9::TRP1 GAL-SMC1(walker B)-HA6::LEU2*
Y839	*MATa smc1-259 TetR-GFP::HIS3 TetOs::URA3 SCC1-myc9::TRP1 GAL-SMC1(walker A)-HA6::LEU2*
Y917	*MATa cdc15-2 TetR-GFP::HIS3 TetOs::URA3 GAL-SMC1-HA6::LEU2*
Y918	*MATa cdc15-2 TetR-GFP::HIS3 TetOs::URA3 GAL-SMC1(c-motif)-HA6::LEU2*
Y956	*MATa pep4::URA3 bar1::hisG SCC1-myc9::TRP1 GAL-SMC1(head)-HA3::LEU2*
Y999	*MATa pep4::URA3 bar1::hisG SCC1-myc9::TRP1 GAL-SMC1(head, c-motif)-HA3::LEU2*
Y1000	*MATa pep4::URA3 bar1::hisG SMC3-myc9::TRP1 GAL-SMC1(head)-HA3::LEU2*
Y1001	*MATa pep4::URA3 bar1::hisG SMC3-myc9::TRP1 GAL-SMC1(head, c-motif)-HA3::LEU2*
Y1065	*MATa smc1-259 TetR-GFP::HIS3 TetOs::URA3 SCC1-myc9::TRP1 GAL-SMC1(head)-HA3::LEU2*
Y1172	*MATa barΔ scc1::URA3 GAL-SCC1-myc18 SMC3-HA3::TRP1 TPI-SMC1(head)-ProtA::LEU2*

Y1225	*MATa smc1-259 TetR-GFP::HIS3 TetOs::URA3 SCC1-myc9::TRP1 GAL-SMC1(headless)-HA3::LEU2*
Y1281	*MATa pep4::URA3 bar1::hisG SMC3-HA3::HIS3 GAL-SCC1(Met269-566)-FLAG::LEU2 TPI-SMC1(head)-ProtA::TRP1*
Y1319	*MATa pep4::URA3 bar1::hisG SCC1-myc9::TRP1 GAL-SMC1(head, walker A)-HA3::LEU2*
Y1320	*MATa pep4::URA3 bar1::hisG SCC1-myc9::TRP1 GAL-SMC1(head, walker B)-HA3::LEU2*
Y1321	*MATa pep4::URA3 bar1::hisG SMC3-myc9::TRP1 GAL-SMC1(head, walker A)-HA3::LEU2*
Y1322	*MATa pep4::URA3 bar1::hisG SMC3-myc9::TRP1 GAL-SMC1(head, walker B)-HA3::LEU2*
Y1418	*MATa barΔ scc1::URA3 GAL-SCC1-myc18 SMC3-TEV-Pk3::TRP1 TPI-SMC1-HA6::LEU2*
Y1419	*MATa barΔ scc1::URA3 GAL-SCC1-myc18 SMC3-TEV-Pk3::TRP1 TPI-SMC1(walker A)-HA6::LEU2*
Y1420	*MATa barΔ scc1::URA3 GAL-SCC1-myc18 SMC3-TEV-Pk3::TRP1 TPI-SMC1(headless)-HA3::LEU2*
Y1478	*MATa pep4::URA3 bar1::hisG SMC3-myc9::TRP1 GAL-SMC1(head, walker A/c-motif)-HA3::LEU2*
Y1565	*MATa MET3-CDC20::TRP1 TetR-GFP::HIS3 TetOs::URA3 GAL-SCC1(Met269-566)-FLAG::LEU2*
Y1573	*MATa smc1-259 TetR-GFP::HIS3 TetOs::URA3 SCC3-Pk3::TRP1 GAL-SMC1-HA6::LEU2*
Y1574	*MATa smc1-259 TetR-GFP::HIS3 TetOs::URA3 SCC3-Pk3::TRP1 GAL-SMC1-HA6(c-motif)::LEU2*
Y1674	*MATa barΔ scc1::URA3 GAL-SCC1-myc18 SMC1-TEV-HA6::HIS3 SCC3-Pk3::LEU2*
Y1719	*MATa pep4::URA3 bar1::hisG SCC1-myc18::HIS3 SMC3-Pk3::TRP1 GAL-SMC1-HA6::LEU2*

Y1720	*MAT*a *pep4::URA3 bar1::hisG SCC1-myc18::HIS3 SMC3-Pk3::TRP1 GAL-SMC1(headless)-HA3::LEU2*
Y1721	*MAT*a *pep4::URA3 bar1::hisG SCC1-myc18::HIS3 SMC1-Pk3::TRP1 GAL-SMC3-HA9::LEU2*
Y1722	*MAT*a *pep4::URA3 bar1::hisG SCC1-myc18::HIS3 SMC1-Pk3::TRP1 GAL-SMC3(headless)-HA3::LEU2*

CHAPTER 8: References

Adams, R. R., Maiato, H., Earnshaw, W. C., and Carmena, M. (2001). Essential roles of Drosophila inner centromere protein (INCENP) and aurora B in histone H3 phosphorylation, metaphase chromosome alignment, kinetochore disjunction, and chromosome segregation. J Cell Biol *153*, 865-879.

Agarwal, R., and Cohen-Fix, O. (2002). Phosphorylation of the mitotic regulator Pds1/securin by Cdc28 is required for efficient nuclear localization of Esp1/separase. Genes Dev *16*, 1371-1382.

Akhemedov, A. T., Frei, C., Tsai-Pflugfelder, M., Kemper, B., Gasser, S. M., and Jessberger, R. (1998). Structural maintenance of chromosomes protein C-terminal domains bind preferentially to DNA with secondary structure. J Biol Chem *273*, 24088-24094.

Akhmedov, A. T., Gross, B., and Jessberger, R. (1999). Mammalian SMC3 C-terminal and coiled-coil protein domains specifically bind palindromic DNA, do not block DNA ends, and prevent DNA bending. J Biol Chem *274*, 38216-38224.

Alexandru, G., Uhlmann, F., Poupart, M.-A., Mechtler, K., and Nasmyth, K. (2001). Phosphorylation of the cohesin subunit Scc1 by Polo/Cdc5 kinase regulates sister chromatid separation in yeast. Cell *105*, 459-472.

Al-Shawi, M. K., and Senior, A. E. (1993). Characterization of the adenosine triphosphatase activity of Chinese hamster P-glycoprotein. J Biol Chem *268*, 4197-4206.

Anderson, D. E., Losada, A., Erickson, H. P., and Hirano, T. (2002). Condensin and cohesin display different arm conformations with characteristic hinge angles. J Cell Biol *156*, 419-424.

Arumugam, P., Gruber, S., Tanaka, K., Haering, C. H., Mechtler, K., and Nasmyth, K. (2003). ATP hydrolysis is required for cohesin's association with chromosomes. Curr Biol *13*, 1941-1953.

Azzaria, M., Schurr, E., and Gros, P. (1989). Discrete mutations introduced in the predicted nucleotide-binding sites of the mdr1 gene abolish its ability to confer multidrug resistance. Mol Cell Biol *9*, 5289-5297.

Bazett-Jones, D. P., Kimura, K., and Hirano, T. (2002). Efficient supercoiling of DNA by a single condensin complex as revealed by electron spectroscopic imaging. Mol Cell *9*, 1183-1190.

Beasley, M., Xu, H., Warren, W., and McKay, M. (2002). Conserved disruptions in the predicted coiled-coil domains of eukaryotic SMC complexes: implications for structure and function. Genome Res *12*, 1201-1209.

Bermudez, V. P., Maniwa, Y., Tappin, I., Ozato, K., Yokomori, K., and Hurwitz, J. (2003). The alternative Ctf18-Dcc1-Ctf8-replication factor C complex required for sister chromatid cohesion loads proliferating cell nuclear antigen onto DNA. Proc Natl Acad Sci U S A *100*, 10237-10242.

Bernard, P., Maure, J. F., Partridge, J. F., Genier, S., Javerzat, J. P., and Allshire, R. C. (2001). Requirement of heterochromatin for cohesion at centromeres. Science *294*, 2539-2542.

Bianchet, M. A., Ko, Y. H., Amzel, L. M., and Pedersen, P. L. (1997). Modeling of nucleotide binding domains of ABC transporter proteins based on a F1-ATPase/recA topology: structural model of the nucleotide binding domains of the cystic fibrosis transmembrane conductance regulator (CFTR). J Bioenerg Biomembr *29*, 503-524.

Biggins, S., and Murray, A. W. (2001). The budding yeast protein kinase Ipl1/aurora allows the absence of tension to activate the spindle checkpoint. Genes Dev *15*, 3118-3129.

Biggins, S., Severin, F. F., Bhalla, N., Sassoon, I., Hyman, A., and Murray, A. W. (1999). The conserved protein kinase Ipl1 regulates microtubule binding to kinetochores in budding yeast. Genes Dev *13*, 532-544.

Birkenbihl, R. P., and Subramani, S. (1995). The *rad21* gene product of *Schizosaccharomyces pombe* is a nuclear, cell cycle-regulated phosphoprotein. J Biol Chem *270*, 7703-7711.

Blat, Y., and Kleckner, N. (1999). Cohesins bind to preferential sites along yeast chromosome III, with differential regulation along arms versus the centric region. Cell *98*, 249-259.

Bloomfield, V., Dalton, W. O., and van Holde, K. E. (1967). Frictional coefficients ofmultisubunit structures. I. Theory. Biopolymers *5*, 135-148.

Boddy, M. N., Shanahan, P., McDonald, W. H., Lopez-Girona, A., Noguchi, E., Yates, I. J., and Russell, P. (2003). Replication checkpoint kinase Cds1 regulates recombinational repair protein Rad60. Mol Cell Biol *23*, 5939-5946.

Britton, R. A., Lin, D. C., and Grossman, A. D. (1998). Characterization of a prokaryotic SMC protein involved in chromosome partitioning. Genes Dev *12*, 1254-1259.

Buonomo, S. B. C., Clyne, R. K., Fuchs, J., Loidl, J., Uhlmann, F., and Nasmyth, K. (2000). Disjunction of homologous chromosomes in meiosis I depends on proteolytic cleavage of the meiotic cohesin Rec8 by separin. Cell *103*, 387-398.

Chan, R. C., Chan, A., Jeon, M., Wu, T. F., Pasqualone, D., Rougvie, A. E., and Meyer, B. J. (2003). Chromosome cohesion is regulated by a clock gene paralogue TIM-1. Nature *423*, 1002-1009.

Cheeseman, I. M., Anderson, S., Jwa, M., Green, E. M., Kang, J., Yates Ill, J. R., Chan, C. S., G., D. D., and Barnes, G. (2002). Phospho-regulation of kinetochore-microtubule attachments by the Aurora kinase Ipl1p. Cell *111*, 163-172.

Chen, J., Gang, L., Lin, J., Davidson, A. L., and Quiocho, F. A. (2003). A tweezers-like motion of the ATP-binding cassette dimer in an ABC transport cycle. Mol Cell *12*, 651-661.

Chiu, A., Revenkova, E., and Jessberger, R. (2004). DNA interaction and dimerization of eukaryotic SMC hinge domains. J Biol Chem *279*, 26233-26242.

Chuang, P. T., Albertson, D. G., and Meyer, B. J. (1994). DPY-27:a chromosome condensation protein homolog that regulates C. elegans dosage compensation through association with the X chromosome. Cell *79*, 459-474.

Ciosk, R., Shirayama, M., Shevchenko, A., Tanaka, T., Toth, A., Shevchenko, A., and Nasmyth, K. (2000). Cohesin's binding to chromosomes depends on a separate complex consisting of Scc2 and Scc4 proteins. Mol Cell *5*, 1-20.

Ciosk, R., Zachariae, W., Michaelis, C., Shevchenko, A., Mann, M., and Nasmyth, K. (1998). An Esp1/Pds1 complex regulates loss of sister chromatid cohesion at the metaphase to anaphase transition in yeast. Cell *93*, 1067-1076.

Cohen-Fix, O., Peters, J.-M., Kirschner, M. W., and Koshland, D. (1996). Anaphase initiation in *Saccharomyces cerevisiae* is controlled by the APC-dependent degradation of the anaphase inhibitor Pds1p. Genes Dev *10*, 3081-3093.

D'Amours, D., and Jackson, S. P. (2002). The Mre11 complex: at the crossroads of dna repair and checkpoint signalling. Nat Rev Mol Cell Biol *3*, 317-327.

Davidson, A. L. (2002). Mechanism of coupling of transport to hydrolysis in bacterial ATP-binding cassette transporters. J Bacteriol *184*, 1225-1233.

Davidson, A. L., Laghaeian, S. S., and Mannering, D. E. (1996). The maltose transport system of Escherichia coli displays positive cooperativity in ATP hydrolysis. J Biol Chem *271*, 4858-4863.

Davidson, A. L., and Sharma, S. (1997). Mutation of a single MalK subunit severely impairs maltose transport activity in Escherichia coli. J Biol Chem *179*, 5458-5464.

de Jager, M., van Noort, J., van Gent, D. C., Dekker, C., Kanaar, R., and Wyman, C. (2001). Human Rad50/Mre11 is a flexible complex that can tether DNA ends. Mol Cell *8*, 1129-1135.

Denison, S. H., Kafer, E., and May, G. S. (1993). Mutation in the bimD gene of *Aspergillus nidulans* confers a conditional mitotic block and sensitivity to DNA damaging agents. Genetics *134*, 1085-1096.

Dewar, H., Tanaka, K., Nasmyth, K., and Tanaka, T. (2004). Tension between two kinetochores suffices for their bi-orientation on the mitotic spindle. Nature *428*, 93-97.

Donze, D., Adams, C. R., Rine, J., and Kamakaka, R. T. (1999). The boundaries of the silenced *HMR* domain in *Saccharomyces cerevisiae*. Genes Dev *13*, 698-708.

Dougherty, W. G., Cary, S. M., and Parks, T. D. (1989). Molecular genetic analysis of a plant virus polyprotein cleavage site: a model. Virology *171*, 356-364.

Edwards, S., Li, C. M., Levy, D. L., Brown, J., Snow, P. M., and Campbell, J. L. (2003). *Saccharomyces cerevisiae* DNA polymerase ε and polymerase σ interact physically and functionally, suggesting a role for polymerase ε in sister chromatid cohesion. Mol Cell Biol *23*, 2733-2748.

Fetsch, E. E., and Davidson, A. L. (2002). Vanadate-catalyzed photocleavage of the signature motif of an ATP-binding cassette (ABC) transporter. Proc Natl Acad Sci U S A *99*, 9685-9690.

Fitch, I. T., Dahmann, C., Surana, U., Amon, A., Nasmyth, K., Goetsch, L., Byers, B., and Futcher, B. (1992). Characterization of four B-type cyclin genes of the budding yeast *Saccharomyces cerevisiae*. Mol Biol Cell *3*, 805-818.

Formosa, T., and Nittis, T. (1999). Dna2 mutants reveal interactions with Dna polymerase alpha and Ctf4, a Pol alpha accessory factor, and show that full Dna2 helicase activity is not essential for growth. Genetics *151*, 1459-1470.

Fousteri, M. I., and Lehmann, A. R. (2000). A novel SMC protein complex in *Schizosaccharomyces pombe* contains the Rad18 DNA repair complex. EMBO J *19*, 1691-1702.

Freeman, L., Aragon-Alcaide, L., and Strunnikov, A. (2000). The condensin complex governs chromosome condensation and mitotic transmission of rDNA. J Cell Biol *149*, 811-824.

Fujioka, Y., Kimata, Y., Nomaguchi, K., Watanabe, K., and Kohno, K. (2002). Identification of a novel non-structural maintenance of chromosomes (SMC) component of the SMC5-SMC6 complex involved in DNA repair. J Biol Chem *277*, 21585-21591.

Funabiki, H., Yamano, H., Kumada, K., Nagao, K., Hunt, T., and Yanagida, M. (1996). Cut2 proteolysis required for sister-chromatid seperation in fission yeast. Nature *381*, 438-441.

Gietz, R. D., and Sugino, A. (1988). New yeast-*Escherichia coli* shuttle vectors constructed with in vitro mutagenized yeast genes lacking six-base restriction sites. Gene *74*, 527-534.

Gruber, S., Haering, C. H., and Nasmyth, K. (2003). Chromosomal cohesin forms a ring. Cell *112*, 765-777.

Guacci, V., Koshland, D., and Strunnikov, A. (1997). A direct link between sister chromatid cohesion and chromosome condensation revealed through analysis of *MCD1* in S. cerevisiae. Cell *91*, 47-57.

Haering, C. H., Löwe, J., Hochwagen, A., and Nasmyth, K. (2002). Molecular architecture of SMC proteins and the yeast cohesin complex. Mol Cell *9*, 773-788.

Hagstrom, K. A., Holmes, V. F., Cozzarelli, N. R., and Meyer, B. J. (2002). C. elegans condensin promotes mitotic chromosome architecture, centromere organization, and sister chromatid segregation during mitosis and meiosis. Genes Dev *16*, 729-742.

Hakimi, M. A., Bochar, D. A., Schmiesing, J. A., Dong, Y., Barak, O. G., Speicher, D. W., Yokomori, K., and Shiekhattar, R. (2002). A chromatin remodelling complex that loads cohesin onto human chromosomes. Nature *418*, 994-998.

Hanna, J. S., Kroll, E. S., Lundblad, V., and Spencer, F. A. (2001). *Saccharomyces cerevisiae* CTF18 and CTF4 are required for sister chromatid cohesion. Mol Cell Biol *21*, 3144-3158.

Hassold, T., and Hunt, P. (2001). To err (meiotically) is human: the genesis of human aneuploidy. Nat Rev Genet *2*, 280-291.

Hauf, S., Waizenegger, I. C., and Peters, J.-M. (2001). Cohesin cleavage by separase required for anaphase and cytokinesis in human cells. Science *293*, 1320-1323.

Hirano, M., Anderson, D. E., Erickson, H. P., and Hirano, T. (2001). Bimodal activation of SMC ATPase by intra- and inter-molecular interactions. EMBO J *20*, 3238-3250.

Hirano, M., and Hirano, T. (1998). ATP-dependent aggregtion of single-stranded DNA by a bacterial SMC homodimer. EMBO J *17*, 7139-7148.

Hirano, M., and Hirano, T. (2002). Hinge-mediated dimerization of SMC protein is essential for its dynamic interaction with DNA. EMBO J *21*, 5733-5744.

Hirano, T. (2002). The ABCs of SMC proteins: two-armed ATPases for chromosome condensation, cohesion, and repair. Genes Dev *16*, 399-414.

Hirano, T., Kobayashi, R., and Hirano, M. (1997). Condensins, chromosome condensation protein complexes containing XCAP-C, XCAP-E and a Xenopus homolog of the Drosophila barren protein. Cell *89*, 511-521.

Hirano, T., and Mitchison, T. J. (1994). A heterodimeric coiled-coil protein required for mitotic chromosome condensation in vitro. Cell *79*, 449-458.

Holland, I. B., and Blight, M. A. (1999). ABC-ATPases, adaptable energy generators fuelling transmembrane movement of a variety of molecules in organisms from bacteria to humans. J Mol Biol *293*, 381-399.

Holt, C. L., and May, G. S. (1996). An extragenic suppressor of the mitosis-defective *bimD6* mutation of *Aspergillus nidulans* codes for a chromosome scaffold protein. Genetics *142*, 777-787.

Hopfner, K.-P., Craig, L., Moncalian, G., Zinkel, R. A., Usui, T., Owen, B. A. L., Karcher, A., Henderson, B., Bodmer, J.-L., McMurray, C. T., *et al.* (2002). The Rad50 zinc-hook is a structure joining Mre11 complexes in DNA recombination and repair. Nature *418*, 562-566.

Hopfner, K.-P., Karcher, A., Craig, L., Woo, T. T., Carney, J. P., and Tainer, J. A. (2001). Structural biochemistry and interaction architecture of the DNA double-strand break repair Mre11 nuclease and Rad50-ATPase. Cell *105*, 473-485.

Hopfner, K.-P., Karcher, A., Shin, D. S., Craig, L., Arthur, L. M., Carney, J. P., and Tainer, J. A. (2000). Structural Biology of Rad50 ATPase: ATP-driven conformational control in DNA double-strand break repair and the ABC-ATPase superfamily. Cell *101*, 789-800.

Hopfner, K. P., and Tainer, J. A. (2003). Rad50/SMC proteins and ABC transporters: unifying concepts from high-resolution structures. Curr Opin Struct Biol *13*, 249-255.

Hoque, M. T., and Ishikawa, F. (2002). Cohesin defects lead to premature sister chromatid separation, kinetochore dysfunction and spindle-assembly checkpoint activation. J Biol Chem *277*, 42306-42314.

Hornig, N. C., and Uhlmann, F. (2004). Preferential cleavage of chromatin-bound cohesin after targeted phosphorylation by Polo-like kinase. EMBO J *23*, 3144-3153.

Hornig, N. C. D., Knowles, P. P., McDonald, N. Q., and Uhlmann, F. (2002). The dual mechanism of separase regulation by securin. Curr Biol *12*, 973-982.

Huang, J., Hsu, J. M., and Laurent, B. C. (2004). The RSC nucleosome-remodeling complex is required for Cohesin's association with chromosome arms. Mol Cell *13*, 739-750.

Hung, L. W., Wang, I. X., Nikaido, K., Liu, P. Q., Ames, G. F., and Kim, S. H. (1998). Crystal structure of the ATP-binding subunit of an ABC transporter. Nature *396*, 703-707.

Irniger, S., Piatti, S., Michaelis, C., and Nasmyth, K. (1995). Genes involved in sister chromatid separation are needed for B-type cyclin proteolysis in budding yeast. Cell *81*, 269-278.

Ivanov, D., Schleiffer, A., Eisenhaber, F., Mechtler, K., Haering, C. H., and Nasmyth, K. (2002). Eco1 is a novel acetlytransferase that can acetylate proteins involved in cohesion. Curr Biol *12*, 323-328.

Jallepalli, P. V., and Lengauer, C. (2001). Chromosome segregation and cancer: cutting through the mystery. Nat Rev Cancer *1*, 109-117.

Janke, C., Ortiz, J., Tanaka, T. U., Lechner, J., and Schiebel, E. (2002). Four new subunits of the Dam1-Duo1 complex reveal novel functions in sister kinetochore biorientation. EMBO J *21*, 181-193.

Jensen, S., Segal, M., Clarke, D. J., and Reed, S. I. (2001). A novel role of the budding yeast separin Esp1 in anaphase spindle elongation: evidence that proper spindle association of Esp1 is regulated by Pds1. J Cell Biol *152*, 27-40.

Jessberger, R. (2002). The many functions of SMC proteins in chromosome dynamics. Nat Rev Mol Cell Biol *3*, 767-778.

Jessberger, R., Riwar, B., Baechtold, H., and Akhemedov, A. T. (1996). SMC proteins constitute two subunits of the mammalian recombination protein complex RC-1. EMBO J *15*, 4061-4068.

Jones, P. M., and George, A. M. (1999). Subunit interactions in ABC transporters: towards a functional architecture. FEMS Microbiol Lett *179*, 187-202.

Kagansky, A., Freeman, L., Lukyanov, D., and Strunnikov, A. (2003). Histone-tail independent chromatin-binding activity of recombinant cohesin holocomplex. J Biol Chem *279*, 3382-3388.

Kaitna, S., Pasierbek, P., Jantsch, M., Loidl, J., and Glotzer, M. (2002). The aurora B kinase AIR-2 regulates kinetochores during mitosis and is required for separation of homologous chromosomes during meiosis. Curr Biol *12*, 798-812.

Kim, S. T., Xu, B., and Kastan, M. B. (2002). Involvement of the cohesin protein, Smc1, in Atm-dependent and independent responses to DNA damage. Genes Dev *16*, 560-570.

Kimura, K., Cuvier, O., and Hirano, T. (2001). Chromosome condensation by a human condensin complex in *Xenopus* egg extracts. J Biol Chem *276*, 5417-5420.

Kimura, K., and Hirano, T. (1997). ATP-Dependent positive supercoiling of DNA by 13S condensin: a biochemical implication for chromosome condensation. Cell *90*, 625-634.

Kimura, K., and Hirano, T. (2000). Dual roles of the 11S regulatory subcomplex in condensin functions. Proc Natl Acad Sci USA *97*, 11972-11977.

Kimura, K., Rybenkov, V. V., Crisona, N. J., Hirano, T., and Cozzarelli, N. R. (1999). 13S condensin actively reconfigures DNA by introducing global positive writhe: implications for chromosome condensation. Cell *98*, 239-248.

Kitagawa, R., Bakkenist, C. J., McKinnon, P. J., and Kastan, M. B. (2004). Phosphorylation of SMC1 is a critical downstream event in the ATM-NBS1-BRCA1 pathway. Genes Dev *18*, 1423-1438.

Kitajima, T. S., Yokobayashi, S., Yamamoto, M., and Watanabe, Y. (2003). Distinct cohesin complexes organize meiotic chromosome domains. Science *300*, 1152-1155.

Klein, F., Mahr, P., Galova, M., Buonomo, S. B. C., Michaelis, C., Nairz, K., and Nasmyth, K. (1999). A central role for cohesins in sister chromatid cohesin, formation of axial elements, and recombination during yeast meiosis. Cell *98*, 91-103.

Kleinschmidt, A. K. (1968). Monolayer technique in electron microscopy of nucleic acid molecules. Method in Enzymology *vol. 12B*, 361-376.

Knop, M., Siegers, K., Pereira, G., Zachariae, W., Winsor, B., Nasmyth, K., and Schiebel, E. (1999). Epitope tagging of yeast genes using a PCR-based strategy: more tags and improved practical routines. Yeast *15*, 963-972.

Kushnirov, V. V. (2000). Rapid and reliable protein extraction from yeast. Yeast *16*, 857-860.

Laloraya, S., Guacci, V., and Koshland, D. (2000). Chromosomal addresses of the cohesin component Mcd1p. J Cell Biol *151*, 1047-1056.

Lavoie, B. D., Hogan, E., and Koshland, D. (2002). In vivo dissection of the chromosome condensation machinery: reversibility of condensation distinguishes contributions of condensin and cohesin. J Cell Biol *156*, 805-815.

Lehmann, A. R., Walicka, M., Griffith, D. J. F., Murray, J. M., Watts, F. Z., McCready, S., and Carr, A. M. (1995). The *rad18* gene of *Schizosaccharomyces pombe* defines a new subgroup of the SMC superfamily involved in DNA repair. Mol Cell Biol *15*, 7067-7080.

Lemon, K. P., and Grossman, A. D. (2000). Movement of replicating DNA through a stationary replisome. Mol Cell *6*, 1321-1330.

Lengronne, A., Katou, Y., Mori, S., Yokobayashi, S., Kelly, G. P., Itoh, T., Watanabe, Y., Shirahige, K., and Uhlmann, F. (2004). Cohesin relocation from sites of chromosomal loading to places of convergent transcription. Nature *430*, 573-578.

Liang, C., and Stillman, B. (1997). Persistent initiation of DNA replication and chromatin-bound MCM proteins during the cell cycle in *cdc6* mutants. Genes Dev *11*, 3375-3386.

Lieb, J. D., Albrecht, M. R., Chuang, P. T., and Meyer, B. J. (1998). MIX-1: an essential component of the C. elegans mitotic machinery executes X chromosome dosage compensation. Cell *92*, 265-277.

Lindow, J. C., Britton, R. A., and Grossman, A. D. (2002). Structural maintenance of chromosomes protein of Bacillus subtilis affects supercoiling in vivo. J Bacteriol *184*, 5317-5322.

Loo, T. W., and Clarke, D. M. (1996). Rapid purification of human P-glycoprotein mutants expressed transiently in HEK 293 cells by nickel-chelate chromatography and characterization of their drug-stimulated ATPase activities. J Biol Chem *270*, 214449-221452.

Loo, T. W., and Clarke, D. M. (1997). Characterization of the adenosine triphosphatase activity of the periplasmic histidine permease, a traffic ATPase (ABC transporter). J Biol Chem *272*, 21883-21891.

Losada, A., Hirano, M., and Hirano, T. (1998). Identification of *Xenopus* SMC protein complexes required for sister chromatid cohesion. Genes Dev *12*, 1986-1997.

Losada, A., Hirano, M., and Hirano, T. (2002). Cohesin release is required for sister chromatid resolution but not for condensin-mediated compaction, at the onset of mitosis. Genes Dev *16*, 3004-3016.

Losada, A., and Hirano, T. (2001). Intermolecular DNA interactions stimulated by the cohesin complex in vitro: Implications for sister chromatid cohesion. Curr Biol *11*, 268-272.

Losada, A., Yokochi, T., Kobayashi, R., and Hirano, T. (2000). Identification and characterization of SA/Scc3p subunits in the *Xenopus* and human cohesin complexes. J Cell Biol *150*, 405-416.

Löwe, J., Cordell, S. C., and van den Ent, F. (2001). Crystal structure of the SMC head domain: an ABC ATPase with 900 residues antiparallel coiled-coil inserted. J Mol Biol *306*, 25-35.

Lupas, A., Van Dyke, M., and Stock, J. (1991). Predicting Coled Coils from Protein Sequences. Science *252*, 1162-1164.

Lupo, R., Breiling, A., Bianchi, M. E., and Orlando, V. (2001). *Drosophila* chromosome condensation proteins topoisomerase II and barren colocalize with polycomb and maintain *Fab-7* PRE silencing. Mol Cell *7*, 127-136.

Mascarenhas, J., Soppa, J., Strunnikov, A., and Graumann, P. L. (2002). Cell cycle-dependent localization of two novel prokaryotic chromosome segregation and condensation proteins in *Bacillus subtilis* that interact with SMC protein. EMBO J *21*, 3108-3118.

Mayer, M. L., Gygi, S. P., Aebersold, R., and Hieter, P. (2001). Identification of RFC(Ctf18p, Ctf8p, Dcc1p): An alternative RFC complex required for sister chromatid cohesion in *S. cerevisiae*. Mol Cell *7*, 959-970.

McDonald, W. H., Pavlova, Y., Yates Ill, J. R., and Boddy, M. N. (2003). Novel essential DNA repair proteins Nse1 and Nse2 are subunits of the fission yeast Smc5-Smc6 complex. J Biol Chem *278*, 45460-45467.

Megee, P. C., Mistrot, C., Guacci, V., and Koshland, D. (1999). The centromeric sister chromatid cohesion site directs Mcd1p binding to adjacent sequences. Mol Cell *4*, 445-450.

Melby, T. E., Ciampaglio, C. N., Briscoe, G., and Erickson, H. P. (1998). The symmetrical structure of structural maintenance of chromosomes (SMC) and MukB proteins: long, antiparallel coiled coils, folded at a flexible hinge. J Cell Biol *142*, 1595-1604.

Michaelis, C., Ciosk, R., and Nasmyth, K. (1997). Cohesins: Chromosomal proteins that prevent premature separation of sister chromatids. Cell *91*, 35-45.

Milutinovich, M., and Koshland, D. E. (2003). SMC complexes - wrapped up in controversy. Science *300*, 1101-1102.

Morishita, T., Tsutsui, Y., Iwasaki, H., and Shinagawa, H. (2002). The Schizosaccharomyces pombe rad60 gene is essential for repairing double-strand DNA breaks spontaneously occurring during replication and induced by DNA-damaging agents. Mol Cell Biol *22*, 3537-3548.

Moriya, S., Tsujikawa, E., Hassan, A. K., Asai, K., Kodama, T., and Ogasawara, N. (1998). A Bacillus subtilis gene-encoding protein homologous to eukaryotic SMC motor protein is necessary for chromosome partition. Mol Microbiol *29*, 179-187.

Nasmyth, K. (2001). Disseminating the genome: Joining, resolving, and separating sister chromatids during mitosis and meiosis. Annu Rev Genet *35*, 673-745.

Niki, H., Jaffe, A., Imamura, R., Ogura, T., and Hiraga, S. (1991). The new gene mukB codes for a 177 kd protein with coiled-coil domains involved in chromosome partitioning of E. coli. EMBO J *10*, 183-193.

Nonaka, N., Kitajima, T., Yokobayashi, S., Xiao, G., Yamamoto, M., Grewal, S. I. S., and Watanabe, Y. (2001). Recruitment of cohesin to heterochromatic regions by Swi6/HP1 in fission yeast. Nat Cell Biol *4*, 89-93.

Ono, T., Losada, A., Hirano, M., Myers, M. P., Neuwald, A. F., and Hirano, T. (2003). Differential contributions of condensin I and condensin II to mitotic chromosome architecture in vertebrate cells. Cell *115*, 109-121.

Onogi, T., Yamazoe, M., Ichinose, C., Niki, H., and Hiraga, S. (2000). Null mutation of the dam or seqA gene suppresses temperature-sensitive lethality but not hypersensitivity to novobiocin of muk null mutants. J Bacteriol *182*, 5898-5901.

Panizza, S., Tanaka, T., Hochwagen, A., Eisenhaber, F., and Nasmyth, K. (2000). Pds5 cooperates with cohesin in maintaining sister chromatid cohesion. Curr Biol *10*, 1557-1564.

Pearson, W. R., Wood, T., Zhang, Z., and Miller, W. (1997). Comparison of DNA sequences with protein sequences. Genomics *46*, 24-36.

Pezzi, N., Prieto, I., Kremer, L., Perez Jurado, L. A., Valero, C., del Mazo, J., Martinez-A., C., and Barbero, J. L. (2000). *STAG3*, a novel gene encoding a protein involved in meiotic chromosome pairing and location of *STAG3*-related genes flanking the Williams-Beuren syndrome deletion. FASEB J *14*, 581-592.

Prieto, I., Suja, J. A., Pezzi, N., Kremer, L., Martinez-A., C., Rufas, J. S., and Barbero, J. L. (2001). Mammalian STAG3 is a cohesin specific to sister chromatid arms in meiosis I. Nat Cell Biol *3*, 761-766.

Rao, H., Uhlmann, F., Nasmyth, K., and Varshavsky, A. (2001). Degradation of a cohesin subunit by the N-end rule pathway is essential for chromosome stability. Nature *410*, 955-959.

Revenkova, E., Eijpe, M., Heyting, C., Gross, B., and Jessberger, R. (2001). Novel meiosis-specific isoform of mammalian SMC1. Mol Cell Biol *21*, 6984-6998.

Rigaut, G., Shevchenko, A., Rutz, B., Wilm, M., Mann, M., and Seraphin, B. (1999). A generic protein purification method for protein complex characterization and proteome exploration. Nat Biotechnol *17*, 1030-1032.

Rollins, R. A., Korom, M., Aulner, N., Martens, A., and Dorsett, D. (2004). *Drosophila* Nipped-B protein supports sister chromatid cohesion and opposes the stromalin/Scc3 cohesion factor to facilitate long-range activation of the *cut* gene. Mol Cell Biol *24*, 3100-3111.

Rollins, R. A., Morcillo, P., and Dorsett, D. (1999). Nipped-B, a Drosophila homologue of chromosomal adherins, participates in activation by remote enhancers in the *cut* and *Ultrabithorax* genes. Genetics *152*, 577-593.

Saitoh, N., Goldberg, I. G., Wood, E. R., and Earnshaw, W. C. (1994). ScII: an abundant chromosome scaffold protein is a member of a family of putative ATPases with an unusual predicted tertiary structure. J Cell Biol *127*, 303-318.

Saka, Y., Sutani, T., Yamashita, Y., Saitoh, S., Takeuchi, M., Nakaseko, Y., and Yanagida, M. (1994). Fission yeast cut3 and cut14, members of a ubiquitous protein family, are required for chromosome condensation and segregation in mitosis. EMBO J *13*, 4938-4952.

Sakai, A., Hizume, K., Sutani, T., Takeyasu, K., and Yanagida, M. (2003). Condensin but not cohesin SMC heterodimer induces DNA reannealing through protein-protein assembly. EMBO J *22*, 2764-2775.

Saraste, M., Sibbald, P. R., and Wittinghofer, A. (1990). The P-loop--a common motif in ATP- and GTP-binding proteins. Trends Biochem Sci *15*, 430-434.

Sawitzke, J. A., and Austin, S. (2000). Suppression of chromosome segregation defects of Escherichia coli muk mutants by mutations in topoisomerase I. Proc Natl Acad Sci U S A *97*, 1671-1676.

Schleiffer, A., Kaitna, S., Maurer-Stroh, S., Glotzer, M., Nasmyth, K., and Eisenhaber, F. (2003). Kleisins: A superfamily of bacterial and eukaryotic SMC protein partners. Mol Cell *11*, 571-575.

Schmitt, L., and Tampé, R. (2002). Structure and mechanism of ABC transporters. Curr Opin Struct Biol *12*, 754-760.

Siegel, L. M., and Monty, K. J. (1966). Determination of molecular weights and frictional ratios of proteins in impure systems by use of gel filtration and density gradient centrifugation. Application to crude preparations of sulfite and hydroxylamine reductases. Biochim Biophys Acta *112*, 346-362.

Sjögren, C., and Nasmyth, K. (2001). Sister chromatid cohesion is required for postreplicative double-strand break repair in *Saccharomyces cerevisiae*. Curr Biol *11*, 991-995.

Skibbens, R. V., Corson, L. B., Koshland, D., and Hieter, P. (1999). Ctf7p is essential for sister chromatid cohesion and links mitotic chromosome structure to the DNA replication machinery. Genes Dev *13*, 307-319.

Smith, C. A., and Rayment, I. (1996). Active site comparisons highlight structural similarities between myosin and other P-loop proteins. Biophys J *70*, 1590-1602.

Smith, P. C., Karpowich, N., Millen, L., Moody, J. E., Rosen, J., Thomas, P. J., and Hunt, J. F. (2002). ATP binding to the motor domain from an ABC transporter drives formation of a nucleotide sandwich dimer. Mol Cell *10*, 139-149.

Sonoda, E., Matsusaka, T., Morrison, C., Vagnarelli, P., Hoshi, O., Ushiki, T., Nojima, K., Fukagawa, T., Waizenegger, I. C., Peters, J. M., *et al.* (2001). Scc1/Rad21/Mcd1 is required for sister chromatid cohesion and kinetochore function in vertebrate cells. Dev Cell *1*, 759-770.

Soppa, J., Kobayashi, K., Noirot-Gros, M. F., Oesterhelt, D., Ehrlich, S. D., Dervyn, E., Ogasawara, N., and Moriya, S. (2002). Discovery of two novel families of proteins that are proposed to interact with prokaryotic SMC proteins, and characterization of the Bacillus subtilis family members ScpA and ScpB. Mol Microbiol *45*, 59-71.

Stemmann, O., Zou, H., Gerber, S. A., Gygi, S. P., and Kirschner, M. W. (2001). Dual inhibition of sister chromatid separation at metaphase. Cell *107*, 715-726.

Stray, J. E., and Lindsley, J. E. (2003). Biochemical analysis of the yeast condensin Smc2/4 complex. An ATPase that promotes knotting of circular DNA. J Biol Chem *278*, 26238-26248.

Strick, T. R., Kawaguchi, T., and Hirano, T. (2004). Real-time detection of single-molecule DNA compaction by condensin I. Curr Biol *14*, 874-880.

Strunnikov, A., Hogan, E., and Koshland, D. (1995). *SMC2*, a *Saccharomyces cerevisiae* gene essential for chromosome segregation and condensation, defines a subgroup within the SMC family. Genes Dev *9*, 587-599.

Strunnikov, A. V., Larionov, V. L., and Koshland, D. (1993). SMC1: an essential yeast gene encoding a putative head-rod-tail protein is required for nuclear division and defines a new ubiquitous protein family. J Cell Biol *123*, 1635-1648.

Sumara, I., Vorlaufer, E., Gieffers, C., Peters, B. H., and Peters, J.-M. (2000). Characterization of vertebrate cohesin complexes and their regulation in prophase. J Cell Biol *151*, 749-761.

Sumara, I., Vorlaufer, E., Stukenberg, P. T., Kelm, O., Redemann, N., Nigg, E. A., and Peters, J.-M. (2002). The dissociation of cohesin from chromosomes in prophase is regulated by Polo-like kinase. Mol Cell *9*, 515-525.

Sutani, T., Yuasa, T., Tomonaga, T., Dohmae, N., Takio, K., and Yanagida, M. (1999). Fission yeast condensin complex: essential roles of non-SMC subunits for condensation and Cdc2 phosphorylation of Cut3/SMC4. Genes Dev *13*, 2271-2283.

Tanaka, K., Hao, Z., Kai, M., and Okayama, H. (2001). Establishment and maintenance of sister chromatid cohesion in fission yeast by a unique mechanism. EMBO J *20*, 5779-5990.

Tanaka, K., Yonekawa, T., Kawasaki, Y., Kai, M., Furuya, K., Iwasaki, M., Murakami, H., Yanagida, M., and Okayama, H. (2000a). Fission yeast Eso1p is required for establishing sister chromatid cohesion during S phase. Mol Cell Biol *20*, 3459-3469.

Tanaka, T., Cosma, M. P., Wirth, K., and Nasmyth, K. (1999). Identification of cohesin association sites at centromeres and along chromosome arms. Cell *98*, 847-858.

Tanaka, T., Fuchs, J., Loidl, J., and Nasmyth, K. (2000b). Cohesin ensures bipolar attachment of microtubules to sister centromeres and resists their precocious separation. Nat Cell Biol *2*, 492-499.

Tanaka, T. U., Rachidi, N., Janke, C., Pereira, G., Galova, M., Schiebel, E., Stark, M. J. R., and Nasmyth, K. (2002). Evidence that the Ipl1-Sli15 (aurora kinase-INCENP) complex promotes chromosome bi-orientation by altering kinetochore-spindle pole connections. Cell *108*, 317-329.

Tomonaga, T., Nagao, K., Kawasaki, Y., Furuya, K., Murakami, A., Morishita, J., Yuasa, T., Sutani, T., Kearsey, S. E., Uhlmann, F., *et al.* (2000). Characterization of fission yeast cohesin: essential anaphase proteolysis of Rad21 phosphorylated in the S phase. Genes Dev *14*, 2757-2770.

Tóth, A., Ciosk, R., Uhlmann, F., Galova, M., Schleiffer, A., and Nasmyth, K. (1999). Yeast Cohesin complex requires a conserved protein, Eco1p (Ctf7), to establish cohesion between sister chromatids during DNA replication. Genes Dev *13*, 320-333.

Toyoda, Y., Furuya, K., Goshima, G., Nagao, K., Takahashi, K., and Yanagida, M. (2002). Requirement of chromatid cohesion proteins Rad21/Scc1 and Mis4/Scc2 for normal spindle-kinetochore interaction in fission yeast. Curr Biol *12*, 347-358.

Uhlmann, F., Lottspeich, F., and Nasmyth, K. (1999). Sister-chromatid separation at anaphase onset is promoted by cleavage of the cohesin subunit Scc1. Nature *400*, 37-42.

Uhlmann, F., and Nasmyth, K. (1998). Cohesion between sister chromatids must be established during DNA replication. Curr Biol *8*, 1095-1101.

Uhlmann, F., Wernic, D., Poupart, M.-A., Koonin, E. V., and Nasmyth, K. (2000). Cleavage of cohesin by the CD clan protease separin triggers anaphase in yeast. Cell *103*, 375-386.

Vagnarelli, P., Morrison, C., Dodson, H., Sonoda, E., Takeda, S., and Earnshaw, W. C. (2004). Analysis of Scc1-deficient cells defines a key metaphase role of vertebrate cohesin in linking sister kinetochores. EMBO Rep *5*, 167-171.

van den Ent, F., Lockhart, A., Kendrick-Jones, J., and Löwe, J. (1999). Crystal structure of the N-terminal domain of MukB: a protein involved in chromosome partitioning. Structure Fold Des *7*, 1181-1187.

van Heemst, D., James, F., Poggeler, S., Berteaux-Lecellier, V., and Zickler, D. (1999). Spo76p is a conserved chromosome morphogenesis protein that links the mitotic and meiotic programs. J Cell Sci *115*, 587-598.

Verkade, H. M., Bugg, S. J., Lindsay, H. D., Carr, A. M., and O'Connell, M. J. (1999). Rad18 is required for DNA repair and checkpoint responses in fission yeast. Mol Biol Cell *10*, 2905-2918.

Volkov, A., Mascarenhas, J., Andrei-Selmer, C., Ulrich, H. D., and Graumann, P. L. (2003). A prokaryotic condensin/cohesin-like complex can actively compact chromosomes from a single position on the nucleoid and binds to DNA as a ring-like structure. Mol Cell Biol *23*, 5638-5650.

Waizenegger, I. C., Hauf, S., Meinke, A., and Peters, J.-M. (2000). Two distinct pathways remove mammalian cohesin complexes from chromosome arms in prophase and from centromeres in anaphase. Cell *103*, 399-410.

Walker, J. E., Saraste, M., Rumswick, M. J., and Gay, N. J. (1982). Distantly related sequences in the α and β subunits of the ATP synthase, myosin, kinases and other ATP requiring enzymes and a common nucleotide binding fold. EMBO J *1*, 945-951.

Weinstock, G. M., McEntee, K., and Lehman, I. R. (1979). ATP-dependent renaturation of DNA catalyzed by the recA protein of Escherichia coli. Proc Natl Acad Sci U S A *76*, 126-130.

Weitao, T., Nordstrom, K., and Dasgupta, S. (1999). Mutual suppression of mukB and seqA phenotypes might arise from their opposing influences on the Escherichia coli nucleoid structure. Mol Microbiol *34*, 157-168.

West, A. G., Gaszner, M., and Felsenfeld, G. (2002). Insulators: many functions, many mechanisms. Genes Dev *16*, 271-288.

Williams, B. C., Garrett-Engele, C. M., Li, Z., Williams, E. V., Rosenman, E. D., and Goldberg, M. L. (2003). Two putative acetyltransferases, san and deco, are required for establishing sister chromatid cohesion in Drosophila. Curr Biol *13*, 2025-2036.

Yamamoto, A., Guacci, V., and Koshland, D. (1996). Pds1p, an inhibitor of anaphase in budding yeast, plays a critical role in the APC and checkpoint pathway(s). J Cell Biol *133*, 99-110.

Yamazoe, M., Onogi, T., Sunako, Y., Niki, H., Yamanaka, K., Ichimura, T., and Hiraga, S. (1999). Complex formation of MukB, MukE and MukF proteins involved in chromosome partitioning in Escherichia coli. EMBO J *18*, 5873-5884.

Yazdi, P. T., Wang, Y., Zhao, S., Patel, N., Lee, E. Y., and Qin, J. (2002). SMC1 is a downstream effector in the ATM/NBS1 branch of the human S-phase checkpoint. Genes Dev *16*, 571-582.

Yoshimura, S. H., Hizume, K., Murakami, A., Sutani, T., Takeyasu, K., and Yanagida, M. (2002). Condensin architecture and interaction with DNA: regulatory non-SMC subunits bind to the head of SMC heterodimer. Curr Biol *12*, 508-513.

Yu, H. (2002). Regulation of APC-Cdc20 by the spindle checkpoint. Curr Opin Cell Biol *14*, 706-714.